

SCHOOL OF  
CIVIL ENGINEERING

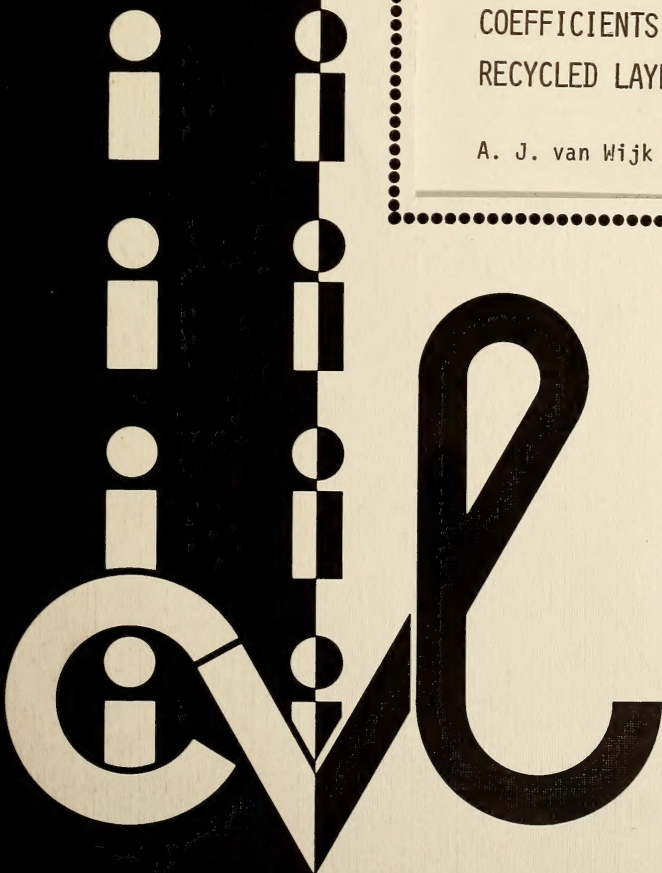
INDIANA  
DEPARTMENT OF HIGHWAYS

JOINT HIGHWAY RESEARCH PROJECT

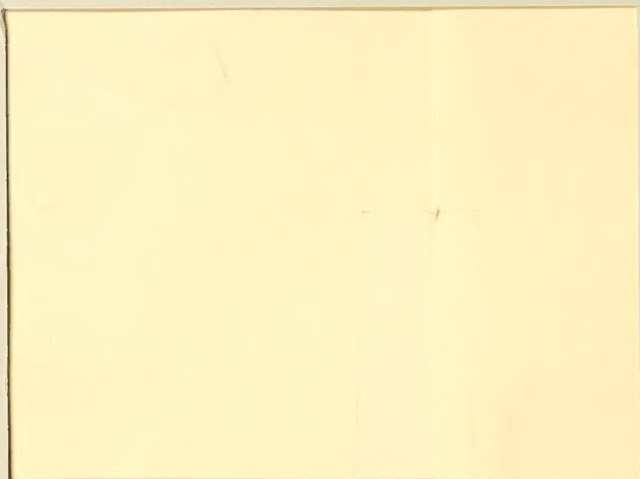
JHRP-84-1

DETERMINATION OF THE STRUCTURAL  
COEFFICIENTS OF A FOAMED ASPHALT  
RECYCLED LAYER

A. J. van Wijk



PURDUE UNIVERSITY

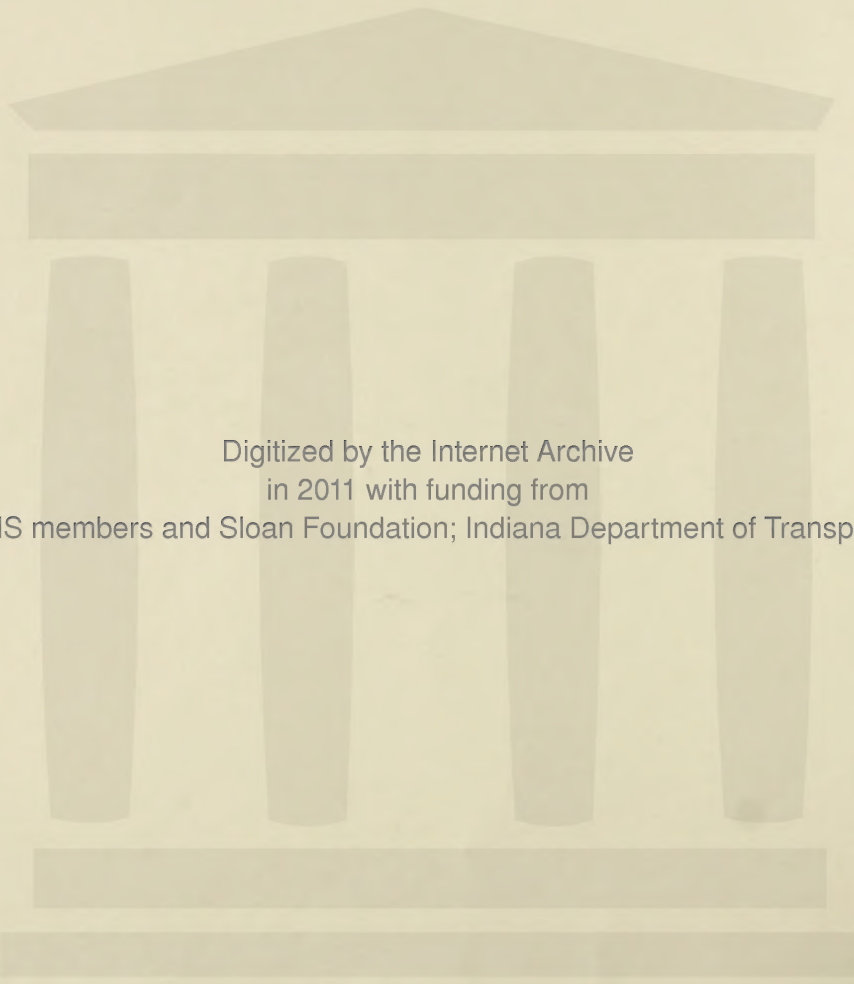


JOINT HIGHWAY RESEARCH PROJECT

JHRP-84-1

DETERMINATION OF THE STRUCTURAL  
COEFFICIENTS OF A FOAMED ASPHALT  
RECYCLED LAYER

A. J. van Wijk



Digitized by the Internet Archive  
in 2011 with funding from  
LYRASIS members and Sloan Foundation; Indiana Department of Transportation



Final Report

DETERMINATION OF THE STRUCTURAL COEFFICIENTS

OF A FOAMED ASPHALT RECYCLED LAYER

TO: H. L. Michael, Director  
Joint Highway Research Project

January 10, 1984

Project: C-36-21F

FROM: L. E. Wood  
School of Civil Engineering

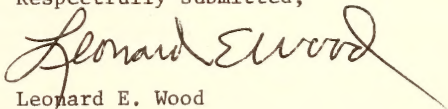
File: 2-8-6

Attached is the Final Report on the JHRP Study titled "Determination of Structural Layer Equivalencies for Material Recycled with Foamed Asphalt". The Report is authored by Adriaan van Wijk, Graduate Instructor in Research on the JHRP staff. Professors E. J. Yoder and L. E. Wood coordinated the research.

Some of the data used in determining the range of structural coefficients recommended for the design of a foamed asphalt recycled layer which would have similar properties to the original layer of bituminous material in the pavement came from a section of SR 16 in Indiana which was reconstructed with a foamed asphalt recycled base course. The research found that the recycled layer was weaker after recycling than it was before recycling but that the recycled layer increased in strength until at 250 days after construction it was as strong or stronger than the original pavement.

The Report is submitted as fulfilling the objectives of the noted JHRP Study as approved in May 1981.

Respectfully submitted,



Leonard E. Wood

LEW:ms

cc: A. G. Altschaeffl  
J. M. Bell  
W. F. Chen  
W. L. Dolch  
R. L. Eskew  
J. D. Fricker  
G. D. Gibson

W. H. Goetz  
G. K. Hallock  
J. F. McLaughlin  
R. D. Miles  
P. L. Owens  
B. K. Partridge  
G. T. Satterly

C. F. Scholer  
R. M. Shanteau  
K. C. Sinha  
C. A. Venable  
L. E. Wood  
S. R. Yoder



Final Report

DETERMINATION OF THE STRUCTURAL COEFFICIENTS  
OF A FOAMED ASPHALT RECYCLED LAYER

by

A. J. van Wijk  
Graduate Instructor in Research

Joint Highway Research Project

Project No.: C-36-21F

File No.: 2-8-6

Prepared as Part of an Investigation

Conducted by

Joint Highway Research Project  
Engineering Experiment Station  
Purdue University

In Cooperation with

Indiana Department of Highways

Purdue University  
West Lafayette, Indiana  
January 10, 1984





## ACKNOWLEDGMENTS

The author would like to express his appreciation to his major professors, Prof. Eldon J. Yoder and Prof. Leonard E. Wood for their guidance and interest throughout the study, as well as the thorough review of the manuscript. He also appreciates their assistance and encouragement in the writing, submitting and presenting of papers regarding this study. Their interest in his and his wife's well-being has been of a constant source of encouragement during the two years of the study.

The author wishes to thank Prof. Virgil Anderson for being on his committee and reviewing the manuscript. The author would further like to thank Dr. Mang Tia for his assistance in helping him to start off in the laboratory and his advice throughout the study. The colleagues of the author in Room 303, especially Messrs. Benjamin Colucci-Rios, Humberto Castedo and Essam Sharaf were always very helpful and interested. The author appreciates that.

The Indiana Department of Highways sponsored the project. The author is extremely grateful to them as well as to the personnel of the Research and Training Center, especially Mr. Keith Kercher for their assistance through the first part of the study.

The author also extends his appreciation to Ms. Marian Sipes for typing the manuscript, Mr. Emmett Black for the photographs and Mr. Brent Phelps for preparing some of the figures.



The study was made easier with the encouragement of the author's family and wife, Una. The author is sincerely thankful to the latter for her understanding, encouragement and assistance throughout the study even with her own busy schedule.





## TABLE OF CONTENTS

	<u>Page</u>
LIST OF TABLES . . . . .	viii
LIST OF FIGURES . . . . .	xi
ABSTRACT . . . . .	xvi
CHAPTER 1: INTRODUCTION . . . . .	1
CHAPTER 2: LITERATURE REVIEW . . . . .	6
2.1. Introduction . . . . .	6
2.2. Foamed Asphalt . . . . .	7
2.2.1. Research . . . . .	7
2.2.2. Application . . . . .	10
2.3. Recycling . . . . .	12
2.3.1. Research . . . . .	12
2.3.2. Application . . . . .	16
2.4. Flexible Pavement Design Methods . . . . .	16
2.4.1. AASHTO Design Procedure . . . . .	18
2.4.2. California Bearing Ratio (CBR) Method . . . . .	20
2.4.3. California Method of Design (Hveem Stabilometer) . . . . .	22
2.4.4. Asphalt Institute Method . . . . .	24
2.4.5. Mechanistic Design Procedures . . . . .	25
2.4.5.1. Pavement Response Models . . . . .	25
2.4.5.2. Material Characterization . . . . .	26
2.4.5.3. Distress Modes . . . . .	27
2.4.6. Summary . . . . .	33
2.5. Determination of Structural Layer Coefficients . . . . .	33
2.5.1. Development of the Structural Layer Coefficients . . . . .	35
2.5.2. Asphalt Institute . . . . .	36
2.5.3. National Crushed Stone Association . . . . .	36
2.5.4. Arizona . . . . .	36
2.5.5. California . . . . .	36
2.5.6. Illinois . . . . .	37
2.5.7. Louisiana . . . . .	37
2.5.8. New Mexico and Wyoming . . . . .	37
2.5.9. Ohio . . . . .	37
2.5.10. Texas . . . . .	38
2.5.11. Pennsylvania . . . . .	38



## TABLE OF CONTENTS (Continued)

	<u>Page</u>
2.5.12. U.S. Forest Service . . . . .	39
2.5.13. Virginia. . . . .	40
2.5.14. Recycled Materials. . . . .	40
2.5.15. Foamed Asphalt Stabilized Layers. . . . .	43
CHAPTER 3: CONSTRUCTION OF THE TEST ROAD. . . . .	47
3.1. Introduction. . . . .	47
3.2. Condition of the Initial Pavement . . . . .	49
3.3. Original Construction Concept . . . . .	49
3.4. Actual Construction . . . . .	57
3.5. Description of the Actual Construction Procedure. . . . .	58
3.6. Control of the Foamed Asphalt Mixture . . . . .	64
3.7. Construction Problems . . . . .	64
3.8. Conclusions . . . . .	65
CHAPTER 4: SAMPLING AND TESTING PROGRAMS ON THE TEST ROAD . . . . .	66
4.1. Introduction. . . . .	66
4.2. Prior to Construction . . . . .	68
4.3. During Construction . . . . .	69
4.4. After Construction. . . . .	72
CHAPTER 5: DESCRIPTION OF TEST EQUIPMENT AND PARAMETERS . . . . .	76
5.1. Introduction. . . . .	76
5.2. Dynamic Cone Penetrometer (DCP) . . . . .	76
5.3. Clegg Impact Soil Tester. . . . .	79
5.4. Dynaflect . . . . .	80
5.5. Kneading Compactor. . . . .	83
5.6. Hveem Stabilometer and Compression Machine. . . . .	85
5.7. Marshall Testing Equipment. . . . .	86
5.8. Vacuum Saturation Equipment . . . . .	89
5.9. Resilient Modulus Testing Equipment . . . . .	89
5.10. Indirect Tensile Strength Testing Equipment . . . . .	93
CHAPTER 6: TESTING PROCEDURE. . . . .	97
6.1. Introduction. . . . .	97
6.2. Subgrade. . . . .	97
6.2.1. In-Situ CBR . . . . .	97
6.2.2. Classification Tests. . . . .	100
6.3. Recycled Foamed Asphalt Mixture . . . . .	100
6.3.1. Laboratory Compacted Samples. . . . .	103
6.3.1.1. Storage . . . . .	103
6.3.1.2. Compaction. . . . .	103
6.3.1.3. Curing. . . . .	106





## TABLE OF CONTENTS (Continued)

	<u>Page</u>
6.3.1.4. Density and Height Determination. . .	107
6.3.1.5. Water Sensitivity Test. . . . .	108
6.3.1.6. Resilient Modulus and Poisson's Ratio Testing . . . . .	108
6.3.1.7. Hveem Resistance Value. . . . .	110
6.3.1.8. Marshall Variables. . . . .	110
6.3.1.9. Indirect Tensile Strength . . . . .	111
6.3.1.10. Moisture Content During Testing . . .	111
6.3.1.11. Miscellaneous Tests . . . . .	112
6.3.2. Cored Samples . . . . .	112
6.4. Asphalt Concrete Surface. . . . .	115
6.5. Evaluation of the Initial Pavement Layer. . . . .	115
6.6. In-Situ Tests on the Pavement Layers. . . . .	116
6.6.1. Clegg Impact Tests. . . . .	116
6.6.2. Deflection Measurements . . . . .	116
CHAPTER 7: RESULTS OF LABORATORY AND IN-SITU TESTS. . . . .	117
7.1. Introduction. . . . .	117
7.2. Subgrade Material . . . . .	117
7.3. Foamed Asphalt Recycled Material. . . . .	123
7.3.1. Main Objectives . . . . .	123
7.3.2. Secondary Objectives. . . . .	134
7.4. Asphalt Concrete Surface Material . . . . .	153
7.5. Initial Asphalt Pavement. . . . .	159
7.6. Fatigue Life. . . . .	159
7.7. Comparison Between Laboratory and Non-Destructive Testing Results . . . . .	159
7.8. Summary of Results. . . . .	162
CHAPTER 8: RESULTS OF NON-DESTRUCTIVE TESTING . . . . .	167
8.1. Introduction. . . . .	167
8.2. Clegg Impact Tests. . . . .	167
8.3. Deflection Tests. . . . .	169
8.4. Comparison of In-Situ CBR and $BCI/D_5$ . . . . .	196
CHAPTER 9: STRUCTURAL COEFFICIENT DETERMINATION . . . . .	199
9.1. The Pavement Response Model . . . . .	199
9.2. Distress Criteria . . . . .	200
9.2.1. Fatigue Cracking. . . . .	202
9.2.2. Rutting . . . . .	212
9.2.3. Deformation . . . . .	212
9.3. Selection of the Pavement Cross Sections. . . . .	212
9.4. Sensitivity Analysis. . . . .	227



## TABLE OF CONTENTS (Continued)

	<u>Page</u>
9.5. Determination of AASHTO Asphalt Concrete Surface Equivalent Thicknesses. . . . .	232
9.6. Determination of Equivalency Factors. . . . .	233
9.6.1. Tensile Strain at the Bottom of the Recycled Layer. . . . .	235
9.6.2. Tensile Strain at the Bottom of the Remaining Initial Pavement Layer. . . . .	236
9.6.3. Compressive Strain on Top of the Subgrade ( $\epsilon_v$ ). . . . .	236
9.6.4. Maximum Deformation of the Subgrade . . . . .	236
9.6.5. Maximum Surface Deflections . . . . .	237
9.6.6. Fatigue Life of the Asphalt Layers. . . . .	237
9.6.7. Results . . . . .	238
9.7. Controlling Criterion . . . . .	257
9.8. Different Recycled Layer Thicknesses. . . . .	258
9.9. Effect of the Elastic Modulus on the Recycled Layer . . . . .	265
9.10. Summary of Results. . . . .	265
9.10.1. Criteria Used in the Final Analysis . . . . .	265
9.10.2. Assumptions Made. . . . .	268
9.10.3. Conclusions . . . . .	270
CHAPTER 10: CONCLUSIONS AND RECOMMENDATIONS . . . . .	274
10.1. Conclusions . . . . .	274
10.2. Recommendations . . . . .	276
10.3. Recommendations for Future Research . . . . .	277
REFERENCES . . . . .	278
APPENDIX . . . . .	286





## LIST OF TABLES

<u>Table</u>		<u>Page</u>
2.1	Properties of Foamed Asphalt Mixtures from the Literature . . . . .	11
2.2	Properties of Cold Recycled Mixtures from the Literature . . . . .	17
2.3	Structural Coefficients from AASHTO Road Test (from Ref. 69) . . . . .	21
2.4	California Gravel Equivalent Factors (after Ref. 76) . . .	23
2.5	Resilient Modulus-Bulk Stress Relationships for Granular Materials . . . . .	28
2.6	Resilient Modulus-Deviator Stress Relationships for Subgrade Materials . . . . .	29
2.7	Subgrade Compression Strain-Fatigue Life Relationships Considered . . . . .	31
2.8	Asphalt Fatigue-Life Relationships Considered. . . . .	34
2.9	Structural Coefficients and Equivalency Factors from the Literature . . . . .	46
3.1	Results of Tests on 24 Core Samples. . . . .	51
3.2	Results of Tests on 8 Core Samples . . . . .	52
3.3	Construction and Material Requirements . . . . .	53
4.1	Position of Samples Taken. . . . .	70
4.2	Number of Samples Taken. . . . .	75
6.1	Number of Laboratory Specimens for Each Storage and Curing Time. . . . .	104
6.2	Number of Laboratory Specimens Used in Each Test . . . . .	105
6.3	Number of Core Specimens Used in Each Test . . . . .	114



## LIST OF TABLES (Continued)

<u>Table</u>		<u>Page</u>
7.1	Dynamic Cone Penetrometer (DCP) Test Results . . . . .	118
7.2	Characteristics of Subbase and Subgrade. . . . .	120
7.3	Results of Resilient Modulus and Poisson's Ratio Tests . .	125
7.4	Results of Indirect Tensile Strength Tests (Unsaturated Specimens). . . . .	126
7.5	Density and Moisture Content of the Unsaturated Samples. .	129
7.6	Results of Tests on the Effects of Curing Time on the Resilient Modulus and Tensile Strength . . . . .	131
7.7	Summary of Results of Tests on the Unsaturated Specimens .	136
7.8	Summary of Results of Tests on Saturated Specimens . . . .	144
7.9	Results of Statistical Comparison Tests. . . . .	146
7.10	Summary of Test Results on the Extracted Asphalt Cement. .	156
7.11	Results of Tests on Asphalt Concrete Surface Mixture . . .	158
7.12	Properties of the Initial Asphalt Layer. . . . .	160
7.13	Fatigue-Life Relationships from Indirect Tensile Tests . .	161
7.14	Comparison Between Laboratory and In-Situ Resilient Modulus Results. . . . .	163
8.1	Deflection Adjustment Factors. . . . .	173
8.2	Summary of Dynaflect Deflection Parameters . . . . .	175
9.1	Fatigue Relationships Used for the Asphalt Concrete. . . .	203
9.2	Fatigue Relationships Used for the Recycled Material . . .	204
9.3	Failure Relationships Based on Strains or Deformations . .	213
9.4	Characteristics of Selected Pavement Sections (Eastbound). .	216
9.5	Characteristics of Selected Pavement Sections (Westbound). .	217
9.6	Pavement Cross-Section Characteristics . . . . .	220



## LIST OF TABLES (Continued)

<u>Table</u>		<u>Page</u>
9.7	Selected Pavement Cross-Sections (Eastbound Lane). . . . .	228
9.8	Selected Pavement Cross-Sections (Westbound Lane). . . . .	229
9.9	Sensitivity Analysis . . . . .	231
9.10	Summary of Coefficients Based on Strains and Deformations.	239
9.11	Summary of Coefficients Based on Fatigue . . . . .	240
9.12	Structural Coefficients Based on the Controlling Criteria.	259
9.13	Effect of Recycled Layer Thickness on the Structural Coefficient (AFTER2-Case). . . . .	262
9.14	Regression Coefficients of the Structural Coefficient vs. Elastic Modulus of the Recycled Layer. . . . .	266
9.15	Assumptions. . . . .	269
9.16	Summary of Structural Coefficients . . . . .	271



## LIST OF FIGURES

<u>Figure</u>		<u>Page</u>
3.1	Location of the Test Road in Indiana . . . . .	48
3.2	Proposed Pavement Cross Section. . . . .	55
3.3	Gradation Analysis of Materials Used in Construction . . .	56
3.4	Flow Diagram of Actual Construction Procedure. . . . .	59
3.5	Diagrammatic Outlay of the Mixing Procedure. . . . .	61
4.1	Strip Map of the Experimental Section. . . . .	67
4.2	Chronological Display of Sampling and Testing Programs . .	74
5.1	Dynamic Cone Penetrometer. . . . .	77
5.2	Dimensions of the Dynamic Cone Penetrometer (from Ref. 61)	78
5.3	Clegg Impact Soil Tester . . . . .	81
5.4	Dynaflect Sensor Arrangement and Deflection Basin (after Ref. 48). . . . .	81
5.5	Kneading Compactor . . . . .	84
5.6	Marshall Test Equipment. . . . .	87
5.7	Typical Load-Deformation Plot from the Marshall Test (from Ref. 22) . . . . .	88
5.8	Resilient Modulus Testing Equipment. . . . .	90
5.9	Typical Deformation Plots from the Resilient Modulus Test (from Ref. 66). . . . .	92
5.10	Stress Distribution Along the Principal Areas (from Ref. 40) . . . . .	94





## LIST OF FIGURES (Continued)

<u>Figure</u>		<u>Page</u>
6.1	Typical Plot from the Dynamic Cone Penetrometer Test . . .	99
6.2	Flow Diagram of Soil Classification Procedure. . . . .	101
6.3	Flow Diagram of the Foamed Asphalt Recycled Specimen Testing Procedure. . . . .	102
7.1	CBR and Thickness of the Subbase and the Subgrade (Eastbound Lane) . . . . .	121
7.2	CBR and Thickness of the Subbase and the Subgrade (Westbound Lane) . . . . .	122
7.3	Effect of Temperature on the Resilient Modulus . . . . .	128
7.4	Effect of Curing Time on the Resilient Modulus . . . . .	132
7.5	Effect of Curing Time and Temperature on Tensile Strength.	133
7.6	Effect of Water on the Hveem-R-Value . . . . .	137
7.7	Effect of Water on the Marshall Stability. . . . .	138
7.8	Effect of Water on the Marshall Index. . . . .	139
7.9	Effect of Water on the Marshall Stiffness. . . . .	140
7.10	Effect of Water on the Specimen Density. . . . .	141
7.11	Effect of Water on the Testing Moisture Content. . . . .	142
7.12	Effect of Water on the Resilient Modulus . . . . .	143
7.13	Effect of Time Stored in a Closed Bag on Resilient Modulus. . . . .	147
7.14	Effect of Storage in Air on the Resilient Modulus. . . . .	149
7.15	Effect of Storage in Air on the Marshall Stability . . . . .	150
7.16	Effect of Storage in Air on the Marshall Index . . . . .	151
7.17	Effect of Storage in Air on the Marshall Stiffness . . . . .	152
7.18	Effect of Compaction Moisture Content on Marshall Stability. . . . .	154



## LIST OF FIGURES (Continued)

<u>Figure</u>		<u>Page</u>
7.19	Effect of Compaction Moisture Content on Resilient Modulus. . . . .	155
7.20	Gradation Analysis of the Recovered Aggregate. . . . .	157
8.1	Changes in the Clegg Impact Values on the Eastbound Lane .	168
8.2	Changes in the Clegg Impact Values on the Westbound Lane .	170
8.3	Changes in Maximum Dynaflect Deflection Before, During and After Construction (Eastbound Lane). . . . .	176
8.4	Changes in Spreadability Before, During and After Construction (Eastbound Lane). . . . .	177
8.5	Changes in Surface Curvature Index Before, During and After Construction (Eastbound Lane). . . . .	178
8.6	Changes in Base Curvature Index Before, During and after Construction (Eastbound Lane). . . . .	179
8.7	Changes in Sensor 5 Deflection Before, During and After Construction (Eastbound Lane). . . . .	180
8.8	Changes in Maximum Dynaflect Deflection Before and After Construction (Westbound Lane). . . . .	181
8.9	Changes in Spreadability Before and After Construction (Westbound Lane) . . . . .	182
8.10	Changes in Surface Curvature Index Before and After Construction (Westbound Lane). . . . .	183
8.11	Changes in Base Curvature Index Before and After Construction (Westbound Lane). . . . .	184
8.12	Changes in Sensor 5 Deflection Before and After Construction (Westbound Lane). . . . .	185
8.13	Comparison of Average Surface Curvature Before, During and After Construction. . . . .	186
8.14	Comparison of Average Maximum Dynaflect Deflection Before, During and After Construction. . . . .	187
8.15	Comparison of Average Spreadability Before, During and After Construction . . . . .	188



## LIST OF FIGURES (Continued)

<u>Figure</u>		<u>Page</u>
8.16	Effects of the Elastic Moduli of the Pavement Layers on the Dynaflect Deflection Basin. . . . .	191
8.17	Effect of Changes in Subbase and Subgrade Elastic Moduli on the Spreadability. . . . .	193
8.18	Effect of Changes in Subbase and Subgrade Elastic Moduli on the Surface Curvature Index. . . . .	194
8.19	Comparison of DCP and BCI Values (Eastbound Lane). . . . .	197
8.20	Comparison of DCP and BCI Values (Westbound Lane). . . . .	198
9.1	Typical Pavement Cross Section Used in the Analysis. . . . .	201
9.2	Fatigue Life-Tensile Strain Relationships for Asphalt Concrete . . . . .	208
9.3	Fatigue Life-Tensile Strain Relationships for the Asphalt Concrete Layer on SR 16. . . . .	209
9.4	Fatigue Life-Tensile Strain Relationships for Asphalt Base Courses . . . . .	211
9.5	Fatigue Life-Compressive Strain Relationships for Subgrades. . . . .	214
9.6	Flow Diagram of the Structural Coefficient Determination Procedure. . . . .	219
9.7	Effect of Changes in the Layer Elastic Moduli on the Dynaflect Deflection Basin . . . . .	222
9.8	Effect of the Inclusion of a Stiff Subgrade Layer at a Depth of 350 inches on the Dynaflect Deflection Basin. . . . .	226
9.9	Effect of Layer Stiffness on the Structural Coefficients (Based on Strains and Deformations). . . . .	242
9.10	Effect of Layer Stiffness on the Structural Coefficients (Based on Fatigue) . . . . .	244
9.11	Effect of Time After Construction on the Structural Coefficients for Low Deflections (Based on Deformations and Strains) . . . . .	246





## LIST OF FIGURES (Continued)

<u>Figure</u>		<u>Page</u>
9.12	Effect of Time After Construction on the Structural Coefficients for Average Deflections (Based on Deformations and Strains). . . . .	248
9.13	Effect of Time After Construction on the Structural Coefficients for High Deflections (Based on Deformations and Strains) . . . . .	250
9.14	Effect of Time After Construction on the Structural Coefficients for Low Deflections (Based on Fatigue). . . .	252
9.15	Effect of Time After Construction on the Structural Coefficients for Average Deflections (Based on Fatigue). . .	254
9.16	Effect of Time After Construction on the Structural Coefficients for High Deflections (Based on Fatigue) . . .	256
9.17	Structural Coefficients Based on the Controlling Criteria (AFTER1 and AFTER2 Cases) . . . . .	261
9.18	Effect of the Recycled Layer Thickness on the Structural Coefficient (AFTER2 Case) . . . . .	264
9.19	Effect of the Layer Elastic Modulus on the Structural Coefficients . . . . .	267
9.20	Recommended Ranges of Structural Coefficients. . . . .	273



## ABSTRACT

Van Wijk, Adriaan Jacobus. M.S.C.E., Purdue University, December 1982. Determination of the Structural Coefficients of a Foamed Asphalt Recycled Layer. Major Professors: E. J. Yoder and L. E. Wood.

The increased interest in, and the actual use of, cold recycling has emphasized the need to know more about the actual field performance of cold recycled pavement layers. Although cold recycling has obvious advantages in energy, construction material and cost savings, these advantages will be of little benefit if the recycled layer does not perform as expected. The performance of a pavement layer is taken into consideration in the AASHTO design method by the structural coefficient. The AASHTO design method is used by more than 65 percent of the states in the United States. Incorrect values used in thickness design can lead to either over expenditure or early failure and unscheduled maintenance. It is therefore important to have reliable structural coefficients to use in pavement design.

The main objective of this research was to determine structural coefficients for a foamed asphalt recycled layer. A linear elastic multi-layer analysis and fatigue characteristics of the recycled layer and subgrade were used to determine the coefficients. Some information used in the analyses was obtained from laboratory tests on samples taken from a section of road SR 16 which was constructed with a foamed asphalt recycled base course. Most of the information was obtained from nondestructive Dynaflect tests on the same road. The



nondestructive tests indicated that the pavement with the foamed asphalt recycled layer had higher deflections and was probably weaker than the initial pavement a few days after construction. The deflections decreased over time and the deflection characteristics 250 days after construction were similar to those of the initial pavement, indicating that the recycled layer is getting stronger and surpassing the initial pavement. Since reliable fatigue life relationships were not available for the recycled layer and the subgrade, a range of structural coefficients was developed which can be used in the design of a foamed asphalt recycled layer with similar properties.



## CHAPTER 1: INTRODUCTION

The energy crisis in 1973 stimulated the search for alternatives for conventional pavement construction methods and materials. Although used since the 1930's, the recycling of pavements, especially asphalt pavements, became a feasible alternative to rehabilitation and reconstruction in the 1970's. Since then the emphasis has shifted from the main concern of saving energy to the more efficient use of highway funds. The construction cost of highways has more than doubled since 1973 (97). The motor fuel tax revenue is the cornerstone of the state highway finance system. In the early 1970's motor fuel tax revenue supplied 63 percent of all state user tax revenue and in 1980 only 55 percent (14). These motor fuel taxes are collected from fuel consumed by the highway user. With the introduction of more fuel-efficient cars, the average fuel consumption (miles per gallon) of new cars has roughly doubled since 1973 (97) while the total fuel consumption has decreased since 1978 (14). Although the tax rate increased slightly, the states' highway departments received less money to construct highways with higher construction costs.

The emphasis further moved from the construction of new highways to the maintenance of existing highways (91). At the end of 1975 more than 100,000 miles of interstate, arterial and collector highways were rated as "poor". Research at the General Motors Research Laboratories (GMR) indicated that 26,000 miles of highways should have been





resurfaced or reconstructed each year since 1975. The cost can increase to as much as \$28.9 billion in ten years until 1985 (55).

In 1979, 94 percent of all paved roads in the U.S. utilized bituminous surfaces. In Indiana approximately 83 percent of the total paved, hard-surface structures under the jurisdiction of the Indiana Department of Highways has bituminous surfaces (48). The possibilities for the use of bituminous pavement recycling are therefore obvious.

Recycling can save energy, pavement material and reduce costs if it performs as expected. The construction of inferior pavements through recycling may lead to the loss of all the benefits of recycling. The strength of the pavement layers is usually taken into consideration in the design of a pavement by the AASHTO structural coefficient or an equivalency factor. The selection of the correct structural coefficient for each layer will lead to the effective use of highway funds, since the performance will be known. The best construction method (conventional or recycled), the optimum layer thicknesses, materials, and maintenance program can be selected with the performance of each pavement section known. The structural coefficients developed during the AASHTO Road Test are unfortunately only truly representative of the pavement materials used in the Road Test and therefore the suggestion after their development that they should be used with care and if possible be verified for a specific material in specific environmental conditions (69). The above verification has been done through the construction of AASHTO Satellite Test Road facilities. The structural coefficient is further dependent on environmental and geometric conditions (69).



A large amount of research has been conducted to determine the properties of various recycled mixtures, but on the other hand, little research has been directed to the establishment of reliable structural coefficients for those mixtures. Layer coefficients vary considerably with material, binder and mixing process (47). A binder that showed promise for use in cold recycling is foamed asphalt. No reliable structural coefficients have been developed for foamed asphalt recycled mixtures, although some have been developed for foamed asphalt stabilized materials (36). Foamed asphalt recycling has only been used to a very limited extent in actual field application in the U.S. and not at all in Indiana.

The main objective of the study was to determine the structural layer coefficients of specific foamed asphalt recycled mixture. An experimental section of 4.2 miles (6.72 km) constructed on State Road 16 approximately 40 miles (64 km) north of Lafayette, Indiana, utilizing foamed asphalt in cold recycling was used as a source for information regarding the properties of the foamed asphalt recycled material and the reconstructed pavement. A computer program (BISTRO) based on the layered elastic theory was used to calculate stresses, strains and deformations in the pavement section. These strains and deformations, with fatigue characteristics were used to compare the foamed asphalt recycled layer with a standard AASHTO (American Association of State Highway and Transportation Officials) Road Test asphalt concrete layer. The BISTRO program requires as input, wheel loads, the elastic properties (elastic moduli and Poisson's ratios) and the thicknesses of the layers.



The main part of this study was the determination of the elastic properties and the thicknesses of the different layers. Information was obtained from two sources, viz. laboratory or in-situ testing and nondestructive testing. The latter was done by means of Dynaflect deflection measurements. Information regarding the subbase and subgrade was obtained from in-situ Dynamic Core Penetrometer (DCP) tests and actual measurements of layer thicknesses. Laboratory compacted and core specimens of the foamed asphalt recycled layer and the surface layer were used to determine the elastic properties and fatigue characteristics of these layers. Since the foamed asphalt recycled material was of primary concern in this study a more detailed testing program was conducted on the foamed asphalt recycled laboratory and core specimens to obtain the following information:

1. The effect of different temperatures on the resilient moduli, Poisson's ratios and tensile strengths.
2. The effect of different curing times on the resilient moduli, Poisson's ratios and tensile strengths.

A secondary study was also performed to investigate the effect of the following factors on the properties of the foamed asphalt recycled material:

1. Water
2. Storage in a closed plastic bag
3. Stockpiling
4. Specimen density
5. Compaction water content
6. Moisture content during testing





In addition to the resilient moduli and tensile strengths used as indicators of the strength of the mixture, the Marshall and the Hveem R-values were also used. The strengths of the laboratory compacted specimens were also compared with those of the core specimens.

The information from the main part of the study was used to determine the structural coefficients in this study.



## CHAPTER 2: LITERATURE REVIEW

### 2.1. Introduction

The properties of any material play an important part in the structural capabilities of the material as a pavement layer. It is therefore important to know what the properties of the foamed asphalt recycled material are. A study of recycling has shown that there is a strong correlation between the structural equivalency of a recycled layer and a conventional mixture with the same binder (18). The first part of this chapter presents a brief overview of properties of recycled and foamed asphalt materials as they relate to the strength of the material, based mainly on laboratory studies. Very few studies have been conducted to investigate the in-situ performance of these materials, but by examining the behavior of all cold recycled mixtures and foamed asphalt mixtures the behavior of foamed asphalt recycled material in actual use can be anticipated. The field applications of cold recycling and foamed asphalt are also briefly summarized.

A summary of the most widely used flexible pavement design methods follows the section on the materials to give some perspective on the significance of structural equivalency factors in the design of pavement structures. This is followed by some of the methods used to determine the structural layer coefficients or equivalency factors, after those established from the AASHTO Road Test.



## 2.2. Foamed Asphalt

### 2.2.1. Research

The process of foaming asphalt was first developed in the mid 1950's by Prof. Csanyi of Iowa State University. He used a steam generator to produce the foam (15). An altered foaming method using only cold water and hot asphalt was developed in Australia, by Mobil Oil, during 1970 (7). This latter method was simpler, readily controlled and more economical and revived interest in the use of foamed asphalt (83).

Research in the properties of foamed asphalt and foamed asphalt mixtures was conducted during that time by Mobil Oil in Australia. They evaluated, among other things, resilient properties, creep properties and determined structural layer equivalencies for these mixtures based on laboratory results (86, 87, 88). This research was supplemented by research on the properties of foamed asphalt sand mixtures in South Africa (3, 4). Research in the United States on the properties of foamed asphalt and foamed asphalt mixtures were done mainly at Purdue (8, 12), Texas A & M (35), Iowa State University (32) and the Colorado Department of Highways (1, 2).

Researchers at Purdue examined the foaming characteristics of various asphalt cements at different temperatures with varying amounts of water. They also studied the properties and factors that affect mixtures of foamed asphalt and three aggregates in Indiana (12).

The Colorado Department of Highways also investigated the foaming properties of different asphalt cements at different temperatures. They also calculated some strength coefficients using the Chevron n-layer



stress-sensitive computer program to calculate tensile strains at the bottom of the asphalt layer for different thicknesses of a foamed asphalt stabilized layer. From these strains and general fatigue life relationships a thickness that would give the same fatigue life as a four inch (100 mm) hot asphalt mixture was determined. The equivalency of the hot mix was taken as 0.44 and the foamed asphalt mixture a fraction thereof depending on its comparative thickness.

Research at Iowa State University evaluated the factors that affect the strength of the mixtures based on Marshall stability or bearing capacity (32).

$$\text{Bearing Capacity} = \left( \frac{\text{Marshall Stability}}{\text{Marshall Flow}} \right) \times \left( \frac{120 - \text{Marshall Flow}}{100} \right) \quad (2.1)$$

Researchers at Texas A & M University examined the structural properties of laboratory foamed asphalt mixtures (35). One set of structural coefficients based on comparisons with AASHTO Road Test materials and another set based on the vertical compressive subgrade strain were determined. The Chevron program was used to calculate the strains. Hveem R-values as a criteria for satisfactory shear resistance were used. Fatigue life characteristics of foamed asphalt mixtures based on maximum tensile strain were developed and compared with those of hot asphalt mixtures to calculate equivalency factors at 68°F (20°C) and 80°F (30°C) for subgrade strengths of 3,000 psi (435 MPa) and 30,000 (4350 MPa). The BISAR computer program was used.

Research performed at Ohio State University for Mobil Oil compared the structural equivalencies of three foamed asphalt mixtures with an





emulsified asphalt mixture as surface and as base course (38). In the analysis the tensile strains at the bottom of the layers were compared for different thicknesses. An elastic layer computer program was again used to determine these strains.

The following is a summary of the major conclusions of the studies mentioned above:

1. The strength of the foamed asphalt increases with curing time (especially the first three days) but the strength after the first day is high enough for the pavement layer to be opened to traffic (12, 32).
2. The mixture stiffens significantly at constant moisture and temperature over time and the stiffness is permanent (88).
3. The mixing water content has a big influence on the strength. It varies for different materials, but is between 65 and 80% of the optimum moisture content for maximum density (32).
4. The percentage of fines in the mixture is very important.
5. The strength of the mixture depends on the asphalt content (32, 12).
6. The mixture is temperature susceptible (12, 86).
7. The mixture is susceptible to water. The strength is reduced substantially when saturated. The rate of water absorption is decreased as curing time is increased. The strength will be restored after drying, but it takes up to 30 days to reach equilibrium (12, 32).
8. The strength of the mixture is still acceptable when mixed at temperatures of 50°F (10°C) (12).



9. Foam half lifes of between 10 and 140 sec. and foam ratios of between 5 and 20 have no significant influence on the properties of the foamed asphalt mixtures (32).
10. There is no apparent difference between the steam and cold water method (32).

Since the properties of foamed asphalt mixtures are influenced by various factors e.g., material, mixing method, environmental conditions, etc., care must be taken in the interpretation of the conclusions given above. The conclusions were made from specific studies and should be verified for specific conditions and materials by tests, but should be true in general. Table 2.1 summarizes some of the properties of the foamed asphalt mixtures obtained in the cited research. Only those properties of importance in this study are given.

The values in Table 2.1 are general and depend on factors such as temperature, asphalt and moisture content, mixing and compaction methods, testing methods and curing times.

#### 2.2.2. Application

In 1956 Csanyi (15) described the in-place bituminous soil stabilization using foamed asphalt in Iowa. This was probably the first field application in the United States. This method, using a steam generator to produce the foam was also used in Maricopa County, Arizona in 1960 (45) and at Nipawin in Canada in 1964 (93). Due to the inconvenience of the steam generator in construction this method was not widely used.



Table 2.1. Properties of Foamed Asphalt Mixtures from the Literature

Reference	Marshall Stability (lb)	Hveem R	E (psi)	Remarks
1,2	--	--	314,000-1,060,000	at 72°F
35	--	86-94	120,000- 300,000	at 72°F
86	--	93-98	350,000-1,050,000	at 72°F
12	2,100-6,000	86-94	95,000- 115,000	at 72°F
8	1,070-1,950	--	--	at 72°F
32	3,000-8,000	--	--	at 77°F

E = elastic modulus

1 psi = 6.9 kPa

1 lb = 4.45N

°C = 5/9 (°F-32)



The modification of this method by Mobil Oil in Australia made the procedure easier and more economical to use in construction. Conventional equipment could be used with only minor modifications. Since 1970 the use of foamed asphalt in construction increased. Foamed asphalt has been used as a binder in bituminous stabilization projects in Australia (7) and in South Africa (4).

Conoco Oil obtained the patent rights for foamed asphalt in the United States after 1970. Foamed asphalt has since been used in various states among others Colorado (1, 2, 44), Michigan (52) and Oklahoma (25). The foamed asphalt base courses have been overlaid by fog sealing, slurry seals (44) and more widely a thin asphalt concrete layer. The base course material has also been mixed in-place (52) and at a central plant (1).

The construction procedure did not cause any serious problems or major equipment changes although some problems occurred in some cases initially (2, 44). The foamed asphalt stabilized layers have performed well this far.

### 2.3. Recycling

#### 2.3.1. Research

After the recycling of asphalt pavements gained prominence various studies were conducted to evaluate the characteristics and performance of recycled materials. The studies examined various types of recycling methods viz. cold, hot, in-place or batch plant mixing and various types of asphalt binders. Most of these research efforts and results were reported and published in proceedings of the Association of





Asphalt Paving Technologists (AAPT) since 1974, and the Transportation Research Record Number 780, which contains the proceedings of the National Seminar on Asphalt Pavement Recycling. None of these studies dealt explicitly with the determination of the structural layer equivalencies of recycled layers.

A study conducted by researchers at Texas A & M University and reported in the National Cooperative Highway Research Program Report (NCHRP) Number 224 (18) and NCHRP Synthesis of Highway Practice Number 54 (17) developed some structural layer equivalencies for various types of recycled mixtures. The structural equivalencies were determined from the maximum vertical (compressive) strain on the subgrade and used to compare the recycled layer with a layer in a certain section of the AASHTO Road Test. The vertical strain on the subgrade has been correlated to the number of repetitions to failure. The thickness of the recycled layer to give the same number of repetitions to failure was compared to the thickness and structural layer coefficient of the Road Test layer. The Texas A & M study also used the maximum tensile strain at the bottom of the asphalt layer and some fatigue characteristics to determine structural layer equivalencies (33). The developed structural equivalencies were very general and not for a specific binder.

Iida, in one of the first studies at Purdue University on cold recycling, investigated the long term behavior based on the creep test. Liquid asphalt, emulsified asphalt and other softening agents as binders were studied (28).



The Iida study was followed by studies to determine the foaming characteristics of asphalts used in Indiana, the performance of Gyratory and Marshall compacted specimens, as well as the effect of curing time and water on the stability of foamed asphalt recycled mixtures (8).

The most recent research is an in-depth study on the characteristics of cold recycled mixtures (66). This study included foamed asphalt as a binder. An AC-2.5 asphalt cement (at 330°F) was mixed with 2% cold water (by weight of asphalt) to produce the foam. The recovered materials were obtained from two sources viz. artificially aged asphalt concrete and asphalt concrete from an in-use pavement. The recovered material had an asphalt content of about 5% by weight of aggregate. The effects of curing time, compactive effort, percent asphalt added, testing temperature and effect of water, were tested. No virgin aggregate was added. The researcher also developed structural layer equivalencies based on the vertical strain on the subgrade, which is directly correlated to the stiffness of the overlaying recycled layer.

The following is a summary of the studies mentioned above on recycling:

1. The binder has a softening effect on the recycled mixture in the first few days after mixing. This is followed by a hardening. This is caused by the diffusion of the virgin binder into the old binder. This diffusion is a function of time, temperature and additional traffic compaction (66). The softening effect is large when the difference between the



viscosities of the old and new binder is large and the dispersing power of the agent is small (28). The resilient modulus and permanent deformation depict this softening for hot recycling. The Marshall stability test is not sensitive enough to show a difference (66). It is unclear whether the creep compliance test shows the effect (28) or is too insensitive to show the effect (66). The effect on creep compliance will depend on the test method, the recycled material and test used.

2. The level of asphalt added has a significant effect on the resilient modulus. The optimum for the study at Purdue was approximately 1% by weight of aggregate (66). It is also a function of the asphalt content of the recycled material.
3. The resilient modulus, Marshall stability and index usually increase with an increase in compaction effort. The Hveem-R-value decreases with the increase in compaction effort with high percentages of asphalt added (66).
4. The stiffness ( $M_R$ ) increases rapidly with curing time in the first 14 days and levels off after 14 days (66).
5. There is a significant difference between the strength after ultimate curing (curing in oven) and after only 28 days curing in air (66). The first is much higher than the latter.
6. All the strength parameters, ( $M_R$ , Hveem-R-value, Marshall stability, and index) are significantly reduced by the exposure to water (66).



7. The stiffness of the recycled layer increases with time after construction due to the densification under wheel loads and the gradual development of creep-actuated stiffening (5).
8. Different added virgin binders have different effects on the old binders and on the mixture properties (65).

Table 2.2 summarizes some of the important material property-values that were obtained in the discussed studies. It is clear that properties of the recycled mixtures vary considerably.

#### 2.3.2. Application

Cold recycling has been used extensively in the United States. States like Arkansas, California, Florida, Illinois, Indiana, Kansas, Kentucky, Louisiana, Maine, Michigan, Nebraska, Nevada, New Jersey, New York, Pennsylvania, Tennessee, Texas, and Washington have used cold recycling to reconstruct pavements. It has also been used in various other places in the world (90). Emulsified asphalt has been used in most cases, with liquid asphalt in some. To date there has not been a reported full scale field application of foamed asphalt as a binder in the recycling of asphalt pavements.

#### 2.4. Flexible Pavement Design Methods

The most widely used flexible pavement design methods are summarized here with special emphasis on the use of the structural equivalency concept.





Table 2.2. Properties of Cold Recycled Mixtures from the Literature

Reference	Stability (lb)	Hveem R	E (psi)	Remarks
66	4,200-9,000	85-95	60,000-200,000	28 day cure Emulsion added at 77°F
66	5,900-8,400	91-95	100,000-200,000	28 day cure Foamed asphalt added at 77°F
32	85-1,394	--	--	at 140°F

E = elastic modulus

1 psi = 6.9 kPa

°C = 5/9 (°F-32)

1 lb. = 4.45N



### 2.4.1. AASHTO Design Procedure

Tests conducted by the American Association of State Highway Officials (AASHO) on a specially constructed loop system near Ottawa, Illinois between October 1958 and late 1960 led to a design procedure that was developed based on the performance of different pavement systems. The serviceability was evaluated by a selected panel of people on an arbitrary scale of 0 to 5 with 5 an excellent pavement. This measure of serviceability was defined as the Present Serviceability Ratio (PSR). The PSR was statistically correlated with different physical measurements to give the following equation:

$$\text{PSI} = 5.03 - 1.91 \log (1 + \overline{\text{SV}}) - 1.38 \overline{\text{RD}}^2 - 0.01 (\text{C} + \text{P})^{1/2} \quad (2.2)$$

where

PSI = p = present serviceability index

SV = slope variance along the wheelpath (a measure of longitudinal roughness)

RD = depth of wheelpath rut (inches)

C = cracked area (ft/1000 ft)

P = pathed area (ft/1000 ft)

An empirical equation was also developed that correlated the axle load applications with the strength of the pavement.

$$\log W_{t18} = 9.36 \log (\text{SN} + 1) - 0.20 + G/\beta + \log \frac{1}{R} + 0.372 (S_i - 0.30) \quad (2.3)$$

$$\text{where } G = \log \frac{4.2 - pt}{4.2 - 1.5} \quad (2.4)$$



$$\beta = 0.40 + \frac{1094}{(SN + 1)^{5.19}} \quad (2.5)$$

where

$W_{t18}$  = total number of equivalent 18 kip (80 kN) load applications after time t.

SN = structural number (measure of strength based on performance)

$P_t$  = serviceability after time t

R = regional factor

$S_i$  = soil support value (measure of subgrade soil strength).

The structural number (SN) is defined as an index number derived from an analysis of traffic, roadbed soil conditions, and regional factors that may be converted to thickness of various flexible pavement layers through the use of suitable layer coefficients related to the type of material being used in each layer of the pavement structure. The layer coefficient (designated by  $a_1$ ,  $a_2$  and  $a_3$  for the surface, base and subbase respectively) is the empirical relationship between the structural number of a pavement structure and layer thickness, which expresses the relative ability of a material to function as a structural component of a pavement (69, 76). The relationship is:

$$SN = a_1 h_1 + a_2 h_2 + a_3 h_3 \quad (2.6)$$

where  $h_1$ ,  $h_2$  and  $h_3$  are the thicknesses corresponding to the three layers (surface, base and subbase) and  $a_1$ ,  $a_2$  and  $a_3$  are corresponding layer coefficients.



The layer coefficients were empirically developed during the AASHTO Road Test. These coefficients (given in Table 2.3) are reliable, but only directly applicable to the types of materials and environmental conditions represented in the Road Test. Procedures similar to those used at the original Road Test have since been used at satellite projects to determine structural coefficients for a specific area and local materials (73, 74). Reliable coefficients are important since they can have a big influence on the design thickness. High stability plant mixed asphalt concrete has the highest coefficient (0.44) and strengths of the other materials (or their influence on performance) are expressed as a fraction of 0.44 to give the structural coefficients.

#### 2.4.2. California Bearing Ratio (CBR) Method

The California Bearing Ratio is a measure of load-carrying capacity. The load-carrying capacity of subgrade and base-type materials are compared with that of a high-quality crushed stone base material (61). The CBR is expressed as a percentage of the penetration resistance to that of a standard value of crushed stone.

This method is used in the US Corps of Engineers and National Crushed Stone Association design procedures. It is an empirical procedure based on the CBR-values of the different pavement components. The basis of this method is to provide adequate thickness and quality of material to prevent repetitive shear deformations within any layer (76).

The general equation is:

$$t = P \left[ \frac{1}{8.1 \text{ CBR}} - \frac{1}{p\pi} \right] \quad (2.7)$$





Table 2.3. Structural Coefficients from AASHTO Road Test  
(from Ref. 69)

Pavement Component	Coefficient		
	$a_1$	$a_2$	$a_3$
Surface course:			
Road mix (low stability)	0.20		
Plant mix (high stability)	0.44		
Sand asphalt	0.40		
Base course:			
Sandy gravel		0.07	
Crushed stone		0.14	
Cement treated		0.15-0.23	
Bituminous treated		0.30-0.34	
Lime treated		0.15-0.30	
Subbase:			
Sandy gravel			0.11
Sand or sandy clay			0.05-0.10



where

$t$  = thickness required above the subgrade

$P$  = wheel load

$p$  = tire pressure

The Federal Aviation Administration (FAA) has developed design curves for flexible airport pavements based on the CBR method of design (85).

Structural layer equivalencies are not explicitly used in the CBR design methods.

#### 2.4.3. California Method of Design (Hveem Stabilometer)

This method is based on the Hveem resistance value, equivalency factors and a measure of the traffic volume and loads (TI). The design was based on field performance. The equation used in the design is:

$$GE = 0.0032 (TI) (100 - R) \quad (2.8)$$

with  $GE$  = gravel equivalent

$TI$  = traffic index (a measure of the wheel loads and volume of traffic)

$R$  = Hveem resistance value

The equation can be used to determine a required gravel equivalent (GE) above each layer. The GE is then adjusted by the equivalency factor to give the final thickness.

The equivalency factors depend on the type of material, in which layer it is used and the Traffic Index (TI) for the asphalt concrete surface (Table 2.4). According to the table a bituminous treated base is approximately 0.60 times as strong as an asphalt concrete surface for a Traffic Index (TI) of 8.0.



Table 2.4. California Gravel Equivalent Factors (after Ref. 76)

Pavement Component	Gravel Equivalent Factor ( $G_f$ )
Asphalt Concrete	1.52-2.50*
Bituminous-Treated Base	1.2
Lime-Treated Base	1.2
Cement Treated Base	1.2 or 1.7
Aggregate Base	1.1
Aggregate Subbase	1.0

\*values depend on Traffic Index.



#### 2.4.4. Asphalt Institute Method

This design method is based on the stresses and strains induced by an axle load on a layered pavement system. The pavement is regarded as a multi-layered elastic system. The material in each layer is characterized by a modulus of elasticity and a Poisson's ratio. The traffic is expressed in terms of repetitions of an 18,000 lb (80 kN) single axle applied to the pavement on two sets of dual tires.

Two limiting strain criteria were used to develop design curves viz.

1. Horizontal tensile strain ( $\epsilon_t$ ) on the underside of the asphalt concrete or asphalt stabilized layer, whichever is closest to the subgrade. Excessive horizontal strains can cause fatigue cracking.
2. Vertical compressive strain ( $\epsilon_c$ ) at the surface of the subgrade. Excessive compressive strains can cause rutting.

The thickness required for a full depth asphalt pavement, emulsified asphalt base (three types) and/or granular base for a given subgrade and expected repetitions of 18,000 lb (80 kN) axle loads can be determined from these design curves (95).

Older design manuals used a substitution ratio ( $S_r$ ) to convert from a thickness of asphalt concrete to an equivalent thickness of some other material. The ratio,  $S_r$ , ranged from 2.0 to 2.7 for untreated base material depending on the quality of the material.





#### 2.4.5. Mechanistic Design Procedures

Pavements can also be designed using an existing computer program which would calculate stresses, strains and deformations in the pavement. The computer programs were developed from theories on the behavior of the pavement layers. The stresses or strains are usually correlated to load repetitions by laboratory tests (9, 10). Structural layer coefficients are not explicitly used in this design method, since the material is characterized by its elastic properties viz. elastic moduli and Poisson's ratio. Pavement response models are widely used in the determination of structural coefficients.

##### 2.4.5.1. Pavement Response Models

Flexible pavements can be represented by the following systems:

1. Multilayer elastic systems
2. Multilayer visco-elastic systems
3. Finite element configuration (both two and three dimensional) (51).

These systems with their appropriate theories have been incorporated in commercially available computer programs to simulate flexible pavement response. The most widely used programs are based on the elastic theory and for multilayered elastic systems are:

BISTRO/BISAR (Shell)

CHEV5L (Chevron Research Co.)

ELSYM5 (University of California, Berkeley)

CRANLAY (Australian Commonwealth Scientific and Industrial  
Research Organization)



PSAD2A (University of California, Berkeley)

PSAD (from NCHRP-1-108) (51, 67)

Programs that use the finite element theory are FEPAVEII and the ILLIPAVE (University of Illinois, Urbana).

The selection of the response model or computer program depends on its availability and the necessary sophistication. The finite element method is probably a more realistic method of simulating a flexible pavement, but it is very expensive. A two way finite element program can be two to five times more expensive than a multilayered elastic program (6). The elastic layered models give a reasonably good correlation with the actual strains in the bound layers (6) although some differ from those obtained by a finite-element model (26). The surface deflections are the same for the two models (BISAR vs. ILLI-PAVE) (26). One of the big limitations of the elastic layered programs are that they assume linear elastic moduli when the moduli are non-linear. Some of the programs e.g. PSAD2A and CHEV5L have included an iteration process to adjust the moduli of the stress-sensitive layers.

#### 2.4.5.2. Material Characterization

The pavement response models use the elastic properties (elastic modulus and Poisson's ratio) and the thickness of the layers as input. The elastic properties are usually obtained from laboratory testing. The elastic moduli of the asphalt mixtures are usually determined as a constant for a given temperature, while the resilient moduli of granular material and subgrade are a function of their stress state in the pavement. The relationships are:



$$M_R = k_1 \theta^{k_2} \quad \text{for granular material} \quad (2.9)$$

where

$M_R$  = resilient modulus

$\theta$  = bulk stress =  $\sigma_1 + \sigma_2 + \sigma_3$

$k_1$  and  $k_2$  are constants determined from laboratory tests.

and

$$M_R = k_1 \sigma_d^{k_2} \quad \text{for subgrade material} \quad (2.10)$$

where

$\sigma_d$  = deviator stress =  $\sigma_3 - \sigma_1$

$k_1$  and  $k_2$  are constants determined from laboratory tests.

The relationships considered for use in this study are given in Table 2.5 for the granular material and Table 2.6 for subgrade material.

#### 2.4.5.3. Distress Modes

The layers in the pavement must either be stiff enough, thick enough or both to withstand the effects of the repeated loads on the pavements without failure. The failure can be structural or functional. Functional failure or failure of the pavement to carry out its intended function without discomfort to the passengers or excessive strains on the vehicles (76) is usually measured by rutting. Other factors like the loss in skid resistance or ravelling can also cause functional failure. Rutting is caused mainly by the vertical strains on the subgrade. The allowable number of load repetitions or equivalent axle loads ( $N_f$ ) to give a certain maximum rut depth have been correlated with the maximum vertical subgrade strain ( $\epsilon_v$ ) in

$$N_f = k_1 (1/\epsilon_v)^{k_2} \quad (2.11)$$



Table 2.5. Resilient Modulus - Bulk Stress Relationships for Granular Materials

$$M_R = k_1 \theta^{k_2}$$

Reference	Material	$k_1$	$k_2$
76	sand	6700	.36
	gravel (clay)	1900	.61
	granular	9600	.55
55	limestone	10000	.4
	bank run gravel	5000	.4
	sand aggregate	3800	.5
	crushed stone	6000	.5
	slag	12500	.35
26	crushed stone	9000	.33
	gravel	6500	.30
33	base	4000	.6
	subbase } fall	5400	.6
	base	3200	.6
	subbase } spring	4600	.6

$\theta$  = bulk stress

$M_R$  = resilient modulus (in psi)

$k_1$  and  $k_2$  = coefficients (constants)

1 psi = 6.9 kPa





Table 2.6. Resilient Modulus - Deviator Stress Relationships for Subgrade Materials

$$M_R = k_1 \sigma_d^{k_2}$$

Reference	Material	$k_1$	$k_2$
33	AASHTO Road Test (fall)	27000	-1.06
	AASHTO Road Test (spring)	8000	-1.06
67	$\sigma_3 = 5$ psi	36300	-1.1
	$\sigma_3 = 2.5$ psi	20900	-1.1

$\sigma_d$  = deviator stress (psi)

$M_R$  = resilient modulus (psi)

$k_1$  and  $k_2$  = coefficients (constants)



where

$N_f$  = number of allowable load repetitions

$\epsilon_v$  = maximum vertical subgrade strain

$k_1$  and  $k_2$  are constants for a specific material.

The relationships considered in this study are summarized in Table 2.7.

Structural failure or the collapse of one or more of the pavement layers is usually caused by fatigue cracking in the asphalt layers, although it can also only be a functional failure (76). The maximum tensile strain or stress at the bottom of the asphalt layers are usually used as a criterion for fatigue cracking. Relationships correlating the number of load repetitions to failure ( $N_f$ ) with either the tensile stress ( $\sigma_t$ ) or strain ( $\epsilon_t$ ) at the bottom of the asphalt layers have been developed. These relationships have mostly been developed through laboratory fatigue testing of asphalt mixtures usually in the form of beam specimens. The loads were usually applied through either a controlled stress or controlled strain conditions. In the controlled stress condition a constant cyclic load is applied throughout the testing process. The deflection is measured to determine the strain. Failure is defined as the point at which the specimen can no longer withstand a desired load. In the case of the controlled stress testing failure occurs at complete fracture of the specimen. In the controlled strain testing procedure the strain is maintained at a constant level in the form of a predetermined value of deflection or strain. The load required to produce this deflection is measured. Failure or the fatigue life is reached when the dynamic load is at a predetermined level of the initial load, usually 50 to 75 percent. The



Table 2.7. Subgrade Compression Strain-Fatigue Life Relationships Considered

Ref.	$N_f$	$(\epsilon_v \cdot 10^{-3})$	Relationship	Comments
18, 76	$10^4$	2.70	$\epsilon_v = 2.8 \cdot 10^{-2} (N_f)^{-0.25}$	Used in the shell design
	$10^6$	1.03		
	$10^8$	0.40		
18, 76	$10^4$	0.64		Used in Kentucky
	$10^6$	0.36		
	$10^8$	0.89		
27	$10^4$	1.66	$\log_{10} \epsilon_v = -1.9765$ $-0.2008 \log_{10} N_f$	Based on AASHTO Road Test
	$10^6$	0.65		
	$10^8$	0.26		
74	$10^4$	--		Prevent rutting of 0.25 inches
	$10^6$	0.450		
	$10^8$	--		
35	$10^4$	--	$\log N_f = 2.05076$ $-597.662(\epsilon_v)$ $-1.32967(\log \epsilon_v)$	
	$10^6$	--		
	$10^8$	--		

$\epsilon_v$  = maximum subgrade compressive strain

$N_f$  = number of load applications to failure

1 inch = 25.4 mm



controlled stress test is used for asphalt layers that give structural support to the pavement (more than three to four inches). The controlled strain test is used for layers less than three to four inches which give no structural support (42). The relationships are in the form:

$$N_f = k_1 (1/\epsilon_r)^{k_2} \quad (2.12)$$

where

$N_f$  = number of load repetitions to failure

$\epsilon_r$  = tensile strain repeatedly applied

$k_1$  and  $k_2$  are constants for a specific material determined from strain controlled tests.

$$\text{or } N_f = k_1 (1/\sigma_r)^k \quad (2.13)$$

where

$N_f$  = as defined before

$\sigma_r$  = tensile stress repeatedly applied

$k_1$  and  $k_2$  are coefficients determined from stress controlled tests.

Laboratory curves can and usually are shifted to recognize crack propagation effects, the possibility of healing between loads, etc. (51). Strains can also have different magnitudes, due to temperature changes over the life of the pavement. If this is considered:

$$\frac{\sum n_i}{N_i} \leq 1 \quad (2.14)$$





where

$n_i$  = number of applications of strain  $\epsilon_i$

$N_i$  = number of applications to failure at strain  $\epsilon_i$  (or stress  $\sigma_i$ ) (16).

The relationships considered for use in the study are summarized in Table 2.8.

#### 2.4.6. Summary

The two currently used design methods in which the structural layer equivalencies or coefficients are used directly, are the AASHTO and California method of design. The AASHTO design method as described in the Interim Guides is used in 33 states in the United States, including Indiana. The Hveem stabilometer method is used by six and the CBR-method by one of the other states (62).

#### 2.5. Determination of Structural Layer Coefficients

Structural layer coefficients and structural layer equivalencies are essentially the same. Both relate the strength or performance capability of the pavement material (according to a specific criteria e.g. cracking) with that of a material with known performance characteristics usually the hot asphalt surface mixture used in the AASHTO Road Test. The coefficient is given as a proportion of the coefficient determined during the AASHTO Road Test. To give the same structural number (SN) the thickness of the layer has to be increased in the same ratio as the coefficients of the layer and the AASHTO hot mix. The structural layer equivalency is given as the thickness of the layer to give the same performance as another layer, usually the AASHTO hot mix surface layer.



Table 2.8. Asphalt Fatigue-Life Relationships Considered

$$N_f = k_1 (1/\epsilon_r)^{k_2}$$

Reference	$k_1$	$k_2$	Comments
35	$9.02 * 10^{-6}$	2.29	Foamed asphalt $M_R=160,000$ psi. Cured for 60 days.
	$8.19 * 10^{-7}$	3.15	ATB emulsion
	$2.01 * 10^{-5}$	2.69	AC Base (Colorado)
56	$4.36 * 10^{-8}$	3.47	Asphalt treated base courses
	$4.78 * 10^{-9}$	3.89	Emulsified mixtures. $E^* = 600,000$ psi (Chevron)
	$7.87 * 10^{-7}$	3.29	Laboratory beam tests on AASHTO Road Test material. For 10% measured cracking (Finn, et.al.)
	$1.084 * 10^{-6}$	3.29	On AASHTO Road Test material. For 45% measured cracking
	$5.33 * 10^{-8}$	3.291	Laboratory beam tests on AASHTO Road Test materials (Monismith)
	$2.16 * 10^{-13}$	4.995	Based on strain at bottom of AASHTO Road Test pavements.
98	Relationship		
	$\log N_f = -17.2278 + 5.57686$		Asphalt concrete base
	$\log(1/\epsilon_r)$ $+ 0.033594(T)$		Controlled stress
	$\log N_f = 06.70799 + 4.19585$		Asphalt concrete surface
	$\log(1/\epsilon_r)$ $- 0.13385(T) + 0.001362(T)^2$		Controlled stress

$N_f$  = number of load applications to failure

$\epsilon_r$  = tensile strain at the bottom of the asphalt layer.

$k_1$  and  $k_2$  = coefficients

T = temperature in °F.



The coefficient can be defined as:

$$a_i = \text{coefficient} = (h_s/h_i) a_s \quad (2.15)$$

$$\text{and the equivalency factor} = (h_i/h_s) \quad (2.16)$$

where

$h_s$  = thickness of a standard material (usually a hot asphalt concrete mixture)

$h_i$  = thickness of the material  $i$

$a_s$  = structural coefficient of the standard material.

Structural coefficients or equivalencies are a function of various factors viz. pavement temperature, surrounding layer thicknesses, loading intensities, moisture changes in the subgrade, material stiffnesses and strengths.

#### 2.5.1. Development of the Structural Layer Coefficients

Coefficients were first developed after the AASHTO Road Test. The structural number (SN) was determined from the AASHTO equation, which was developed based on performance. The layer thicknesses were then used as independent variables to predict SN. The regression coefficients were used as the structural coefficients (69).

The coefficients developed at the Road Test were for the types of material used in the Road Test. Coefficients used for other materials were established by rationalization and a study of comparative cohesion, stability and bearing values obtained in the laboratory. It was emphasized that further experience and research would be necessary to establish valid coefficients for all materials (69). This led to further research by various agencies to modify old or develop new



structural equivalencies. The following is a summary of some of the coefficients currently used for bituminous mixes and methods used to develop them.

#### 2.5.2. The Asphalt Institute

Based on an extensive survey of prior performance of asphalt pavements and theoretical considerations the structural equivalencies or substitution ratios discussed in section 2.4.4 were determined.

#### 2.5.3. National Crushed Stone Association

Layer equivalencies, using normal gravel as a standard, were developed by dividing the vertical pressure at failure for each material by that for the standard gravel at given lateral pressures. The researcher (Nichols) concluded that a constant value cannot be assigned to a specific material. It varies with wheel loads (69).

#### 2.5.4. Arizona

The original coefficients were modified by including the effects of grading, stability, thickness, abrasion and type of asphalt for bituminous surfaces and bases. Similar modifications were made for other types of materials (69).

#### 2.5.5. California

Research showed that the magnitude of the load has a marked influence on the equivalency of a bituminous base. The property of cohesion was used to develop an empirical relationship to adjust mixes which did not have tensile strength characteristics similar to that of the asphaltic concrete at the AASHTO Road Test (69).





#### 2.5.6. Illinois

Studies showed that the coefficients vary with the strength of material used in the pavement. The coefficients of the surface ( $a_1$ ) and the base course ( $a_2$ ) were correlated with the Marshall stability for bituminous mixes. The upper value of 0.44 represents the asphalt concrete used in the Road Test. The modification of the coefficients was based on tests conducted by the state and experience with coefficients developed during the Road Test (69).

#### 2.5.7. Louisiana

The coefficients were modified based on the strength of the material. The coefficients of the bituminous mixes vary as a function of the Marshall stability (69).

#### 2.5.8. New Mexico and Wyoming

The structural coefficients were also varied as a function of the Marshall stability for asphalt concrete surface layers (69).

#### 2.5.9 Ohio

Theoretical asphalt concrete equivalencies were calculated on a continuous hourly or fourth-hourly basis for a 245-day period. Equivalence was defined as that thickness of base necessary to replace one inch of surfacing for equal deflection. Deflections were calculated using the layer elastic theory and the results of static and dynamic laboratory tests of the pavement materials in the frequency domain. 19 kip (84 kN) single axle loadings moving at 50 mph (80 kmh) were assumed (13).



### 2.5.10. Texas

The coefficients of asphalt-treated bases were determined from the Texas triaxial class at 140°F (60°C) and the asphalt concrete on cohesiometer values (69).

### 2.5.11. Pennsylvania

Research was conducted at the Pennsylvania Transportation Research Facility which is a one-mile, one-lane test road composed originally of 17 test pavements. It was constructed in 1972. Four of the sections were replaced by eight shorter segments in 1974. The structural coefficients of the base course materials were determined by using two different methods of analysis viz:

1. AASHTO performance analysis: serviceability indicators (e.g., rut depth, cracks, patching etc.) were monitored bi-weekly to calculate PSI. The pavement life expressed in terms of 18 kip (80 kN) equivalent axle loads (EAL) ( $N_f$ ) and the rate of change of serviceability loss ( $\beta$ ) could also be determined throughout the experiment. Regression analysis of  $\beta$  or  $\log \rho$  with thicknesses of surface course and base course was used to determine the coefficients  $a_1$  and  $a_2$  in the equation:

$$SN = a_1 h_1 + a_2 h_2 + a_3 h_3 \quad (2.6)$$

2. Limiting criteria concept. The tensile strain at the bottom of the asphalt layer and the maximum surface deflection were used to predict fatigue cracking. Maximum compressive strain on top of the subgrade was used to predict rutting. All three



strain criteria were related to the number of EAL to cause the appropriate type of failure (fatigue cracking or rutting). The BISAR elastic layer program was used to determine the coefficients for the most critical of the three cases:

$$\rho = 0.64 (SN + 1)^{9.36} \quad (72, 73, 74) \quad (2.17)$$

#### 2.5.12. US Forest Service (24)

Researchers used two methods to determine structural coefficients viz.

1. The AASHTO method: The actual number of EAL and PSI were used to back-calculate  $a_i$ -values for open graded asphalt emulsion mixes (OGAEM).
2. The limiting strain criteria: The maximum tensile strain under the OGAEM layer and the maximum compressive strain on top of the subgrade were used to determine the number of load repetitions to failure ( $N_f$ ) for the critical case. Strain to failure and  $N_f$  relationships developed by Chevron were used. The strains were calculated by a computer program. The coefficients were determined by the following equation:

$$a_{\text{OGAEM}} = \frac{d_{\text{hot}}}{d_{\text{OGAEM}}} (a_{\text{hot}}) \quad (2.18)$$

where

$a_{\text{OGAEM}}$  = structural coefficient of OGAEM

$a_{\text{hot}}$  = 0.44

$d_{\text{hot}}$  = thickness of hot mix asphalt concrete

$d_{\text{OGAEM}}$  = thickness of the OGAEM to give the same  $N_f$ -value at failure as the hot mix asphalt concrete.



The structural coefficients are a function of EAL, the subgrade modulus and the modulus of the OGAEM layer.

### 2.5.13. Virginia

The following equation and regression analysis were used to determine equivalency factors for base course layers:

$$\log d = a_0 + a_1 \left( h_1 + \frac{a_2}{a_1} h_2 + \frac{a_3}{a_1} h_3 + \frac{a_s}{a_1} G_s \right) \quad (2.19)$$

where

$d$  = maximum deflection during the spring

$a_s/a_1$  = thickness equivalency factor of the subgrade

$G_s$  = equivalency grading of the subgrade soil

$h_1, h_2, h_3$  = thickness of the surface, base and subbase course respectively

$a_0, a_1, a_2, a_3$  = regression coefficients (70).

### 2.5.14. Recycled Materials

The following methods were used in a comprehensive study to determine structural equivalencies to evaluate the characteristics of recycled materials (34):

1. The subgrade deformation was used to determine structural coefficients for the recycled layers. The subgrade deformation correlates well with the performance loss, as measured by rut depth and riding quality, in the AASHTO Road Test. A typical AASHTO section (loop 4) was modeled by the stress-sensitive layered elastic Chevron computer program. A relationship between the number of 18,000 lb (80 kN) single axles





to produce a PSI of 2.5 and the vertical subgrade deformation (induced by the vertical compressive strain on top of the subgrade) was developed:

$$N_{18(2.5)} = 0.098e^{-3.39 \ln W_s} \quad (2.20)$$

with  $N_{18(2.5)}$  = the number of 18000 lb (80 kN) load repetitions to cause a reduction in the present service-ability to a value of 2.5.

$W_s$  = vertical subgrade deformation (inches).

The recycled material was characterized by its resilient modulus ( $M_R$ ) and Poisson's ratio and substituted in the AASHTO model. The thickness of the recycled layer to give the same subgrade deformation as in the original pavement system was compared with the thickness of the corresponding layer in the AASHTO modelled pavement.

2. The maximum tensile strain at the bottom of the surface layer was also used to determine the structural coefficients of recycled surface material (33). The model of the pavement in loop 4 of the AASHTO Road Test was again used. The thickness of the recycled layer to give the same number of load repetitions to failure as a standard quality hot asphalt mix (representing the AASHTO Road Test pavement surface) was used to determine the structural coefficients, since the structural numbers (SN) were the same:

$$a'_1 = \frac{a_i h_i}{h'_1} \quad (2.21)$$



with  $a'_1$  = structural coefficient of the recycled layer

$a_1$  = structural coefficient of the laboratory standard  
= 0.44

$h'_1$  = thickness of the recycled layer

$h_1$  = thickness of the asphalt concrete.

The materials were characterized at 68°F (20°C). Laboratory tensile strain versus fatigue life relationships were determined for the recycled materials and the laboratory standard hot asphalt mixture.

3. Based on the concept that if a uniform pavement of a given elastic modulus is increased in thickness above a semi-infinite subgrade the maximum deflection would decrease and the spreadability would increase, charts were plotted using layered elastic computer programs displaying spreadability against maximum surface deflection for different thicknesses and subgrade moduli. The Dynaflect maximum deflection was adjusted to correspond with the maximum deflection under a dual wheel load of 4500 lb (20 kN) per wheel. The spreadability of the Dynaflect deflection basin is approximately equal to that measured under the dual 4500 lb (20 kN) wheel load (32).

The in-situ structural response of a recycled layer was compared with that of a control section by obtaining the effective thicknesses from the chart. The effective thickness is basically:

$$h_e = \sum_{i=1}^N b_i t_i \quad (2.22)$$



where

$h_e$  = effective thickness

$b_i$  = effective thickness factor of layer  $i$

$t_i$  = actual thickness of layer  $i$

$N$  = number of pavement layers

The thickness equivalency ratio was defined as the ratio of the recycled  $b_i$  to the control  $b_i$ .

This method is generally the most reliable in the comparison of structural responses of pavements with comparable cross sections.

#### 2.5.15. Foamed Asphalt Stabilized Layers

1. The AASHTO structural layer coefficients of the foamed asphalt were calculated and compared with those established for bituminous stabilized bases at the Road Test (35). The procedure was exactly the same as the one described in section 2.2.14. It is based on the vertical deformation of the subgrade.
2. The maximum vertical strain on top of the subgrade was used to calculate structural coefficients. By using the Chevron layered elastic program the subgrade strains were calculated for a pavement system to get a thickness of the foamed asphalt layer that would give the same strain as a six inch hot asphalt mix. The thickness equivalency was taken as the ratio of the thickness of the foamed asphalt layer to that of the hot asphalt mix layer of six inches (150 mm). This was done for different subgrade moduli and different temperatures, which implies different resilient modulus values of the asphalt layers (35, 66).



3. The thickness of the foamed asphalt stabilized layers could be determined such as to give a specific fatigue life from laboratory developed tensile strain ( $\epsilon_r$ )-fatigue life ( $N_f$ ) relationships.

$$N_f = k_1 (1/\epsilon_r)^{k_2} \quad (2.11)$$

where  $k_1$  and  $k_2$  are coefficients (constants) to be determined for each material through testing.

This thickness was then compared with the thickness of the hot asphalt mix to give the same fatigue life (35). The tensile strains at the bottom of the asphalt layer were taken as the critical tensile strains and they were calculated with the Chevron computer program.

Another study used a similar method to determine the structural coefficients, but instead of developing strain-fatigue life relationships for foamed asphalt mixes relationships for asphalt and emulsified asphalt mixes were used (1).

4. An additional study used the maximum tensile strain at the bottom of the foamed asphalt layer to compare thicknesses of foamed asphalt layers with an emulsion layer. The structural equivalencies were given as the ratio between the foamed asphalt and emulsion mix thicknesses to give the same tensile strains when used as surface and similarly as base course (38).

There are therefore a variety of methods available to determine structural coefficients or equivalencies. The best method would be one that would include fatigue, stiffness and the permanent deformation characteristics.





Table 2.9 summarizes some of the structural coefficients or equivalency factors developed in the studies described in this chapter. The values vary considerably and are a function of the method used as well as the properties and thickness of the surrounding layers and the temperature.



Table 2.9. Structural Coefficients and Equivalency Factors from the Literature

Reference	Material	Coefficient	Equivalency Factor	Remarks
24	Open graded	--	1.21-1.25	1
	Emulsion Mix	--	1.23-1.29	2
70	Asphalt base	--	1.33	Based on regression
1,2	Foamed asphalt	0.23-0.44	--	2
35	Foamed asphalt	0.24-0.35	--	Based on AASHTO procedures
			1.18-2.00	1 ( $E_s = 3000$ )
			1.16-1.81	1 ( $E_s = 30000$ )
			2.93-3.91	2 ( $E_s = 3000$ )
			2.84-3.92	2 ( $E_s = 30000$ )
	Asphalt base		1.19	Based on AASHTO
38	Foamed asphalt base		0.46-0.75	Based on strength of emulsion
	Foamed asphalt surface		0.50-0.85	
5	Cold recycled material	.30-.38		
46	In-place recycled concrete base		1.13-2.00	
69	Bituminous-treated base	0.30 0.30-0.35 0.25 0.34 0.34		Illinois Arizona Wyoming Louisiana (hot mix) AASHTO Road Test

1. Based on subgrade deformation.

2. Based on the tensile strength in the asphalt layer.

$E_s$  = elastic modulus of the subgrade.



## CHAPTER 3: CONSTRUCTION OF THE TEST ROAD

### 3.1. Introduction

During 1980 the decision was made by the Indiana Department of Highways to construct an experimental section using foamed asphalt and asphalt emulsion as binders in cold recycling. The road selected for this purpose was a 8.8 mi. segment of SR 16 from the junction with SR 231 to the Jasper-White County line. It was a road which was to be resurfaced during the same year. Figure 3.1 shows the location of the road. This segment was divided into two approximately equal segments, one utilizing foamed asphalt as the binder and one using emulsion. The main objectives of this experimental section were (30):

1. To determine the feasibility and suitability of the use of cold recycling.
2. To monitor the performance of such a pavement under actual conditions of traffic and weather.
3. To determine the cost and time required for the project.
4. To determine the interest and ingenuity of the contractors in this project.
5. To gain experience in the use of foamed asphalt and emulsion in recycling.

This was especially true for the construction of the foamed asphalt section, since foamed asphalt has not been previously used in Indiana. Conventional construction equipment had to be modified to be able to



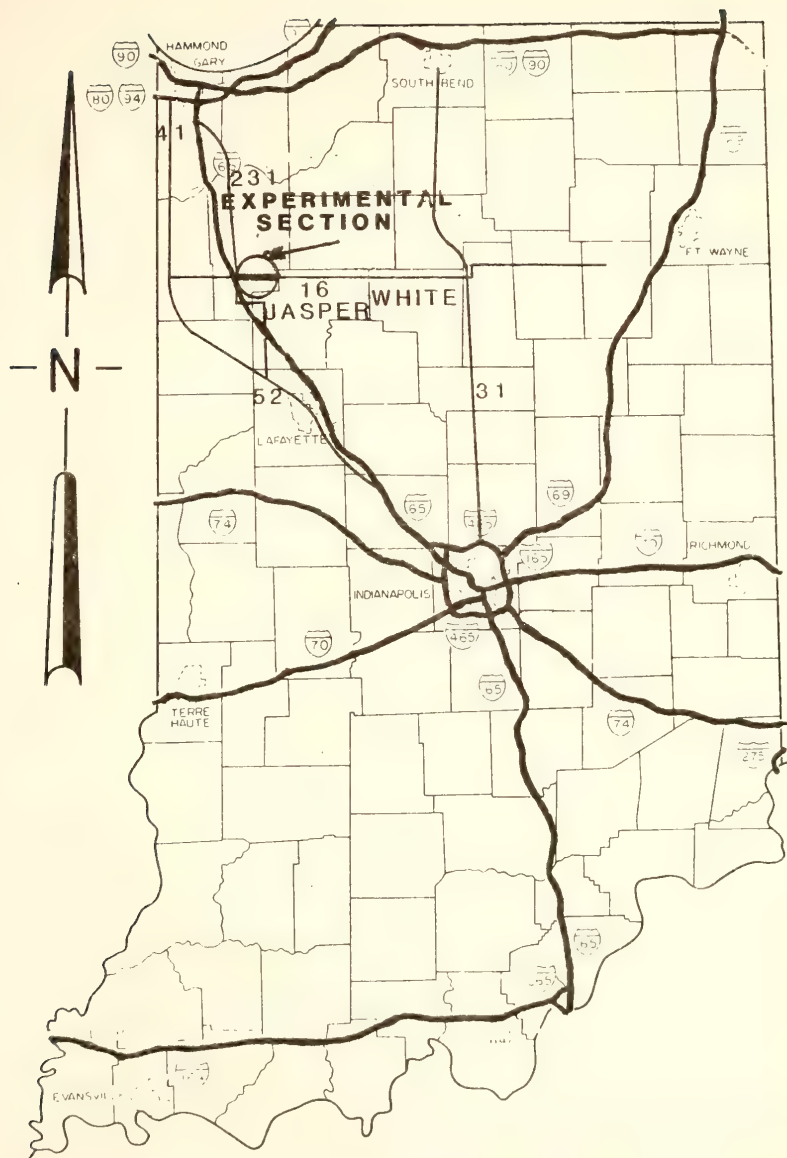


FIGURE 3.1 LOCATION OF THE TEST ROAD  
IN INDIANA





produce and mix foamed asphalt. The rest of the chapter will center around the construction of the foamed asphalt section.

### 3.2. Condition of the Initial Pavement

The initial pavement was 18 foot (5.5 meter) wide. It showed a few longitudinal cracks, some rutting, some consolidation and extensive flushing. The longitudinal cracks appeared mostly along the wheelpath closest to the centerline. These cracks could have been caused by the lack of internal friction in the sandy subgrade (17) and/or excessive bending stresses in the wheelpath (18). None of these pavement defects caused serious performance problems. The flushing created an unsafe roadway in wet weather and the road needed an improved cross section.

The traffic volume as determined in 1978 consisted of approximately 550 vpd in both directions with 18% trucks.

### 3.3. Original Construction Concept

The plan was to reconstruct the pavement using the pulverized in-place pavement material mixed with additional aggregate and foamed asphalt as a base course. It was felt that cold in-place recycling could provide a low cost simple construction procedure.

In order to design the recycled mixture and to determine the thickness, tests were conducted on cores obtained from the initial pavement. Approximately 100 four inch (100 mm.) cores were taken over the 8.8 mile (14 km.) section.



At first 24 core samples from six sites were analyzed to determine the grading and the asphalt content. The results are given in Table 3.1. In a second investigation eight cores from four different locations were analyzed to determine the penetration and the kinematic viscosity of the asphalt concrete in the initial pavement. The results are given in Table 3.2. The average asphalt penetration was 41 pens. and the average kinematic viscosity 460 cSt. Both the penetration and the viscosity values had large variances. The average asphalt content was 6.1 percent, with a small variance.

Ten extra four inch (100 mm) cores were analyzed to determine the resilient modulus ( $M_r$ ) at different temperatures and for the top and the bottom 2.5 inches (65 mm.) There is no significant difference (at  $\alpha = 0.05$ ) between the  $M_r$ -values obtained from the top and the bottom 2.5 inches (65 mm.). The average total thickness was 5.8 inches (170 mm.). Visual inspection seemed to indicate that the top half had more asphalt than the bottom half. This was not verified through testing. The in-situ CBR-values were also determined through Dynamic cone penetrometer (DCP) tests at 28 locations at the center of the lanes. The average CBR of the sandy silt subgrade was approximately 12, with a standard deviation of 4.3. The subgrade was overlaid by a, on the average, 4.8 inch (120 mm.) thick granular layer with a CBR of 30 (standard deviation of 11).

Information obtained from the above tests, results from research at Purdue and practical experience were used to establish the material and construction requirements. The requirements are summarized in Table 3.3.



Table 3.1. Results of Tests on 24 Core Samples

			Ave.	S.D.	Range
% Asphalt			6.10	0.40	5.06-6.79
% Passing Sieve	0.75 inches		0.83	1.21	0-4.18
	0.50 inches		8.56	2.89	4.19-14.72
	0.375 inches		16.90	2.75	11.46-21.50
	#4		34.50	2.74	27.39-39.14
	#6		9.12	0.89	7.67-11.14
	#200		25.11	4.09	18.93-37.10
<#200			4.39	0.81	2.39-5.76

S.D. = standard deviation

1 inch = 25.4 mm



Table 3.2. Results of Tests on 8 Core Samples

		Ave.	S.D.	Range
Penetration (in pens)		41	12.18	28-63
Kinematic viscosity (cSt)		459.9	155.5	195.2-651.4
% Passing Sieve	#8	28.3	2.43	25.8-33.3
	#30	15.1	1.41	13.4-17.9
	#40	13.4	1.09	11.9-15.0
	#50	11.9	1.07	10.1-12.5
	#100	8.6	0.79	7.3-9.5
	#200	5.5	0.41	4.6-5.9

S.D. = standard deviation

1 inch = 25.4 mm





Table 3.3. Construction and Material Requirements

---

1. Foamed Asphalt:

Asphalt concrete: AC-5

Mixing temperature:  $330 \pm 15^{\circ}\text{F}$  ( $165 \pm 5^{\circ}\text{C}$ )

Amount of water: 2% by weight of asphalt

Expansion ratio = (volume of foamed asphalt)/(volume of asphalt cement)

Half life = 20 seconds = time it takes the volume of foam to reduce from its maximum volume to one-half of the maximum volume

Temperature during processing  $> 50^{\circ}\text{F}$  ( $10^{\circ}\text{C}$ ) during non-work periods and it had to be graded and compacted.

---

2. Milled Material:

Maximum size: three inch (75 mm)

90 to 100 percent less than 1-1/2 inch (38 mm)

Free moisture during mixing = 2.5 - 3.5%

---

3. Additional Aggregate:

The construction section had to be open to two-way traffic.

Grading: meeting section 903 of IDOH standard specifications

Coarse aggregate: meet requirements of Class C aggregate

Free moisture during mixing = 2.5 - 3.5%

---

4. Geometry of the Pavement:

Minimum thickness of the recycled base: four inch (100 mm)

---

5. Construction:

The construction section had to be open to two-way traffic during non-work periods and it had to be graded and compacted.

---



The plan was to reconstruct the road to a width of 22 feet (6.7 meter) by increasing the width by two foot (600 mm.) on each side. Excavations had to be made to a depth of five inches (125 mm) to extend the five inch (125 mm.) base course. The excavated material was to be used on the shoulders. Some additional aggregate had to be added to maintain the four inch (100 mm.) thickness of the base course. Figure 3.2 shows a cross section of proposed final pavement.

A thickness of four inches (100 mm) of recycled base course and a 1-1/2 inch (38 mm.) hot mix asphalt concrete surface seemed to be sufficient to carry the traffic on this road. No structural coefficients were available to be used in the design. The selection of the thickness of the stabilized base was made strictly from a practical viewpoint.

Cold in-place recycling was specified in the construction proposal. The initial pavement had to be ripped, milled, scarified or pulverized to a depth of four inches (100 mm) to such an extent that 100% of the material passed the three inch (75 mm.) sieve and 90 to 100% the 1-1/2 inch (38 mm) sieve. After the excavations on the sides were made, the additional aggregate had to be placed on top of the reduced and shaped material at a rate of approximately 160 lbs. per square yard (87 kilograms per square meter). The additional aggregate could be crushed stone, crushed blast furnace slag, natural or blast furnace slag, sand or a combination of these materials meeting a standard specification. A material complying to the specifications of the Indiana Department of Highways for a #53 crushed stone would be acceptable, as shown in Figure 3.3.



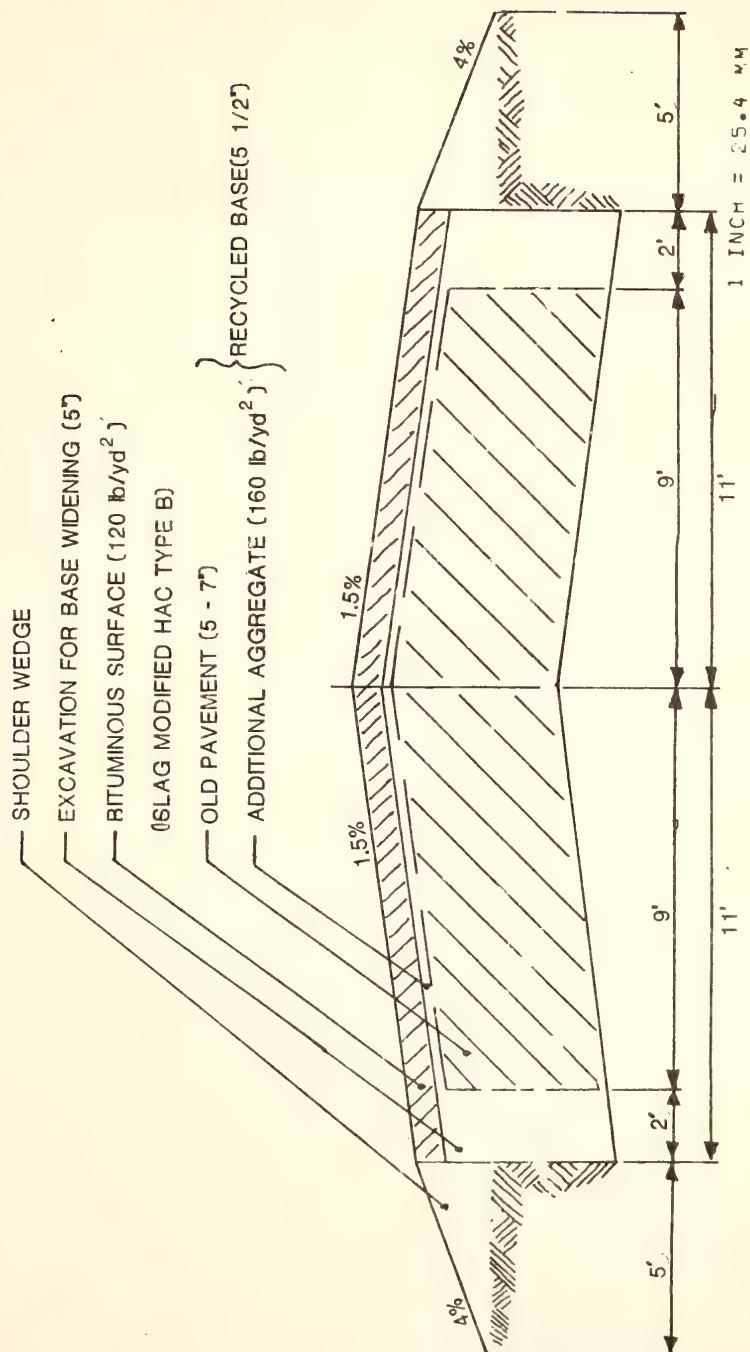


FIGURE 3.2 PROPOSED PAVEMENT CROSS SECTION



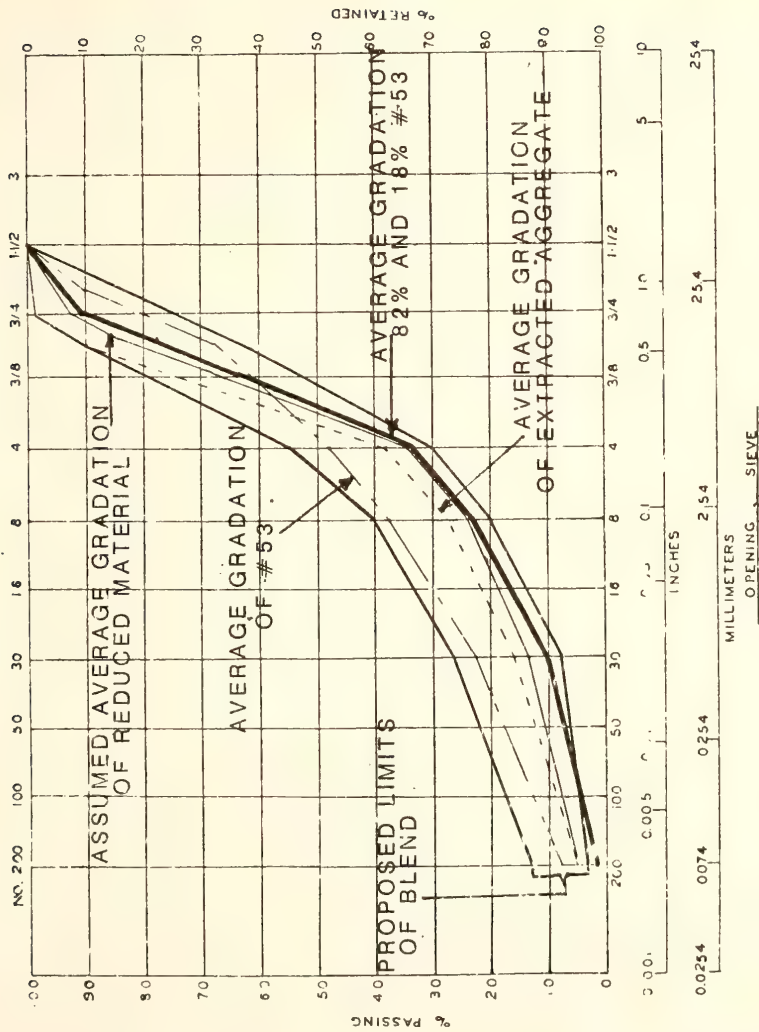


FIGURE 3.3 GRADATION ANALYSIS OF MATERIALS USED IN CONSTRUCTION





The first application of foamed asphalt had to be applied directly to the additional aggregate at a rate of approximately 0.75 gallons per square yard (3.5 liters per square meter) (4% by weight of aggregate) and simultaneously shallow mixed to a depth of not more than a 1/2 inch (13 mm) below the additional aggregate layer. A second application of foamed asphalt had then to be applied at 1.0 gallon per square yard (5 liters per square meter) (1.5% by weight of material) and mixed to full depth. The hot mix surface at a rate of 20 lbs. per square yard (11 kg per square meter) had to be placed on top of the recycled base (the specifications are summarized in Table 3.3).

The bid was made on the basis of in-place recycling (30). The unit prices were \$0.40 for the shallow mixing, \$1.00 for full depth mixing and \$0.25 for the spreading and compaction of the recycled base. The successful low bidder was A. Metz, Inc. The contractor was given 60 working days to finish the 8.8 mile (14 km) section. Adjustments to the proportions of the materials could be, and were, made if necessary.

#### 3.4. Actual Construction

The construction of the foamed asphalt section started in August 1981. It was the first experience the contractor had with foamed asphalt.

The contractor got permission to mix the milled material and the additional aggregate at a central plant instead of in-place. The main reasons for this were:

1. The contractor had a mixing plant available approximately 5 to 10 miles (8 to 16 km) from the construction site.



2. The milling machine had difficulty milling to a depth of four inches (100 mm) in one pass. The twin shafted pugmill the contractor originally intended to use was no longer available.
3. The mixing control would be better at a central plant.

During trial runs at the central plant the proportion of the additional aggregate to be added was changed from 29% to approximately 33% by weight of reduced material or 25% by total weight of material. This small change did not seem to influence the quality of the mixture. #53 crushed stone was to be used as additional aggregate. It was readily available to the contractor.

The centerline of the initial pavement was used as reference height. This meant that the transverse slope was measured from the centerline. The depth of the intended excavation of five inches (125 mm) on the sides of the pavement therefore varied since the initial pavement did not have a constant transverse slope.

The construction procedure was changed from cold in-place recycling to cold recycling at a central plant. Figure 3.4 displays a flow diagram of the actual construction procedure. The specifications given in Table 3.3 were still valid.

### 3.5. Description of the Actual Construction Procedure

In order to keep the road open to traffic during non-work periods the milling was done in two layers. A CMI rotomill was used. The milling was done by a subcontractor. The pavement also had to be safe for traffic during non-work periods and no dropoffs were allowed overnight. First a layer of 2.5 inches (65 mm) was removed. The remaining 2.5 inches (65 mm) of initial pavement was sufficient to sustain traffic



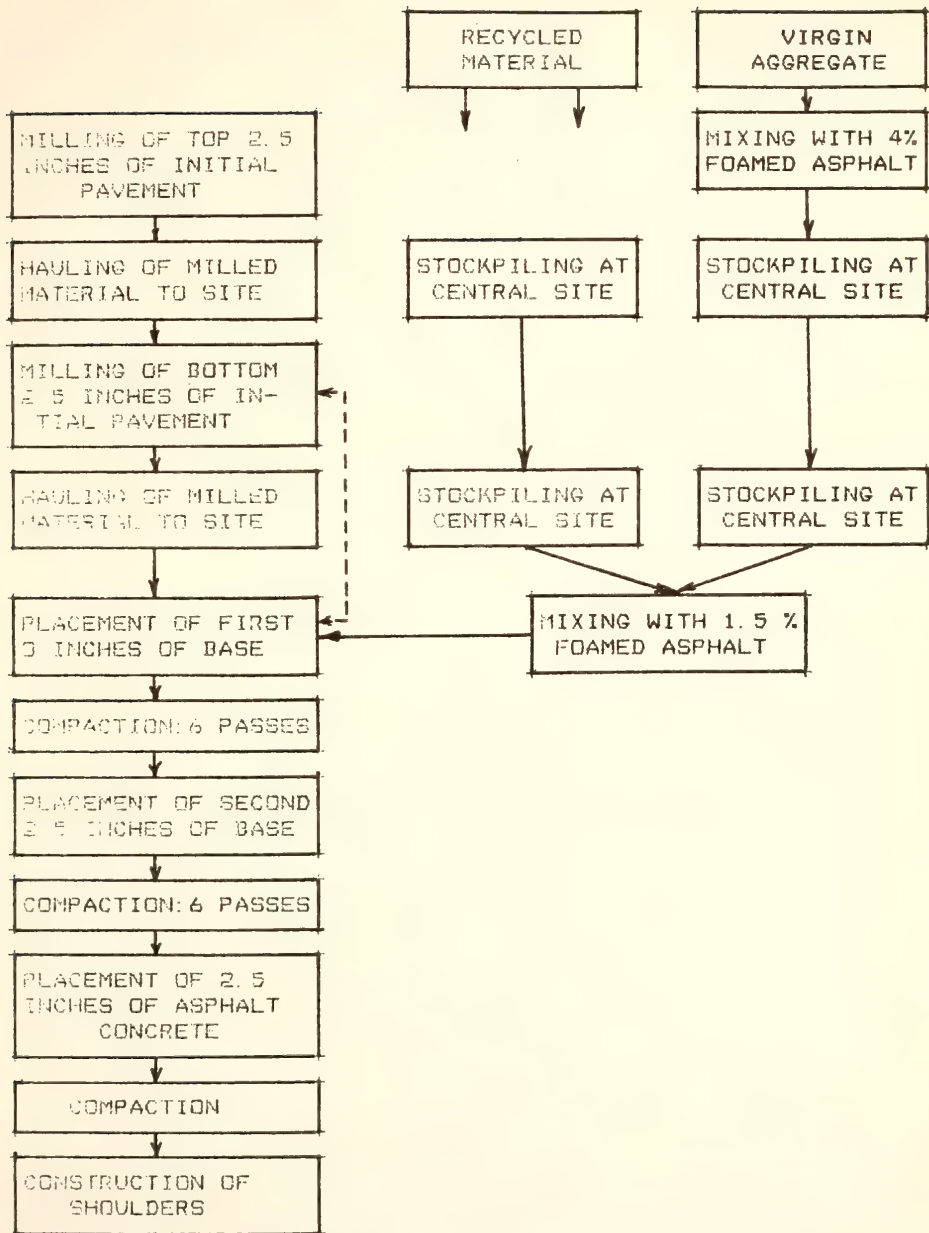


FIGURE 3.4 FLOW DIAGRAM OF ACTUAL CONSTRUCTION PROCEDURE

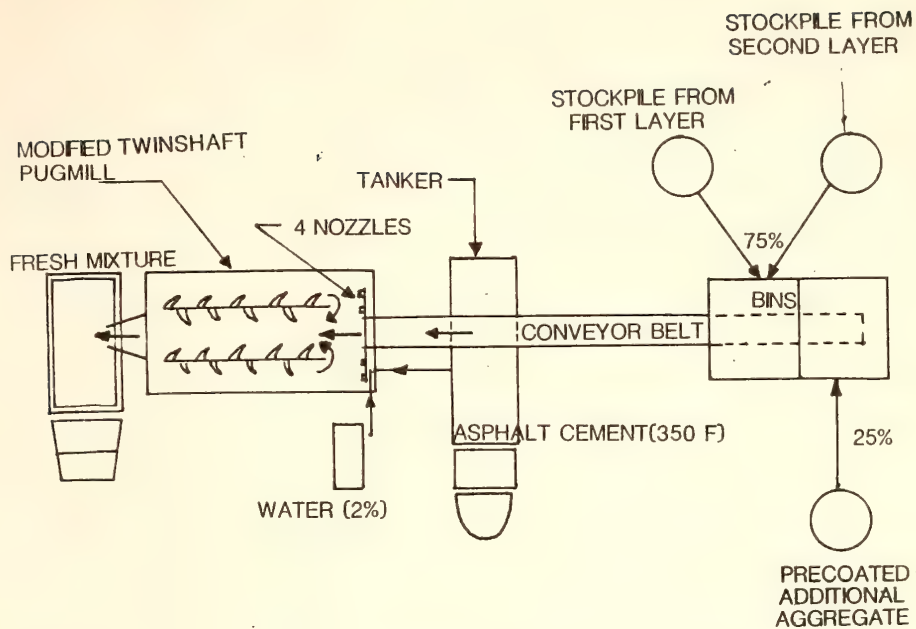


during construction. Approximately 8,000 to 10,000 linear feet (2400 to 3000 linear meter) of milling of this 9 feet (2.75 meter) wide and 2.5 inch (65 mm) thick pavement layer could be done in a day. The milling was done to the width of a lane (9 feet or 2.75 meter) at a time. It was found that the milling was faster and fewer pieces larger than three inch (75 mm) were created during colder weather. The milling was therefore done mainly from early morning (6:30 a.m.) to just after noon (2:30 p.m.). The milled material was hauled to the central plant and stockpiled.

During the first milling operation the additional aggregate (#53B) was mixed with 4 percent foamed asphalt (by weight of aggregate) and stockpiled. The mixing was done at the central plant with a modified twin-shaft pugmill. Figure 3.5 shows the process schematically. An old Barber-Greene twinshaft pugmill was modified to be able to mix the foamed asphalt. Four large nozzles were installed to spray the foamed asphalt into the mixing chamber. The water was stored in a tank on the ground and pumped under pressure to the nozzles. The asphalt cement came directly from an asphalt tanker at approximately 330° F (165° C). The asphalt was also pumped to the nozzles where it came into contact with the water at the nozzles. The foam was produced with this contact between the water and the hot asphalt cement. The mixing time was approximately 45 seconds. This modified pugmill could produce up to 240 ton (120 tons) of a foamed asphalt mixture per hour. The foamed asphalt coated the fines better than the coarse aggregate, as expected, since it relies on the mastic properties of the fines. The premixed stockpile had the color of wet aggregate and not asphalt coated aggregate.







PLAN VIEW

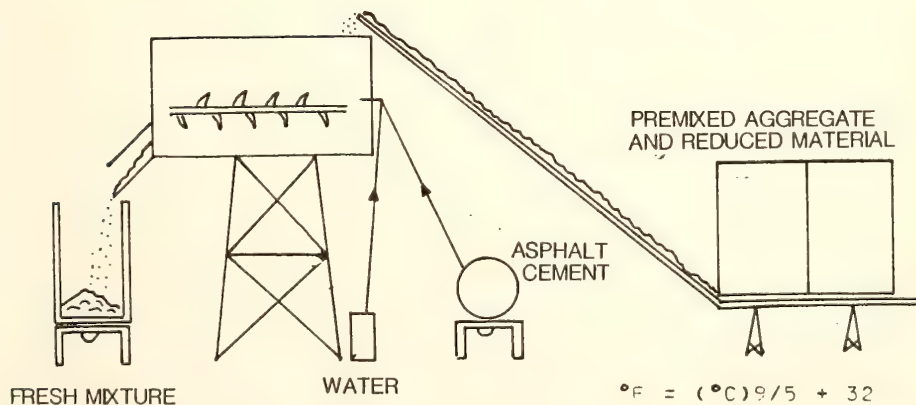


**FIGURE 3.5** DIAGRAMMATIC OUTLAY OF THE MIXING PROCEDURE



The second milling operation followed the first one and removed an additional 2.5 inches (65 mm) of initial pavement. A thickness of 1 inch (25 mm), on average, of initial pavement was left on top of the underlying layers. This protected the subgrade and avoided problems with heavy construction equipment on places where very soft subgrades appeared.

The second milling operation was followed closely, at approximately 1000 feet (300 meter), with the placement of the first three inches (75 mm) of the intended 5.5 inches (140 mm) of recycled base course. The placement was done by a conventional asphalt paver to a width of 11 feet (3.35 meter), which was the lane width. The 2 foot (600 mm) on the sides was cleared by a motor grader. Since the centerline height was taken as reference height and transverse slope had to be 1-1/2% no excavations (as originally specified) were made. The paver completed the portion that had been previously milled by the end of the construction day. This provided a graded, compacted and safe roadway during non-work periods. Care was taken, through the milling of a few centimeters at the side of the placed recycled material, to provide a good bond between the recycled material to be placed in the opposite lane and the recycled layer which had already been placed.

The mixture used in the paving operation was mixed in the twin-shaft pugmill at the central plant. The reduced material was mixed with the premixed additional aggregate in the ratio of 3 to 1. The percentage of foamed asphalt added was 1-1/2% of the total mixture.

The compaction was started immediately after the placement of the first lift by two passes of a steel wheel roller. This was followed by



two passes of a rubber wheel roller after a few hours and another two passes of the same roller at the end of the day. Nuclear density tests showed that six passes gave adequate compaction. Since the road was opened to traffic after a few hours, traffic and especially the heavy construction trucks travelling to and from the central plant caused extra compaction.

The placement of the second lift of 2.5 inches (65 mm) to reach a base thickness of 5.5 inches (140 mm) followed the first lift. It was placed and compacted in the same way as the first lift. An uncompacted placed layer of 4 inches (100 mm) compacted to a thickness of approximately 2.5 inches (65 mm). This is completely different from hot asphalt mixes.

Material from the first and second milling operation was stockpiled in separated piles. Material from both these stockpiles was used simultaneously in the mixing process to minimize the effect of possible unequal asphalt contents of the top and bottom of the initial bituminous pavement. The mixed material was generally transported directly from the pugmill to the paver to be placed. Only in a few cases, when some additional aggregate had to be coated was the recycled mixture stored for a few days.

The placement of the second lift (top) of base course was followed after about 3 days with an AE-T tack coat of 0.05 gal/syd ( $0.25 \text{ l/m}^2$ ) and the hot asphalt surface of 120 lbs/syd ( $65 \text{ kg/m}^2$ ). A shoulder, using one size material obtained as a by-product from the production of crushed stone, completed the construction. The construction of the foamed asphalt section took between 20 and 25 days, including the milling of the initial pavement.



### 3.6. Control of the Foamed Asphalt Mixture

The properties of the foamed asphalt were checked before construction and it was found that a reasonable coating could be obtained by using a halflife of only 12 seconds and an expansion ratio of 10. These properties were checked frequently during construction.

It was never necessary to adjust the free moisture content of the material, since it was between 2.5 and 3.5 percent for most of the time.

Only a small amount of material larger than three inches (75 mm) was obtained through the milling operation. No effort was made to remove these pieces, since it was assumed that they would be broken down during the mixing.

### 3.7. Construction Problems

No serious problems occurred during construction. One of the minor problems was that milling during high pavement temperatures caused the milled material to stick together due to the high asphalt content. Another minor problem was that the larger pieces of reduced material were dragged along by the paver and the scars had to be corrected manually.

The biggest problem was ravelling. This was fortunately a problem only during the first few days of placement. It usually appeared on the outside few feet of the pavement. It occurred soon after placement and was initiated by the wheels of the heavy construction vehicles. The reasons for the ravelling appear to have been a too low binder content, inadequate compaction for heavy vehicular use, as well as a very soft or improperly prepared subgrade. The existence of some organic material e.g. grass could have prevented proper compaction. The





ravelling was compacted by the traffic to a distress pattern similar to rutting and was corrected by the placement of either the second lift of base course material or the surface. It was not necessary to remove these sections.

### 3.8. Conclusions

Foamed asphalt seems to be an acceptable binder in cold recycling. No major equipment changes had to be made during construction to accommodate the foamed asphalt. Conventional equipment could be used with only minor modifications. The construction procedure could also be kept simple and progress maintained at an acceptable rate. The construction crew adjusted well to the placement of the new material although they said that it was easier to place hot asphalt concrete.

The pavement could be opened to traffic soon after construction and it performed well. Even the heavy construction vehicles had no detrimental effect on the recycled layer.

The initial and short term performance of this foamed asphalt recycled layer seems to be satisfactory. The pavement was still in good condition after eight months. The surface layer showed some thin cracks at the centerline of the lanes. These cracks appear to be in the surface layer only and not caused by the recycled layer.



## CHAPTER 4: SAMPLING AND TESTING PROGRAMS ON THE TEST ROAD

### 4.1. Introduction

The sampling and testing for this study were tailored to obtain information regarding the properties of the recycled foamed asphalt mixture that could be used to determine the structural layer equivalencies as well as to use the equipment available at Purdue University and the Indiana Department of Highways.

An elastic layer computer program (BISTRO) was used to calculate stresses, strains and deflections in the pavement layer. The program uses as input the moduli of elasticity, the Poisson's ratios and the thicknesses of the pavement layers. Tests were primarily performed to obtain these values and the sampling was done according to that. The investigation into how these and some other properties were affected by factors such as water, stockpiling, compaction moisture content temperature and curing (which was done as a substudy), did not influence the sampling process. The objectives of this substudy were stated earlier.

The foamed asphalt section of the project of 4.2 mi. (6.72 km) was divided up into 0.1 mile segments for both the eastbound and westbound lanes. This formed a grid with 42 points (stations) on the eastbound and 42 points on the westbound lanes as shown in Figure 4.1. The stations were numbered from 0 at the intersection of SR 16 with SR 231 eastwards to 42 (0.42 miles) on top of the bridge over the



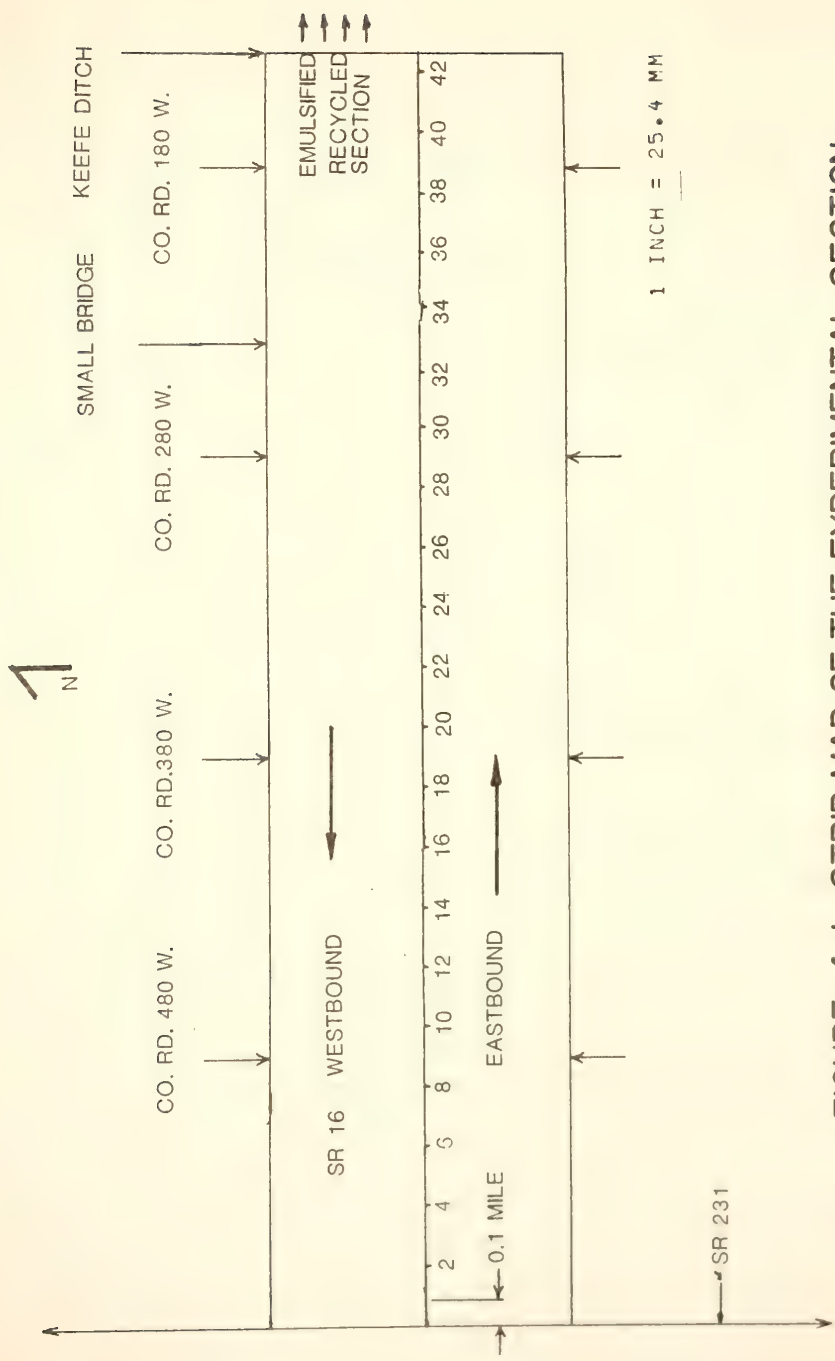


FIGURE 4.1 STRIP MAP OF THE EXPERIMENTAL SECTION



Keefe Ditch (Figure 4.1: Test section), which is the end of the foamed asphalt section. The stations on the eastbound lane were designated S (south) and those on the westbound lane by N (north). The eastbound lane therefore had 43 stations, from 0S to 42S and the westbound lane also 43 stations from 0N to 42N.

These 86 stations established the positions from where all the samples were taken and the tests were conducted. It was not practical to get samples or to perform tests at all those positions, but enough were chosen for each specific test to get a representative sample and to cover the entire foamed asphalt project.

#### 4.2. Prior to Construction

Approximately 100 five inch (125 mm.) cores were taken by personnel of the IDOH over the 8.8 mile (6.72 km) section as described in Chapter 3. Ten four inch (100 mm) cores, taken at randomly selected positions, were used to test the properties of the initial pavement asphalt concrete layer.

Dynamic cone penetrometer tests were conducted to determine the in-situ strength of the layers underlying the asphalt concrete layer of the initial pavement. Ten tests were done on the eastbound lane and seven on the westbound lane. The positions were selected to cover both lanes.

Samples for the determination of the Unified Classification and the moisture content were taken from ten positions on the eastbound and six on the westbound lane. A sample of at least five lb. (2.3 kg) of each of the distinguishable layers of the subgrade were placed in a plastic bag, sealed and stored for further testing. The samples were





taken from holes made at the edge of the pavement on the shoulder. All were done on one day in April 1981 as were the strength tests.

Table 4.1 gives the exact positions of these tests and samples.

Deflection measurements were taken during November 1980 and May 1981 at every 0.1 mile (160 m) in both lanes.

#### 4.3. During Construction

During the construction period, August and September 1981, additional in-situ strength values for the underlying layers were obtained - eight from the eastbound and three from the westbound lane. This gave a total of 18 in-situ strength tests for the eastbound lane and 10 for the westbound lane for a total of 28. These tests were conducted on the same day.

The thickness of the remaining initial pavement asphalt concrete layer and the thickness of the top underlying granular layer were also measured at fourteen different positions on the eastbound lane and eleven on the westbound lane. These positions were selected to cover the entire section and were influenced by the construction. The tests had to be run between the second milling operation and the placement of the first recycled layer. The tests were performed during a two day period.

The relative in-situ strength of the recycled base course was determined with a Clegg impact tester at 14 different positions on the westbound and 19 on the eastbound lane. These positions were also selected to cover the whole section and were influenced by the construction, since it had to be done after the compaction of the base course layer and before the placement of the following layer. The



Table 4.1. Position of Samples Taken

	Prior to Construction			During Construction			After Construction			
	Subgrade Strength	Class. †	Deflection	Subgrade Strength	Thick- ness*	Material Samples	Deflection	Clegg	Cores	Deflec- tion
0			X				X			0
1	X	X	X				X			X
2			X				X			0
3	X	X	X		X		X			X
4	0		X				X			0
5	X	X	X				X		X	0
6			X			X <sub>T</sub>	X		X*	0
7	X	X	X			X <sub>T</sub>	X		XXX*	0
8	0		X				X		0	0
9	X	X	X		X		X		X	0
10			X				X			0
11	X	X	X				X			0
12	0		X				X	0		0
13	X	X	X		0 X	O <sub>T</sub>	X		XXXX	0
14			X		0	O <sub>T</sub>	X			0
15			X				X			0
16	0		X		0		X			0
17			X	X	0 X	O <sub>B</sub>	X	0	0000 X	0
18			X		0		X			0
19			X				X		00	0
20	0		X				X			0
21			X	X	X 0		X		X	0
22			X		0	O <sub>B</sub>	X			0
23		0	X				X	0000		0
24	0		X				X	0		0
25		0	X	X	X		X	X 0	0	0
26			X	X 0	X 0	O <sub>B</sub> X <sub>B</sub>	X	X 0	X	0



Table 4.1. Continued

Prior to Construction			During Construction			After Construction		
Subgrade Strength	Class. <sup>†</sup>	Deflection	Subgrade Strength	Thickness*	Material Samples	Deflection	Clegg	Cores Deflection
27	X	X	0			X	X	X 0
28		X	0	0	O <sub>B</sub>	X	0	X 0
29	0	X	X	X		X	X	X 0
30		X	0			X		X 0
31		X	0			X		X 0
32	0	X	0	X 0		X	0	X 0
33		X	0	X	X <sub>B</sub> X <sub>T</sub>	X	X	XX**
34		X	0		X <sub>T</sub> X <sub>T</sub>	X		XXX
35		X	0	X	X <sub>T</sub>	X		X 0
36	X 0	X	0	0		X	X 0	X 0
37		X	X	X		X	X	X 0
38		X	0			X		X 0
39		X	0			X		X 0
40	0	X	0			X		X 0
41		X	0			X		X 0
42	X	X	0	X		X	*	X 0
43		X	0			X		X 0

<sup>†</sup> Classification (Unified) and moisture content samples.

\* Thickness of the remaining initial pavement surface layer and the top subgrade granular layer.

X - on Eastbound lane

0 - on Westbound lane

X<sub>T</sub> and O<sub>T</sub> - top recycled layer (second lift)

X<sub>B</sub> and O<sub>B</sub> - bottom recycled layer (first lift)

\* - unusable core from eastbound lane

\*\* - unusable core from westbound lane



measurements were taken on two consecutive days. One set was taken approximately six hours after construction and another set on the next day. Most of the measurements were taken on the first layer. All were taken at the center of each lane.

Thirteen samples were taken from the paver during construction. Each sample weighed approximately 25 lb. (12 kg) and was placed in a plastic bag and sealed. Two samples were taken from the first lift on the eastbound lane and four on the westbound lane at six different positions. Two samples were taken from the second lift on the westbound lane and five on the eastbound lane at six different positions. Two samples were taken per day except for the last day when three were taken. The positions were determined by the position of the paver. The placement of the two lifts took about ten to twelve working days. It was not practical to sample every day and therefore the samples were taken on six different days. This was determined to be sufficient to characterize the properties of the foamed asphalt mixture across the whole section. The material from these samples were used to compact specimens in the laboratory.

Deflection measurements were taken on top of the completed foamed asphalt recycled base coarse on the eastbound lane only at 0.1 mile (160 m) intervals.

The exact positions of all the tests are shown in Table 4.1.

#### 4.4. After Construction

Four inch cores were taken, during October 1981. Twenty four were taken at eleven different positions on the eastbound lane and twenty at nine different positions on the westbound lane for a total of forty





four cores. Of these forty four only thirty four could be used in further tests. The cores were taken over a period of about five working days. The positions were chosen to coincide with those where material samples were taken from and in-situ strength tests of the sub-grades were conducted. It was very difficult to get full size cores. The cores tended to break at the weak bond between the two lifts. The bottom part then remained in the hole or fell apart. This is the reason why so few specimens from both layers at the same position could be obtained.

The positions are shown in Table 4.1.

Deflection measurements were also taken on top of the hot surface mixture overlaying the recycled base course in both the eastbound and westbound lanes at 0.1 mile (160 m) intervals. The measurements were taken only a few (approximately three to six) days after construction. The measurements were taken at the center of each lane.

Figure 4.2 shows the chronological order in which the sampling and testing were done. The types of tests and the number of samples taken are for each test are summarized in Table 4.2.



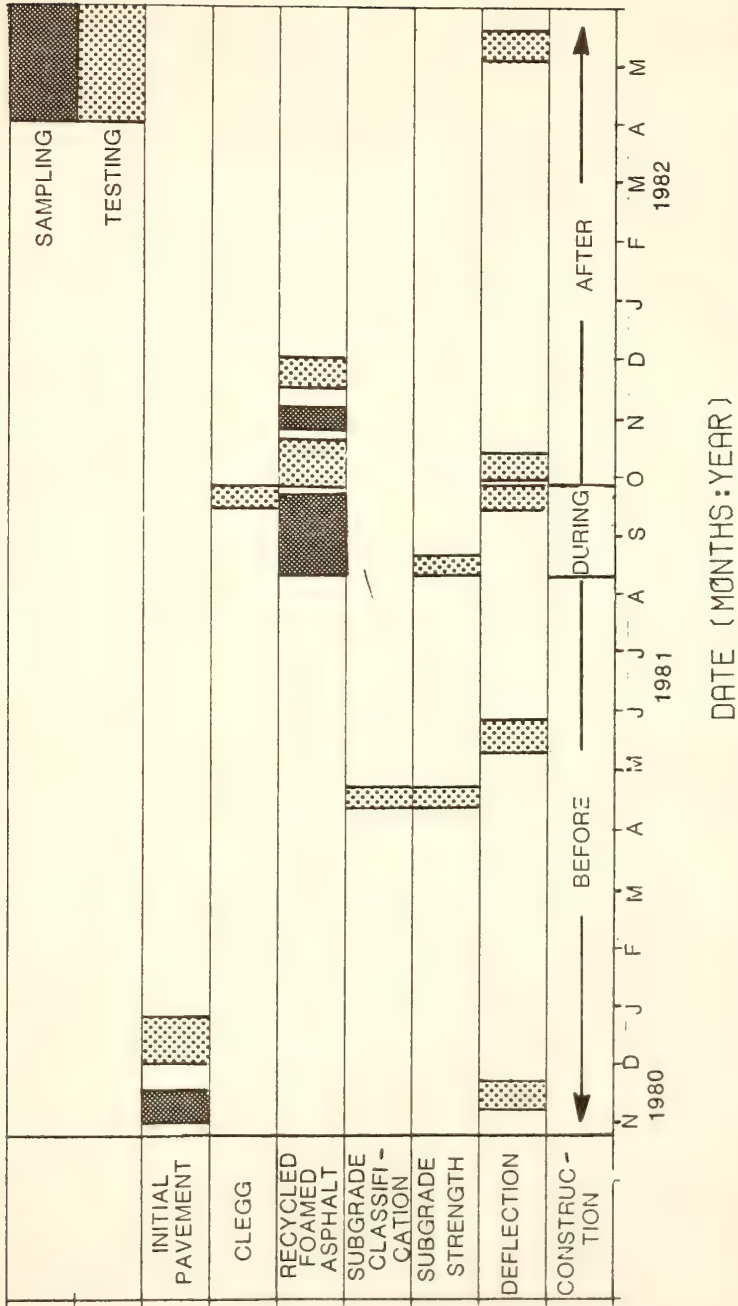


#### FIGURE 4.2 CHRONOLOGICAL DISPLAY OF SAMPLING AND TESTING PROGRAMS



Table 4.2. Number of Samples Taken

Lane	<u>Before Construc- tion</u>		<u>During Construc- tion</u>		<u>After Construc- tion</u>		Total
	E	W	E	W	E	W	
Subgrade strength	10	7	8	3	-	-	28
Samples for Classification	10	6	-	-	-	-	16
Thickness of Initial Pavement and Granular Layer	-	-	14	11	-	-	25
Recycled Material Samples	-	-	7	6	-	-	13
Relative Strength of the Base	-	-	19	14	-	-	33
Total Usable Cores	-	-	-	-	24	21	35
Deflections	44	44	43	-	43	44	-

E = eastbound

W = westbound



## CHAPTER 5: DESCRIPTION OF TEST EQUIPMENT AND PARAMETERS

### 5.1. Introduction

The major pieces of equipment used for the in-situ testing in this study were the dynamic cone penetrometer (DCP), the Clegg Impact Soil Tester and the Dynaflect. The equipment used in the laboratory study included the Hveem kneading compactor, Hveem compression machine, the resilient modulus test equipment and the Marshall testing equipment. Various other types of equipment were used to perform the standard tests done in this study. Since the latter are standard tests using standard equipment and not of primary concern in this study they will not be described here.

### 5.2. Dynamic Cone Penetrometer (DCP)

The DCP is a modified version of the penetrometer used by the Country Roads Board, Victoria, Australia. It consists of a long rod with a cone point. A 4.55 lb. (10 kg) hammer is dropped a distance of 18.11 inches (460 mm) sliding along the upper part of the drive rod until it strikes an anvil at the lower end (Figure 5.1). This forces the hardened steel cone, 0.787 inches (20 mm) in diameter into the soil. The penetration is then measured on gradations on the top rod by comparing it to a fixed reference point. In this case a tripod with a pointer was used to measure the penetration (Figure 5.2). A penetration of at least 12 inches (305 mm) is suggested per test and a set of three tests per position (61).





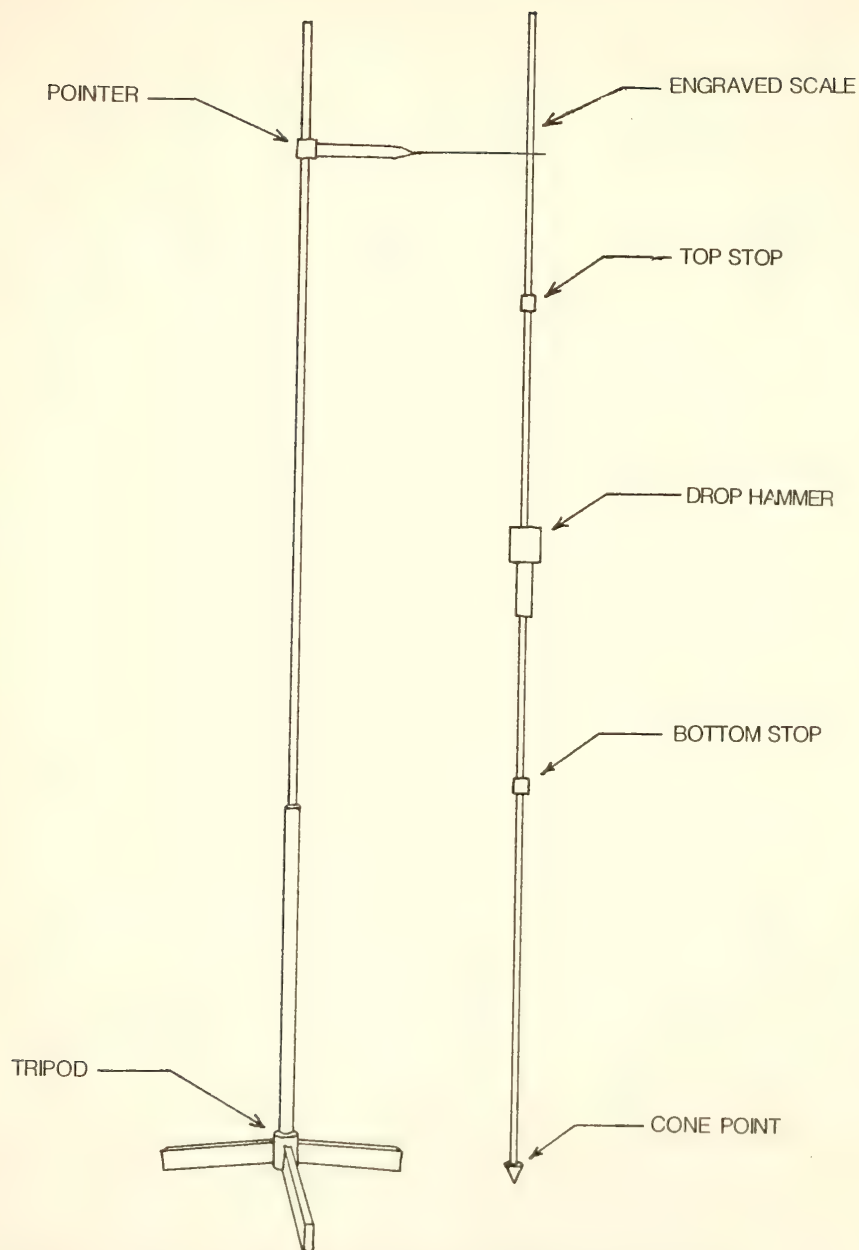


FIGURE 5.1 DYNAMIC CONE PENETROMETER



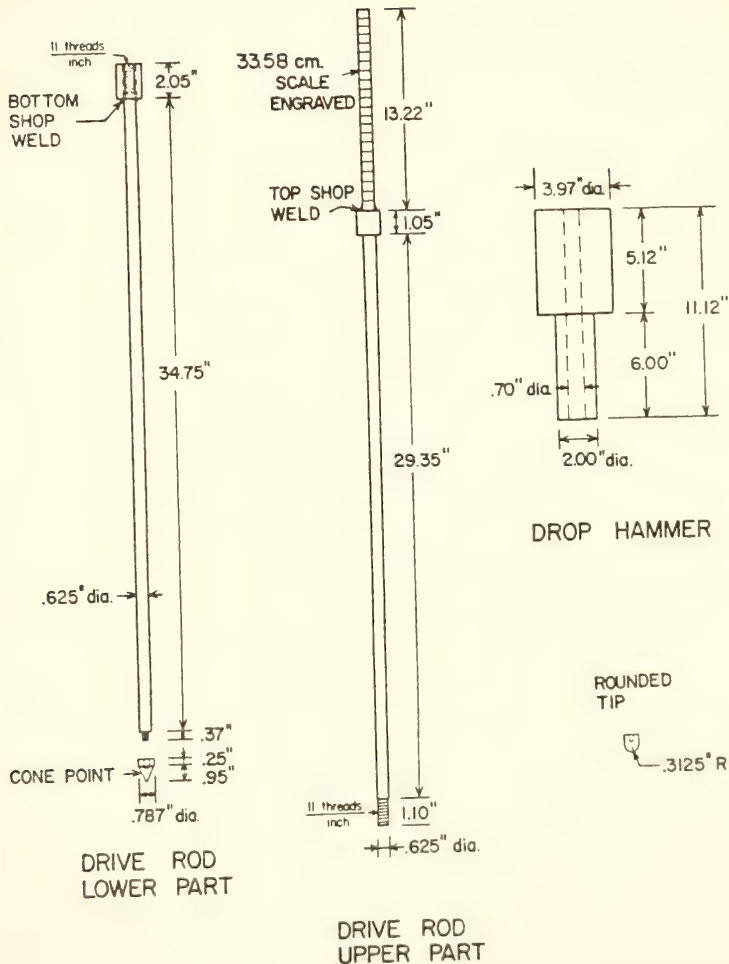


FIGURE 5.2 DIMENSIONS OF THE DYNAMIC CONE PENETROMETER (from ref. 61)



The DCP provides an easy to operate, inexpensive and fast test to determine the strength of the in-situ soil, especially for subgrade soils with CBR values up to 50.

The penetration has been correlated with CBR-values by the following equation (19):

$$\text{CBR} = 230/p \quad (5.1)$$

where:

CBR = California Bearing Ratio (percent)

p = penetration (mm/blow)

The range is from 1 to 50 CBR.

### 5.3. Clegg Impact Soil Tester

The impact soil tester was developed by Dr. Baden Clegg at the University of Western Australia. It consists essentially of a heavy compaction hammer of 10 lb. (4.5 kg) (Figure 5.3). An accelerometer attached to the hammer generates an electrical output which is fed to a peak level hold meter. The meter registers the peak deceleration in units of 10 gravities. The level reached after the fourth blow is referred to as the Impact Value (IV).

The test is conducted by placing the guide tube on top of the layer and held in place by one foot. The hammer is then lifted to a height of 12 inches (305 mm) and dropped. The reading is recorded after the fourth drop (82).

The Clegg impact soil tester is used to test the strength of granular material and is correlated with CBR-values (82).

In this study it was used to compare the relative strengths (or stiffnesses) of the foamed asphalt recycled base course at different



positions. It is not possible at this stage to compare these values with other measures of stiffness or strength e.g. elastic modulus or CBR for asphalt stabilized layers.

#### 5.4. Dynaflect

The Dynaflect has been used widely to measure pavement deflections. The instrument is reliable, relatively simple and fast to use. It also provides more information than just maximum deflections (58).

The Dynaflect is mounted on a small two-wheel trailer and towed by a pick-up truck. At the test section a pair of steel wheels are lowered to the pavement, the pneumatic wheels lifted and an oscillating load is generated by eccentric weights rotating eight revolutions per second. The peak to peak load applied is 1000 lb. (455 kg). The peak to peak deflections are measured by five geophones, placed as indicated in Figure 5.4.

The Dynaflect can be moved using the steel wheels at very slow speeds (up to 4 mph). The trailer can be towed over longer distances by using the pneumatic wheels at higher speeds.

The deflections obtained from the Dynaflect form a deflection basin, as shown in Figure 5.4. The shape of the deflection basin is important and research has shown that it can be used to investigate various properties of the materials in the layer (43,5,71,59,18,48).

The following terms are commonly used with Dynaflect deflection basins and can be used to describe various properties of the pavement.

1. Dynaflect maximum deflection (DMD) which is the deflection at the center between the Dynaflect loading wheels as measured by the first sensor ( $D_1$ ). This deflection has been correlated







FIGURE 5.3 CLEGG IMPACT  
SOIL TESTER

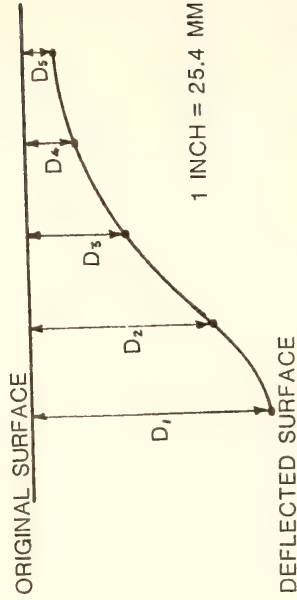
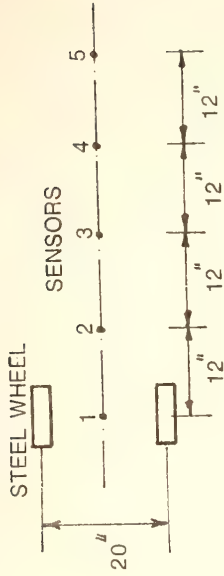


FIGURE 5.4 DYNAFLECT SENSOR  
ARRANGEMENT AND DEFLECTION BASIN  
(after ref.48)



with the Benkelman Beam deflection. The relationships is (80)

$$\text{Benkelman Beam Deflection} = 20.63 * \text{DMD} \quad (5.2)$$

2. Surface curvature index (SCI). It is defined as

$$\text{SCI} = D_1 - D_2 \quad (5.3)$$

where

$D_1$  = deflection at the first sensor

$D_2$  = deflection at the second sensor.

The SCI is an indicator of the stiffness of the surface course.

It increases as the stiffness decreases (48).

3. Base curvature index (BCI) is defined as the difference between the deflections at the fourth and fifth sensors.

$$\text{BCI} = D_4 - D_5 \quad (5.4)$$

where

$D_4$  = deflection at the fourth sensor

$D_5$  = deflection at the fifth sensor

The BCI and the deflection at  $D_5$  are indicative of the pavement

support conditions (48). The deflection at the fifth sensor

has been correlated with the subgrade modulus ( $E_s$ ). The re-

lationship is: (18)

$$\text{for } \gamma = 0.50: E_s = 5190 D_5^{-0.997} \quad (5.5)$$

$$\text{for } \gamma = 0.40: E_s = 6350 D_5^{-0.992} \quad (5.6)$$

where

$E_s$  = elastic modulus of the subgrade (psi)

$D_5$  = deflection at the fifth sensor ( $10^{-3}$  inches)

$\gamma$  = Poisson's ratio.



4. The spreadability is defined as follows:

$$SPD = (D_1 + D_2 + D_3 + D_4 + D_5) * 100/5D_1 \quad (5.7)$$

where

$D_1$  = deflection at the first sensor

$D_2$  = deflection at the second sensor

$D_3$  = deflection at the third sensor

$D_4$  = deflection at the fourth sensor

$D_5$  = deflection at the fifth sensor

The SPD is indicative of the distribution of loads by the pavement to the underlying layers. Pavements with higher spreadability values will distribute the wheel loads more effectively and therefore induce smaller stresses and strains on the subgrade (28).

5. Slope of the deflection basin is defined as the difference between the deflection at  $D_1$  and  $D_5$ .

$$\text{Slope of the deflection basin} = D_1 - D_5 \quad (5.8)$$

where  $D_1$  and  $D_5$  are as defined above.

The slope is also indicative of the surface stiffness (43).

#### 5.5. Kneading Compactor

The standard California kneading compactor as described in ASTM D1561 (Compaction of test specimens of bituminous mixtures by means of California Kneading Compactor) and the Asphalt Institute design procedures (92) was used to compact the specimens. The compactor is designed to consolidate the material by a series of individual "kneading action" impressions made by a moving ram having a face shaped as a sector of four inches (102 mm) diameter circle (Figure 5.5).



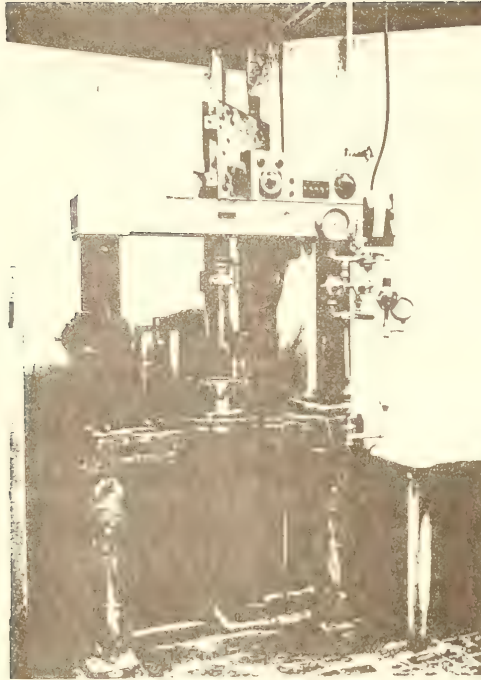


FIGURE 5.5 KNEADING COMPACTOR





The force under the tamper foot can be controlled. It has a maximum force of 500 psi (34.5 kPa). The time a certain pressure can be applied can also be varied to comply to the ASTM test.

#### 5.6. Hveem Stabilometer and Compression Machine

The Hveem stabilometer and compression machine was used to determine the R-values of the specimens in this study. The Hveem stabilometer is a triaxial testing device which measures the horizontal pressure developed by a test specimen as a vertical pressure is applied. The compression machine is capable of applying the required loads at a head speed of 0.05 inch per minute (0.02 mm per second) as specified by the ASTM standards for this test.

The R-value is usually used to determine the strength of soils and the stability or bearing capacity of cold asphalt stabilized mixtures at a temperature of  $73 \pm 5^\circ\text{F}$  ( $23 \pm 2.8^\circ\text{C}$ ). The R-value is defined as:

$$R = 100 - \frac{100}{\frac{2.5}{D} \left( \frac{P_v}{P_h} - 1 \right) + 1} \quad (5.9)$$

where

$P_v$  = 160 psi (1103 kPa) vertical pressure

$D$  = turns displacement reading

$P_h$  = horizontal pressure at  $P_v$  (psi) (77).

A correction factor has to be applied to specimens not 2.5 inches (63.5 mm) in height.

The compression machine was also used to compress the specimen after the kneading compaction to a static pressure of 1000 psi (6.9 MPa) with a head speed of 0.25 inch per minute (6.3 mm per minute).



The same machine was also used to remove the specimen from the mold.

### 5.7. Marshall Testing Equipment

The Marshall testing apparatus (Figure 5.6) was used to conduct Marshall stability as well as indirect tensile tests on the foamed asphalt recycled mixture.

In order to determine the Marshall stability the specimen is loaded to failure at a constant head speed of two inches (51 mm) per minute. The Marshall equipment used gives a continuous load-deformation plot during the test (77,92).

The load required to produce failure is defined as the Marshall stability. The flow value is the vertical deformation of the specimen during the test until failure occurs. The Marshall stability is a measure of strength and resistance to deformation under load and the flow of the plasticity and flexibility of the mix (22). It is widely used.

The Marshall stiffness ( $S_m$ ) is defined as:

$$S_m = \text{stability/flow} \quad (5.10)$$

and the Marshall index ( $I_m$ ) as the slope of the linear portion of the load-deformation trace obtained from the autographic Marshall equipment. These two parameters provide some extra measures for the mixture characteristics and can be used in conjunction with the conventional used values of stability and flow (22).

Figure 5.7 shows a typical plot and the discussed parameters. Marshall stability, index, stiffness and flow will be referred to as Marshall variables in this report.



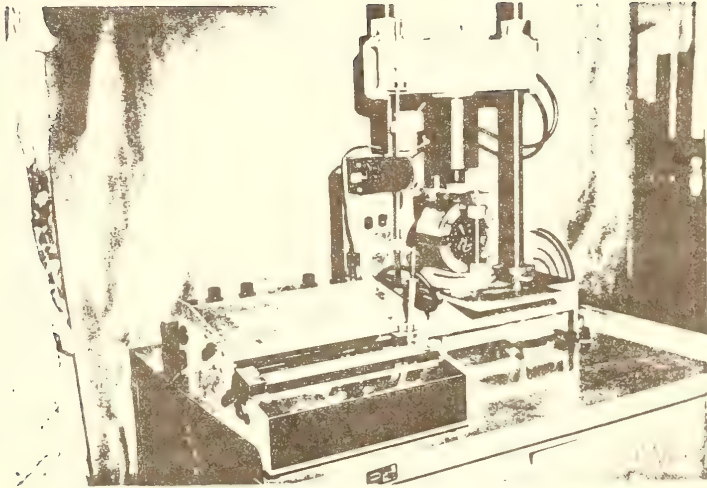
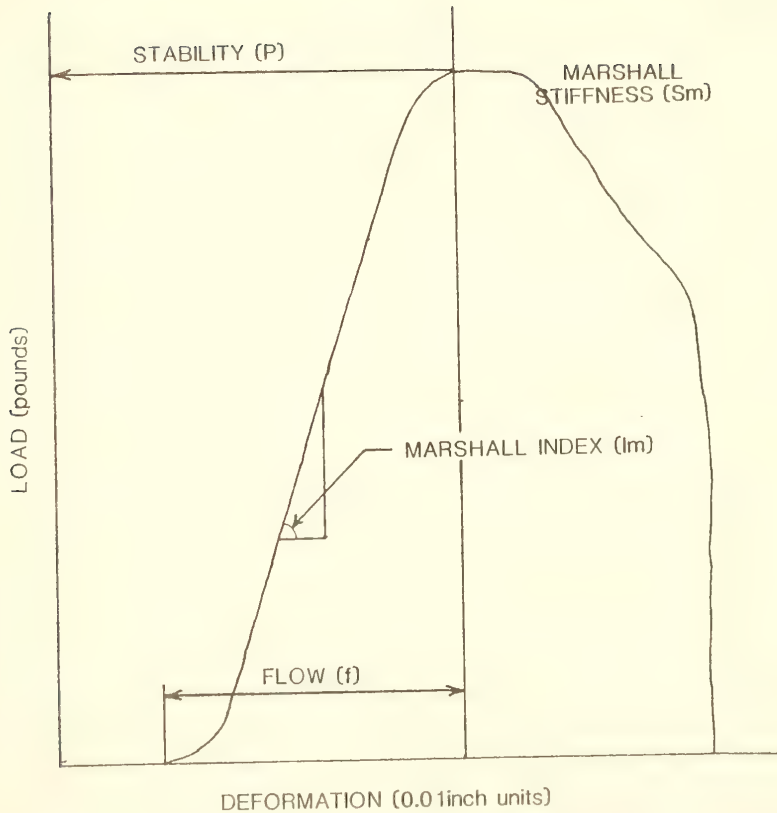


FIGURE 5.6 MARSHALL TEST EQUIPMENT





1 LB (F) = 4.45 N  
 1 INCH = 25.4 MM

FIGURE 5.7 TYPICAL LOAD-DEFORMATION PLOT  
 FROM THE MARSHALL TEST  
 (from ref. 22)





### 5.8. Vacuum Saturation Equipment

The vacuum saturation test was conducted to investigate the effect of prolonged exposure to subsurface water on the foamed recycled mixture.

The vacuum manometer and desicator used were similar to those described in an interim guide of the Asphalt Institute (72). A vacuum pump capable of pulling four inches (100 mm) of Hg was also used.

### 5.9. Resilient Modulus Testing Equipment

The resilient modulus test used in this study was based on the diametrical resilient modulus test proposed by Schmidt (57). The test equipment is shown in Figure 5.8. It consisted mainly of a loading frame, a diaphragm air cylinder, a solenoid valve system, a compressed air source, three DC LVDT's, a two channel chart recorder and a DC voltage source for the DC LVDT's.

A vertical load of 50 lb. (22.7 kg) was applied diametrically every 3 seconds for a duration of 0.1 second. This load was applied through a 0.5 inch (13 mm) steel strip to the specimen. The vertical deformation as well as the horizontal deformations were measured.

Based on the analyses of Timochenko and Froeht on the behavior of specimen as a linear elastic material under dynamic loads Schmidt (57) derived a relationship between the resilient modulus and the induced horizontal deformation of the specimen in the diametral resilient modulus test.

Using the analysis of the stresses in a circular disc under a short strip loading developed by Hondros and the elastic-strain relationships the following relationships were reported by various sources (23, 66):



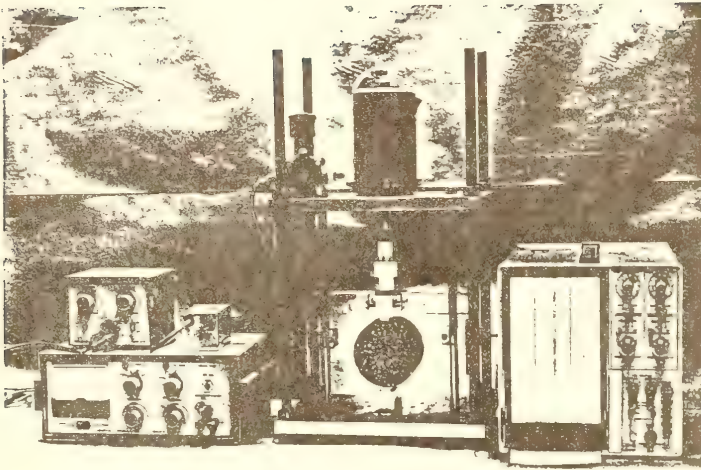


FIGURE 5.8 RESILIENT MODULUS TESTING EQUIPMENT



$$E = \frac{P}{\pi t dv} (11.257 - 0.193\gamma) \quad (5.11)$$

$$E = \frac{P}{\pi t dh} (0.841 + 3.141\gamma) \quad (5.12)$$

$$\gamma = 3.59 dh/dv - 0.27 \quad (5.13)$$

where

E = modulus of elasticity

P = load

t = thickness of specimen

dv = vertical deformation

dh = horizontal deformation

$\gamma$  = Poisson's ratio

In this study, the following equation was used to calculate the resilient modulus:

$$E = \frac{3.583P}{t \cdot dv} \quad (5.14)$$

The effect of the Poisson's ratio on the resilient modulus is very small when the vertical deflection is used in the calculation (66).

Two types of resilient moduli can be calculated by these equations depending on the value measured viz. total or instantaneous. The instantaneous resilient modulus was calculated throughout this study from the appropriate instantaneous measured values. Figure 5.9 shows a typical deformation plot indicating the measurements which were used in the calculations.



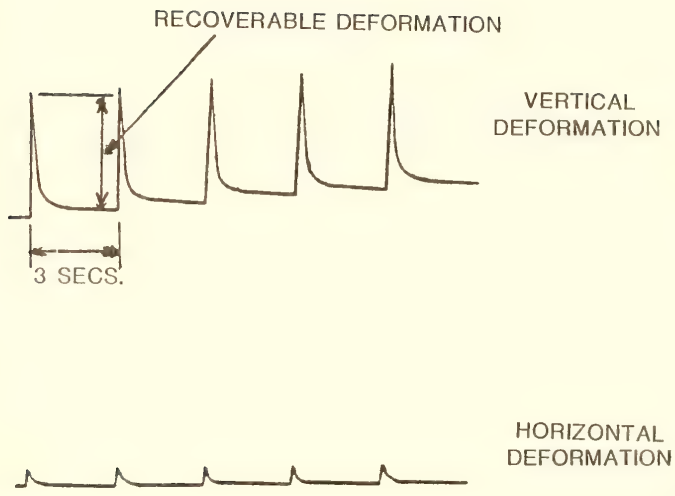


FIGURE 5.9 TYPICAL DEFORMATION PLOTS FROM  
THE RESILIENT MODULUS TEST  
(from ref. 66)





### 5.10. Indirect Tensile Strength Testing Equipment

The indirect elastic theory has been proved to be valid when testing elastic materials with loads applied through a short curved loading strip. The test provides useful information on the tensile properties of the mixture (23,40).

The Marshall equipment was also used to perform indirect tensile tests on the specimens. A load was applied at two inches (51 mm) per minute until the specimen failure. Only the vertical deformation could be measured.

Based on the stresses in a circular disc and elastic-strain relationships the following equations were derived (32,40,89,41,29): (Figure 5.10 illustrates the occurrence of stresses and strains).

$$S_T = 0.156 \frac{P_{fail}}{h} \quad (5.15)$$

$$E = S_H / h(0.9976\gamma + 0.2692) \quad (5.16)$$

$$\gamma = \frac{0.0673 \text{ DR} - 0.8954}{-0.2494 \text{ DR} - 0.0156} \quad (5.17)$$

$$\epsilon_T = X_T \left[ \frac{0.1185\gamma + 0.03896}{0.2494\gamma + 0.0673} \right] \quad (5.18)$$

$$\epsilon_C = Y_T \left[ \frac{-0.03896\gamma + 0.1185}{+0.0156 \gamma - 0.8954} \right] \quad (5.19)$$

where

$S_T$  = tensile strength (psi)

$\gamma$  = Poisson's ratio



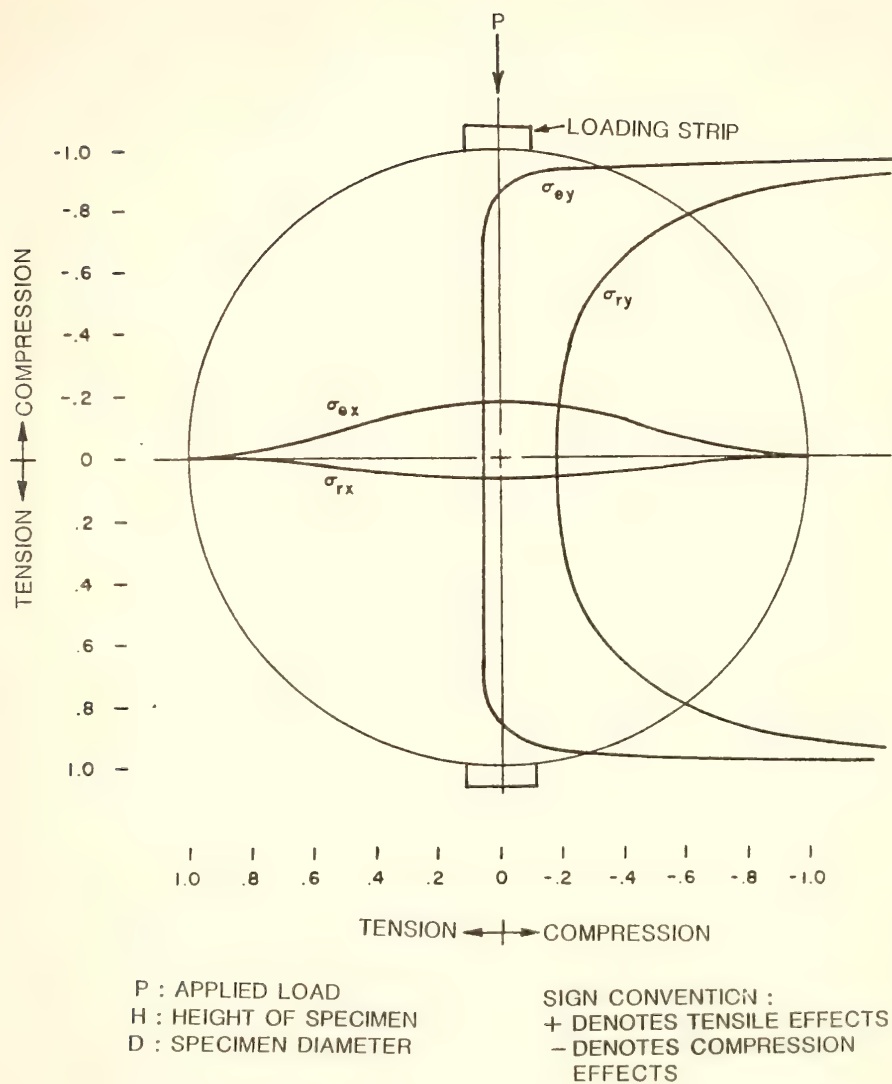


FIGURE 5.10 STRESS DISTRIBUTION ALONG THE PRINCIPAL AXES (from ref. 40)



- $D_R$  = deformation ratio  $Y/X$  (the slope of line of best fit between the vertical deformation and the horizontal deformation)  
 $X_T$  = total horizontal deformation (inches)  
 $Y_T$  = total vertical deformation (inches)  
 $S_H$  = horizontal tangent modulus  $P/X_T$  (the slope of the line of best fit between load  $P$  and horizontal deformation)  
 $E$  = static modulus of elasticity (psi)  
 $\epsilon_T$  = tensile strain  
 $\epsilon_C$  = compressive strain  
 $h$  = height of specimen (inches)  
 $P_{fail}$  = total load at failure (lb)

The equations cited above are valid for specimens of four inches (102 mm) in diameter and under static loading conditions.

The indirect tensile strength can also be used to predict the fatigue life to failure ( $N_f$ ) of bituminous mixtures. Eight bituminous concretes from five different areas viz. California, Utah, Ohio, Pennsylvania and Virginia were used by Maupin and Freeman (42) to determine the following relationships:

1. For constant stress testing:

$$N_f = k_1 (1/\sigma)^{k_2} \quad (5.20)$$

with

$$k_2 = 11.6 - 0.000396 E \quad (5.21)$$

$$k_1 = e^{k_2 \ln(12.6 \sigma_{IT}^{-558})} \quad (5.22)$$

$E$  = static elastic modulus



$S_T$  = tensile strength =  $\epsilon_{IT}$

$N_f$  = cycles to failure

$\sigma$  = maximum bending stress

2. For constant strain testing:

$$N_f = k_1 (1/\epsilon)^{k_2} \quad (5.23)$$

with

$$k = 0.03746 - 0.744 \quad (5.24)$$

$$\log k_1 = 7.92 - 0.122 \sigma_{IT} \quad (5.25)$$

$N_f$  = cycles to failure (the number of cycles to produce a 1/3 reduction in initial stiffness calculated at approximately 200 cycles).

The researchers recommend that the relationships be used for mixtures with aggregate smaller than one inch size and primarily for dense-graded bituminous concretes.

The equations cited above are true for specimens of 4 inches (102 mm) in diameter and under static loading conditions.





## CHAPTER 6; TESTING PROCEDURE

### 6.1. Introduction

As mentioned earlier, tests were conducted to fulfill the objectives of the study. Standard testing procedures as described by the American Society for the Testing of Materials (ASTM), the American Association of State Highway and Transportation Officials (AASHTO) and the Asphalt Institute were used when possible. This allows comparisons to be made to results obtained in other studies.

As described in Chapter 4 (Sampling) the sampling and testing were conducted prior, during and after construction. The tests on the subgrade, in-situ strength and classification were conducted before and during the early stages of the construction. The tests on the initial pavement were performed before construction. Tests on the recycled foamed asphalt mixture were conducted during and after construction. Deflection measurements were taken before, during and after construction. The chronological order has been shown in Figure 4.1.

### 6.2. Subgrade

#### 6.2.1. In-Situ CBR

The in-situ CBR values of the subgrade were obtained from dynamic cone penetrometer (DCP) tests. The tests were conducted on the subgrade through five inch diameter core holes in the initial pavement in seventeen cases. Three DCP tests were run in such a hole. The



penetration of the rod after each blow (fall of the 10 lb. (45 kg) hammer) was recorded up to a depth of at least 12 inches (30 cm). In cases where no changes in the penetration per blow for the first 12 inches could be detected the penetration was continued to 24 inches (50 cm).

The number of blows were then plotted against the penetration depth for all three tests. The slope of the line (penetration per blow) is an indicator of the in-situ strength and was correlated with CBR-values (Chapter 5). A change in slope indicated a change in subgrade strength. The depth at which the slope changed indicated the depth of a layer with a different strength. This was used to determine the thicknesses and strengths of different subgrade layers. Figure 6.1 shows a typical number of blows versus penetration plot. The values taken were the average of the three tests at each position (hole). In a few cases the third DCP test could not be run because of disturbance of the subgrade by the previous two tests, since the hole was only 5 inches in diameter. This problem was detected either during the testing or during the plotting of the data. In such cases only results from the first two tests were used.

Another eleven holes were made after the first milling operation through the remaining 2-1/2 inches (65 mm) of initial pavement with a hammer and a chisel to open up the subgrade material. A procedure similar to that described in the previous paragraphs was followed to obtain the in-situ strength of the subgrade with the DCP. Three DCP tests could be run in all cases in these holes.



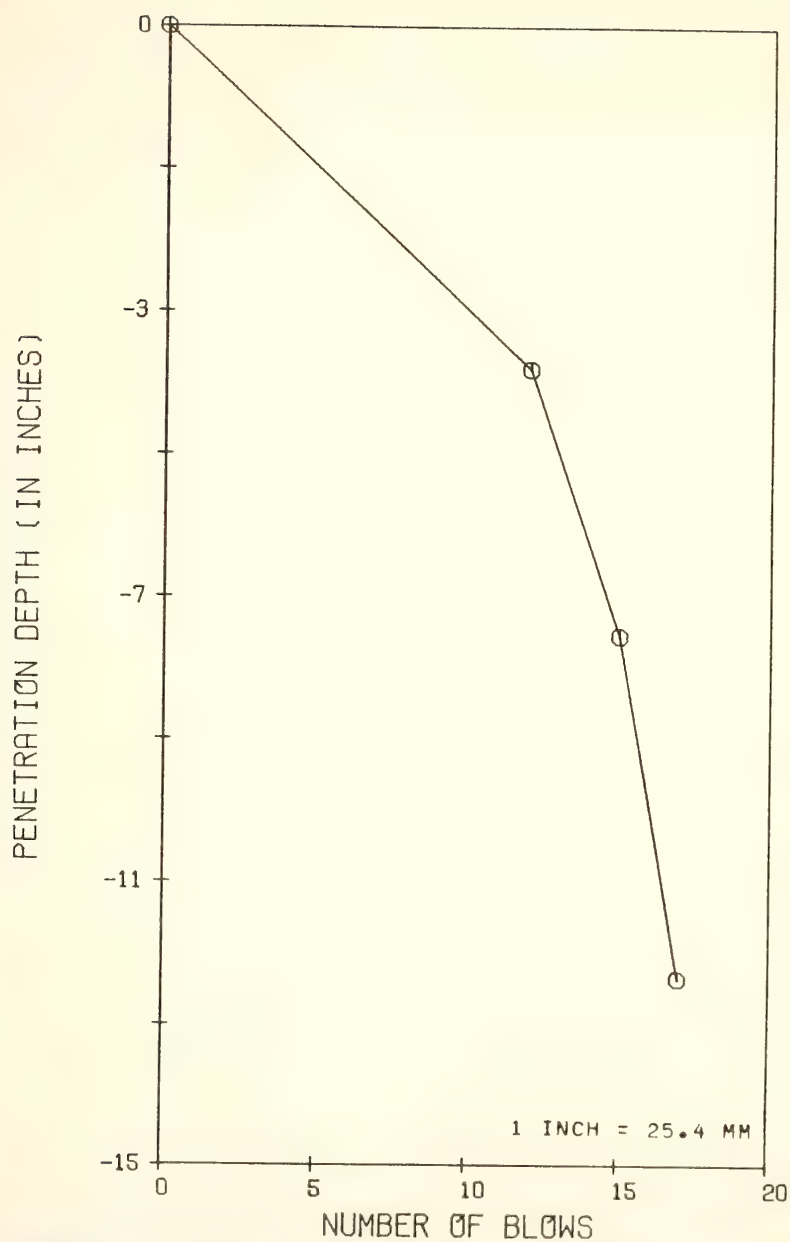


FIGURE 6.1 TYPICAL PLOT FROM THE DYNAMIC CONE PENETROMETER TEST



### 6.2.2. Classification Tests

Classification tests were conducted on the sixteen samples taken at the edge of the pavement. Standard AASHTO or ASTM testing procedures were used.

The samples were stored in a plastic bag until it could be tested. The sample preparation, the grading analysis of the coarse aggregate, the grading analysis and the determination of the hydrosopic moisture content of the fine aggregate (passing the #10 (2.0 mm) sieve) were done according to the AASHTO T87-76 or the ASTM D421-58 (reapproved in 1978) testing procedure. The liquid limit (L.L.) and the plastic limit (P.L.) determination on the material passing the #40 (0.425 mm) sieve were done in accordance to the AASHTO T89-76 (ASTM D423-66 (reapproved 1970)) and AASHTO T90-70 (ASTM D424-59 (reapproved 1971)) test procedures respectively. The latter procedure also indicated how the plastic limit should be calculated.

The Unified Classification system was used to classify the material underlying the initial pavement. The percentage of material passing the #200 (0.475 mm) sieve, the percentage passing the #4 (6.25 mm) sieve, the grain size curve, the liquid limit (L.L.) and the plastic limit (P.L.) were used in the classification (94).

The testing and classification procedures are displayed in Figure 6.2.

### 6.3. Recycled Foamed Asphalt Mixture

A flow diagram describing the testing procedure for the foamed asphalt recycled mixtures is given in Figure 6.3.





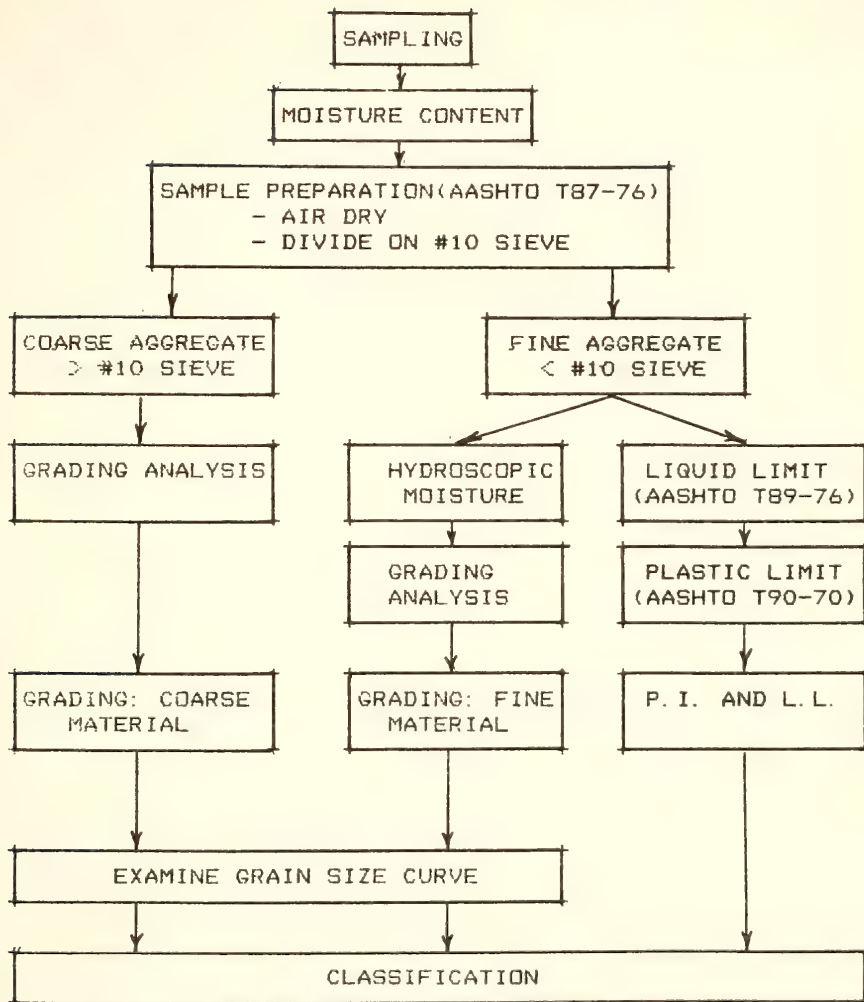


FIGURE 6.2 FLOW DIAGRAM OF SOIL CLASSIFICATION PROCEDURE



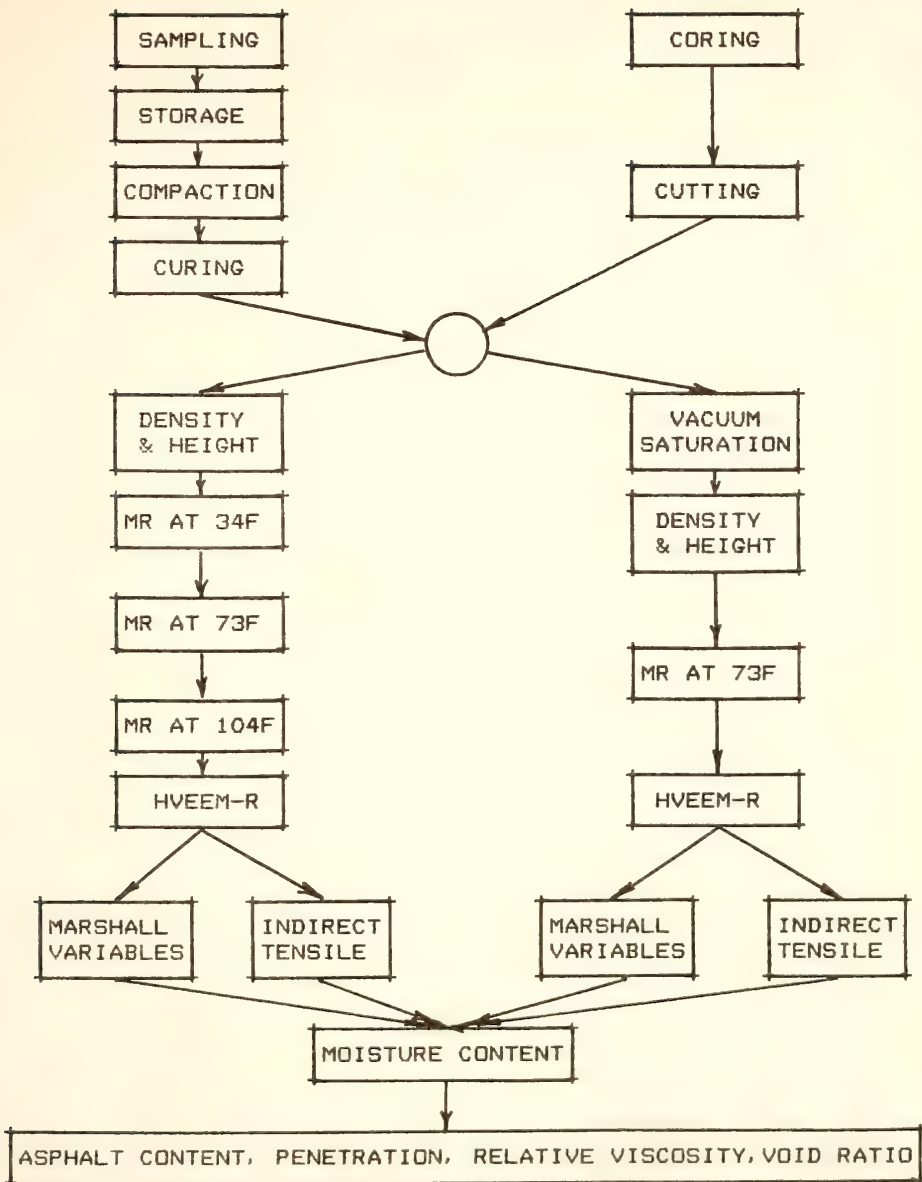


FIGURE 6.3 FLOW DIAGRAM OF THE FOAMED ASPHALT RECYCLED SPECIMEN TESTING PROCEDURE



### 6.3.1. Laboratory Compacted Samples

#### 6.3.1.1. Storage

The samples of the recycled foamed asphalt mixture, taken during construction, were stored in air tight plastic bags. Most of the specimens were stored in the plastic bag for less than ten hours.

The influence of storage of the mixture in a plastic bag was determined by compacting a few specimens after storage of between one and twenty-one days. A few specimens were compacted after ten days in air to investigate the effect of stockpiling in the open on the mixture.

Table 6.1 summarizes the storage times and the number of specimens in each, while Table 6.2 summarizes the number of specimens used in each test.

#### 6.3.1.2. Compaction

The California kneading compactor, as described in Chapter 3, was used to compact all the specimens. A standard procedure suggested by the Asphalt Institute for asphalt mixtures (MS-2) or ASTM-D1561 was used. The same method was used by other researchers at Purdue University on cold asphalt mixtures (28,39). This was one of the reasons for selecting this compaction procedure. Some of the other reasons were that this method is widely used and very well documented and it simulates compaction during construction better than the Marshall compaction method. The kneading compaction method represents the pavement density and stability after approximately one year in service. Although the gyratory compaction method also simulates the compacted during construction well it is less widely used and more cumbersome to use. The



Table 6.1. Number of Laboratory Specimens for Each Storage and Curing Time

		Curing (Days)				Total	
		Air			Oven		
		1	10	14			
Storage	Closed in Bag	0	6	78	-	6	90
		1	-	6	-	-	6
		3	-	4	-	-	4
		4	-	2	-	-	2
		5	-	2	-	-	2
		6	-	2	-	-	2
		7	-	2	-	-	2
		10	2	4	2	-	8
		14	-	2	-	-	2
		21	-	4	-	-	4
	Open	10	2	-	-	-	6
	Total		10	106	6	6	128





Table 6.2. Number of Laboratory Specimens Used in Each Test

	Storage											Curing			
	Closed						Open					Air			
	0	1	3	4	5	6	7	10	14	21	10	1	10	14	Oven
Total Unsaturated	55	6	2	2	2	2	2	8	2	4	6	10	71	6	6
1	55	6	2	2	2	2	2	8	2	4	6	10	71	6	6
2	55	6	2	2	2	2	2	8	2	4	6	10	70	6	6
3	27	4	2	2	2	2	2	8	2	4	6	10	49	6	-
4	28	2	2	-	-	-	-	-	-	-	-	-	21	-	6
Total Saturated	35												35		
1	35												35		
2	35												35		
3	26												26		
4	9												9		
Total	90	6	2	2	2	2	2	8	2	4	6	10	106	6	6

Test 1 = Hveem R-value

2 =  $M_R$  at 3 temperatures, except on the saturated specimens

3 = Marshall test.

4 = Indirect tensile test.



Indiana Department of Highways uses the kneading compactor for the compaction of asphalt mixtures.

The Asphalt Institute procedure specifies that 1150 grams of the mixture be placed into a mold while rodding the mix twenty times in the center and twenty times along the edge. The tamper foot pressure was set at 250 psi (1.7 MPa) for one minute to accomplish preliminary consolidation of the mix. This was followed by the compaction of the mixture with a tampering foot pressure of 500 psi (3.45 MPa) for 5 minutes.

The mold and specimen were then removed from the kneading compactor, the mold inverted and the specimen pushed to the opposite end of the mold by applying a static load of 1000 psi (7.9 MPa) with a head speed of 0.25 inches per minute (7.3 mm/min.). This was done in the compression machine.

The same machine was also used to remove the specimen from the mold immediately after compaction.

The moisture content of the mixture during compaction was determined by oven drying a sample at constant temperature.

#### 6.3.1.3. Curing

The primary objective of this study was to determine the material properties of the foamed asphalt recycled mixture in actual use. The material properties during three stages in the life of the pavement layer seem to be important viz. just after construction, after a few months in use and after a longer period of use under ideal conditions (ultimate strength). The first stage, soon after construction, can be simulated by a specimen with no curing time. The intermediate stage



was simulated by curing the specimens for 10 days in air. This would be the strength of the mixture for most of its life since it would be difficult to reach higher levels due to environmental conditions. The ultimate strength is an attempt to simulate the strength the material can have if it is cured under ideal conditions for a long period of time. It is unlikely that this condition will be reached due to the effect of the environmental conditions. After a long period of time the pavement will start losing strength again due to cracking of the asphalt layer. The cracking can be induced by oxidation and aging of the asphalt and by excessive strains due to traffic loads and volumes. The ultimate curing condition was simulated in the laboratory by air curing for ten days followed by fifty hours at 140°F (60°C).

Since the intermediate curing (ten days air curing) was taken as the condition that would be prevailing in the pavement most of the specimens were cured for ten days. A few specimens were cured for only one day in order to assess the strength of the pavement during the critical period soon after construction. A few specimens were also cured in air and in the oven to obtain maximum strengths.

Table 6.2 is a summary of the curing times and the number of specimens in each.

#### 6.3.1.4. Density and Height Determination

The height of the specimen is important in the determination of the resilient modulus, Marshall stability, Hveem resistance value and the tensile strength. The height of the specimen was measured at three different positions and the average taken as the height of the specimen.



The density was determined in accordance with the ASTM D2776-71 test procedure. The procedure specified that the air dry weight, the weight in water and the saturated surface dry weight be measured and used in the calculation of the density.

This procedure was followed for all the specimens. The specimens that were placed in the vacuum saturation apparatus were weighed after the saturation.

#### 6.3.1.5. Water Sensitivity Test

This test method was designed by the Asphalt Institute to simulate the effect of prolonged exposure to subsurface water on other than open graded bases and temporary wearing surfaces (72).

The specimen was subjected to a vacuum of 1.25 inches (30 mm) Hg for one hour. Water at room temperature (73°F or 23°C) was then drawn into the vacuum chamber, submerging the specimen. The vacuum was then released and the specimen left submerged in water for 24 hours.

The vacuum saturation equipment is described in Chapter 6.

#### 6.3.1.6. Resilient Modulus and Poisson's Ratio Testing

The unsaturated samples were tested at three different temperatures viz. 34°F (1°C), 73°F (23°C) and 104°F (40°C), while the vacuum saturated samples were tested at 73°F (23°C) only. The three temperatures were selected to represent the following conditions:

1. Cold but unfrozen (34°F or 1°C). This would represent pavement conditions when the subgrade is unfrozen. Temperatures below freezing cause the subgrade to freeze and would therefore change the subgrade modulus to that of a stiff layer.





The cold but unfrozen condition will occur during the beginning of the winter and the spring thaw period.

2. Average temperature. The average temperature of approximately 70°F (21°C) represents the average temperature in the pavement. This is also about the temperature used in other studies to determine structural layer equivalencies (1,24, 35,72).
3. High pavement temperature (104°F or 40°C). This represents the condition during the warm summer months. Although pavement temperatures can be higher than 104°F (40°C) during the summer months it is difficult and impractical to determine the resilient modulus at much higher temperatures (35).

The same test specimen was tested at all three temperatures. The specimen was left in a temperature controlled room or oven for between 2 to 4 hours before testing. The specimen was taken from the controlled temperature condition and placed into the resilient modulus testing device at laboratory temperature (73°F). Care was taken to center the specimen and to keep the loading strips clean.

The pulsating load of 50 lb. (22.7 kg) was then applied to the specimen. Ten to twenty pulse loads were applied to precondition the specimen before the vertical and horizontal deformation readings were recorded. The vertical and horizontal deformations were measured by the three LVDT's and plotted on the chart recorder. Deformations for at least three pulse loads were taken before the load was turned off.

The specimen was rotated 120 degrees and the whole process repeated. The specimen was turned another 120 degrees and another set of readings taken.



The resilient modulus and Poisson's ratio were calculated from the resilient (or recoverable) deformations. The resilient modulus of a specimen was taken as the average of the three resilient moduli. Typical deformation plots were shown in Figure 5.11.

#### 6.3.1.7. Hveem Resistance Value

All the specimens were tested at room temperature (73°F or 23°C) in the Hveem stabilometer to determine the resistance (R) value. The procedure suggested by the Asphalt Institute was used (77). It is the same method that is used for the determination of the resistance value of soils.

The reasons for the determination of the Hveem-R-value rather than the Hveem-S-value were that the use of the R-value is suggested by the Asphalt Institute for cold mixtures, it was used by other researchers at Purdue University in studies on foamed asphalt and cold recycled mixtures and the static load on the specimen is only 2000 lb. (909 kg). This load of 2000 lb. (909 kg) is lower than the 6000 lb. (2727 kg) used to determine the Hveem stability (S) value. The specimen was therefore stressed to a lower level and this made the determination of the R-value more reliable.

#### 6.3.1.8. Marshall Variables

The Marshall testing equipment was used to determine the Marshall stability, flow, index and stiffness.

The method used was the one adopted by the Asphalt Institute and specified in ASTM D1559, except the test temperature was 73°F (23°C). The specimen was placed into the apparatus and loaded at a rate of



2 inches (51 mm) per minute until failure. The load and vertical deformation were recorded up to failure. These plots were used to calculate the Marshall stability, stiffness, index and flow as described in Chapter 6.

Eighty-nine of the specimens were tested using the Marshall equipment to determine the Marshall variables. All the tests were conducted at room temperature (73°F or 23°C).

#### 6.3.1.9. Indirect Tensile Strength

The Marshall equipment was used to determine the tensile strength at failure. The upper and lower test head of the compression testing machine were replaced with two 1/2 inch wide steel loading strips. The specimen was placed in between the two loading strips and centered. The load was then applied at a constant rate (2 inches or 51 mm per minute) until the specimen fail. The load and vertical deformations to failure were recorded. The failure load was used to calculate the tensile strength at failure ( $S_T$ ).

Forty-one specimens were tested in this way at three different temperatures viz. 34°F (1°C), 73°F (23°C) and 104°F (40°C). The specimens were kept at the testing temperature for between two and four hours before testing.

#### 6.3.1.10. Moisture Content During Testing

After the determination of the Marshall variables or the tensile strength the moisture contents of fifty specimens, representing all the combinations of storage time, curing time and temperatures were determined. The specimens were weighed after the tests and then dried to a



constant temperature of 230°F (110°C) to determine the dry weight.

These weights were used to determine the moisture content.

#### 6.3.1.11. Miscellaneous Tests

The following standard tests were also conducted on the laboratory compacted samples.

1. ASTM 2172-75 Method A Quantitative Extraction of bitumen from bituminous paving mixtures.
2. ASTM D2176-76 Test for kinematic viscosity of asphalt.
3. ASTM D5-73 Test for penetration of bituminous materials.
4. ASTM D70-76 Test of specific gravity of semi-solid bituminous materials.
5. ASTM D127-77 Test for specific gravity and absorption of coarse aggregate.
6. ASTM D128-78 Test for specific gravity and adsorption of fine aggregate.

#### 6.3.2. Cored Samples

The cores were taken approximately three to four weeks after construction. The thirty-five cores were cut into specimens with a height of approximately 2-1/2 inches (65 mm) when possible. The thin asphalt concrete layers were cut off first. The remaining core consisted of the recycled foamed asphalt base. Since the two base layers were approximately 2-1/2 inches thick, two specimens could be cut from each core. In cases where the cores were broken, specimens to a thickness as close as possible to 2-1/2 inches (65 mm) were cut.

The cut specimens were stored for another five to six weeks at room temperature (73°F or 23°C) before testing.





The testing procedure was exactly the same as that for the laboratory compacted specimens. The procedure described in paragraphs 6.3.1.4 to 6.3.1.10 was followed. Due to the roughness on the surfaces, some of the specimens could not always be rotated with 120 degrees when determining the resilient modulus.

Sixty-three core specimens were tested. Only forty-five specimens were higher than 2 inches (55 mm) and could be used to determine the Hveem-R-value. Fifteen of them had cracks, were badly broken or too uneven on the surface to be tested in the stabilometer. Therefore only thirty-one specimens were used to determine the Hveem-R-value. Only eighteen specimens were used in the determination of the Marshall indices. The indirect tensile test was conducted on the rest, since the height is not such an important factor in the test itself. The equation to calculate the tensile strength incorporates any height. This is not true for the determination of the Hveem-R-value and the Marshall stability, where corrections have to be made depending upon specimen heights.

The resilient modulus test can be and was conducted on specimens of any height. The test was also conducted on the specimens at three different temperatures as described earlier. The tests and the number of specimens in each test are summarized in Table 6.3.

Only five specimens were tested after vacuum saturation, since the influence of water was already investigated with the laboratory samples. In this study it was more important to obtain reliable values for the properties of the recycled material that could be used in the calculation of stresses, strains and deflections.



Figure 6.3. Number of Core Specimens Used in Each Test

		Dry	Vac. Sat.	Total
Total		58	5	63
Tests	1	26	5	31
	2	52	5	57
	3	13	5	18
	4	45	-	45

Test 1 = Hveem R value.

2 =  $M_R$  at 3 temperatures, except on the saturated specimens.

3 = Marshall test.

4 = Indirect tensile test.



#### 6.4. Asphalt Concrete Surface

Sixteen asphalt concrete surface specimens cut from the cores were tested to determine the resilient modulus and indirect tensile strength at three different temperatures as described above. Only three had heights of more than 2.2 inches (55 mm). The rest had heights of approximately 1.2 inches (30 mm).

Three specimens from a mixture sample taken during construction were compacted using the kneading compactor and the method described for the recycled mixtures (ASTM-D1561). They were cured in air for approximately a week. The resilient modulus and tensile strength were determined following the same testing procedure and equipment as described earlier. The testing temperature was 73°F (23°C).

#### 6.5. Evaluation of the Initial Pavement Layer

The testing conducted by personnel of the IDOH prior to construction has been described in Chapter 3. Ten four inch cores were analyzed as part of this study to determine the resilient modulus of the initial surface layer at three different temperatures viz. 34°F (1°C), 73°F (23°C) and 104°F (40°C). The cores were taken at random from the entire 8.8 mile (14 km) section. The cores were divided into a top and a bottom 2-1/2 inches (65 mm). From the ten cores nine specimens from the top 2-1/2 inches (65 mm) and five from the bottom 2-1/2 inches (65 mm) were obtained. A procedure similar to the one described in Section 6.3.1.6 was used to determine the resilient moduli. The Marshall stability, index, stiffness, and flow values at 73°F (23°C) were also determined using the procedure described in section 6.3.1.8.



## 6.6. In-Situ Tests on the Pavement Layers

### 6.6.1. Clegg Impact Tests

The Clegg impact soil tester and procedure described earlier were used to obtain a measure of the relative strength of the recycled base coarse layer. Tests were conducted at the center of each lane and in the wheel path on the layer a few hours after construction and at the same positions the following day. A set of data were also taken to investigate the variability on the pavement cross section.

The readings were in all cases taken after the fourth drop of the hammer.

### 6.6.2. Deflection Measurements

Deflection measurement using the Dynaflect were also taken by personnel of the Research and Training Center as described in Chapter 6. They were taken before, during and after construction at 0.1 mile intervals in the center of each lane.





## CHAPTER 7: RESULTS OF LABORATORY AND IN-SITU TESTS

### 7.1. Introduction

As described earlier the main objective of this study is to determine the structural layer equivalencies of the foamed asphalt recycled layer. This can and will be done by looking at the stresses, strains and deflections in the pavement as calculated with the layered elastic theory. The material properties (resilient moduli and Poisson's ratios) and the thicknesses of the layers must be known to use the theory. These properties can be determined mainly by two methods viz. direct in-situ or laboratory tests on the material from each layer or by nondestructive testing devices e.g. Dynaflect. The fatigue of the material is also of importance in the determination of structural coefficients. The fatigue characteristics were tested by means of indirect tensile tests.

The results from the direct in-situ and laboratory tests will be summarized and discussed in this chapter. The results of the secondary study on the foamed asphalt recycled material will also be summarized and discussed.

### 7.2. Subgrade Material

The results of the in-situ strength tests, performed with the DCP (dynamic cone penetrometer) and correlated with the CBR-values are given in Table 7.1. In all the cases at least two distinct layers could be detected. The top layer, with an average thickness of 4.8 inches



Table 7.1. Dynamic Cone Penetrometer (DCP) Test Results

Num.	Ave. Total 12"	Ave. 12" Subgr.	Ave. 24" Subgr.	CBR Gran. Layer	Thick- ness Gran. Inches	No. of Layers Detected
<u>Eastbound</u>						
1	19.8	9	9	33	5.4	2
3	14.9	12.5	12.5	20	3.8	2
5	9.9	5.5	5.5	14	6.2	2
7	16.8	9.2	7.1	40	2.6	3
9	12.9	8	8	16	7.4	2
11	17.2	12.5	10.8	40	1.8	3
13	16.0	13.6	10.9	23	4.0	3
17	15.3	11.6	9.6	21	3.6	3
21	29.9	18.7	16.8	40	5.0	3
25	13.1	12.7	9.7	14	4.8	3
27	20.2	14.5	11.8	29	3.4	4
29	13.6	10.5	8.5	22	2.4	3
33	19.7	14.7	12.8	31	3.0	3
36	16.0	14.0	10.6	21	3.2	4
37	21.3	11.1	10.1	45	3.6	3
39	8.2	5	5	14	4.2	2
41	13.9	11.4	7.5	22	2.6	3
42	14.8	9.9	7.9	29	2.6	3
<u>Westbound</u>						
4	14.5	7	7	25	5.0	2
8	11.9	6	6	19	5.4	2
12	21.5	12.6	9.8	45	2.8	3
16	23.8	11.9	9.9	50	3.4	3
20	26.8	22	22	37	3.8	2
24	12.0	8.5	8.5	14	7.6	2
28	30.0	10.0	10.0	40	4.2	2
32	25.0	15.0	11.0	18	5.4	2
36	13.0	8.0	7.0	24	3.2	3
40	27.0	22.0	22.0	37	4.2	2
Ave.		11.69		27.96	4.8	
S.D.		4.29		10.94		

1 inch = 25.4 mm



(120 mm) consisted of granular material with a GW-GM Unified Classification. The plasticity index (PI) was less than 2 in all cases. The average moisture content during sampling was 5.8% with a standard deviation of 2.6%.

The subgrade material underlying this granular layer consisted of a layer with only one CBR-value in approximately half of the positions tested. The rest of the positions had subgrade layers with two different CBR values, except for two which had three detectable different strengths at three different depths. All the layers had a Unified Classification of SM. The PI was in all cases less than 7 with an average of between 1 and 2. The average moisture content during the sampling was 15.2% with a standard deviation of 3.1%.

Table 7.2 summarizes these results of both the layers.

Figure 7.1 displays the manner in which the thickness and strength of the granular layer as well as the strength of the underlying layer (subbase) vary along the eastbound lane. The strength of the subbase is taken as the weighted average of the top 12 inches (300 mm).

The strength values and the thickness of the granular layer vary considerably. It will not be possible to select only one value to represent the strengths or thicknesses of the layers. Figure 7.2 shows that it is also true for the westbound lane.

Although the DCP was developed to get quick and approximate readings, the differences in thicknesses and strengths are large enough to detect these differences. For the same reason the order of accuracy of the thicknesses and strengths obtained from DCP-tests must be kept in mind.



Table 7.2. Characteristics of Subbase and Subgrade

		Granular Layer	Subgrade Soil
Moisture Content During Sampling (in %)	Mean	5.8	15.2
	S.D.	2.6	3.1
	Range	3.8-8.7	10.5-21.1
<hr/>			
PI ave.		1.0	2.0
range		NP-2	NP-7
<hr/>			
Unified Classification		GW-GM*	SM**
n		6	12

\*GW-GM = fines interfere with the free draining properties of the well graded coarse gravel.

\*\*SM = coarse grained silty sand.





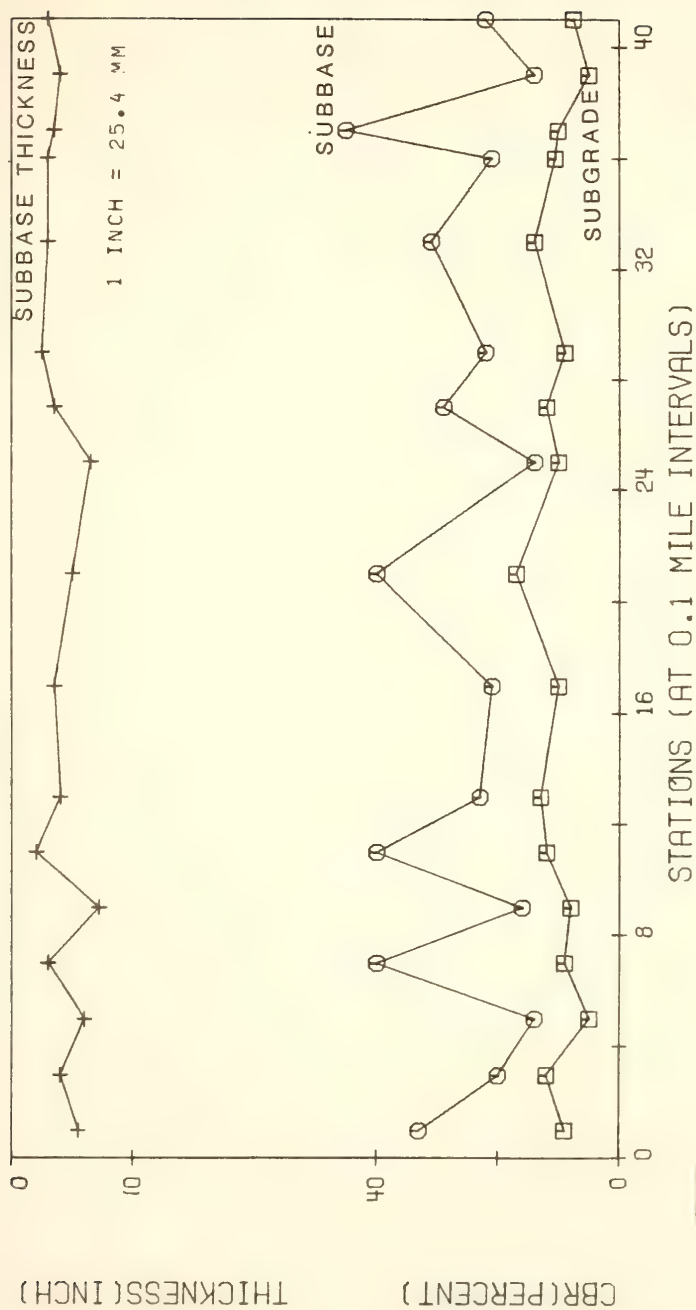


FIGURE 7.1 CBR AND THICKNESS OF THE SUBBASE AND THE SUBGRADE  
(EASTBOUND LANE)



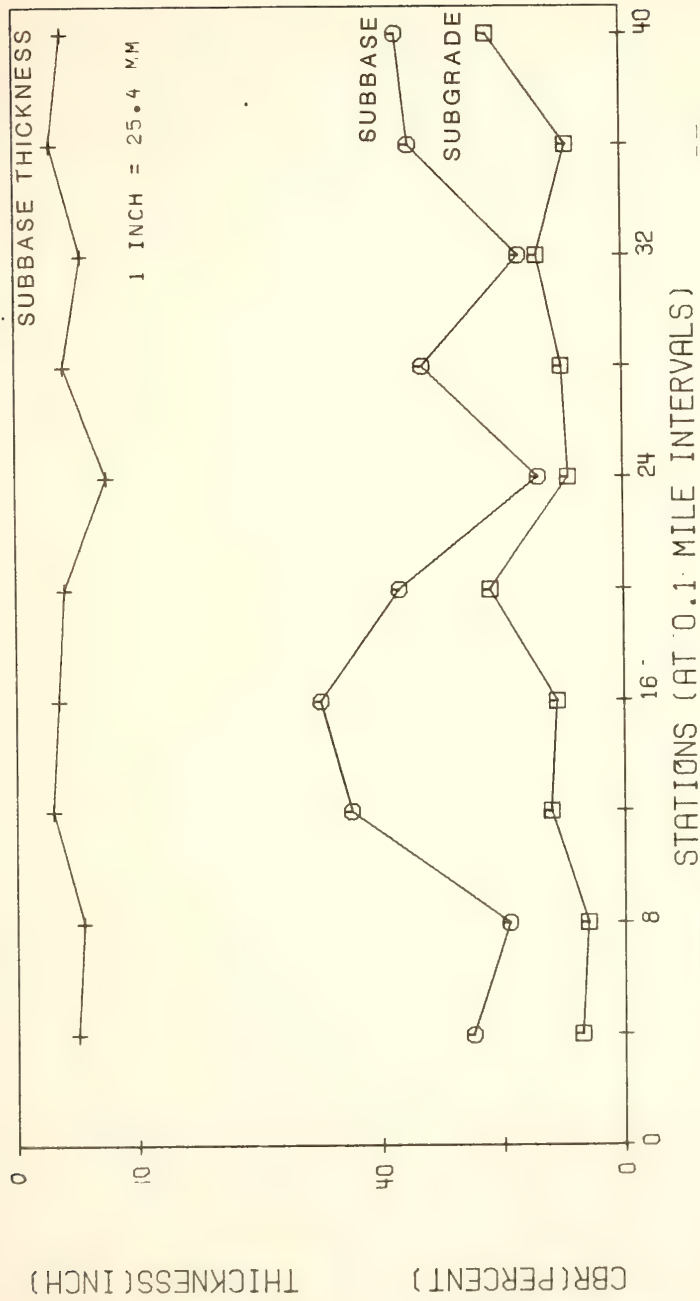


FIGURE 7.2 CBR AND THICKNESS OF THE SUBBASE AND THE SUBGRADE  
(WESTBOUND LANE)



### 7.3. Foamed Asphalt Recycled Material

This study was done to determine the layer equivalencies of the foamed asphalt recycled layer. A detailed study was conducted to determine the elastic parameters (resilient modulus and Poisson's ratio) and the tensile strength of the unsaturated samples. The unsaturated samples were chosen since the side drainage of the test road was adequate. All of the in-situ tests and deflection measurements were taken with the pavement layers in an unsaturated condition.

The specimens were obtained from two sources viz. laboratory compacted specimens and cores.

The results as they pertain to the main objectives of this study will be discussed in the first part of this section and in the second part as they pertain to the secondary objectives.

#### 7.3.1. Main Objectives

The laboratory compacted specimens were prepared from samples taken at twelve different positions in two different layers. The first step therefore was to find out if there are any differences between the elastic properties of the two layers, as well as if the properties at all the positions are the same.

Although the resilient modulus ( $M_R$ ) values at each of the six positions vary considerably, no statistical difference could be detected at  $\alpha = 0.05$  for the resilient moduli at 34°F (1°C), 73°F (23°C) and 104°F (40°C) respectively for the bottom layer. Not enough tensile strength values were available to test if they are the same at the six positions.



The resilient modulus values at 34°F (1°C) and 104°F (40°C) are statistically the same at  $\alpha = 0.05$ , while the  $M_R$ -values at 73°F (23°C) are statistically the same at  $\alpha = 0.01$  for the six locations in the top layer (second lift).

The standard one way analysis of variances was used to compare the means at the different positions. It also showed that all the values are homogeneous. Using the same procedure the resilient modulus values at 73°F (23°C) for all 12 locations show a statistical difference at  $\alpha = 0.05$  but they are all from a homogeneous subset according to the Student-Newman-Keuls procedure at  $\alpha = 0.05$ .

The standard t-test was used to compare the parameter mean values of the two layers. Since the  $M_R$ -values at the three temperatures, and the tensile strengths at 73°F (23°C) were the same at  $\alpha = 0.05$  respectively, average values were used to characterize the parameters for both layers combined. These values as well as the values for each layer separately are summarized in Tables 7.3 and 7.4.

It was not possible to compare the values of the parameters at different locations for the cored specimens, since only one specimen was tested from each core position in most cases. The resilient moduli at 34°F (1°C), 73°F (23°C) and 104°F (40°C) as well as the tensile strength values at 73°F (23°C) were the same at  $\alpha = 0.05$  respectively for both layers. The t-test was again used. The values are summarized in Tables 7.3 and 7.4.

The resilient modulus testing equipment is extremely sensitive and data are therefore influenced by factors such as humidity, air temperature, equipment temperature and noise and vibrations caused by other laboratory equipment. This is especially significant during the





Table 7.3. Results of Resilient Modulus and Poisson's Ratio Tests

(Unsaturated Specimens)						
		Temp (°F)	M <sub>R</sub> (psi)	S.D.	n	
Lab. Specimens	Top Layer	34	191,209	77,942	14*	
		73	93,897	20,517	19**	
		104	41,415	8,867	18*	
	Bottom Layer	34	214,209	120,450	17*	
		73	90,045	21,382	18*	
		104	40,274	9,824	18*	
	Both Layers	34	203,940	102,481	31***	
		73	92,024	20,741	37***	
		104	40,894	9,194	35***	
	-----					
	Core Specimens	Top Layer	34	168,451	75,335	18
			73	81,922	30,815	24
104			51,776	8,946	10	
Bottom Layer		34	174,169	89,309	13	
		73	73,516	17,681	19	
		104	48,642	9,177	11	
Both Layers		34	170,849	80,092	31***	
		73	78,207	25,919	43***	
		104	50,134	8,943	21***	
-----						
γ						
Poisson's Ratio	34	0.043	----	36		
	73	0.138	----	106		
	104	0.524	----	43		

\* means at 6 locations equal at  $\alpha = 0.05$ .

\*\* means at 6 locations equal at  $\alpha = 0.01$ .

\*\*\*means of both layers equal.

1 psi = 6.9 kPa

Note:  $M_R$  values homogeneous

Randomness was assumed, although the sampling was not completely random.



Table 7.4. Results of Indirect Tensile Strength Tests (Unsaturated Specimens)

		$S_T$ (psi)	sd (psi)	n
Samples	Top Layer	34.5	6.7	6
	Bottom Layer	32.4	7.4	4
	Both Layers	33.6	6.6	10*
Cores	Top Layer	29.3	11.9	16
	Bottom Layer	38.0	10.7	8
	Both Layers	28.9	11.0	24*

1 psi = 6.9 kPa

\* means of both layers equal.

Note:  $S_T$  values homogeneous.

Randomness was assumed, although the sampling was not completely random.



recording of very small deformations, which occur during the testing of stiff specimens. The cyclic load of 50 lb. (22.4 kg) is also too small to determine the  $M_R$  accurately due to the influence of the outside factors.

The reasons mentioned in the previous paragraph and the fact that the LVD's took approximately 20 min. to obtain a stable and uniform temperature (which was impractical to reach in this study) gave erratic and possibly unreliable Poisson's ratio values. The average Poisson's ratio values for both the laboratory compacted and core specimens are nevertheless given in Table 7.3.

The mean  $M_R$ -value at 34°F (1°C) and the tensile strength value at 73°F (23°C) were the same for the laboratory compacted and the core samples at  $\alpha = 0.05$ . This was not the case for the  $M_R$ -values at 73°F (23°C) and 104°F (40°C) respectively.

The resilient moduli for the laboratory compacted and core specimens are shown in Figure 7.3 at different temperatures. The resilient modulus values change, as expected, significantly with temperature.

The main reasons for the differences in  $M_R$ -values seem intuitively to be due to differences in densities, asphalt contents, moisture contents during compaction and testing. There are differences between the densities and testing moisture content, but not between the asphalt contents. The main reason for these differences seems to be the density, since higher densities give higher  $M_R$ -values as can be seen in Table 7.5. It can be seen from the same table that although the testing moisture contents differ, a high moisture content does not



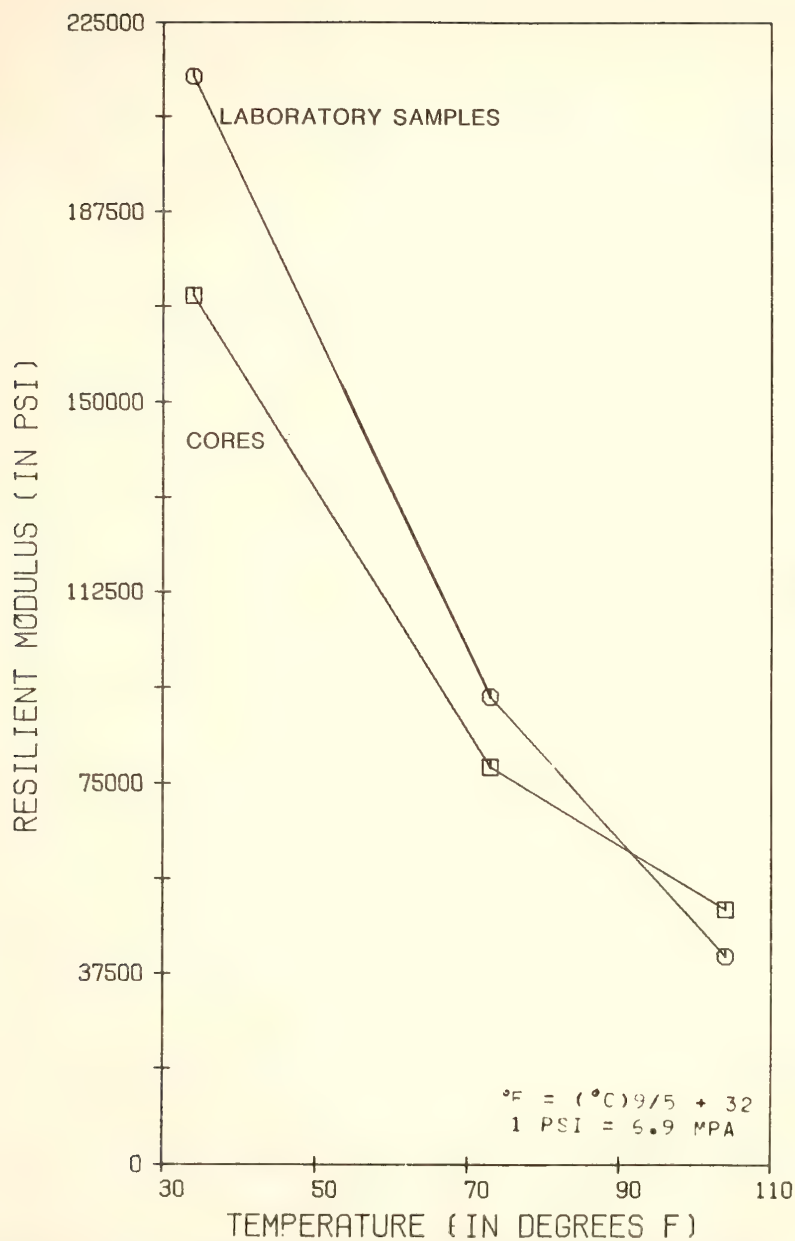


FIGURE 7.3 EFFECT OF TEMPEATURE ON THE RESILIENT MODULUS





Table 7.5. Density and Moisture Content of the Unsaturated Samples

			$\bar{X}$	S.D.	n	$\bar{M}_R(73^\circ\text{F})$
Samples	Top Layer	w	0.58	0.12	6	93,897
		$\gamma$	148.01	1.12	18	
	Bottom Layer	w	0.73	0.08	16	90,045
		$\gamma$	147.01	1.31	17	
	Both Layers	w	0.66	0.12	12**	92,024
		$\gamma$	147.51	1.31	35	
Cores	Top Layer	w	0.27	0.19	5	81,922
		$\gamma$	138.59	2.93	20	
	Bottom Layer	w	0.23	0.11	4	73,516
		$\gamma$	137.16	6.61	8	
	Both Layers	w	0.25	0.15	9*	78,207
		$\gamma$	137.90	5.05	38	

$\bar{X}$  = average value

w = moisture content during testing (%)

$\gamma$  = density (pcf)

\* means of 2 layers equal at  $\alpha = 0.05$

\*\*means of 2 layers not equal at  $\alpha = 0.05$

1 pcf =  $0.0160 \text{ gm/cm}^3$

1 psi = 6.9 kPa

Note:  $\gamma$  not homogeneous

w homogeneous

Randomness was assumed, although the sampling was not completely random.



ensure a high  $M_R$ . These factors are further explored later on in this chapter. The compaction moisture content cannot be compared since the values for the core specimens were not available.

The laboratory compacted specimens are expected to have higher densities since the kneading compaction method was used and it simulates the density in the pavement after one year in use.

In a study on eighteen laboratory compacted specimens from one sample the influence of curing time and temperature on the resilient modulus and indirect tensile strength were investigated. Three different curing times viz. 1 day in air, 10 days in air and 10 days in air plus an additional 50 hours at 140°F (60°C), as described in the previous chapter, were used.

There were no statistical differences at  $\alpha = 0.05$  among the means of the densities and asphalt contents of the eighteen specimens.

Table 7.6 summarizes the results, while Figures 7.4 and 7.5 display the results graphically. The  $M_R$  increased substantially from the 10 day air curing to the optimum curing condition at all temperatures. The increase from the 1 day curing to the 10 day curing condition was also significant, but less profound. The  $M_r$  at 73°F (23°C) after only 1 day of air curing is more than 50,000 psi (207 MPa) and stiff enough to be opened to traffic.

The 10 day air curing simulates the condition of the pavement layer after a few months in service. The ultimate curing simulates the condition after a few years in service under ideal conditions viz. no water in the layer, no freeze-thaw cycles, no fatigue cracking, no noticeable oxidation of the asphalt cement. This condition is very



Table 7.6. Results of Tests on the Effect of Curing Time on the Resilient Modulus and Tensile Strength

	Temp (°F)	$\bar{S}_T$ (psi)	S.D.	$\bar{M}_R$ (psi)	S.D.	n	w test(%)
Curing Time	0 Day	34	71.6	168558	7540	2	1.5
		73	21.5	52947	15855	2	1.3
		104	7.3	31432	2072	2	1.1
	10 Days	34	132.1	187716	53869	2	0.75
		73	40.0	103990	2901	2	0.65
		104	9.9	39693	5786	2	0.74
	Maximum	34	200.0	519728	112438	2	0.27
		73	40.2	303576	36381	2	0.28
		104	13.6	65537	15529	2	0.20

1 psi = 6.9 kPa



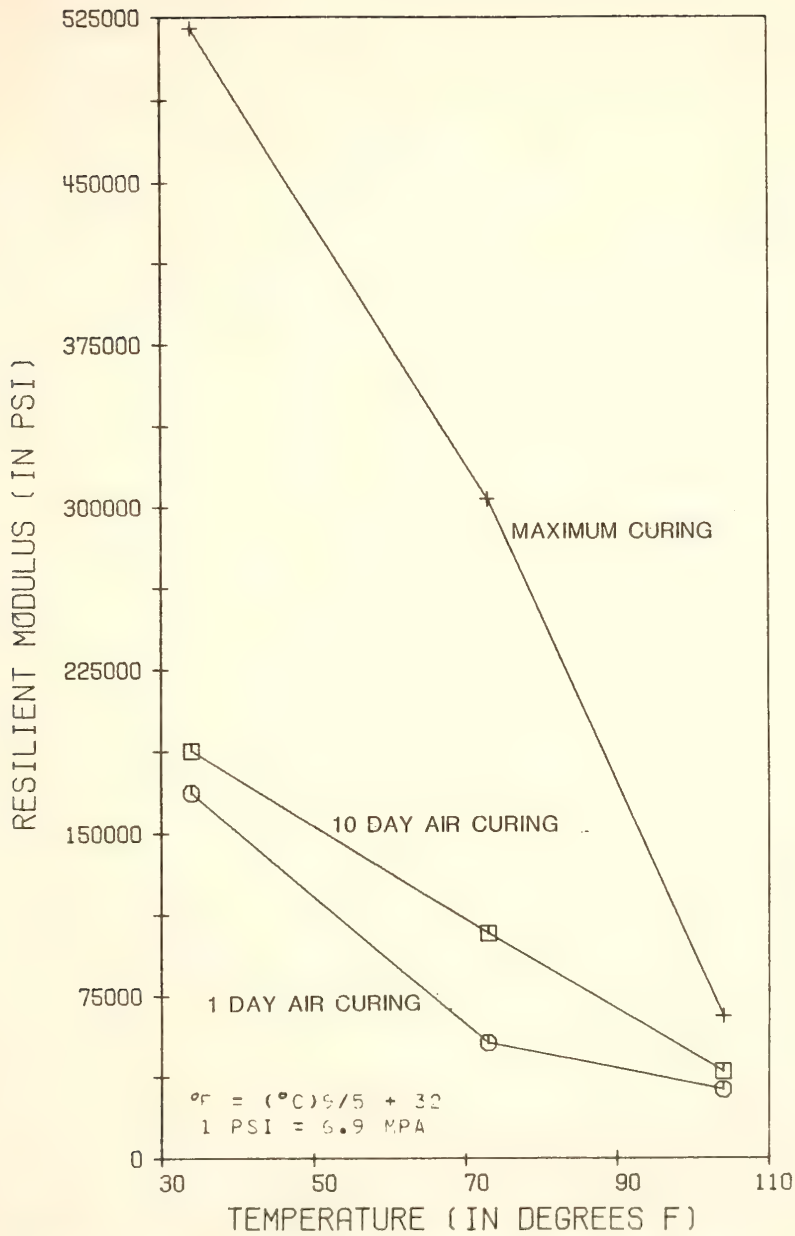
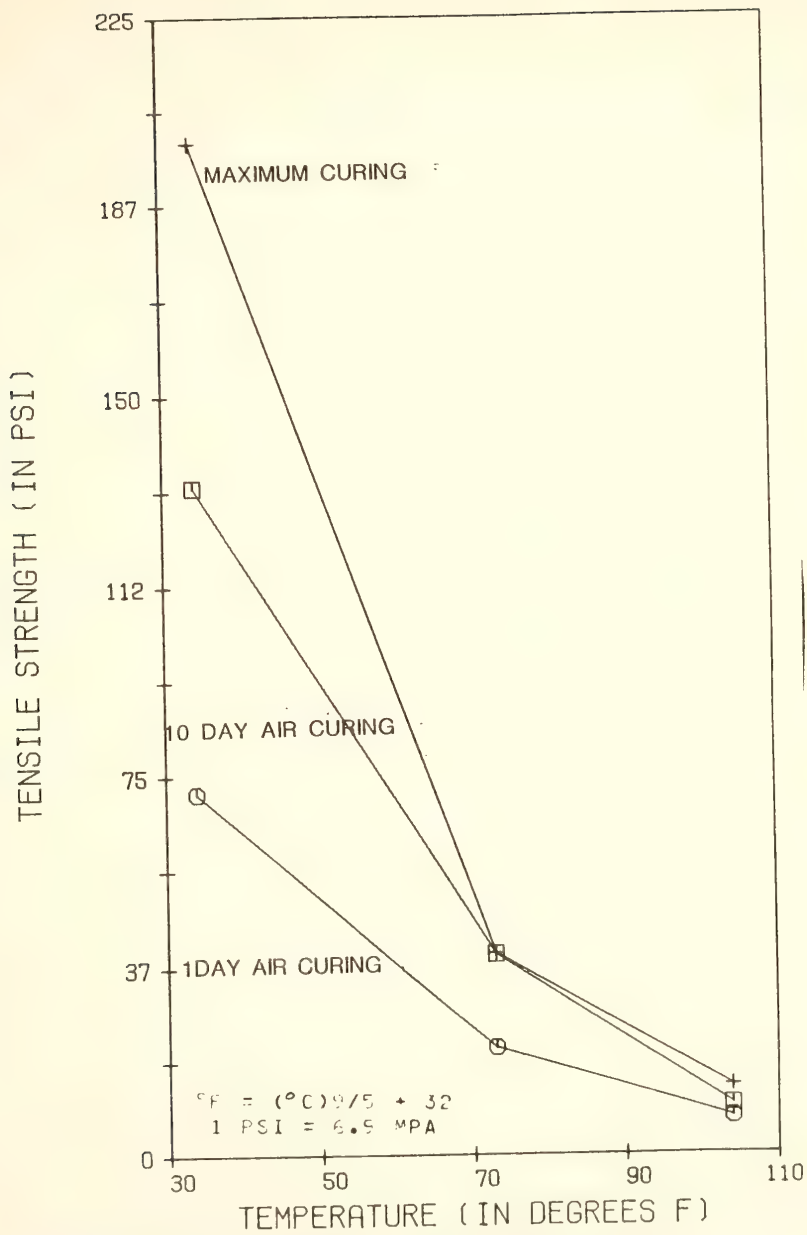


FIGURE 7.4 EFFECT OF CURING TIME ON THE RESILIENT MODULUS







**FIGURE 7.5 EFFECT OF CURING TIME AND TEMPERATURE ON TENSILE STRENGTH**



unlikely to be reached in the pavement and therefore the maximum  $M_R$  will lie between the 10 day air curing values and the ultimate curing values at all temperatures.

The influence of curing time is less profound on the indirect tensile strength ( $S_T$ ). The largest increase seems to be between the 1 day and 10 day air curing condition at 73°F (23°C). At 104°F (40°C) the biggest increase occurred after the 10 day air curing period. The increase in tensile strength was equally distributed among the three curing times at 34°F (1°C). The maximum tensile strength should, as with the  $M_R$ , be between the 10 day air curing and ultimate curing values.

Both the  $M_R$  and the  $S_T$  are influenced significantly by temperature. The  $S_T$  is influenced more than the  $M_R$ .

The values for the  $M_R$  and  $S_T$  obtained from these eighteen specimens correspond very well with the values obtained from the specimens prepared from the samples taken at the same position and used in the comparisons and results described in the beginning of this section (Tables 7.3 and 7.4). It is therefore a representative sample and the foamed asphalt recycled material can be expected to behave similarly and have approximately the same values.

#### 7.3.2. Secondary Objectives

The same specimens that were used to obtain the results presented in the previous section were used to obtain information regarding the Hveem-R and Marshall variable values. These values can be used to compare the recycled foamed asphalt mixture with other asphalt stabilized mixtures and specifications for asphalt base courses. An



attempt was also made in this section to explain the behavior of the mixture based on density, asphalt content and moisture content. The influence of water on the mixture was also investigated. For this part of the study extra specimens had to be compacted.

Table 7.7 summarizes the results of the tests mentioned in the previous paragraph on the unsaturated specimens. A one way analysis of variance procedure was again used to conclude that the mean values at each location in each of the two layers were equal at  $\alpha = 0.05$  where possible. The means of each of the two layers were compared using the standard t-test. The means of the Marshall stability, stiffness, flow, Hveem-R-value and density of the laboratory compacted samples are significantly higher at  $\alpha = 0.05$  than the appropriate mean values of the core specimen values (Table 7.9). This is to be expected since the laboratory samples are compacted to a higher density and some of the core samples were slightly cracked and disturbed. Figures 7.6 to 7.12 depict these differences.

The influence of vacuum saturation on the test parameters of 36 laboratory compacted specimens from the six different positions in each of the two layers is summarized in Table 7.8. Only five core specimens were exposed to water. The test parameters obtained from them have large variances and the test parameter values of the saturated and unsaturated core specimens are the same at  $\alpha = 0.05$ . This is not reliable due to the small number of saturated specimens. The saturated laboratory compacted specimens have lower Marshall stability, stiffness, index, Hveem-R and  $M_R$  at 73°F (23°C) values, but only the difference in mean  $M_R$ -values is significant at  $\alpha = 0.05$ . The rest of the differences



Table 7.7. Summary of Results of Tests on the Unsaturated Specimens

	Top Layer			Bottom Layer			Both Layers		
	$\bar{X}$	S.D.	n	$\bar{X}$	S.D.	n	$\bar{X}$	S.D.	n
R	84.9	2.6	18	86.6	2.41	18	85.8	2.6	36
Marshall									
Stab. (1b) <sup>3</sup>	3280	190	18	2640	630	18	2960	560	36*
Index (x 10 <sup>3</sup> lb/inch)	43.1	5.4	18	47.3	11.1	18	45.2	8.6	36*
Stiffness (x 10 <sup>3</sup> lb/inch)	18.2	3.1	18	22.8	4.5	18	20.5	4.5	36*
Flow (0.01 inch)	18.9	3.2	18	12.2	2.7	18	16.3	4.2	36**
$\gamma$ (pcf)	147.01	1.31	17	148.01	1.12	18	147.5	1.31	35
$w_{comp}$ (%)	2.40	0.28	6	3.02	0.76	6	2.53	0.75	12*
$w_{test}$ (%)	0.58	1.46	6	0.73	0.08	6	0.66	0.12	12*
R	80.8	6.9	12	76	10.6	13	78.3	9.2	25
Marshall									
Stab. (1b) <sup>3</sup>	2580	1430	5	1720	640	7	1960	1050	12*
Index (x 10 <sup>3</sup> lb/inch)	21.7	10	5	13.5	4.9	7	16.0	8.6	12*
Stiffness (x 10 <sup>3</sup> lb/inch)	9.2	3.8	5	5.6	1.7	7	7.3	4.2	12*
Flow (0.01 inch)	28.0	4.0	5	36.0	14.7	7	32.0	13.0	12*
$\gamma$ (pcf)	137.16	6.61	18	138.59	2.93	20	137.9	5.05	38
$w_{test}$ (%)	0.27	0.19	5	0.23	.11	3	0.25	0.15	9*

\* means of values for the two layer equal at  $\alpha = 0.05$ .\*\*means of values for the two layer not equal at  $\alpha = 0.05$ .

1 inch = 25.4 mm  
 1 lb = 4.45 N  
 1 pcf = 0.0160 gm/cm<sup>3</sup>

Note : All values except R and  $\gamma$  are homogeneous  
 Randomness was assumed, although the sampling  
 was not completely random.





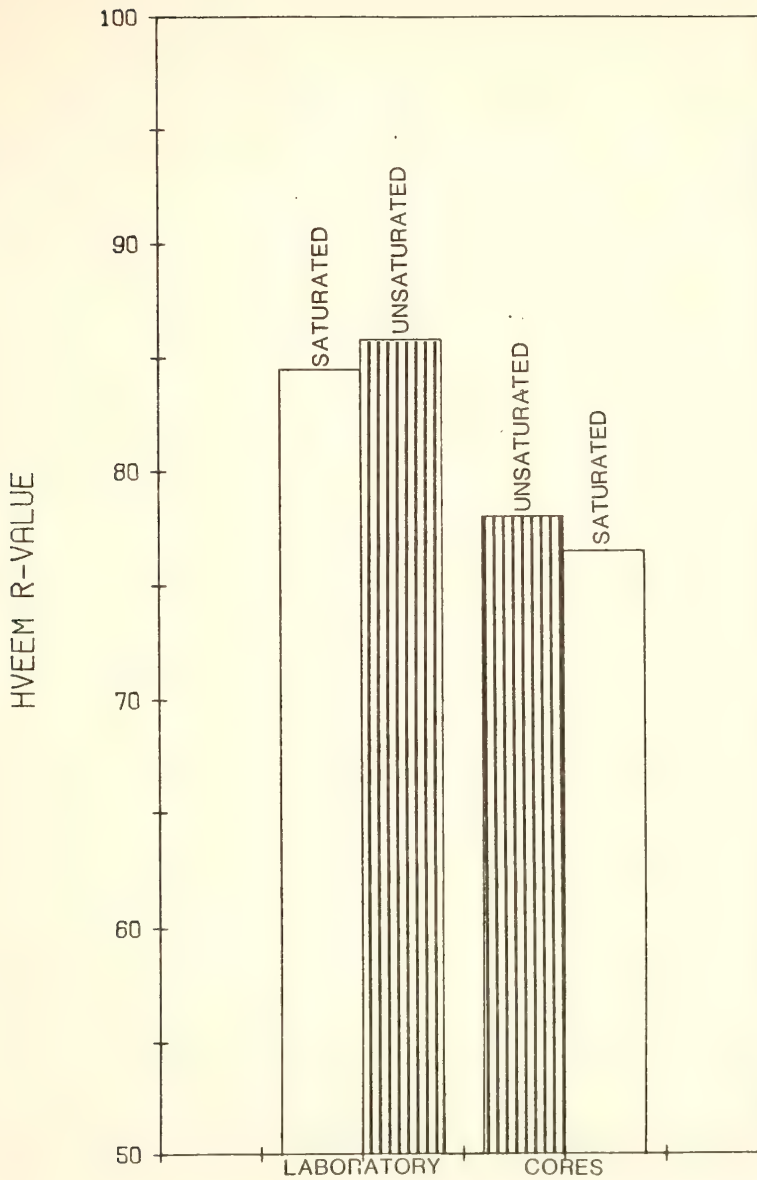


FIGURE 7.6 EFFECT OF WATER ON THE HVEEM-R-VALUE



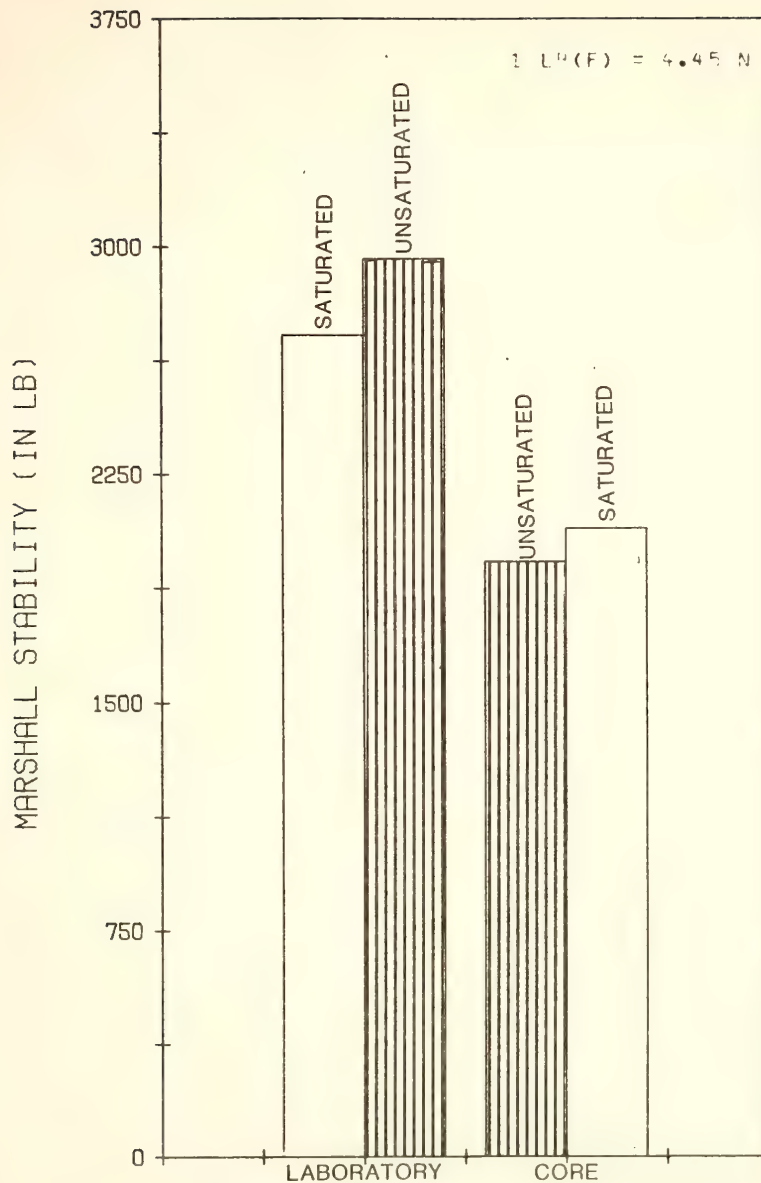


FIGURE 7.7 EFFECT OF WATER ON THE MARSHALL STABILITY



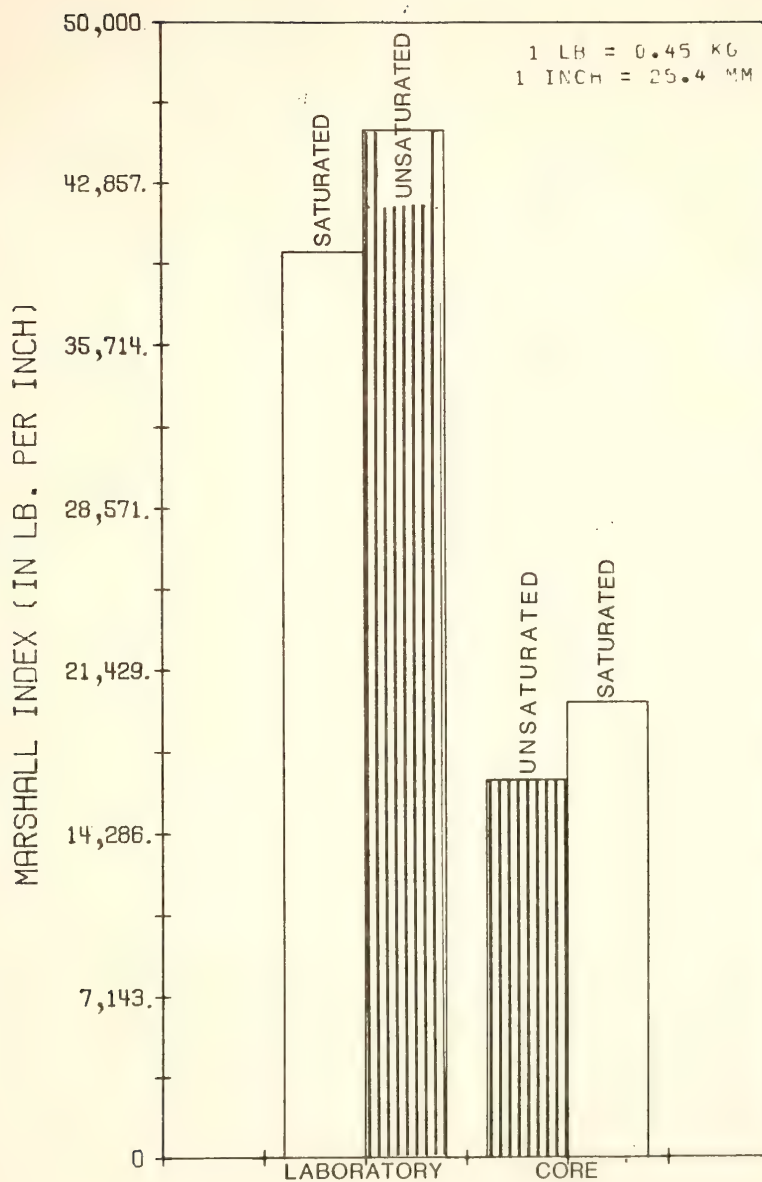


FIGURE 7.8 EFFECT OF WATER ON MARSHALL INDEX



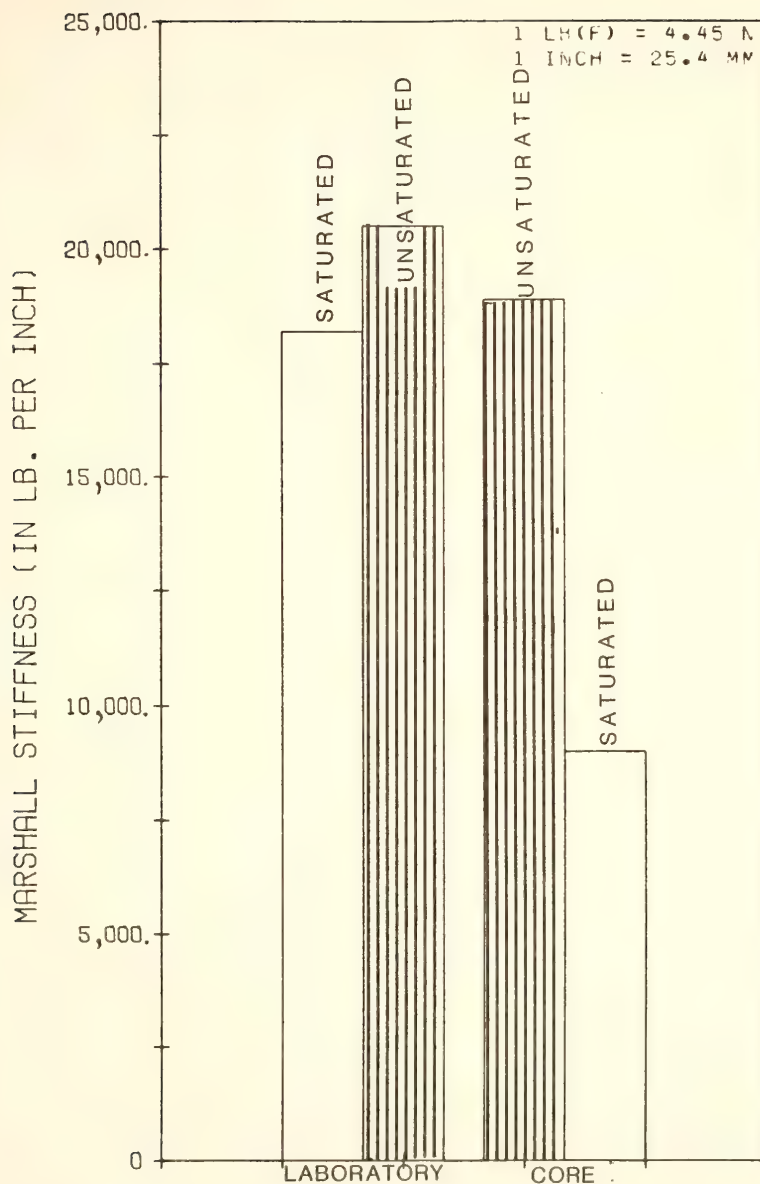


FIGURE 7.9 EFFECT OF WATER ON THE MARSHALL STIFFNESS





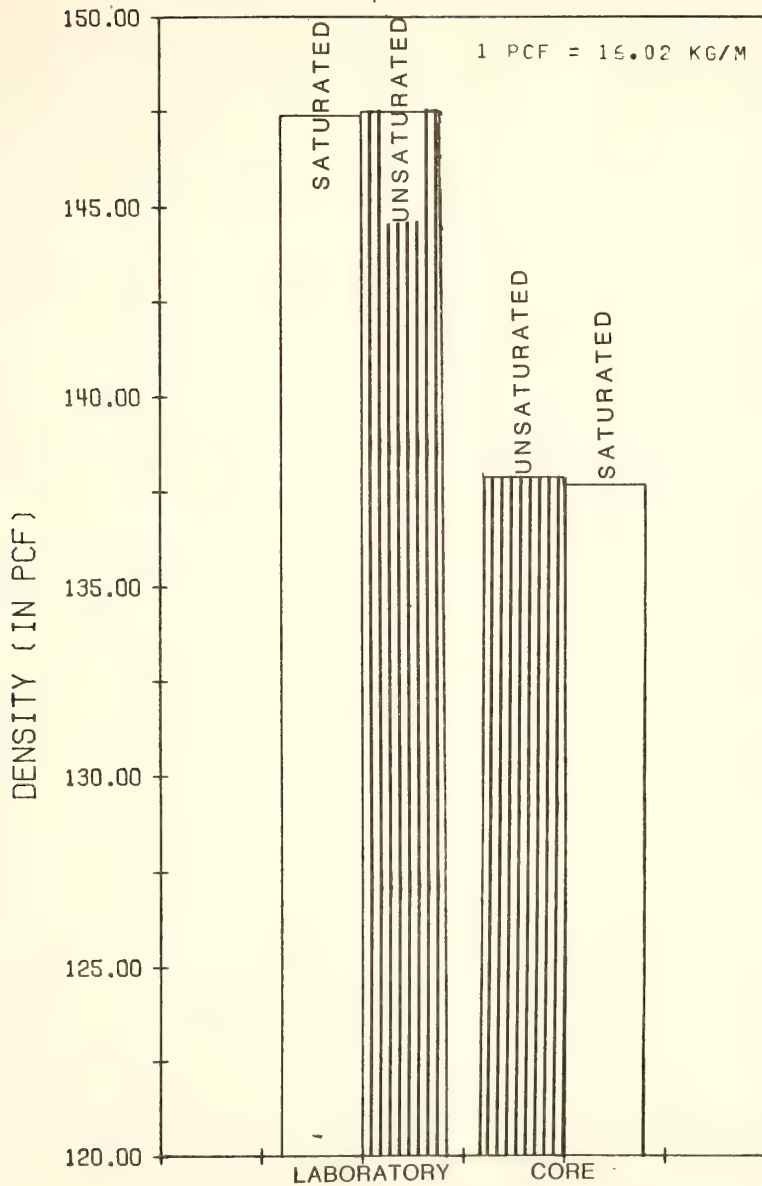


FIGURE 7.10 EFFECT OF WATER ON THE SPECIMEN DENSITY



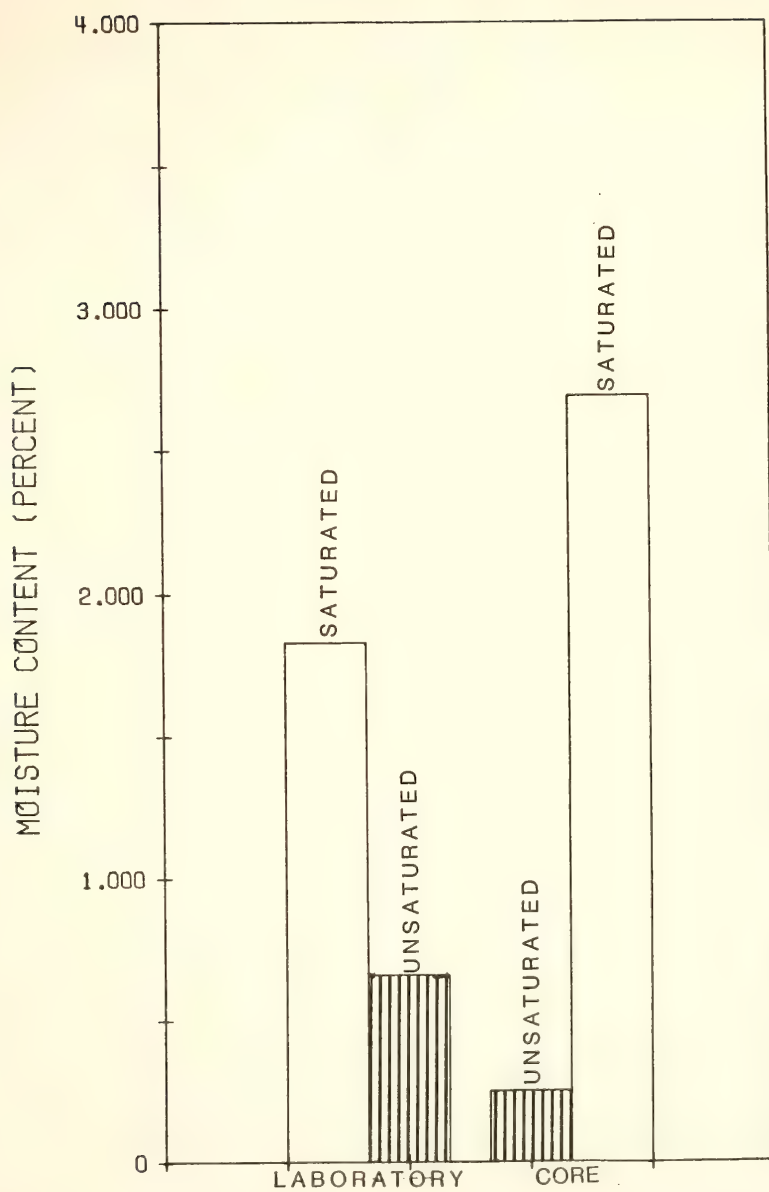


FIGURE 7.11 EFFECT OF WATER ON THE TESTING MOISTURE CONTENT



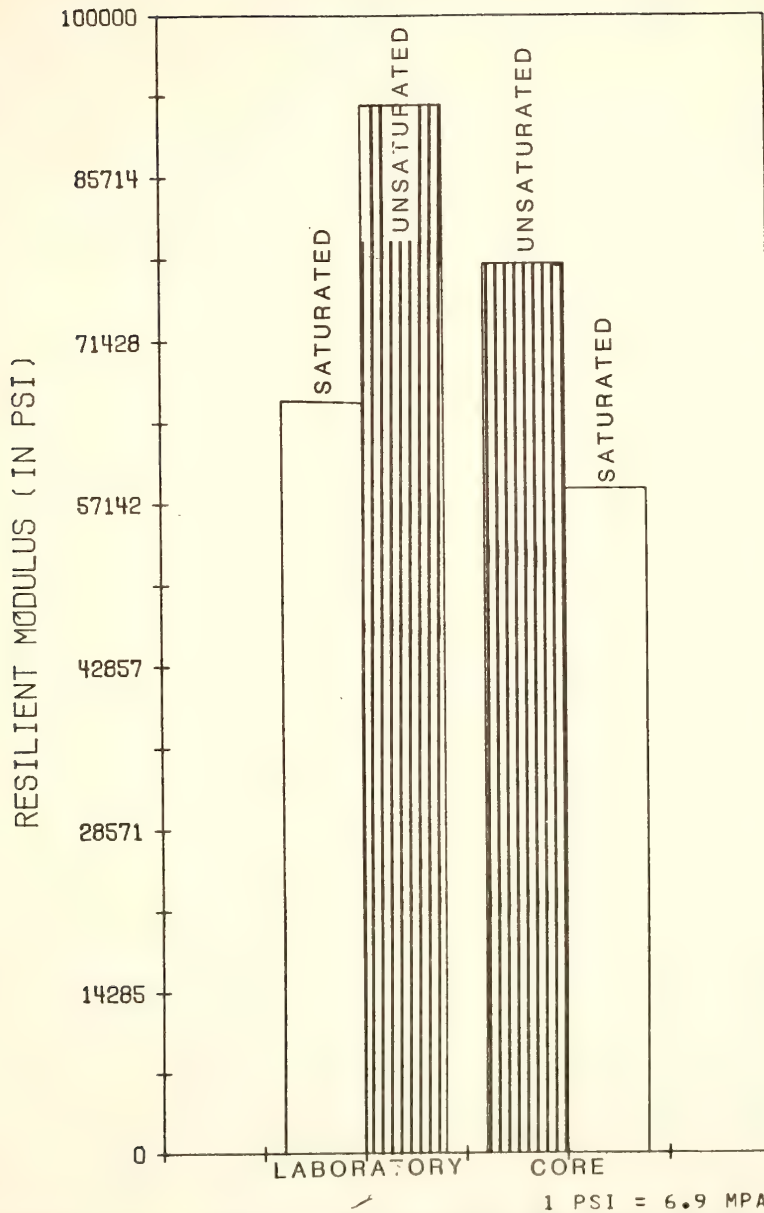


FIGURE 7.12 EFFECT OF WATER ON THE RESILIENT MODULUS



Table 7.8. Summary of Results of Tests on Saturated Specimens

Lab	Top Layer			Bottom Layer			Both Layers		
	$\bar{X}$	S.D.	n	$\bar{X}$	S.D.	n	$\bar{X}$	S.D.	n
R Marshall	83.7	2.7	18	85.4	4.4	17	84.5	3.6	35*
Stab. (lb) <sup>3</sup>	2830	240	12	2440	522	13	2710	522	25*
Index (x 10 <sup>3</sup> lb/inch)	37.2	5.3	12	42.2	8.3	13	39.7	7.11	25*
Stiffness (x 10 <sup>3</sup> lb/inch)	17.3	2.6	12	19.5	4.2	13	18.4	3.5	25*
Flow (.01 inch)	19.0	3.2	12	13.6	3.2	13	16.3	4.2	25**
M <sub>R</sub> (73°F) (psi)	69434	16563	17	63038	8258	18	66236	13289	35*
S <sub>T</sub> (73°F) (psi)	32.9	6.5	5	34.1	6.9	3	33.9	5.9	8*
γ (pcf)	148.2	0.87	18	146.8	1.87	16	147.4	1.50	34*
w <sub>comp</sub> (%)	2.04	0.28	6	3.02	0.76	6	2.53	0.75	12*
w <sub>test</sub> (%)	1.62	0.31	6	2.03	0.50	6	1.83	0.70	12*
R Marshall	83	1.4	2	70.0	11.3	2	76.5	10.0	4*
Stab. (lb) <sup>3</sup>	2250	140	3	1810	1004	2	2070	1020	5*
Index (x 10 <sup>3</sup> lb/inch)	20.7	10.7	3	19	19.8	2	20	12.5	5*
Stiffness (x 10 <sup>3</sup> lb/inch)	8	3	3	10.5	12.05	2	9.0	6.5	5*
Flow (0.01 inch)	28	14	3	30	24.0	2	28.8	15.6	5*
M <sub>R</sub> (73°F) (psi)	53640	1200	2	61225	10860	2	58430	7500	4*
S <sub>T</sub> (73°F) (psi)	--	--	--	--	--	--	--	--	--
γ (pcf)	138.3	4.43	3	135.60	3.79	2	137.7	3.95	5*
w <sub>test</sub> (%)	3.97	--	1	2.10	--	1	2.69	1.11	3*

\* means of both layers equal at  $\alpha = 0.05$ .\*\*means of both layers not equal at  $\alpha = 0.05$ .

1 inch = 25.4 mm

1 lb = 4.45 N

1 pcf = 0.0160 gm/cm<sup>3</sup>





are significant at an alpha value of approximately 0.10 (Table 7.9). These differences were again depicted in Figures 7.6 to 7.12.

Table 7.9 gives a summary of the results of statistical tests on the test parameters to verify that there are differences in the mean values at  $\alpha = 0.05$ . In the cases where the differences are not significant it is not possible to conclude that one value is different from another. The level of significance can be increased by taking more observations.

Another objective was to investigate the influence of storage of the foamed asphalt recycled mixture on the test parameters. Twenty eight specimens were compacted after 1, 3, 4, 5, 6, 7, 10, 14 and 21 days in a closed plastic bag and then air cured for 10 days before testing. The Hveem-R-values, Marshall variables, resilient modulus density and moisture content were determined. The strength parameter,  $M_R$ , showed a decrease in strength after 10 days when the mixture is stored in a closed plastic bag (Figure 7.13). The  $M_R$  increased after that. The density and compaction moisture content did not follow the same trend and were essentially constant. The Marshall variables and Hveem-R-value showed changes, but no definite trend could be detected. Since the strength gain should be the same for all the specimens it can be hypothesized that the reasons for the differences in  $M_R$  values after 10 days occurred because the initial  $M_R$  modulus values were different. The additional asphalt cement seemed to have had a softening effect on the original asphalt as has been reported by others (28,66). This softening effect is easier to detect in the  $M_R$  values which is a measure of the stiffness of the mixture, than in the Marshall variables and Hveem-R-values. The equipment used to measure these parameters



Table 7.9. Results of Statistical Comparison Tests

	Lab.		Cores		Sat.		Unsat.	
	Sat. vs.	Unsat.	Sat. vs.	Unsat.	Lab. vs.	Cores	Lab. vs.	Unsat.
$M_R$ (34°F)	*		*		*			NS
(73°F)	S		NS		S			NS
(104°F)	*		*		*			S
ST (73°F)	NS		*		*			NS
R	S ( $\alpha=.10$ )		NS		S			S
Marshall								
Stability (1b)	S ( $\alpha=.10$ )		NS		S			S
Stiffness( $\times 10^3$ lb/inch)	S ( $\alpha=.10$ )		NS		S			S
Index ( $\times 10^3$ lb/inch)	S		NS		S			S
Flow (0.01 inch)	NS		NS		S			S
$\gamma$ (pcf)	NS		NS		S			S
$w_{comp}$ (%)	NS		*		*			*
$w_{test}$ (%)	S		S		S ( $\alpha=.10$ )			S

\* = no values to be compared

S = means significant at  $\alpha=0.05$ , except where indicated otherwise.NS = not significant at  $\alpha=0.10$ .

1 inch = 25.4 mm

1 lb = 4.45 N

1 pcf = 0.0160 gm/cm<sup>3</sup>



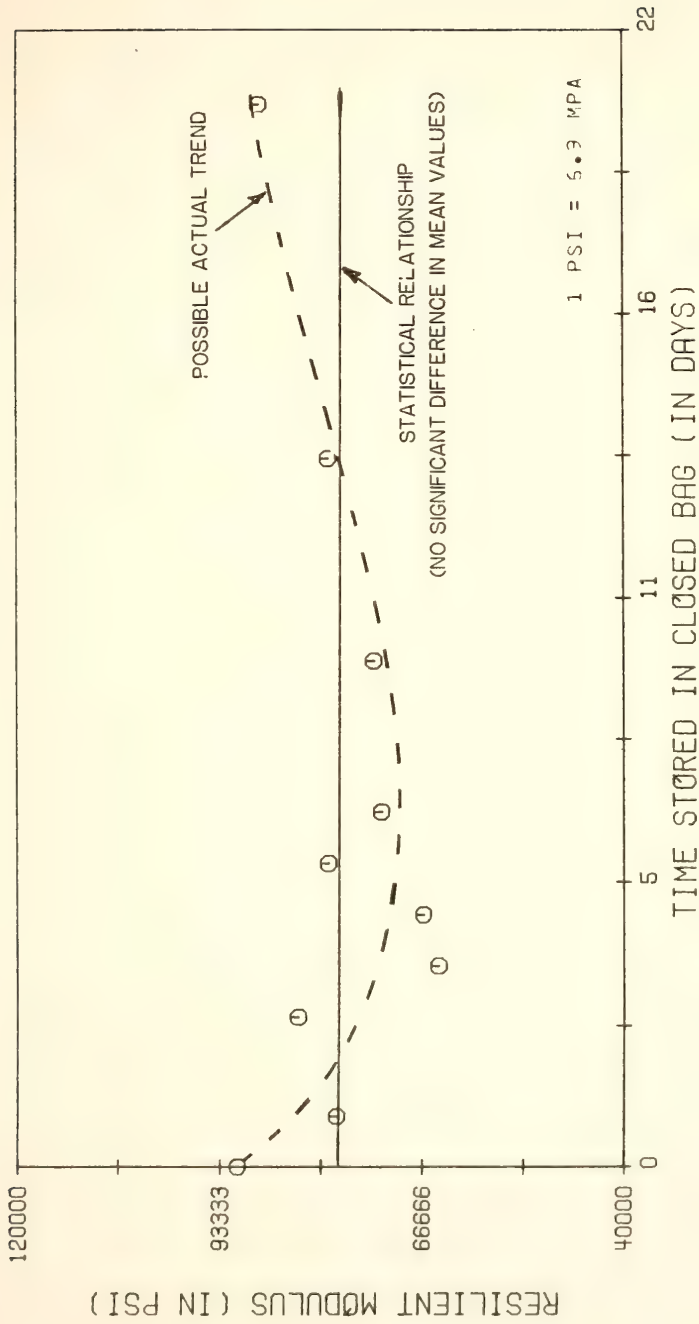


FIGURE 7.13 EFFECT OF TIME STORED IN A CLOSED BAG ON RESILIENT MODULUS



might also not be sensitive enough to measure the parameters to the required level of accuracy. The storage of the mixture in a plastic bag has some influence on the  $M_r$  and to a smaller extent the Marshall variables and Hveem-R-value, but the exact magnitude and reasons cannot be obtained from this study. No curing seems to occur during the storage period.

In a comparison between the strengths of the foamed asphalt recycled mixture when stored open in air against storage in a closed plastic bag it was found that the resilient moduli of the specimens compacted from the mixture stored in the closed bag were significantly higher (at  $\alpha = 0.05$ ) than those from mixtures stored in the open. The Marshall variables are different at a level of  $\alpha = 0.10$ , but the Hveem-R-values are not different. Although the densities and the testing moisture contents of the specimens compacted from the mixture stored in the closed bag were higher than those compacted from a mixture stored in the open they were not significantly different at  $\alpha = 0.05$  (Figures 7.14 to 7.17).

Stockpiling (storage in the open) will reduce the  $M_R$  of the mixture, but will have little effect on the Marshall stability and R-value. Recycled foamed asphalt mixtures can be stored in closed plastic bags and used in laboratory tests without seriously influencing the Marshall variables and R-value. The effect on the  $M_r$  does not seem to be large, but is present.

In an attempt to explain the behavior of the strength parameters, they ( $M_R$ , R-value and Marshall variables) were related to density, compaction moisture content, testing moisture content and the loss of moisture





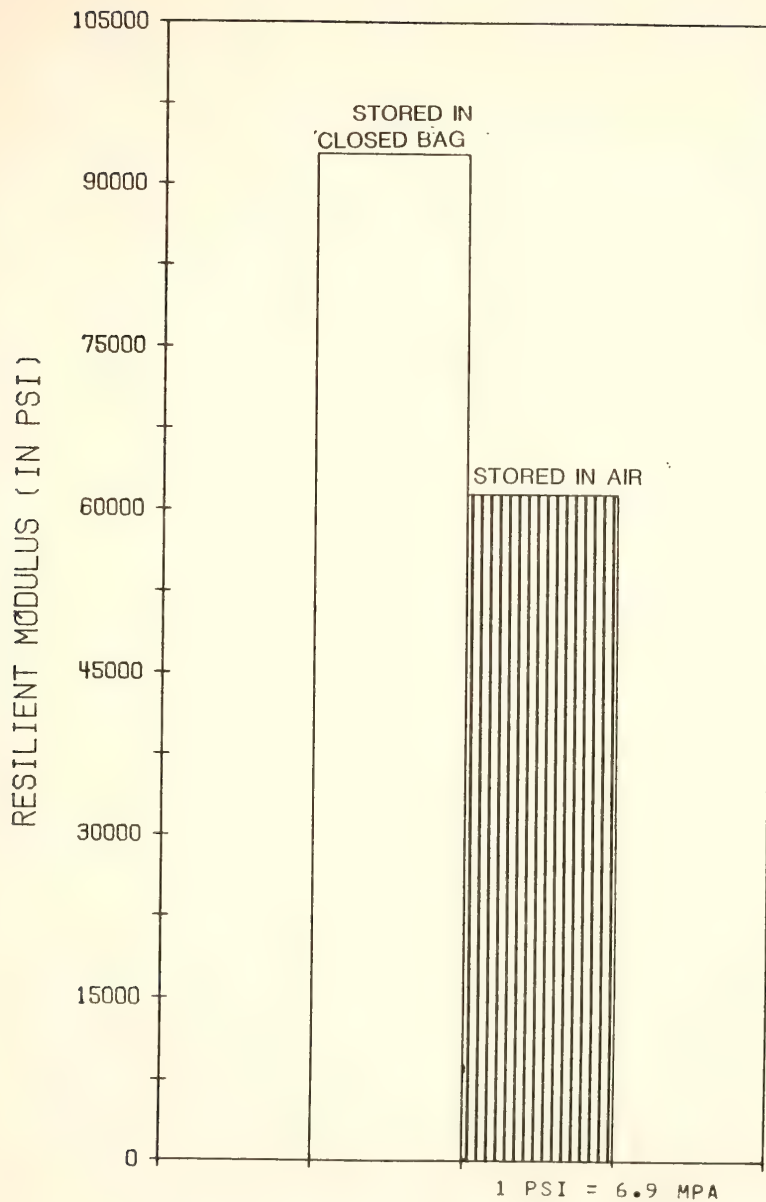


FIGURE 7.14 EFFECT OF STORAGE IN AIR ON THE RESILIENT MODULUS



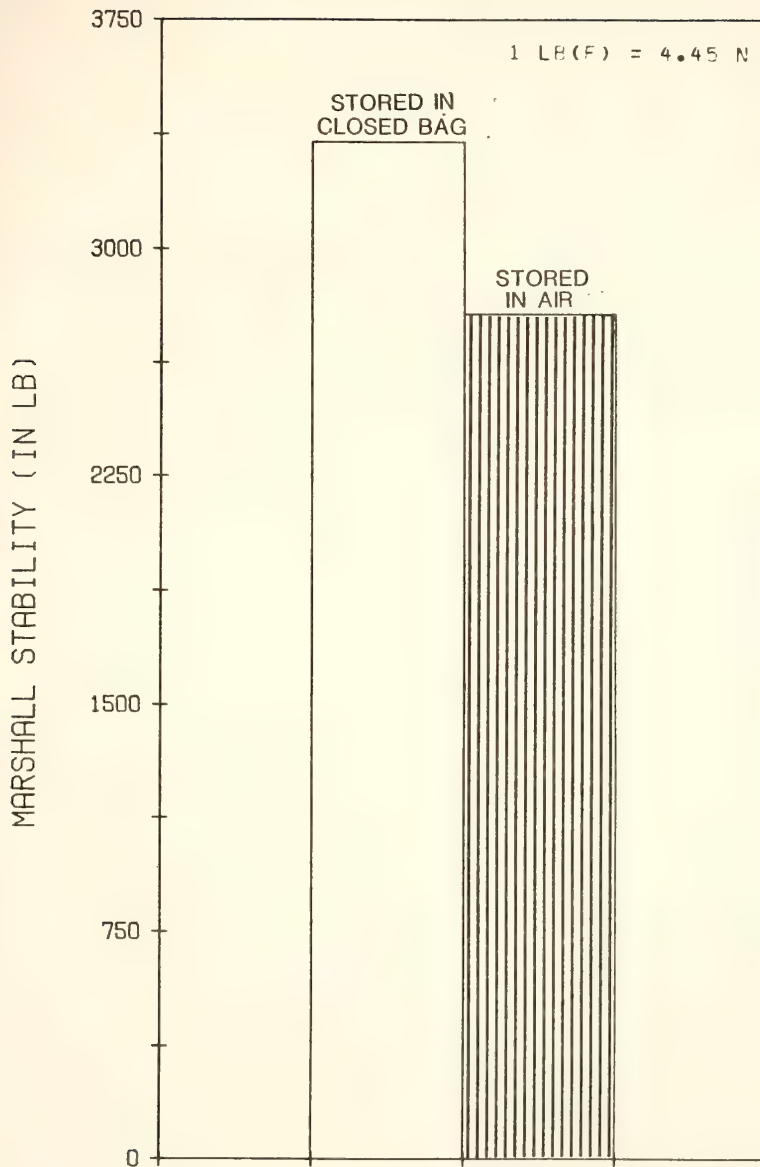


FIGURE 7.15 EFFECT OF STORAGE IN AIR ON THE MARSHALL STABILITY



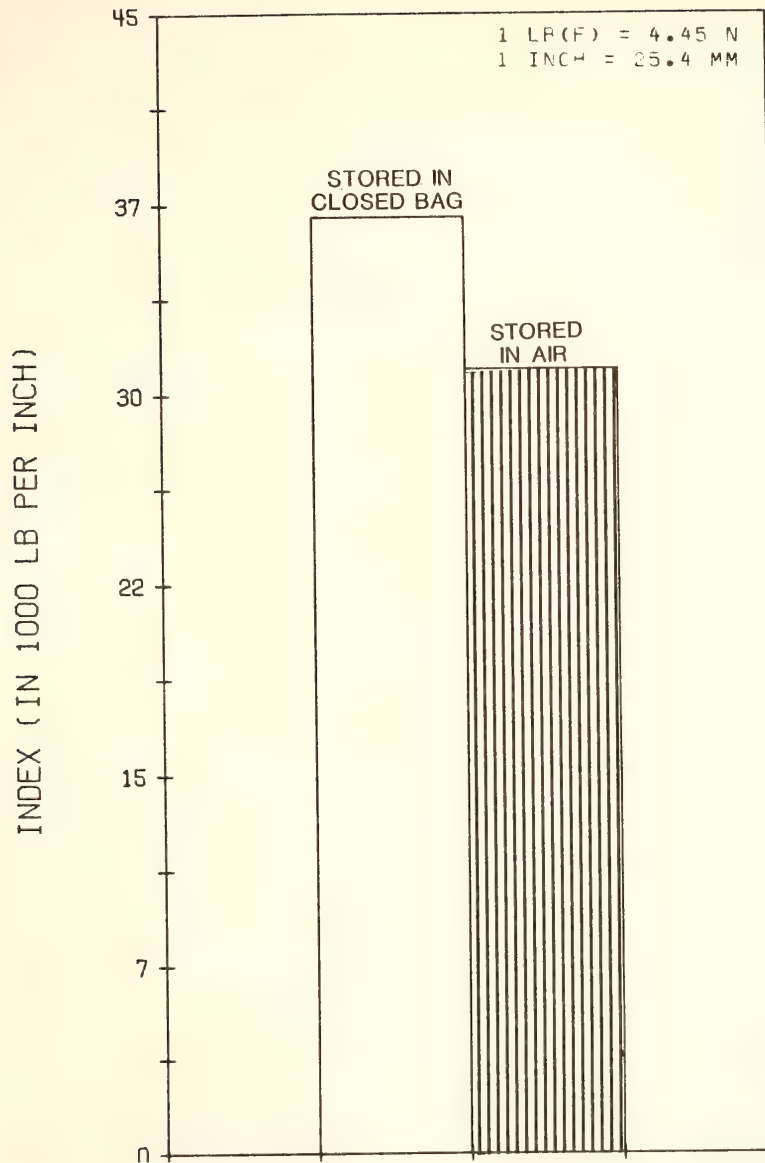


FIGURE 7.16 EFFECT OF STORAGE IN AIR ON THE MARSHALL INDEX



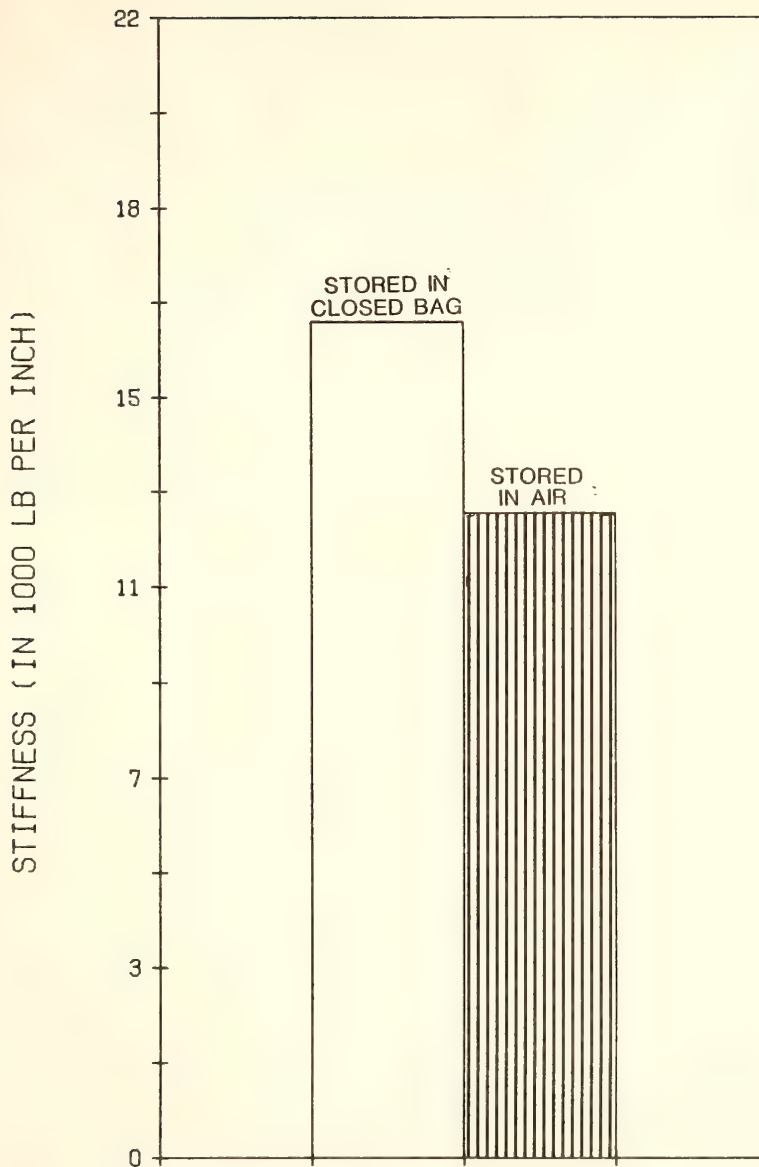


FIGURE 7.17 EFFECT OF STORAGE IN AIR ON THE MARSHALL STIFFNESS





during curing. The compaction moisture content was the only parameter that could be related successfully to the Marshall stability and  $M_R$ . These relationships for the laboratory compacted samples are shown in Figures 7.18 and 7.19. An optimum  $M_R$  and Marshall stability can be obtained by using the correct compaction moisture content. For this foamed asphalt recycled mixture it was approximately 2.3%.

The asphalt contents of the specimens were fairly constant, but the penetration and kinematic viscosity of the recovered asphalt cement varied considerably. The asphalt contents were close to the desired and specified asphalt contents. The results are summarized in Table 7.10.

The gradation of the recovered aggregate fell within the specification limits and close to the gradation assumed during the design (Figure 7.20).

#### 7.4. Asphalt Concrete Surface Material

The results of tests on the specimens obtained from cores and on the three laboratory compacted specimens are given in Table 7.11. Only the properties important to the determination of the structural layer equivalencies viz. resilient moduli at different temperatures on the indirect tensile strengths ( $S_T$ ) at 73°F (23°C) were determined. No reliable values for the Poisson's ratio could be obtained due to the sensitivity of the recording equipment.  $M_R$ -values at low temperatures (stiff specimens) are for the same reason not very reliable.



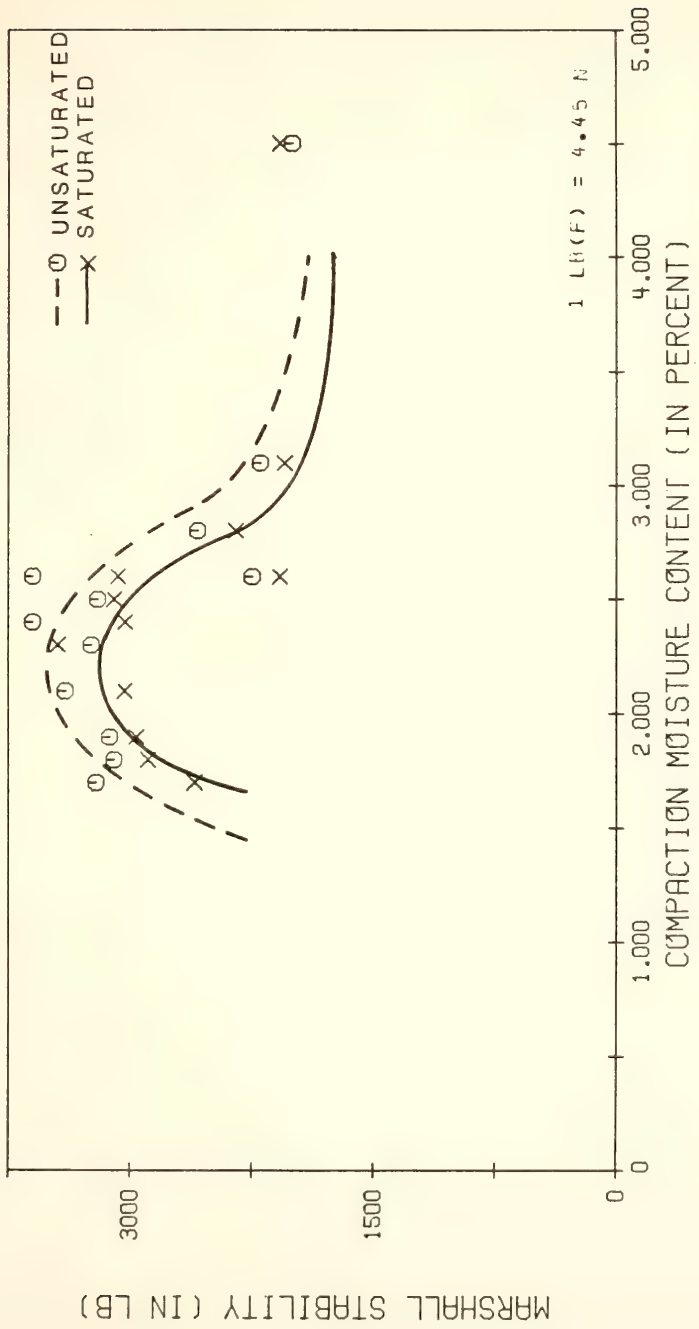


FIGURE 7.18 EFFECT OF COMPACTION MOISTURE CONTENT ON MARSHALL STABILITY



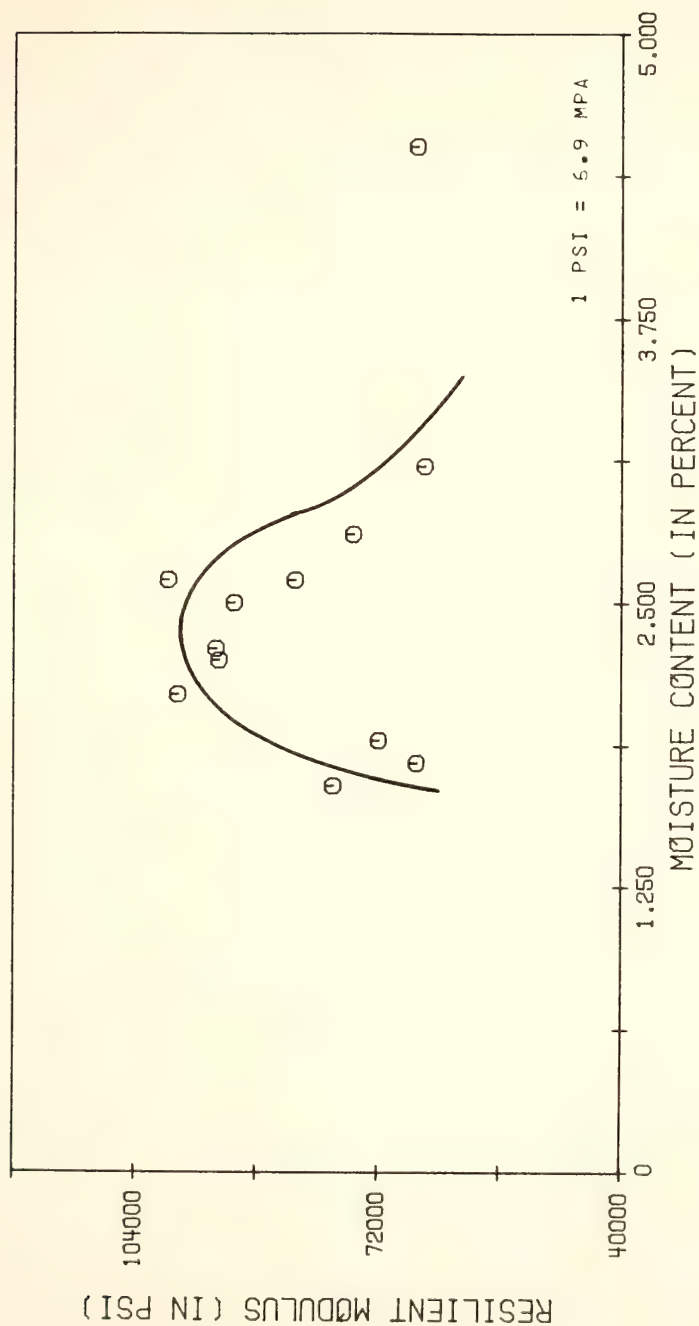


FIGURE 7.19 EFFECT OF COMPACTION MOISTURE CONTENT ON  
RESILIENT MODULUS



Table 7.10. Summary of Test Results on the Extracted Asphalt Cement

		$\bar{X}$	S.D.	n
Asphalt content	1	7.15	-	6
(%) Actual	2	7.70	-	6
	3	7.93	1.32	6
Expected*	1	7.33		
(%)	2	7.12		
	3	6.64		
Penetration (pens)		42	9.5	3
Kinematic visc (cSt)		481		
% voids (samples)**		2.8		
% voids (cores)**		9.2		

\* Based on information in the construction proposal.

\*\* Values based on average gradation, asphalt content and density.

1. By weight of mix
2. By weight of wet aggregate
3. By weight of dry aggregate





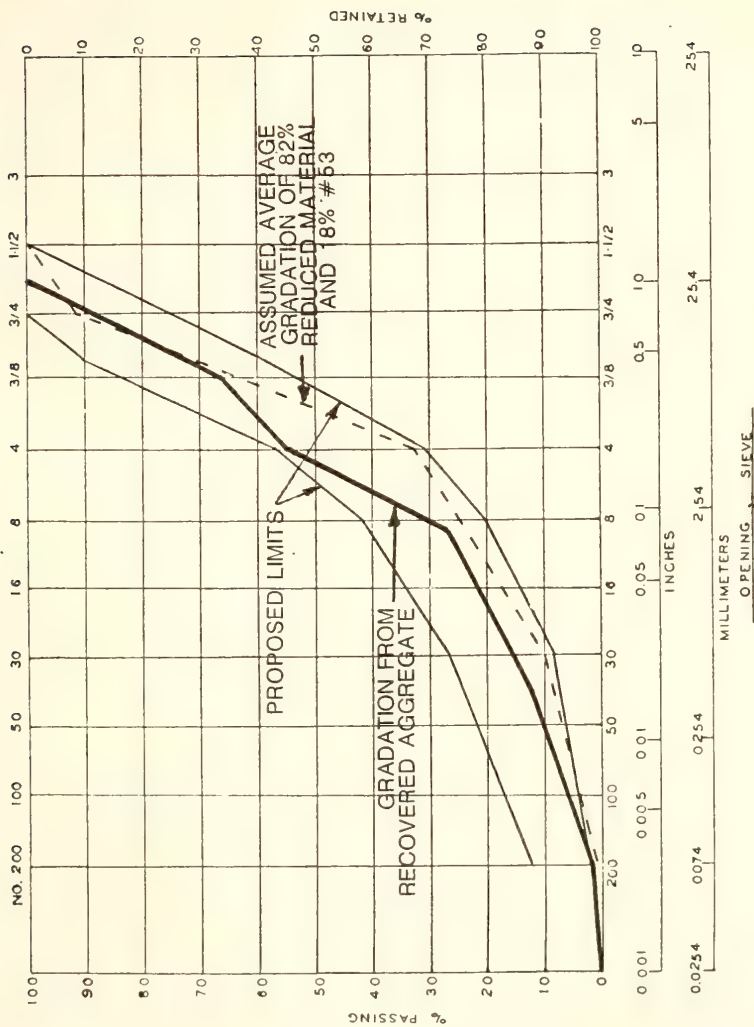


FIGURE 7.20 GRADATION ANALYSIS OF THE RECOVERED AGGREGATE



Table 7.11. Results of Tests on Asphalt Concrete Surface Mixture

	Temp (°F)	Cores	Laboratory
Resilient Modulus (psi)	34	360,000	--
	73	300,000	300,000
	104	71,000	--
Tensile Strain (psi)	73	109	185

1 psi = 6.9 kPa



### 7.5. Initial Asphalt Pavement

The results of the tests on the ten cores taken before construction are summarized in Table 7.12. These values were used as an indication of the properties of the remaining critical pavement layer.

### 7.6. Fatigue Life

The indirect tensile strengths were used to predict the fatigue life of the foamed asphalt recycled and the hot asphalt surface mixture. The correlations were developed for asphalt concrete mixtures (42). The horizontal deformations were not measured and the static elastic modulus could not be calculated. The relationships for controlled strain could therefore not be used to determine the fatigue life characteristics. The fatigue life-tensile strain relationships calculated for the recycled and surface material based on correlations developed from the indirect tensile test and constant strain tests are given in Table 7.13. The relationships for the recycled material seems to be unrealistic. The relationships are therefore not valid for these foamed asphalt materials.

### 7.7. Comparison Between Laboratory and Nondestructive Testing Results

Chapter 9 describes how the deflections measurements and the BISTRO-program, based on the elastic layered theory were used to calculate the resilient modulus for all the layers.  $M_R$ -values were obtained for the foamed asphalt recycled layer at 1, 12 and 250 days after construction. The pavement temperatures were not the same during all the deflection measurements. The laboratory  $M_R$ -results were adjusted to correspond with the temperatures of the pavement during the non-destructive testing.



Table 7.12. Properties of the Initial Asphalt Layer

	Average	S.D.	n
$M_R$ at 34°F	82000	18	12
(psi) 72°F	64000	17.7	14
104°F	38500	10.9	14
Hveem-R	89	3	14
Marshall Stability (lb)	4480	1120	14
Marshall Flow (0.01 inch)	8	3	10

1 psi = 6.9 kPa

1 inch = 25.4 mm

1 lb = 4.45 N

°C = 5/9 (°F-32)





Table 7.13. Fatigue-Life Relationships from Indirect Tensile Tests

$$N_f = k_1 (1/\epsilon_r)^{k_2}$$

Layer	$k_1$	$k_2$
Foamed asphalt:		
Laboratory	6000	0.53
Cores	24000	0.34
Asphalt Concrete Surface:		
Laboratory	$2.24 \times 10^{-5}$	6.18
Cores	$4.19 \times 10^{-6}$	3.33

$N_f$  = number of load applications to failure

$\epsilon_r$  = tensile strain at the bottom of the asphalt layer

$k_1$  and  $k_2$  = coefficients.



Table 7.14 summarizes the results of the laboratory and non-destructive test results. The resilient modulus of the 10 day air cured specimens seems to be approximately equal to the in-situ resilient modulus of the recycled layer 250 days after construction.

### 7.8. Summary of Results

1. The soil underlying the base course consisted of a granular layer of between three and five inches (75 and 125 mm) thick on top of a finer grained sandy silt. The granular layer had strengths (CBR-values) ranging from 14 to 50. The sandy silt layer had strengths varying from 10 to 30% CBR (for the top 12 inches or 305 mm). A uniform strength cannot be assigned to the strengths of these two layers. The test section will have to be divided into sections with equal granular layer and sandy silt layer strengths for further analysis.
2. Although the  $M_R$  values differ at the twelve different sampling locations the two layers and the locations can be represented by an average value for each of the three temperatures. The  $M_R$  at 34°F (1°C) was approximately 240,000 psi, at 73°F (23°C) 92,000 psi and at 104°F (40°C) 41,000 psi for the laboratory compacted specimens. The  $M_R$  at 34°F (1°C) was approximately 171,000 psi, at 73°F (23°C) 78,000 psi and at 104°F (40°C) approximately 50,000 psi for the core specimens.
3. The indirect tensile strength at 73°F (23°C) was approximately 34 psi (235 kPa) for the laboratory compacted specimens at 29 psi (200 kPa) for the core specimens.



Table 7.14. Comparison Between Laboratory and In-Situ Resilient Modulus Results

Days After Construction	In-Situ Resilient Modulus (psi)		Pavement Temp (°F)	Laboratory Resilient Modulus (psi)		
	Average	Range		1 day	Curing Time 10 days	max. cores
1	40000	14000-100000	77	55000	85000	280,000 75000
12	40000	20000-120000	72	60000	95000	320,000 80000
12	40000	20000-130000	80	52000	80000	253,000 70000
250	75000	20000-130000	85	50000	70000	220,000 180000*

1 psi = 6.9 kPa

°C = 5/9 (°F-32)

\* From 3 cores taken 250 days after construction and tested at 70 F (s.d. = 85000 psi.)



4. No reliable values for the Poisson's ratio could be obtained. The values ranged from 0.043 (at 34°F) to 0.524 (at 104°F).
5. The resilient moduli and indirect tensile strengths ( $S_T$ ) increased with a decrease in temperature.
6. The  $M_R$  and indirect tensile strength values increased with an increase in curing time. The low value was sufficient to support traffic immediately after construction. The  $M_R$  values changed from 53,000 psi (359 kPa) at 73°F (23°C) with no curing to 304,000 psi (2097 kPa) with maximum curing. The  $S_T$  values changed from 22 psi (152 Pa) at 73°F (23°C) with no curing to 40 psi (276 Pa) with maximum curing.
7. The maximum curing condition will most probably never be reached and the maximum strength of the pavement will be close to the values obtained after 10 days air curing. The strength of the mixture in the pavement will increase from the values obtained for the core specimens during use, since the density and stiffness will increase.
8. The average Marshall stability of the laboratory compacted specimens was 3000 lb. (13.35 kN), the average flow 0.16 inches (4 mm) and the average R-value 86. For the core specimens the average Marshall stability was 2000 lb. (8.9 kN), the average flow 0.32 inches (8 mm) and the R-value 78. The average densities were 148 pcf and 138 pcf (2.37 and 2.21 gmcm<sup>2</sup>) respectively.





9. Water had a detrimental effect on the strength of the foamed asphalt recycled mixture. It reduced the Marshall stability, the R-value and the  $M_R$ . The effect on the  $M_R$  was the most profound. The  $M_R$  was reduced by between 25 and 30% for both the laboratory compacted and core specimens. Water should therefore be kept out of the pavement.
10. Storage of the mixture in closed plastic bags had only a slight influence on the Marshall stability and Hveem-R-value, but a larger influence on the  $M_R$ . The additional asphalt seemed to soften the mixture during the first few (5) days which caused the mixture to be less stiff (lower  $M_R$ ).
11. Stockpiling in the open reduced the  $M_R$ .
12. The compaction moisture content influenced the  $M_R$  and Marshall stability. Optimum values can be obtained for this foamed asphalt recycled mixture with a compaction moisture content of approximately 2.3%.
13. The asphalt content of 7.15% by weight of mix and the grading of the recovered aggregate were close to the proposed values. The asphalt cement penetration and kinematic viscosity remained approximately the same.
14. The asphalt concrete surface layer can be represented by a  $M_R$ -value of more than 360,000 psi (233 MPa) at 34°F (1°C), 300,000 psi (2069 MPa) at 73°F (23°C) and 71,000 psi (490 MPa) at 104°F (40°C). The indirect tensile strength at 73°F (23°C) was approximately 150 psi (1034 MPa).



15. The fatigue life-tensile strain relationships determined from the results of the indirect tensile test cannot be used for the foamed asphalt recycled material.
16. The average resilient modulus of the recycled layer determined from the deflection measurements 250 days after construction (Chapter 9 ) corresponds well with the  $M_R$  of the laboratory sample after 10 day air curing.



## CHAPTER 8: RESULTS OF NON-DESTRUCTIVE TESTING

### 8.1. Introduction

The results of the nondestructive tests viz. Clegg impact soil tests and the Dynaflect deflection measurements are summarized and discussed in this chapter. The Dynaflect is widely used in nondestructive testing. It is generally used to compare different pavements and/or the uniformity of a pavement section.

The Dynaflect deflections have been correlated with Benkelman beam deflections which are actual deflections of the pavement under a 18,000 lb (80 kN) dual wheel load.

The Clegg impact soil tester is, and was designed to be, used to measure the in-situ strength of granular materials. The Clegg Impact Value (CIV) has also been correlated with CBR-values. The Clegg impact tester was not used on the recycled layer in this study to determine absolute values for strength, but to see if it is possible to compare the relative strengths of the different sections of the foamed asphalt recycled layer.

### 8.2. Clegg Impact Tests

The results of the tests on the eastbound lane are shown in Figure 8.1. The relative strength of the recycled layer as measured at the center of the lane increased substantially with increased compaction. The first set of observations was taken approximately six hours after



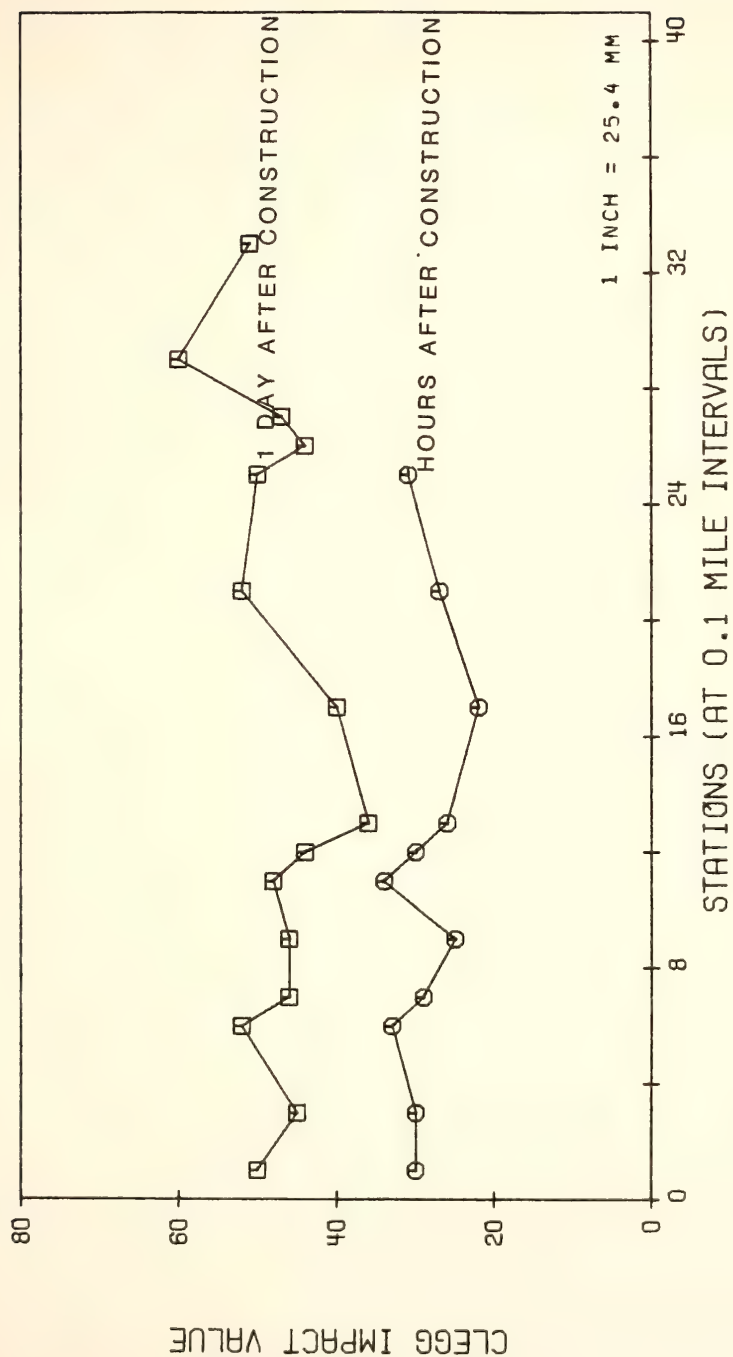


FIGURE 8.1 CHANGES IN THE CLEGG IMPACT VALUES  
ON THE EASTBOUND LANE





placement. The material was at that time compacted by four passes of the compaction machine. The next set of observations was taken the following morning. The recycled material was compacted by two additional passes of the compaction equipment and traffic after the first observations were taken. The density as specified by the IDOH was reached and was approximately the same as the density obtained during the Dynaflect deflection measurements before the surface was placed. The Clegg impact tests were conducted on the bottom layer only.

The average CIV-value before final compaction was 33.5 (standard deviation was 10.8) and after final compaction 46.5 with a standard deviation of 5.2.

Figure 8.2 shows the results of the tests on the westbound lane. All the tests were performed after the final compaction. Both these figures show that differences in strengths or densities can be detected by the Clegg impact soil tester. It is not possible at this point to relate these relative CIV-values to absolute values e.g. elastic modulus for asphalt stabilized or recycled layers. Since the Clegg tests were conducted on the bottom recycled layer and the deflection tests on the top and surface layers the values for stiffness of the two tests cannot be compared.

### 8.3. Deflection Tests

Dynaflect pavement deflections are usually characterized by the maximum deflection (DMD), the surface curvature index (SCI), the base curvature index (BCI), the deflection of the fifth sensor ( $D_5$ ) and the spreadability (SPD). The significance of all the parameters are explained in Chapter 6. Metwali (48) showed that the DMD, SCI and  $D_5$



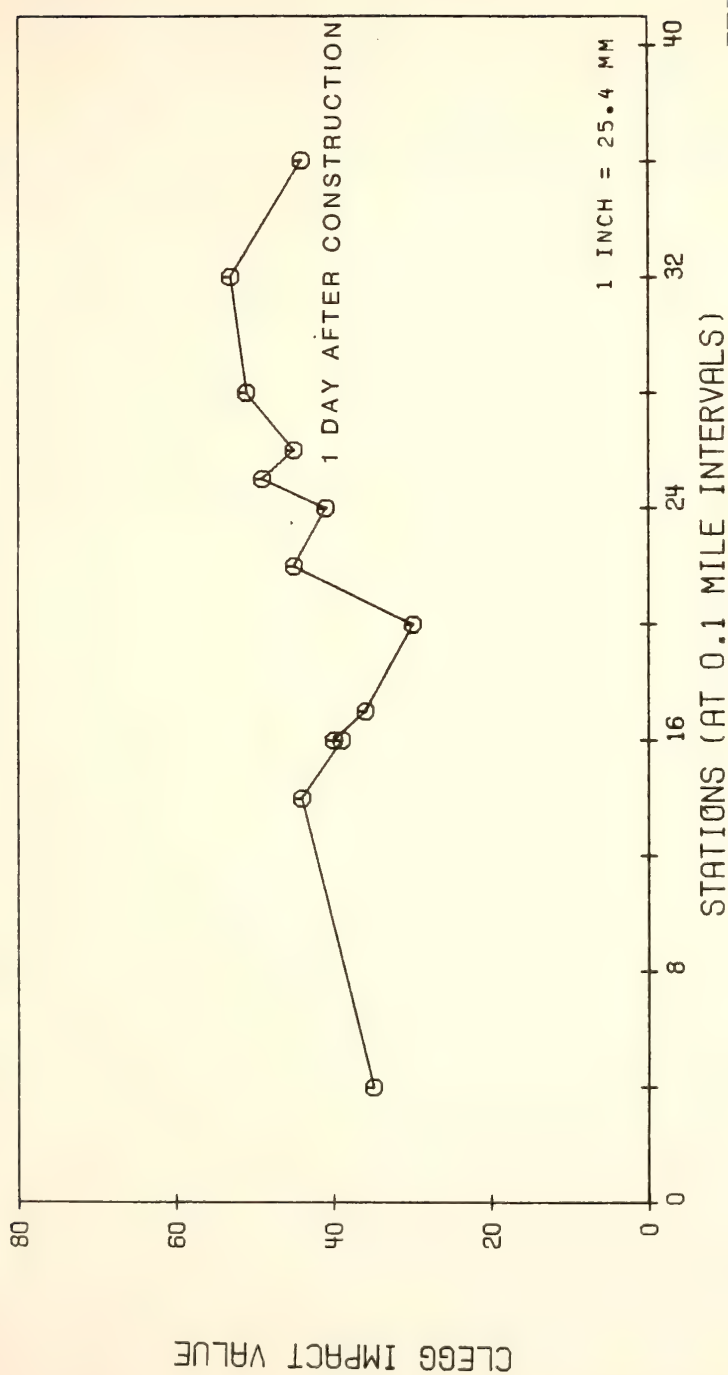


FIGURE 8.2 CHANGES IN THE CLEGG IMPACT VALUES ON THE WESTBOUND LANE



have significantly (at  $\alpha = 0.01$ ) lower values in the fall when compared with the spring values. The SPD is not influenced by seasonal differences. Since the deflection measurements were taken in different seasons they cannot be compared without appropriate adjustments or the realization that the values could have been influenced by seasons.

Deflections, for a constant pavement cross section, are influenced mainly by the temperature in the asphalt layers and the moisture content of the subbase and especially the subgrade, except for temperatures below freezing point when the subgrade can be frozen. This latter case was not present. The maximum deflections occur during the spring thaw period.

Relationships based on the time of year were developed to compare DMD values (Metwali (48)). Researchers in Kentucky (59) developed relationships to compare the deflections under the first three sensors of the Road Rater based on the temperature of the asphalt layers. Although they concluded that moisture content in the subgrade has an influence on the deflections the effect of the temperature is more important. Higher temperatures give lower elastic moduli of the asphalt layer and therefore higher deflections. Since the SCI is an indication of the stiffness of the surface layer and the difference between the deflections of the first and second sensors of the Dynaflect it will be influenced mainly by the temperature. Adjustments should therefore be made based on temperature. The spreadability (SPD) does not have to be adjusted, because it is not influenced by time of year. Even if the deflections of the first three sensors, which are influenced by changes in the moduli of the surface layers, were to be adjusted, the SPD value



would not change substantially due to the method of determining SPD. The values of BCI and D5 are influenced by the season, but relationships are not available to adjust them according to the season. The fall values are higher and this must be considered in the comparison of deflections taken at different times. Table 8.1 gives a summary of the adjustment factors used for the different parameters in this chapter. The factors were selected from both methods mentioned above. They were in most cases very similar. In the one instance where the factors were completely different the factor developed based on the time of year only was used, since the other method relies on the mean ambient temperature five days prior to measuring the pavement temperature during deflection measurements and it was difficult to obtain accurate values for the latter. All the adjustment factors were adjusted to compare the deflections and deflection parameters to those taken during and soon after construction (in September 1981). The average temperature during that time was close to 70°F (21°C) and the deflections were used to determine the structural layer equivalencies. Table 8.1 also shows which deflection data sets were available and could be used for each of the lanes.

Four sets of deflection data were available for each of the lanes. Deflection measurements were taken before construction on the initial pavement during November 1980 (BEFORE1) and May 1981 (BEFORE2) on both lanes. The measurements taken during May 1981 on the eastbound lane could not be used due to a calibration error. A set of deflection measurements was taken on the recycled foamed asphalt layer during construction in September 1981 (DURING) in the eastbound lane only. Two sets of deflection measurements were taken after construction on both





Table 8.1. Deflection Adjustment Factors

	Time	D <sub>1</sub>	SCI	SPD	BCI	D <sub>5</sub>	Designation
<b>Eastbound</b>							
Prior to Construction	Nov. 1980	1.15	1.15				BEFORE1
During Construction**	Sept. 1981	1.00	1.00				DURING
Less than 10 days after Construction	Sept. 1981	1.00	1.00	None	None*	None*	AFTER1
8 months after Construction	May 1982	0.80	0.80				AFTER2
<b>Westbound</b>							
Prior to Construction 1	Nov. 1980	1.15	1.15				BEFORE1
Prior to Construction	May 1981	0.80	0.80				BEFORE2
Less than 10 days after Construction	Sept. 1981	1.00	1.00	None	None*	None*	AFTER1
8 months after Construction	May 1982	0.80	0.80				AFTER2

\* Adjustments ought to be made, but no adjustment factors were available.

\*\*On top of the foamed asphalt layer.

D<sub>1</sub> = maximum Dynaflect deflection (sensor 1).

SCI = surface curvature index.

BCI = base curvature index.

SPD = spreadability.

D<sub>5</sub> = deflection of sensor 5.



lanes. The first set was taken ten to twelve days after the placement of the asphalt concrete surface in September 1981 (AFTER1) and the second set approximately 8 months after construction in May 1982 (AFTER2). The Dynaflect deflection parameters are summarized in Table 8.2. Figures 8.3 to 8.7 display these parameters for the eastbound and Figures 8.8 to 8.12 for the westbound lane.

The maximum deflections were higher a few days after construction (AFTER1) than those taken before the construction (BEFORE1 and BEFORE2) (Figure 8.13). The maximum deflections decreased (an indication that the pavement stiffness increased) during the first eight months after construction, but were still higher than the deflections before construction. The surface curvature index (SCI), as an indicator of the stiffness of the surface layers (base course and surface), shows the same trend (Figure 8.14). A low SCI-value indicates a high stiffness. According to the SCI values is the stiffness of the top layers approximately the same with and without the 1-1/2 inch asphalt concrete surface layer (DURING and AFTER1). The addition of the 1-1/2 inch (38 mm) asphalt concrete surface increased the spreadability of the pavement structure. The spreadability increased during the first eight months after construction, but was still lower than the spreadability of the initial pavement if the deflections taken during November 1980 (BEFORE1) were taken as a reference (Figure 8.15). If the deflections taken during May 1981 (BEFORE2) were taken as a reference the spreadability of the new recycled pavement is higher after eight months.

This apparent inconsistency with the spreadability shows how difficult it is to compare pavement structures based on some Dynaflect



Table 8.2. Summary of Dynaflect Deflection Parameters

		$D_1$ (mils)	SCI (mils)	SPD (%)	BCI mils	$D_5$
Eastbound						
BEFORE1	$\bar{X}$	1.743	.466	51.90	.144	.229
(Nov. 1980)	S.D.	.639	.269	4.60	.072	.094
DURING	$\bar{X}$	2.105	.640	46.02	.168	.192
(Sept. 1981)*	S.D.	.636	.263	5.03	.068	.087
AFTER1	$\bar{X}$	1.819	.650	48.22	.183	.257
(Sept. 1981)**	S.D.	.562	.221	4.56	.072	.150
AFTER2	$\bar{X}$	1.706	.502	49.56	.195	.273
(May 1982)***	S.D.	.584	.193	5.21	.089	.126
Westbound						
BEFORE1	$\bar{X}$	1.631	.437	52.37	.150	.22
(Nov. 1980)	S.D.	.541	.231	5.292	0.076	.085
BEFORE2	$\bar{X}$	1.546	.526	47.72	.181	.209
(May 1981)	S.D.	.434	.224	5.860	.141	.075
AFTER1	$\bar{X}$	2.055	.758	46.68	.205	.226
(Sept.)**	S.D.	.870	.350	4.142	.093	.075
AFTER2*	$\bar{X}$	1.917	.599	48.67	.211	.285
(May)	S.D.	.877	.294	5.100	.121	.136

All values have been adjusted according to the factors in Table 9.1.

1 inches = 25.4 mm

n = 42

$D_1$  = maximum Dynaflect deflection (sensor 1)

SCI = surface curvature index

SPD = spreadability

BCI = base curvature index

$D_5$  = deflection of sensor 5



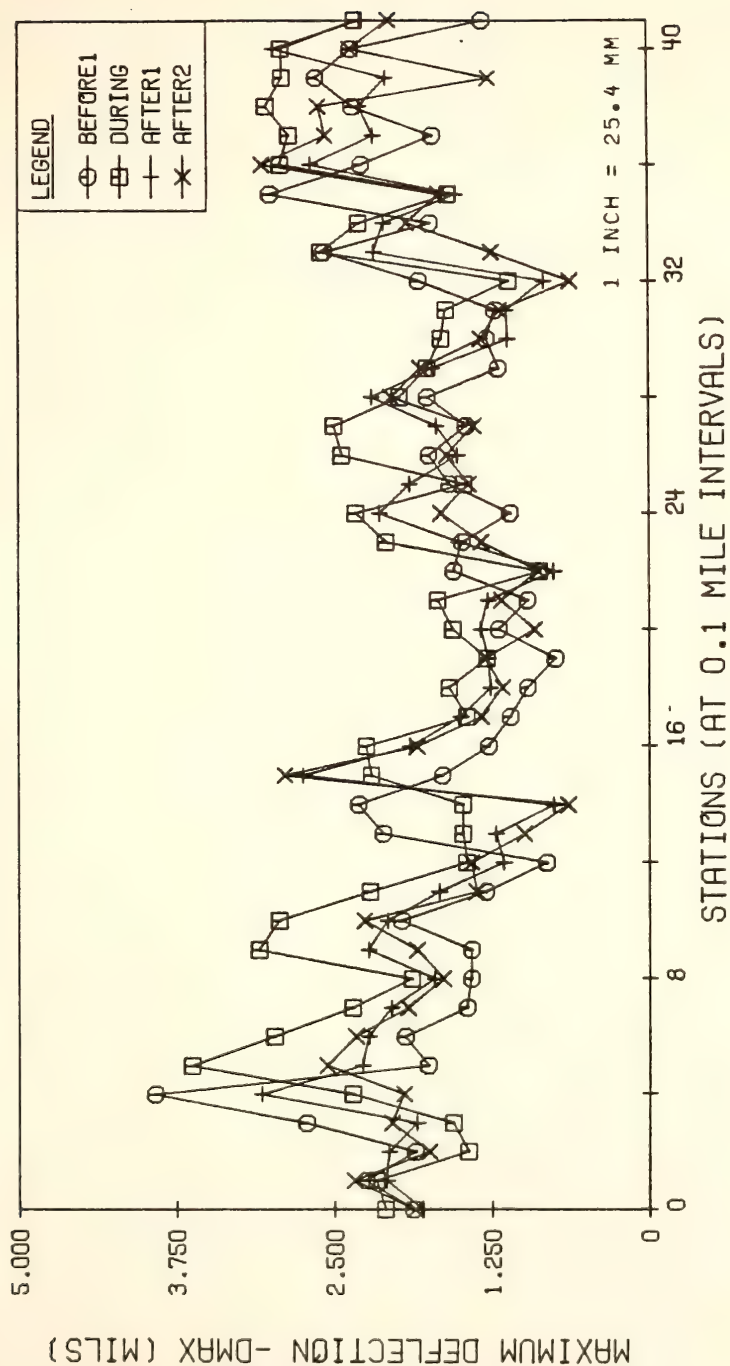


FIGURE 8.3 CHANGES IN MAXIMUM DYNAFLECT DEFLECTION BEFORE, DURING AND AFTER CONSTRUCTION (EASTBOUND LANE)





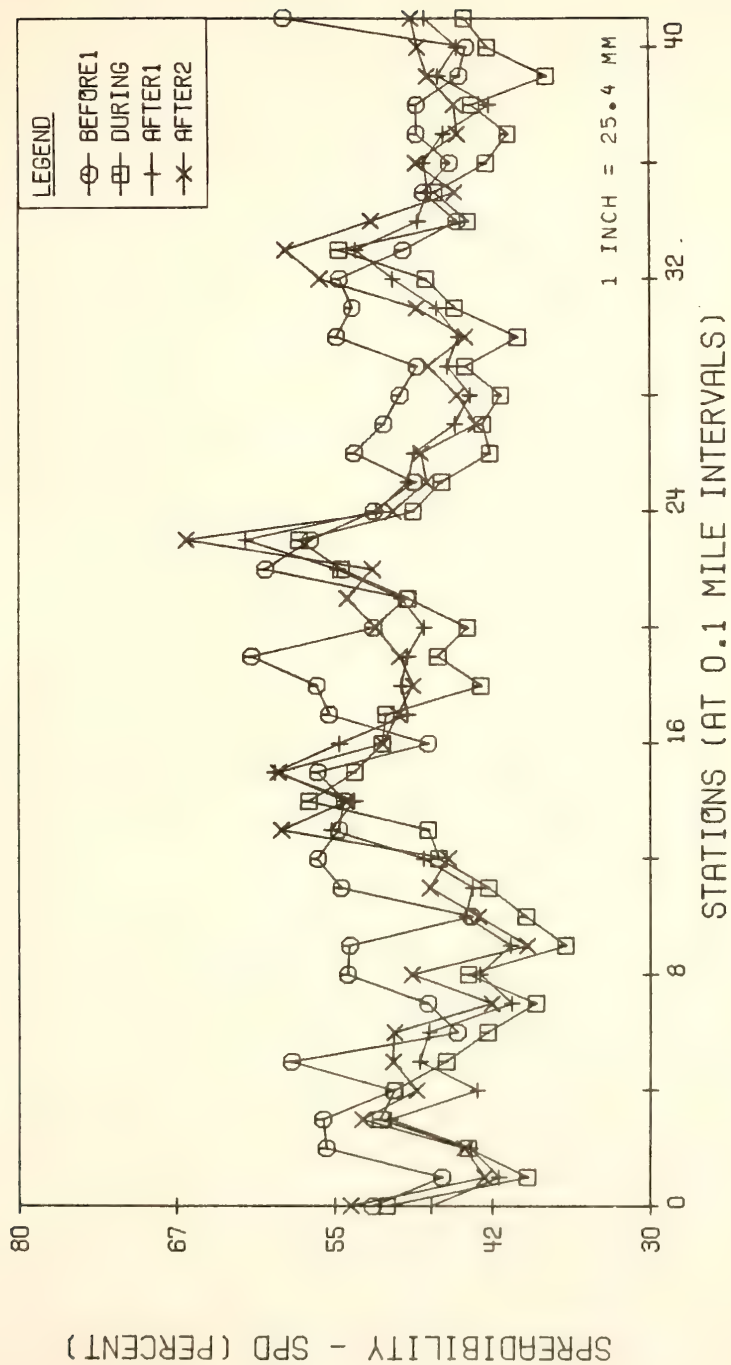
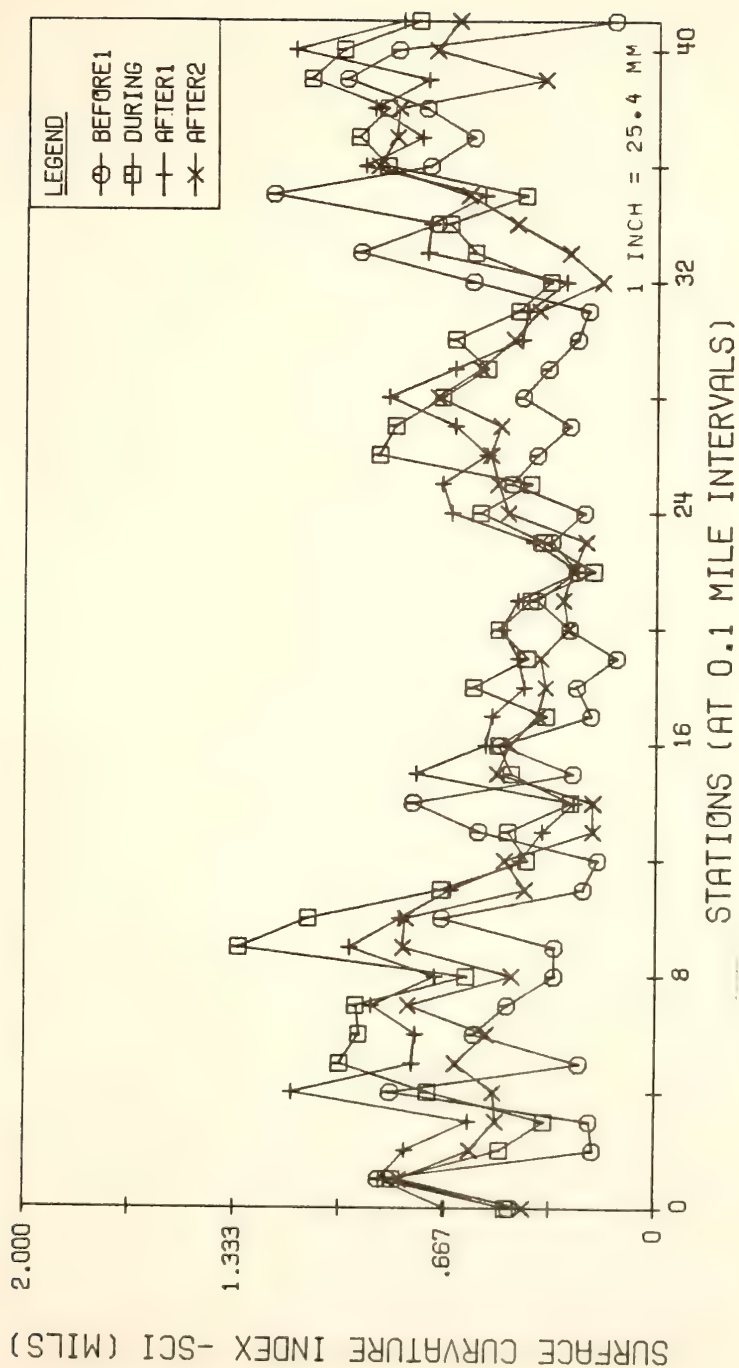


FIGURE 8.4 CHANGES IN SPREADABILITY BEFORE, DURING AND AFTER CONSTRUCTION (EASTBOUND LANE)





**FIGURE 8.5 CHANGES IN SURFACE CURVATURE INDEX BEFORE, DURING AND AFTER CONSTRUCTION (EASTBOUND LANE)**



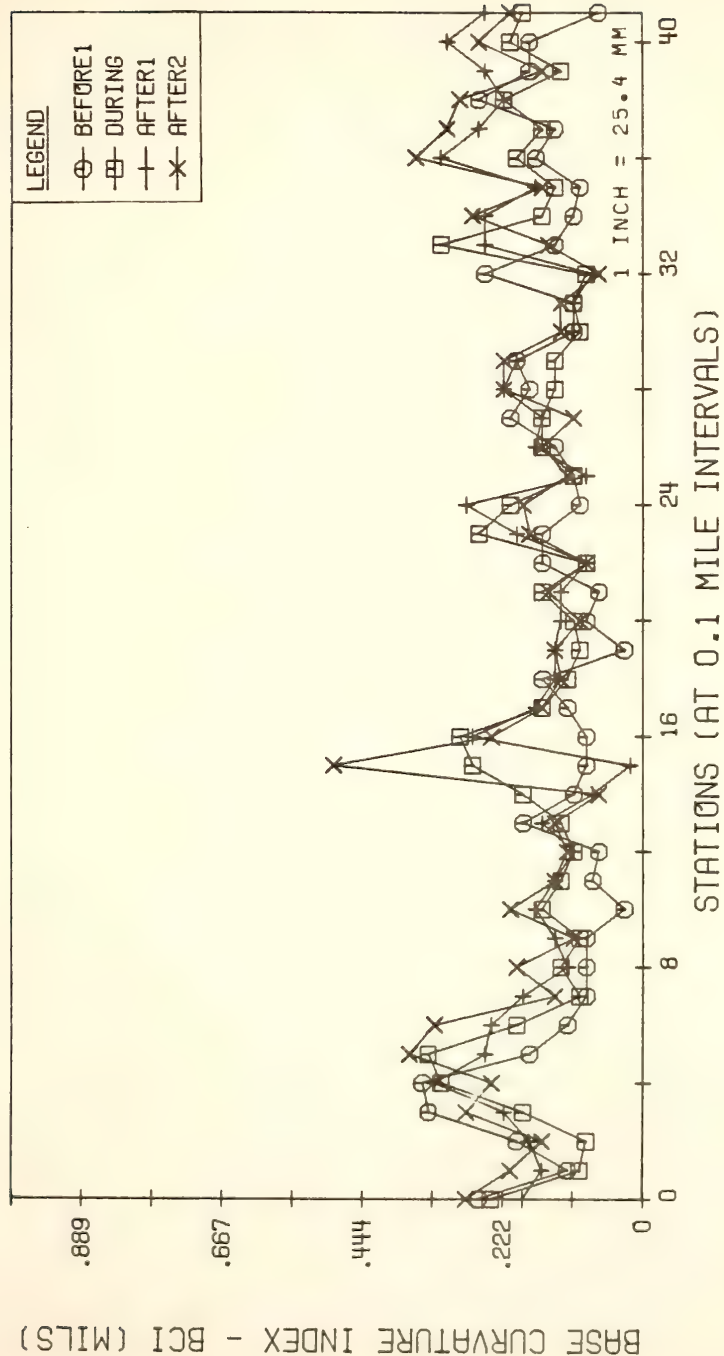


FIGURE 8.6 CHANGES IN BASE CURVATURE INDEX BEFORE, DURING AND AFTER CONSTRUCTION (EASTBOUND LANE)



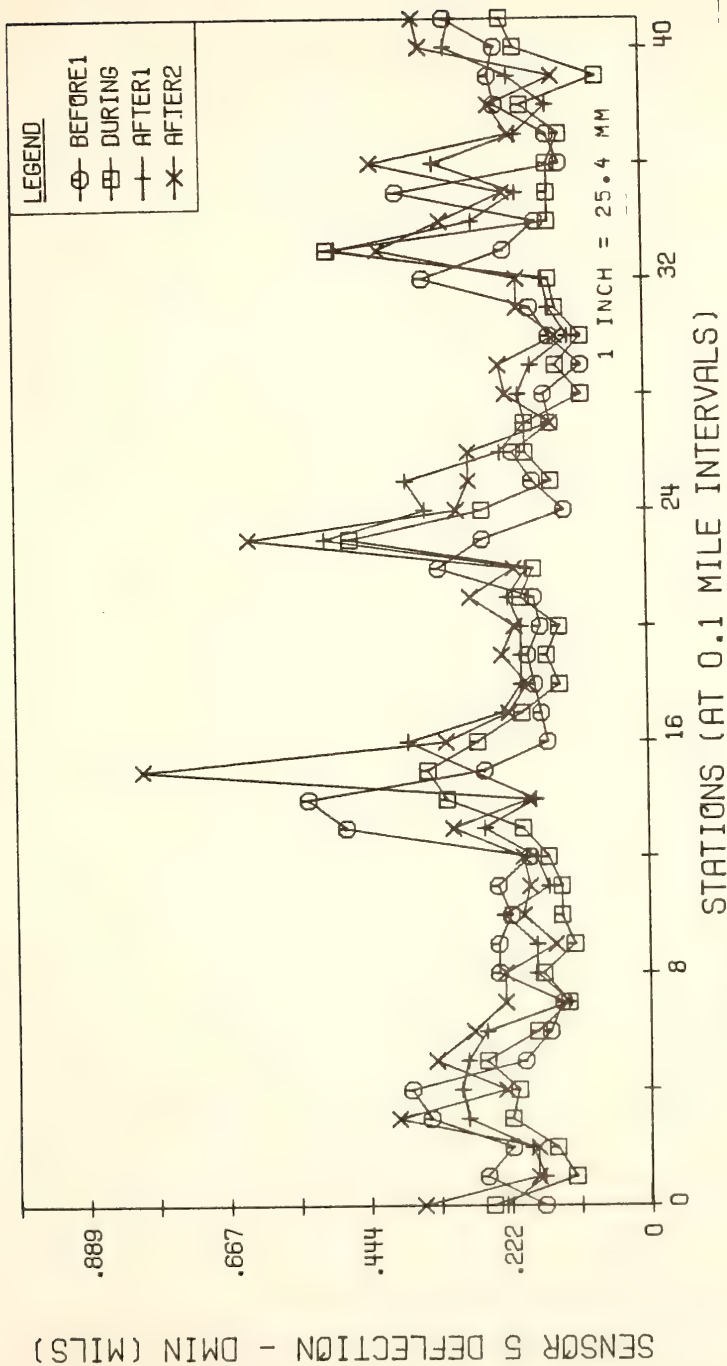


FIGURE 8.7 CHANGES IN SENSOR 5 DEFLECTION BEFORE, DURING AND AFTER CONSTRUCTION (EASTBOUND LANE)





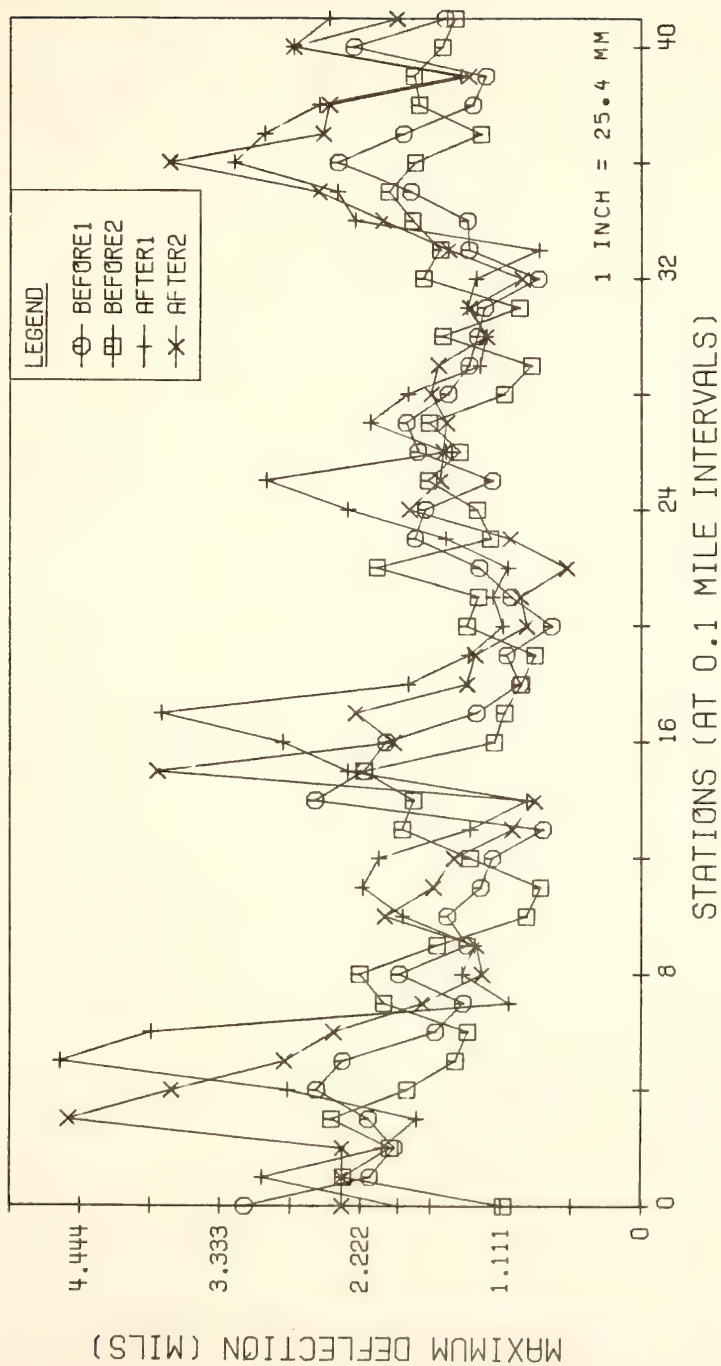
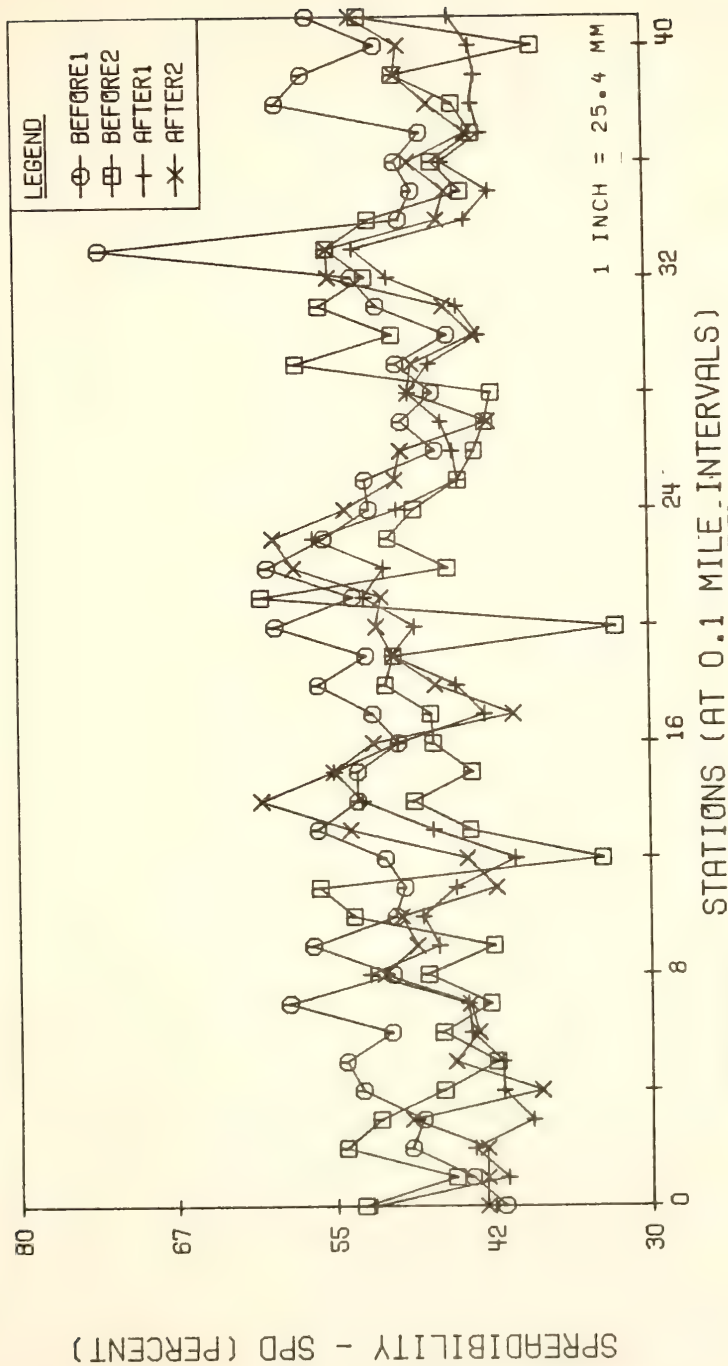


FIGURE 8.8 CHANGES IN MAXIMUM DYNAFLECT DEFLECTION BEFORE AND AFTER CONSTRUCTION (WESTBOUND LANE)





**FIGURE 8.9 CHANGES IN SPREADABILITY BEFORE AND AFTER  
CONSTRUCTION (WESTBOUND LANE)**



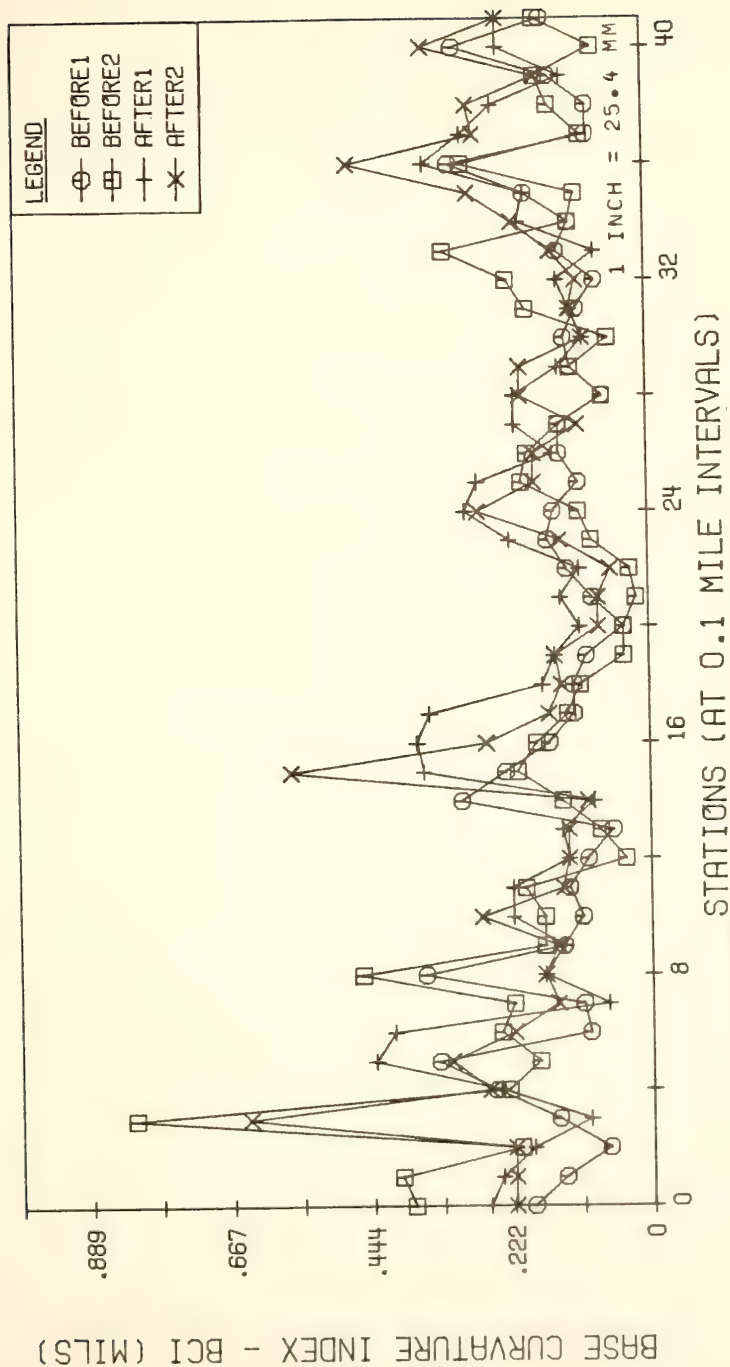


FIGURE 8.10 CHANGES IN SURFACE CURVATURE INDEX BEFORE AND AFTER CONSTRUCTION (WESTBOUND LANE)



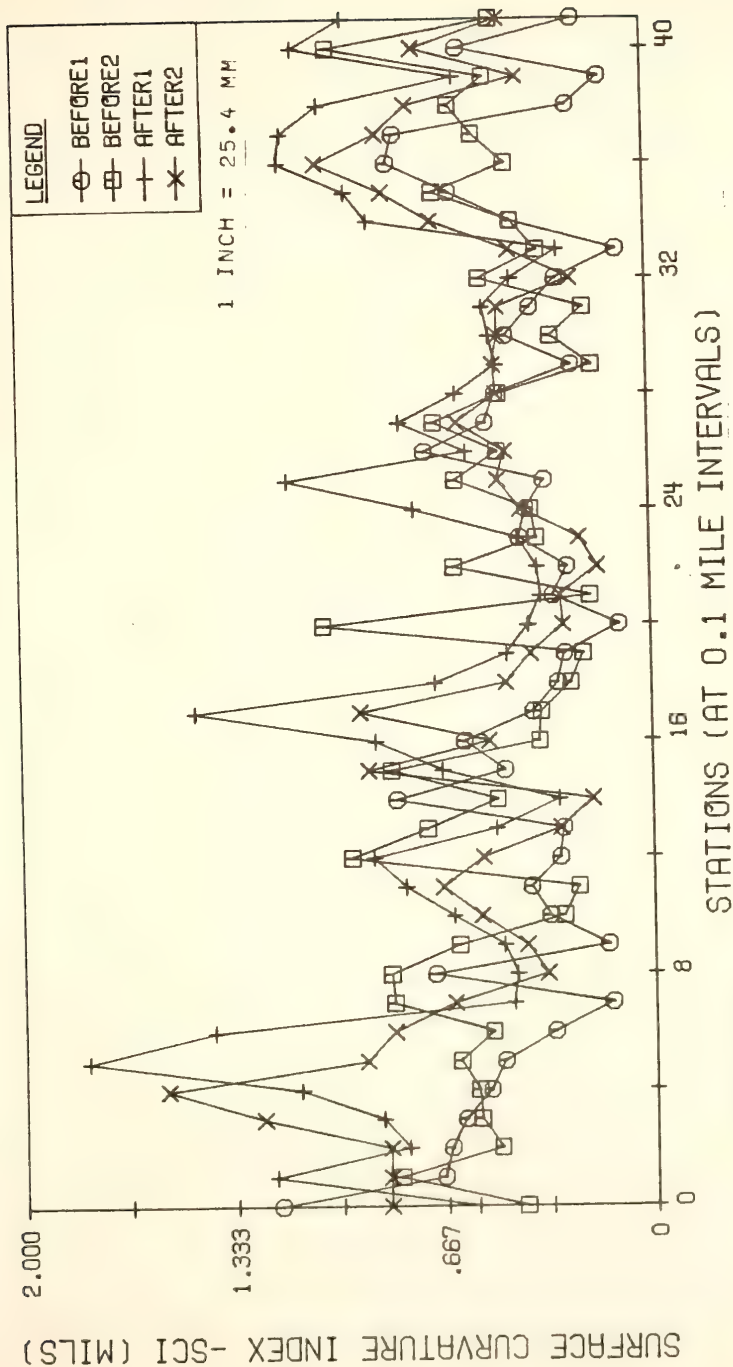


FIGURE 8.11 CHANGES IN BASE CURVATURE INDEX BEFORE AND AFTER CONSTRUCTION (WESTBOUND LANE)





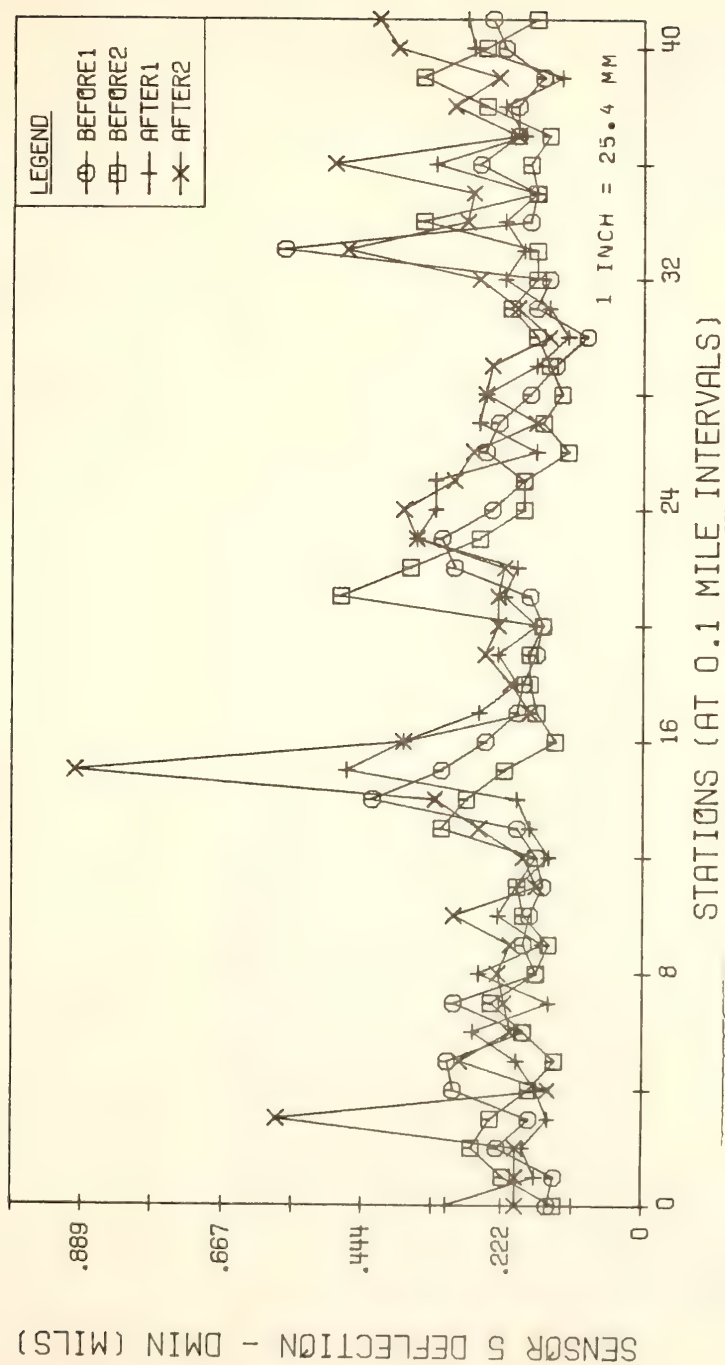


FIGURE 8.12 CHANGES IN SENSOR 5 DEFLECTION BEFORE AND AFTER CONSTRUCTION (WESTBOUND LANE)



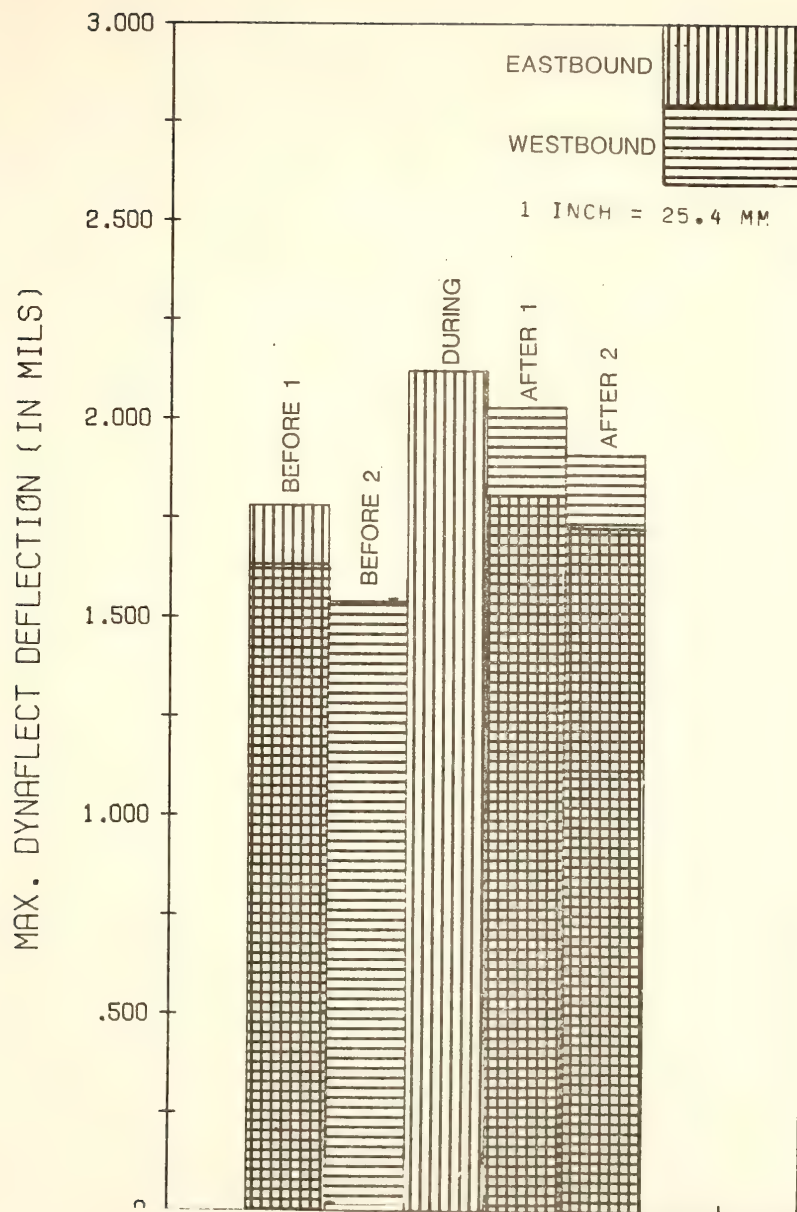


FIGURE 8.13 COMPARISON OF AVERAGE SURFACE CURVATURE BEFORE, DURING AND AFTER CONSTRUCTION



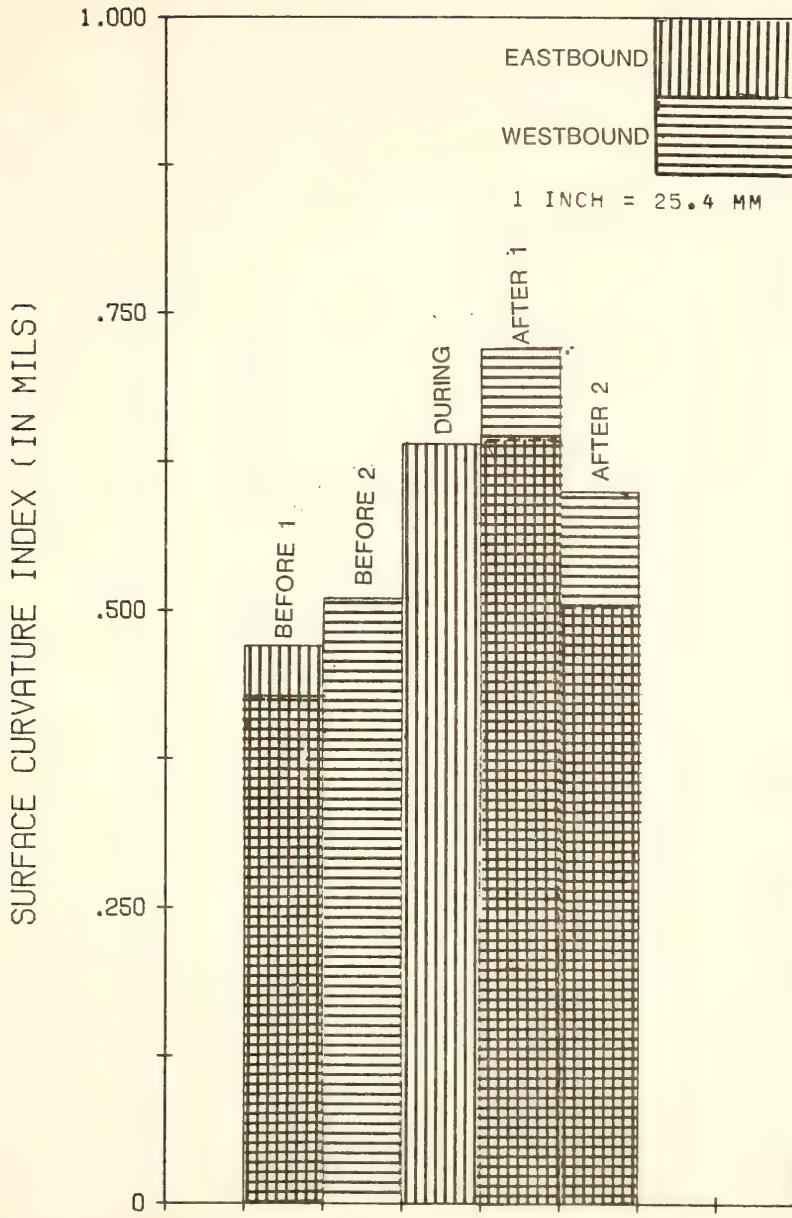


FIGURE 8.14 COMPARISON OF AVERAGE MAXIMUM DYNAFLECT DEFLECTION BEFORE, DURING AND AFTER CONSTRUCTION



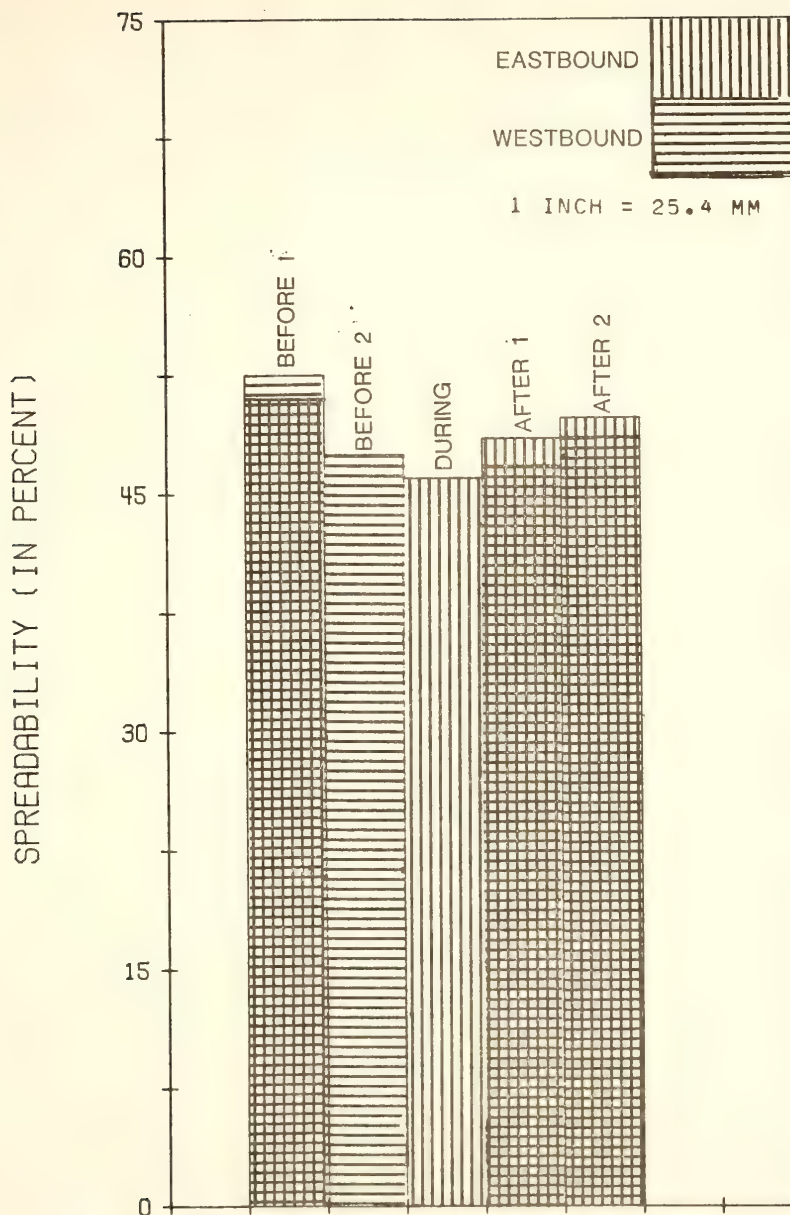


FIGURE 8.15 COMPARISON OF AVERAGE SPREADABILITY BEFORE, DURING AND AFTER CONSTRUCTION





deflection parameters only. The maximum deflections are influenced to a large extent by the subgrade. The deflection of the fifth sensor and the base curvature index (BCI), as indicators of the strength of the subgrade, vary considerably among testing dates. The moisture content of the subgrade plays a major role in its strength. It is unlikely that the moisture contents would have been the same even within a specific season. That can be seen by the difference in  $D_5$  and BCI values between the DURING and AFTER1 testing times, which were not more than twelve days apart. Another important characteristic of the subgrade is its stress sensitivity. A low deviator stress ( $\sigma_d$ ) results in a high resilient modulus value. A stiff layer overlaying a subgrade will induce smaller deviator stress values than a less stiff layer on a similar subgrade. The same subgrade can therefore have different  $M_r$  or strength values which will influence the maximum deflection. Although adjustments have been made to the maximum deflection values the influence of the strength of the subgrade must be kept in mind in the use of maximum deflections to compare different pavements.

The spreadability as an indicator of the strength of a pavement also has some inherent inconsistencies. The deflection values at the first two sensors are influenced mainly by temperature and the fourth and fifth sensors mainly by moisture content in the subgrade for a pavement structure with specific pavement layer characteristics (Figure 8.16). An increase in the temperature of the asphalt layers will decrease the stiffness and therefore results in higher deflection values of sensors one to three while four and five remain the same. This will cause the spreadability to decrease which is correct. On the other hand, if only





**FIGURE 8.16 EFFECTS OF THE ELASTIC MODULI  
OF THE PAVEMENT LAYERS ON THE  
DYNAFLECT DEFLECTION BASIN**

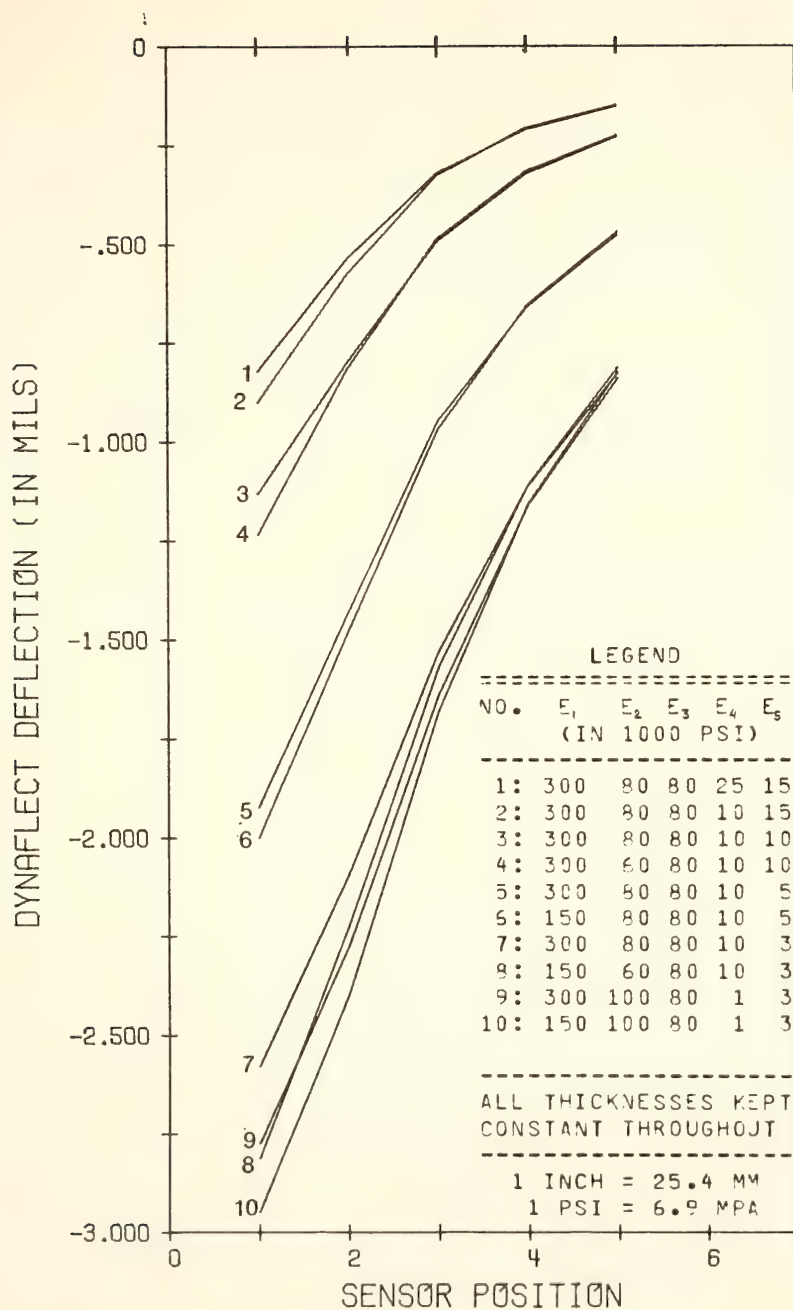


FIGURE 8.16



the moisture content in the subgrade increases the deflection values at all the sensors will increase, but more at the first and second sensors than at the other three. This will result in a smaller spreadability than for a similar pavement structure on a stronger subgrade. The spreadability can be a good indicator of the pavement strength if the subgrade strength remains the same. This unfortunately is not the case in this study. Pavements with strong subgrades tend to have lower spreadability values than a similar pavement structure on a weaker subgrade indicating low strengths as shown in Figure 8.17, while they should be the same.

The opposite is true for the SCI. Pavements with subgrades with high strengths will have lower SCI values, indicating a higher strength than a similar pavement with a soft subgrade (Figure 8.18). The SCI is a function of both the strengths of the surface and the base course materials. A high SCI value does not necessarily indicate a stiff surface layer, even if the subgrade is the same. A stiff base course and a flexible surface course will also give a high SCI-value. The surface curvature index cannot be used as an indicator of the stiffness of the surface layer (in this case the recycled layer) alone.

In spite of all the limitations of the Dynaflect deflection parameters that are indicators of the strength of the surface layer and by looking at all the five parameters simultaneously it can be concluded that the strength of the pavement was lower than the original during and soon after construction, but it increased and after eight months was at least as strong as the original pavement before construction. The foamed asphalt recycled base course layer of 5.5 inches (140 mm) and the 1-1/2 inch (38 mm) hot asphalt surface layer after





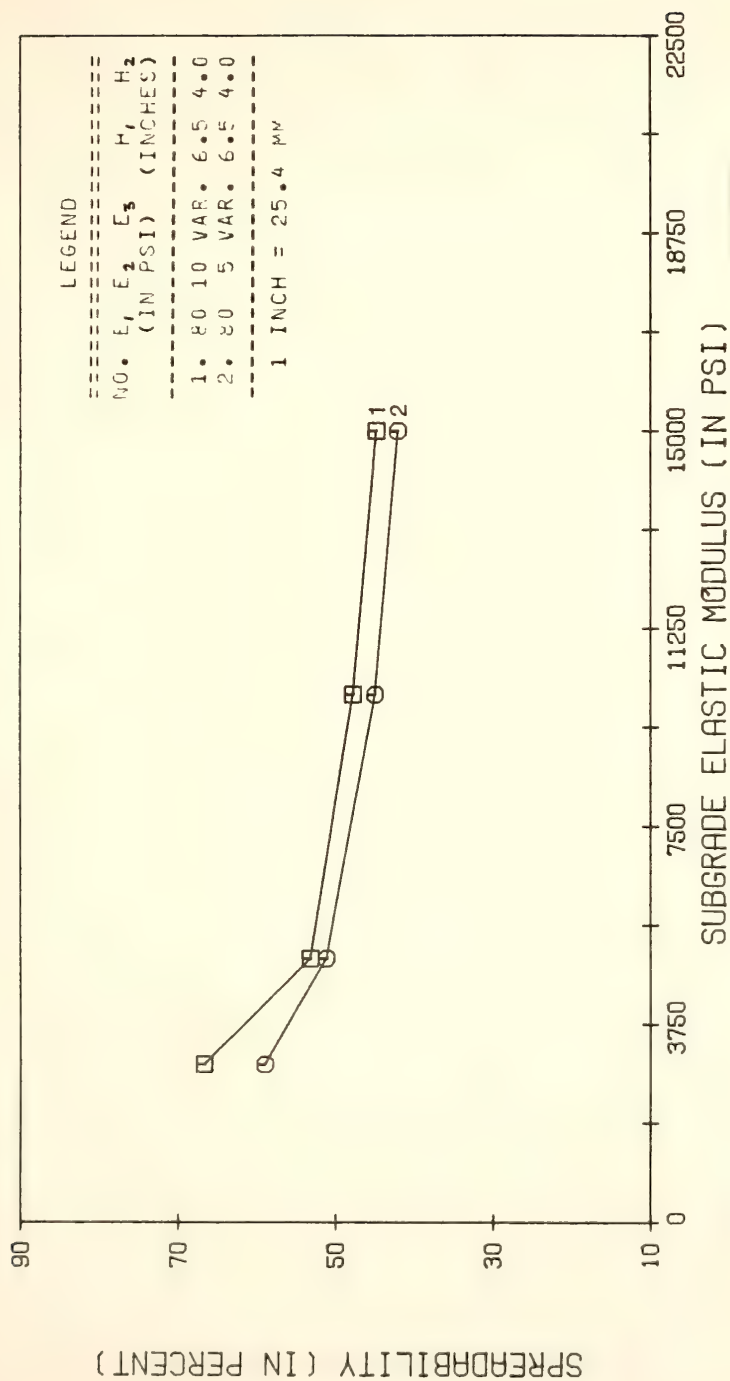


FIGURE 8.17 EFFECT OF CHANGES IN SUBBASE AND SUBGRADE ELASTIC MODULI ON THE SPREADIBILITY



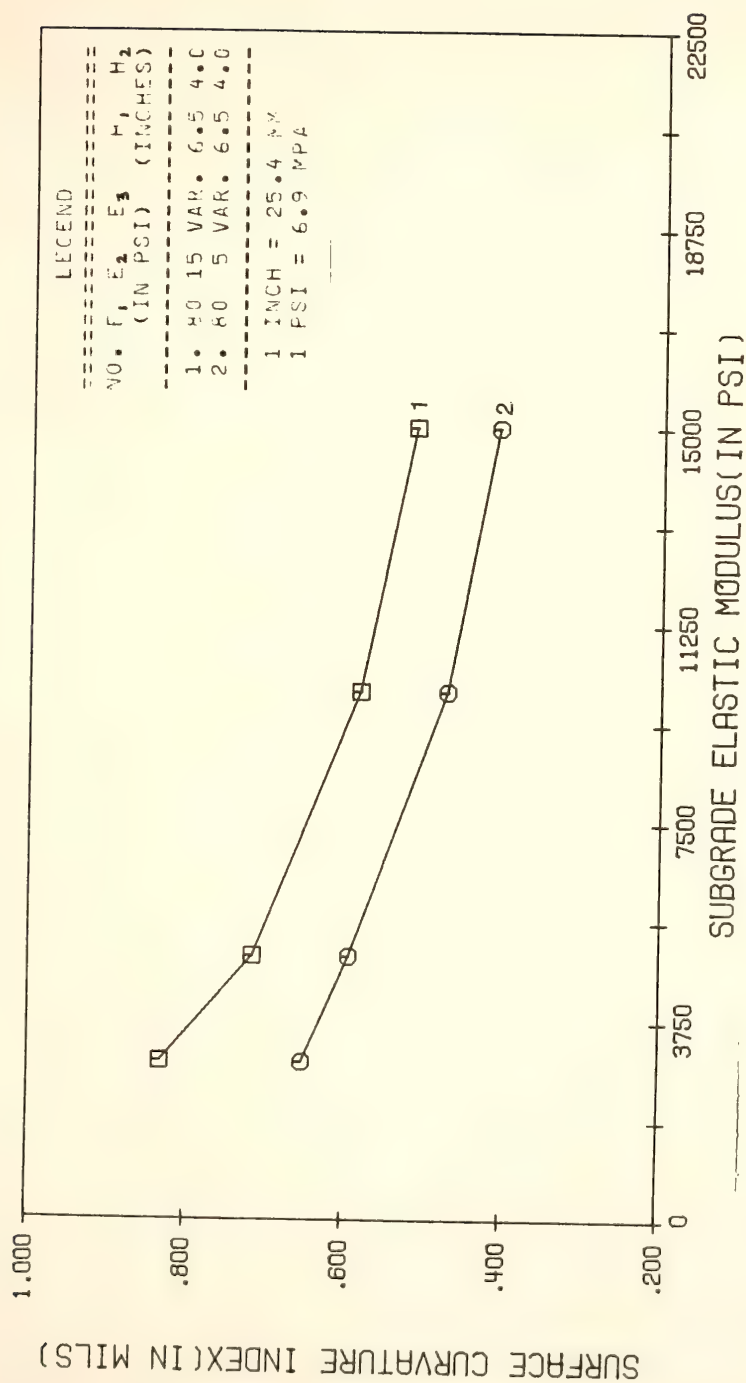


FIGURE 8.18 EFFECT OF CHANGES IN THE SUBBASE AND SUBGRADE ELASTIC MODULI ON THE SURFACE CURVATURE INDEX



eight months is at least as strong as the original asphalt concrete pavement of approximately 5.8 inches (170 mm). The original asphalt layer showed no severe distress patterns before it was removed.

The behavior of the foamed asphalt recycled pavement layer is thus in concordance with the behavior of conventional pavements, namely that the life of the pavement consists of three phases (11,70). During the first or consolidation phase the pavement layers, in this case the recycled and surface layers, undergo some consolidation due to the vehicle wheel loads. This phase can last from three to eighteen months depending on the rigidity (70). Since the recycled layer is not very rigid and the traffic volume is low, this phase will probably last a fairly long time. During this phase the deflections decrease. This is another indication that the recycled pavement is still in this phase. This phase should be followed by an elastic phase in which the pavement is elastic and the deflections constant. Pavements with low deflections usually have a longer elastic phase than those with high deflection (11). During the final phase the tensile strain will cause cracking in the asphalt layers and subsequent failure.

The deflections of the foamed asphalt recycled pavements are likely to become smaller than the values measured after eight months due to consolidation and curing of the foamed asphalt recycled material as described in Chapter 7.

The Dynaflect deflection parameters are very useful in the comparison of relative values on the same pavement from measurements taken at the same time. The SCI and BCI or  $D_5$  can be used to select sections with uniform subgrade or surface layers strengths. This was done in this study to select the sections used in the next chapter.



#### 8.4. Comparison of In-Situ CBR and BCI/D<sub>5</sub>

The in-situ CBR-values obtained from DCP tests were compared with BCI-values obtained from deflections taken during May 1981 (BEFORE2) and September 1981 (DURING and AFTER1). No significant statistical relationship could be found. The values are displayed in Figure 8.19 for the eastbound and Figure 8.20 for the westbound lane. The DCP-values shown are the average over the top 24 inches (610 mm) of the sandy silt subgrade. The deflections of the fifth sensor were also compared with the DCP values, but showed an even worse correlation.

One of the reasons for the poor correlations probably is that both BCI and D<sub>5</sub> are not unique indicators of the subgrade strength.





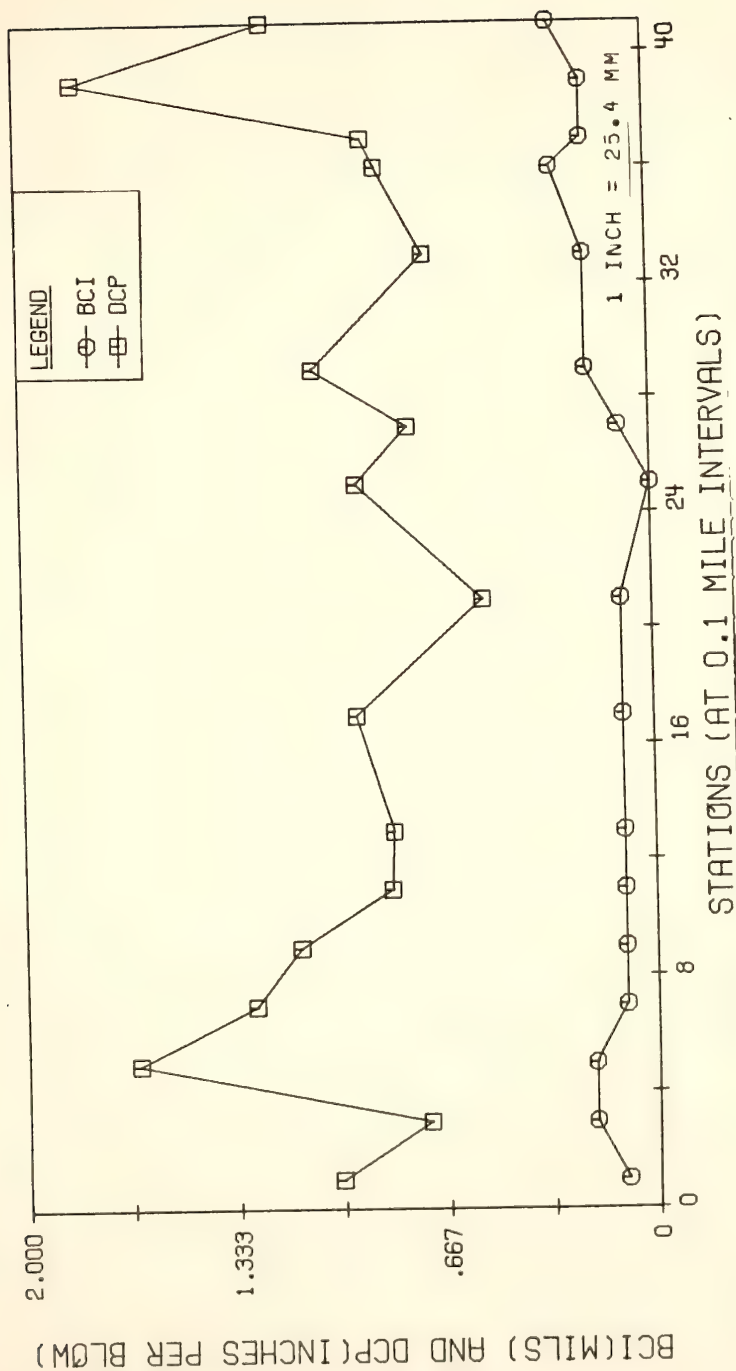


FIGURE 8.19 COMPARISON OF DCP AND BCI VALUES (EASTBOUND LANE)



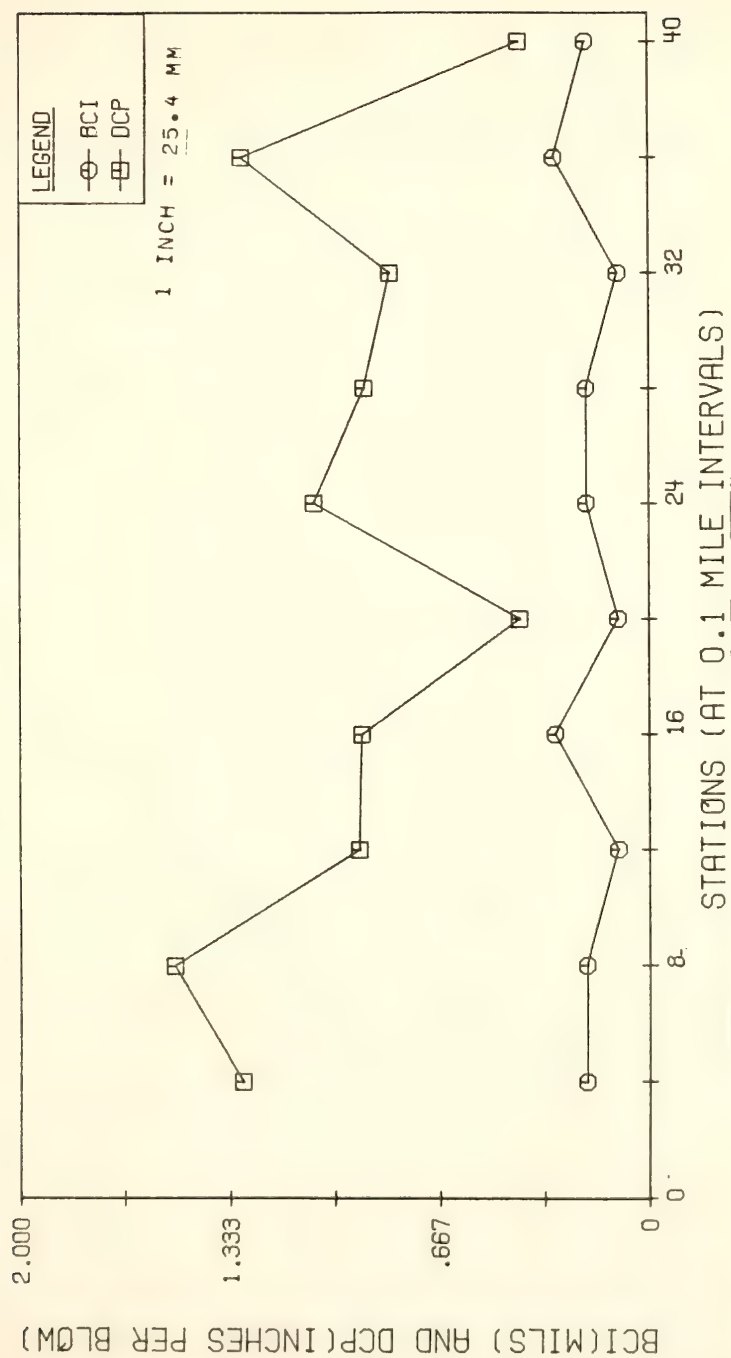


FIGURE 8.20 COMPARISON OF DCP AND BCI VALUES (WESTBOUND LANE)



## CHAPTER 9: STRUCTURAL COEFFICIENT DETERMINATION

### 9.1. The Pavement Response Model

Various pavement response models in general use are described in Chapter 2. The BISTRO program was used in this study due to its availability. The BISTRO computer program is based on the elastic layer theory and can calculate stresses, strains and deformations at various places in the pavement for virtually any number of layers. The BISTRO program is not stress-sensitive (non-linear). The elastic moduli of the stress-sensitive layers had to be adjusted independently of the computer program.

The analysis used in the BISTRO program is based on the theory of stress distribution in an unstratified semi-infinite elastic medium under the compressive action of a rigid body as presented by Boussinesq in 1885 and generalized to layered systems by Burmister in 1943. It also uses the Hankel transform theory. The following assumptions are made in the program.

1. Each layer is a homogeneous ideally elastic material with a uniform finite thickness, but infinite dimensions in the horizontal directions.
2. All the overlying layers are stratified vertically over the semi-infinite base (bottom) layer.
3. Each layer is physically defined by its elastic parameters, modulus of elasticity ( $E$ ) and Poisson's ratio ( $\gamma$ ).



4. The system is uniformly loaded over circular area axisymmetric surface loads.
5. The adjacent layers are bonded and no slip occurs at the interface.
6. The layers remain in contact and the vertical stress and displacement are continuous at the layer interfaces.
7. Displacements, stresses and strains are finite at infinite depth (81).

### 9.2. Distress Criteria

The selection of the distress criteria is an essential and very important part of the rational design procedure and the determination of structural equivalencies (16). The distress criteria are used to predict the performance of the pavement. The performance is usually measured as the number of equivalent 18000 lb (80 kN) axle loads (EAL) to cause some type of failure. The failure can either be structural or functional. Structural failure occurs when the pavement is not capable of carrying out its intended function without causing discomfort to the passengers or high stresses to the vehicles (76). This condition can occur due to excessive rutting, reduction in skid resistance or excessive deformations. Functional failure is defined as the collapse of the pavement structure due to the breakdown of one of the pavement layers. Fatigue cracking of any of the asphalt layers is usually used as a criterion.

The three criteria used in this study are fatigue cracking of the asphalt layers, excessive rutting and deformation. Figure 9.1 depicts these criteria and indicates where they occur in the pavement.





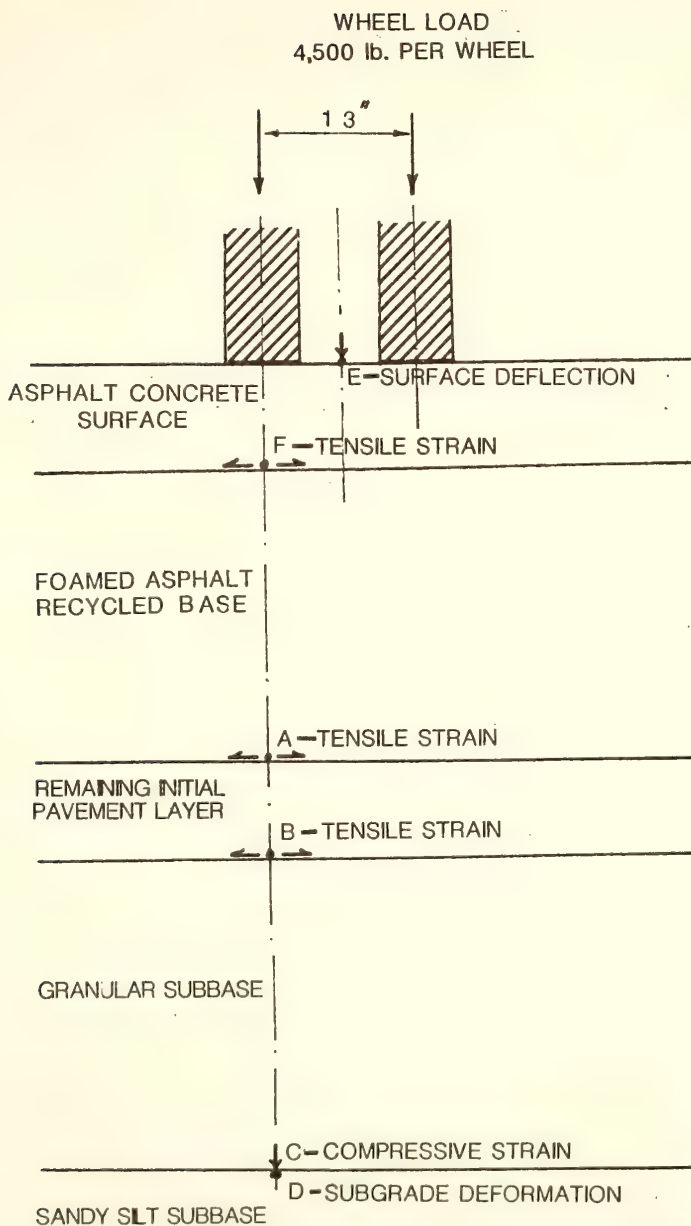


FIGURE 9.1 TYPICAL PAVEMENT CROSS SECTION  
USED IN THE ANALYSIS



### 9.2.1. Fatigue Cracking

Fatigue cracking in asphalt layers are caused by excessive radial stresses or strains at the bottom of the asphalt layers through repeated traffic load applications. The controlled stress (excessive strains) failure mode is usually used for asphalt layers of more than three to four inches thick and the controlled strain (excessive stress) failure mode for thinner layers (50). These strains or stresses are related to the number of load applications to failure ( $N_f$ ). The controlled stress failure mode relationships were used in this study to predict the number of load applications to failure for specific tensile strains at the bottom of the foamed asphalt recycled layer as well as the standard AASHTO asphalt surface layer. The controlled strain failure mode was used to check if the asphalt concrete surface on the experimental road would not fail before the recycled layer.

The relationships used are summarized in Tables 9.1 and 9.2. They are based on results from the indirect tensile tests and on relationships given in the literature. The relationships are valid for asphalt layers at 70°F (21°C). Rauhut and Kennedy (56) have developed procedures whereby the coefficients in the fatigue life tensile strain relationships can be adjusted for stiffnesses and temperatures. The mix stiffness can be adjusted by:

$$k_{1i} = k_{1j} (E_j/E_i)^4 \quad (9.1)$$

where

$E_j$  = elastic modulus of the reference mixture (for the best results it should be close to 500 kpi (3.45 MPa)).



Table 9.1. Fatigue Relationships Used for the Asphalt Concrete

$$N_f = k_1 (1/\epsilon_r)^{k_2}$$

Designation	$k_1$	$k_2$	Temp. (°F)	Ref.	Description
<u>Asphalt Concrete (Experimental Road)</u>					
X	$4.997 \times 10^{-14}$	5.10	85	12	From indirect tensile tests. - laboratory specimen
Y	$1.83 \times 10^{-6}$	3.20	85	11	- strength after eight months
<u>Asphalt Concrete (AASHTO material)</u>					
X	$7.87 \times 10^{-7}$	3.29	70	20	Developed from laboratory beam tests on AASHTO Road Test materials for <10% cracking
	$3.11 \times 10^{-6}$	3.14	72		
	$1.15 \times 10^{-6}$	3.25	77		
	$5.83 \times 10^{-6}$	3.07	80		
	$1.76 \times 10^{-5}$	2.95	85		
Y	$2.16 \times 10^{-13}$	4.995	70	56	Based on the tensile strain at the bottom of the AASHTO Road Test pavements (used elastic layer theory and psi = 2.5)
	$8.54 \times 10^{-13}$	4.79	72		
	$3.16 \times 10^{-13}$	4.90	77		
	$1.60 \times 10^{-12}$	4.72	80		
	$4.82 \times 10^{-12}$	4.60	85		

$N_f$  = number of load applications to failure.

$\epsilon_r$  = tensile strain at the bottom of the asphalt layer.

$k_1$  and  $k_2$  = coefficients.



Table 9.2. Fatigue Relationships Used for the Recycled Material

$$N_f = k_1 (1/\epsilon_r)^{k_2}$$

Designa- tion	$k_1$	$k_2$	Temp (°F)	Ref.	Description
1	$4.36 \times 10^{-8}$	3.47	70	56	For asphalt treated bases
	$6.37 \times 10^{-8}$	3.56	72		
	$1.72 \times 10^{-7}$	3.45	77		
	$3.23 \times 10^{-7}$	3.39	80		
	$9.73 \times 10^{-7}$	3.26	85		
2	$2.20 \times 10^{-6}$	3.29	70	20	From laboratory fatigue tests on AASHTO material with E = 150000 psi.
	$5.95 \times 10^{-6}$	3.17	72		
	$8.69 \times 10^{-6}$	3.12	77		
	$1.63 \times 10^{-5}$	3.07	80		
	$4.91 \times 10^{-5}$	2.95	85		
3	$4.47 \times 10^{-15}$	4.83	68	35	From laboratory fatigue tests on foamed asphalt stabil- ized material E = 190000 psi.
	$1.21 \times 10^{-15}$	4.73	72		
	$1.77 \times 10^{-14}$	4.69	77		
	$3.32 \times 10^{-14}$	4.62	80		
	$9.99 \times 10^{-14}$	4.50	85		





Table 9.2. Continued

Designa- tion	$k_1$	$k_2$	Temp (°F)	Ref.	Description
4	$9.02 \times 10^{-6}$	2.29	68	35	Same as 3 but a different mixture E = 160000 psi
	$1.32 \times 10^{-5}$	2.25	72		
	$3.57 \times 10^{-5}$	2.14	77		
	$6.70 \times 10^{-5}$	2.07	80		
	$1.95 \times 10^{-4}$	1.95	85		

$N_f$  = number of load applications to failure.

$\epsilon_r$  = tensile strain at the bottom of the asphalt layer.

$k_1$  and  $k_2$  = coefficients.



$E_i$  = elastic modulus of the mixture used.

$k_{1i}$  and  $k_{1j}$  are the coefficients in the fatigue life ( $N_f$ ) tensile strain ( $\epsilon_r$ ) relationship.

$N_f = k_1 (1/\epsilon_r)^{k_2}$  for the respective mixtures.

The adjustment for temperature is:

$$\log [k_1(T_1)/k_2(T_2)] = 0.00058 (T_1^2 - T_2^2) \quad (9.2)$$

where

$T_1$  = temperature of the reference relationship (in °F)

$T_2$  = actual temperature (in °F)

$k_1$  = coefficient in the fatigue life tensile strain relationship.

$k_2$  = exponent in the fatigue life tensile strain relationship.

The pavement temperatures at mid depth of the asphalt layer were determined at the time the deflection measurements were taken. A procedure developed by Southgate et.al (72) was used. The mean daily temperature for the five days prior to deflection measurement and the asphalt pavement surface temperature at the time of measurement were used. Temperatures at mid depth (3 inches or 75 mm) of 77°F (25°C), 72°F (22°C), 80°F (27°C) and 85°F (29°C) for the measurements taken during construction (DURING), after construction on the eastbound lane (AFTER1), after construction on the westbound lane (AFTER1) and eight months after construction (AFTER2) were used.

Rauhut suggests that any of the two adjustments viz. based on stiffness or on temperature can be used (56). In this study the temperature adjustment were used since:



1. It gives slightly lower load repetition values ( $N_f$ ) at a moduli of 200,000 psi (1380 MPa) or temperature of 80°F (27°C).
2. The fatigue relationships used for the recycled layer cannot be adjusted using the stiffness since the moduli at 70°F are now known in all cases.
3. The fatigue relationships developed from the indirect tensile testing, can better be adjusted by temperature.

The number of load repetitions increases as the temperature increases or the stiffness decreases.

The fatigue relationships chosen to be used in this study are:

1. A relationship developed by Finn et.al (56) from laboratory beam tests on AASHO Road Test materials and shifted to predict cracking of less than 10 percent.
2. A relationship developed by Witczak (56) from elastic layer predictions of the tensile strain at the bottom of the AASHO Road Test pavements.

These relationships are displayed in Figure 9.2.

Two relationships developed from the indirect tensile tests on the asphalt concrete used on the experimental section (SR16), one from laboratory compacted samples and one from cores taken eight months after construction were used to predict the service life of the surface layer (Figure 9.3). Four different relationships were used to predict the fatigue life of the foamed asphalt recycled layer. The relationships developed from the indirect tensile tests could not be used and therefore no relationships were available for the foamed asphalt recycled material. The following relationships were selected from the literature:



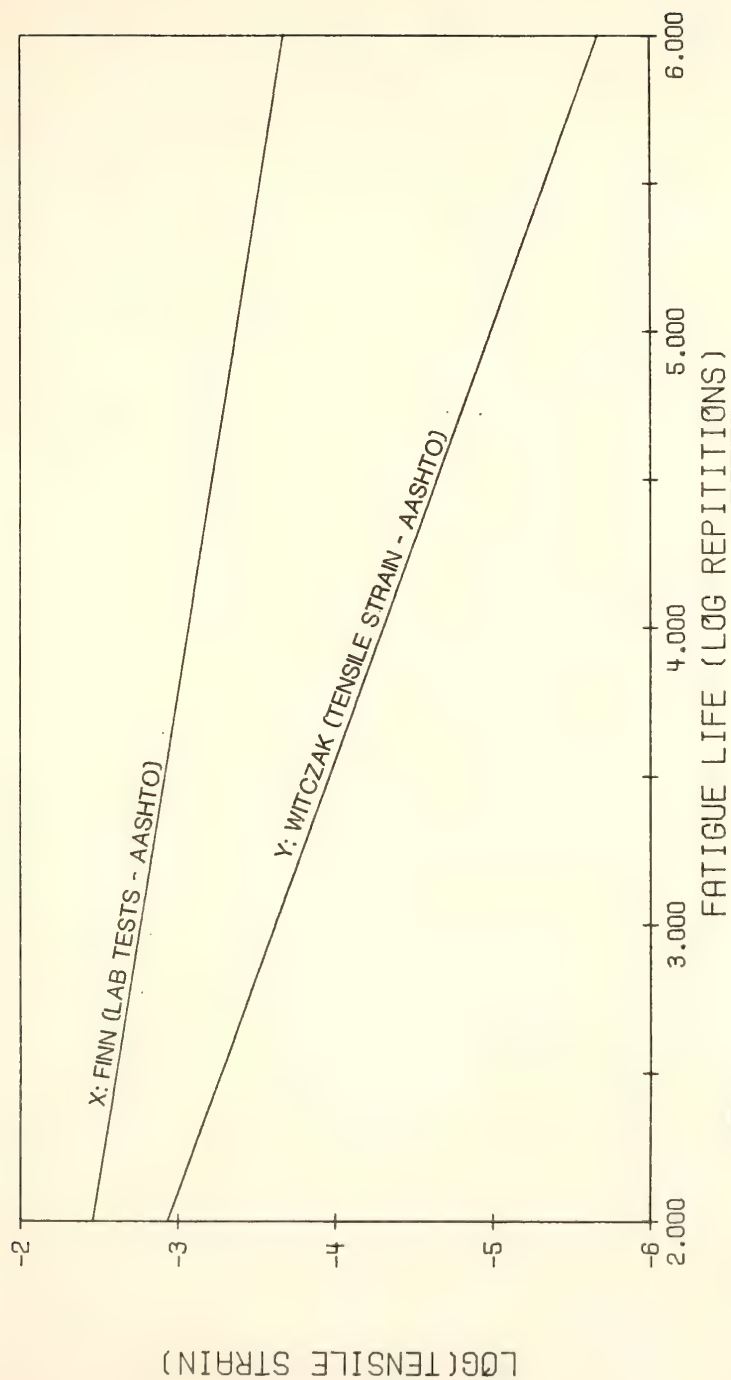


FIGURE 9.2 FATIGUE LIFE - TENSILE STRAIN RELATIONSHIPS FOR  
ASPHALT CONCRETE





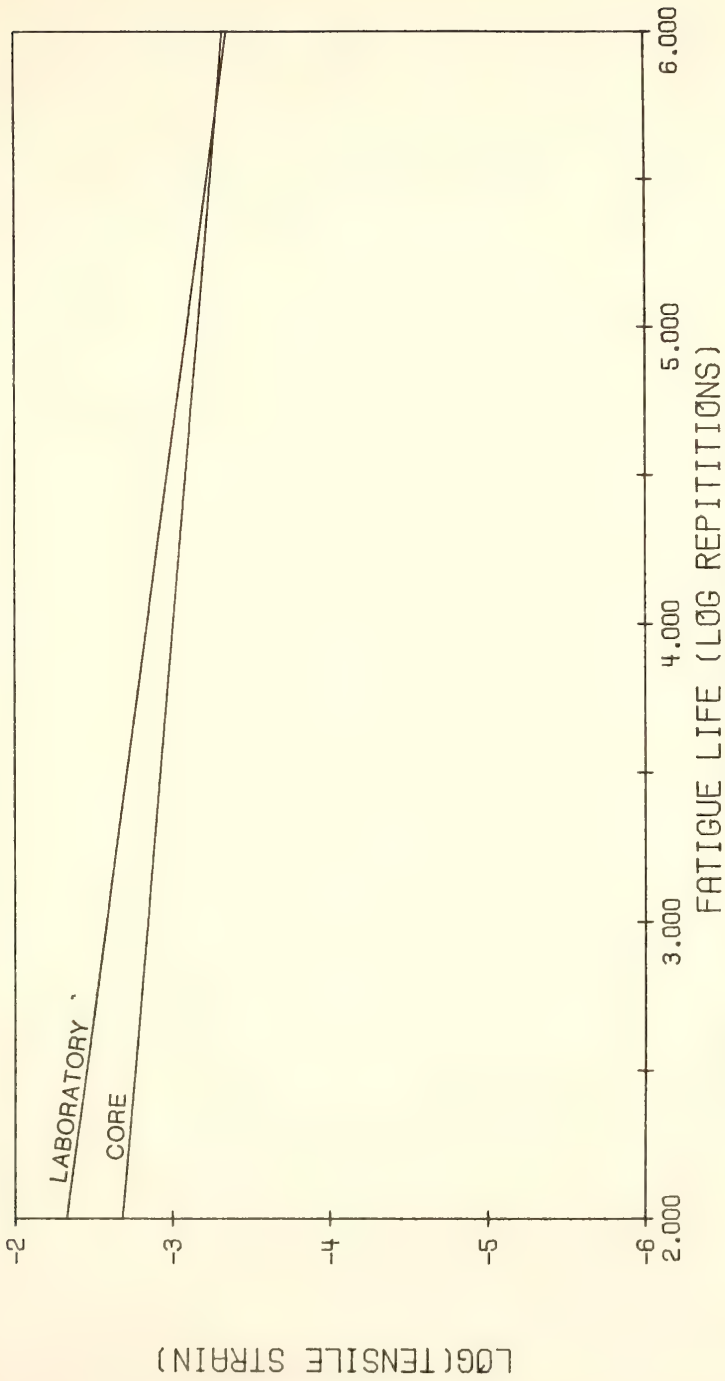


FIGURE 9.3 FATIGUE LIFE - TENSILE STRAIN RELATIONSHIPS FOR THE  
ASPHALT CONCRETE LAYER ON SR 16



1. Finn et.al (20) developed a relationship that can be adjusted for the stiffness of the asphalt layer. They suggest that it can be used for asphalt treated materials. Sufficient information regarding the cracking in asphalt-treated base courses were not available from the AASHO Test Road to develop separate relationships. An elastic modulus of 150,000 psi (1035 MPa) was used. This is approximately 50 percent higher than the strength of the laboratory compacted samples after ten days curing and tested at 72°F. Samples taken from the test road eight months after construction gave an average elastic modulus of 180,000 psi (1242 MPa) with a very large standard deviation of 84,000 psi (579 MPa) for only three samples. A conservative value would therefore be 150,000 psi (1035 MPa).
2. Smith and Nair (56) developed a relationship for asphalt treated materials. Since the foamed asphalt recycled layer can be considered as an asphalt treated material, this relationship was used in the study.
3. Epps and Little (35) developed fatigue relationships for foamed asphalt stabilized material from stress controlled laboratory tests. Two of these relationships were used in this study to predict the fatigue life of the foamed asphalt recycled material. It was shifted with a factor of 13 to take field conditions into consideration (35).

Figure 9.4 shows the large differences among these curves. All the fatigue life relationships used to predict fatigue cracking were summarized in Tables 9.1 and 9.2.



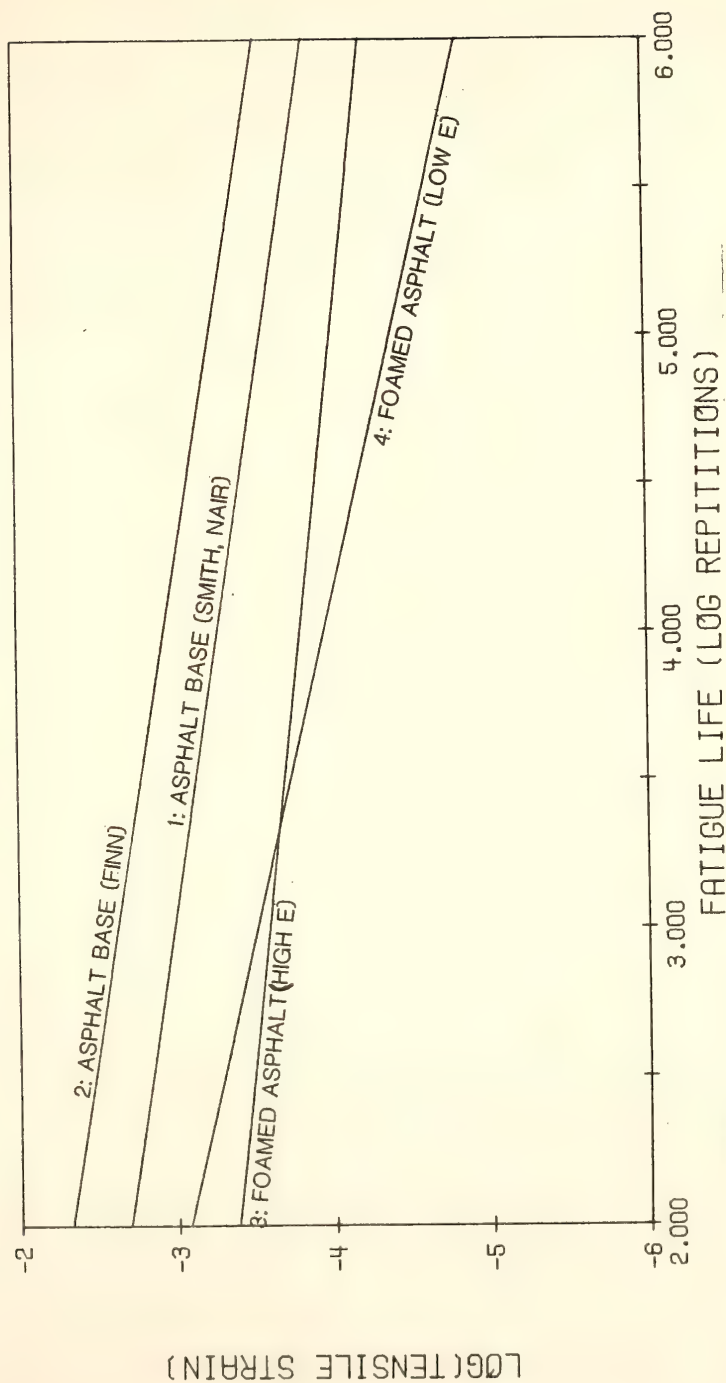


FIGURE 9.4 FATIGUE LIFE - TENSILE STRAIN RELATIONSHIPS FOR  
ASPHALT BASE COURSES



### 9.2.2. Rutting

The maximum vertical subgrade strain ( $\epsilon_v$ ) is used to predict the number of loads on a pavement to reach a certain rut depth. The maximum compressive strain on the subgrade has been related to the number of EAL that would cause undesirable rutting as well as with the structural number (SN). The relationships used in this study were selected from relationships given in the literature and described in Chapter 2. The maximum deformation of the subgrade ( $W_g$ ) has also been related to the number of 18,000 lb. (80 kN) axle loads to cause Present Serviceability (PSI) to be reduced to 2.5 (33). These relationships are summarized in Table 9.3 and displayed in Figure 9.5.

### 9.2.3. Deformation

Although maximum deflection is not very frequently used as a distress mode it was used in this study to determine the structural layer equivalencies. The relationships correlated maximum deflection with the structural number and EAL for a reduction of 1.5 or 2.0 in the psi. These relationships were obtained from a study done on an AASHTO satellite project in Pennsylvania (72). They are summarized in Table 9.3.

## 9.3. Selection of the Pavement Cross Sections

The Dynaflect deflections taken during and after construction were used to select uniform sections. Each of the lanes were divided into sections with approximate equal deflections at each of the five sensors. This was done for the three sets of deflection readings, one during and two after construction (DURING, AFTER1 and AFTER2) on the eastbound





Table 9.3. Failure Relationships Based on Strains or Deformations

Designation	Relationship	Ref.	Description
A.	Tensile strain at the bottom of the recycled layer ( $\epsilon_{r2}$ )		
B.	Tensile strain at the bottom of the remaining initial layer ( $\epsilon_{r3}$ )		
C.	Compressive strain on the subgrade ( $\epsilon_v$ )		
	$\log \epsilon_v = -1.9765 - 0.2008 \log(N_f)$	76	For AASHTO materials
	$\log N_f = 2.05076 - 597.662 (\epsilon_v)$	51	Regression on AASHTO Road Test results
	$\epsilon_v = 2.8 \times 10^{-2} (N)^{-0.25}$	51	Used by Shell in their design
	$\epsilon_v = 14.81 + 14805.05(SN + 1)$	74	From analysis of AASHTO satellite test road
D.	Deformation of the subgrade ( $\delta_s$ )		
	$N_f = 0.098e^{-3.39 \ln \delta_s}$	34	From results of an analysis on Loop 4 of the AASHTO Road Test
E.	Maximum deformation at the surface ( $\delta_m$ )		
	$\log RR = -6.866 + 4.325 \log(\delta_m)$	56	From AASHTO Road Test results
	$\delta_m = 0.85 + 1287.30(SN + 1)$	74	From analysis of AASHTO satellite test road

$N_f$  = number of load applications to failure.

$\epsilon_v$  = subgrade compressive strain (maximum).

SN = structural number.

RR = rate of rutting.

$\delta_m$  = surface deflection.

$\delta_s$  = subgrade deformation (vertical).



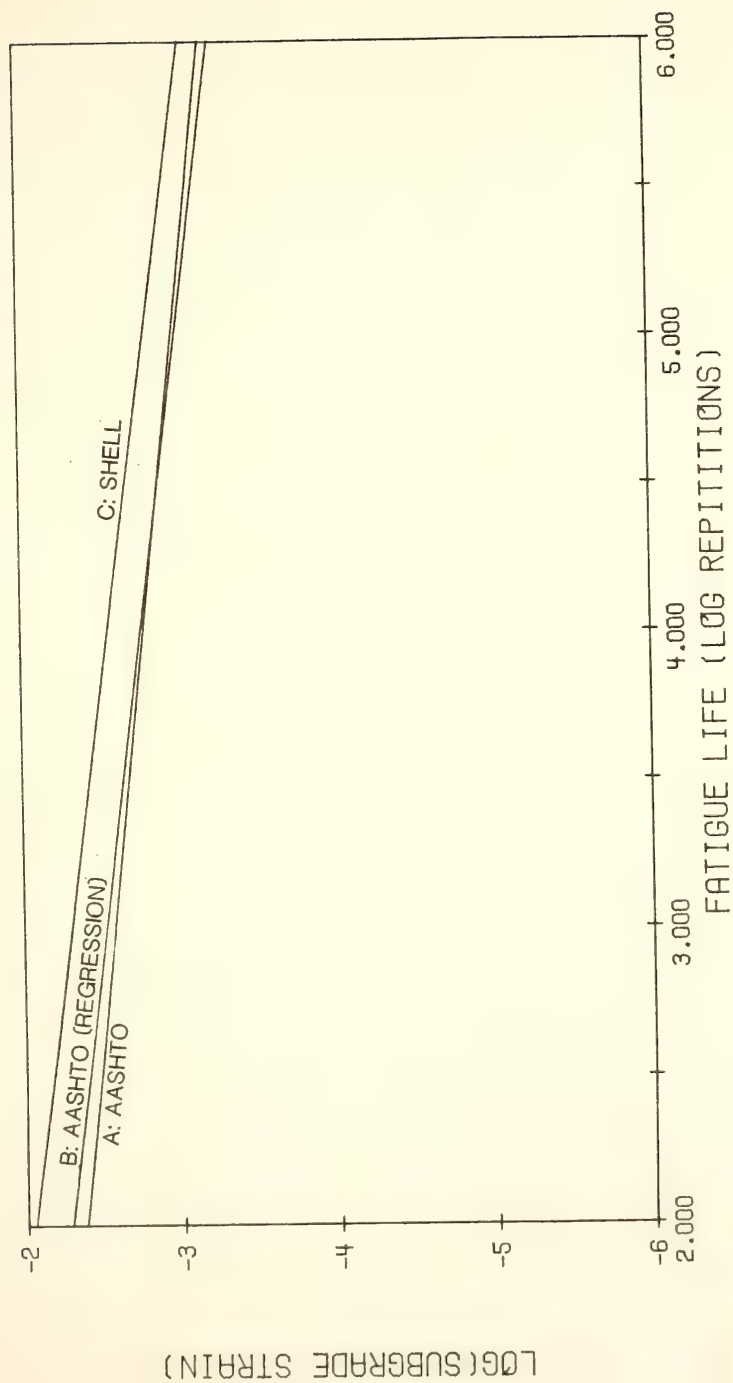


**FIGURE 9.5 FATIGUE LIFE – COMPRESSIVE STRAIN RELATIONSHIPS FOR SUBGRADES**



lane and two sets of readings, both after construction (AFTER1 and AFTER2) on the westbound lane. From each of these five sets of readings five sections were chosen to represent the two sections with the highest deflections, the two with the lowest deflections and the average deflections. The values are given in Table 9.4 for the eastbound and Table 9.5 for the westbound lanes. As expected the section with the lowest deflections during construction also gave the lowest deflections during the measurements taken after construction. This was also the case for the other sections.

These 25 different cross sections were simulated by pavement cross sections that would give the same deflections (deflection basin) at the five sensors when analyzed by the BISTRO elastic layer program. A load of 9000 lb (40 kN) applied through two wheels at a pressure of 80 psi (550 Pa) each and spaced 13 inches (330 mm) apart was used in the program. It is the same as the standard load used during the Benkelman Beam deflection measurements. No information besides the results from the laboratory compacted cores was available regarding the properties of the recycled layer material or the asphalt concrete surface material for the deflections taken during (DURING) or soon after (AFTER1) construction. The laboratory testing on the cores was conducted approximately two to three months after construction and therefore the information obtained from the tests could not be used to characterize the foamed asphalt recycled and asphalt surface material during and soon after construction. Iterations had to be made to select the correct characteristics. The BISTRO program assumes constant elastic moduli ( $E$ ) for each of the layers. Since the granular subbase and



Table 9.4. Characteristics of Selected Pavement Sections (Eastbound)

	D <sub>1</sub>	D <sub>2</sub>	D <sub>3</sub>	D <sub>4</sub>	D <sub>5</sub>	SCI	Slope	BCI	SPD (%)
	in Mils (from Dynaflect)								
DURING									
high1	3.02	1.81	.56	.26	.13	1.21	2.89	.13	38.28
high2	2.82	1.90	.73	.35	.16	.92	2.66	.19	42.27
low1	1.47	1.03	.49	.30	.18	.44	1.29	.12	47.21
low2	1.51	1.07	.51	.30	.17	.44	1.34	.13	47.15
ave	2.10	1.46	.66	.36	.20	.64	1.90	.16	45.52
AFTER1									
high1	2.16	1.27	.63	.36	.21	.89	1.95	.15	42.87
high2	2.41	1.54	.85	.52	.25	.87	2.16	.27	46.22
low1	1.19	.80	.51	.36	.22	.39	.97	.14	51.76
low2	1.29	.84	.49	.34	.21	.45	1.08	.13	49.15
ave	1.79	1.16	.66	.44	.26	.63	1.53	.18	48.16
AFTER2									
high1	2.57	1.58	.73	.34	.18	.99	2.39	.16	42.02
high2	3.43	2.37	1.28	.61	.29	1.06	3.14	.32	46.53
low1	1.36	.97	.58	.35	.22	.39	1.14	.13	51.18
low2	1.58	1.12	.64	.37	.23	.46	1.35	.14	49.87
ave	2.13	1.51	.86	.47	.27	.62	1.86	.20	49.20

D<sub>1</sub> to D<sub>5</sub> = deflections of Dynaflect sensors 1 to 5 respectively.

SCI = surface curvature index.

BCI = base curvature index.

SPD = spreadability.

1 inch = 25.4 mm.





Table 9.5. Characteristics of Selected Pavement Sections (Westbound)

	D <sub>1</sub>	D <sub>2</sub>	D <sub>3</sub>	D <sub>4</sub>	D <sub>5</sub>	SCI	Slope	BCI	SPD (%)
	in Mils								
AFTER1									
high1	2.79	1.72	.88	.50	.23	1.07	2.56	.27	43.87
high2	2.99	1.99	1.15	.73	.37	1.00	2.62	.36	48.36
low1	1.11	.75	.45	.32	.20	.36	.91	.12	50.99
low2	1.37	.91	.55	.37	.21	.46	1.16	.16	49.78
ave	2.06	1.31	.74	.47	.26	.75	1.80	.21	46.99
AFTER2									
high1	3.53	2.44	1.30	.64	.32	1.09	3.21	.32	46.63
high2	3.36	2.38	1.40	.82	.49	.98	2.87	.33	50.30
low1	1.17	.82	.48	.31	.23	.35	.94	.08	51.45
low2	1.62	1.14	.66	.38	.22	.48	1.40	.16	49.63
ave	2.40	1.65	.91	.50	.29	.75	2.11	.21	47.92

D<sub>1</sub> to D<sub>5</sub> = deflections of Dynaflect sensors 1 to 5 respectively.

SCI = service curvature index

BCI = base curvature index

SPD = spreadability



sandy silt subgrade layers are stress-sensitive, iterations were made to obtain the correct moduli values for each of these layers. The following procedure was followed (Figure 9.6):

1. Molds were prepared plotting each of the 25 selected deflection basins on transparent paper.
2. The thicknesses of the asphalt concrete surface ( $h_1$ ), the foamed asphalt recycled layer ( $h_2$ ), the layer of initial pavement that remained between the recycled layer and the granular layer ( $h_3$ ) and the granular layer ( $h_4$ ) were obtained from the results of the tests conducted prior and during construction. Poisson's ratio values of 0.35 for the asphalt layers, 0.40 for the granular layer and 0.50 for the subgrade were arbitrarily selected to represent the material. Although Poisson's ratios of 0.40 are also widely used for asphalt layers a lower value gives higher stresses and strains and therefore more conservative values. Table 9.6 summarizes the thicknesses and Poisson ratios used.  
  
A large number of deflection basins were obtained by using the BISTRO program for low, intermediate and high values of the elastic moduli of the different layers. Examples are displayed in Figure 9.7 as well as Figure 8.13. All the deflections were divided by 20.63 to be compatible with the Dynaflect values (80,18).
3. Cross sections with specific moduli were then selected by comparing the actual deflection basins (on the transparent paper) with the developed deflection basins. The subgrade modulus could be (uniquely) identified by these deflection



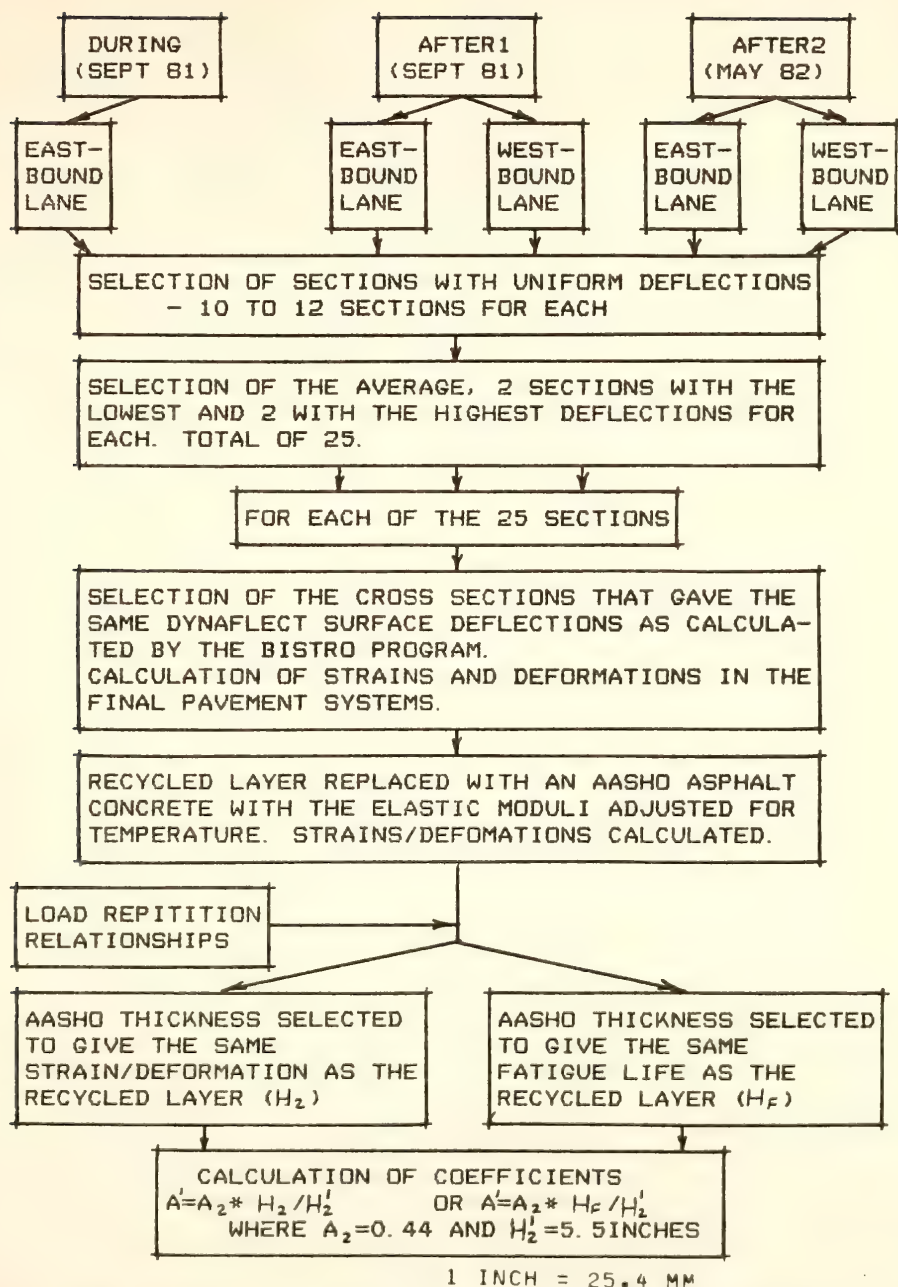


FIGURE 9.6 FLOW DIAGRAM OF THE STRUCTURAL  
COEFFICIENT DETERMINATION PROCEDURE



Table 9.6. Pavement Cross-Section Characteristics

Layer	Poisson's Ratio	Elastic Modulus (in psi)	Thickness (inches)	Description of Layer
1	0.35	120000-250000*	1.25	Asphalt concrete surface
2	0.35	14000-13000	5.50	Foamed asphalt recycled
3	0.35	10000-50000*	1.00	Remaining initial pavement
4	0.40	4700-12200	3,4,5	Granular subbase
5	0.50	2350-9600	100-450	Sandy silt subgrade
<hr/>				
6	0.50	Varied	Var.	Extra layer where necessary
7	0.50	>1000000		Stiff subgrade layer at 350 inches minimum

\*E-values arbitrarily chosen in this range.

1 inch = 25.4 mm

1 psi = 6.9 kPa







**FIGURE 9.7 EFFECT OF CHANGES IN THE LAYER  
ELASTIC MODULI ON THE DYNAFLECT  
DEFLECTION BASIN**

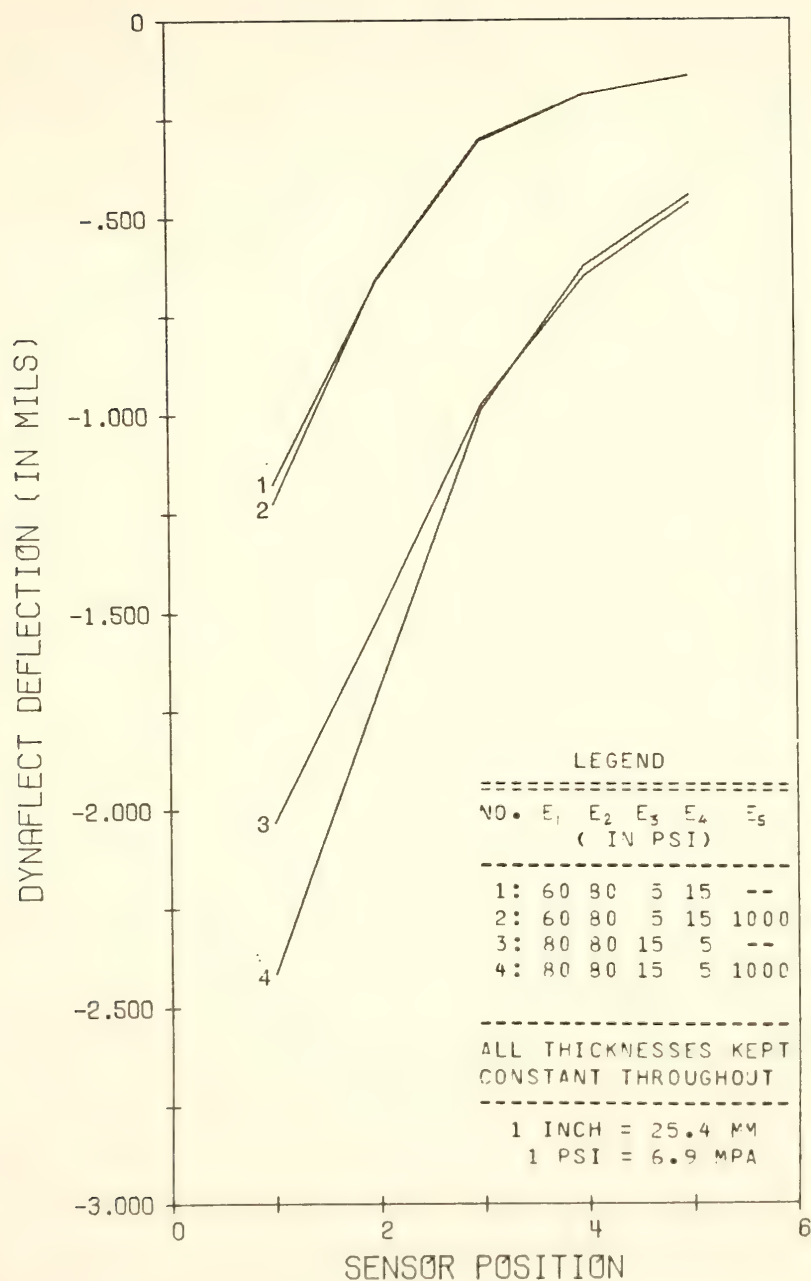


FIGURE 9.7



basins, since they are essentially insensitive to changes in elastic moduli and thicknesses of the overlaying layers for the combinations tested (Figure 9.7). None of the deflections at the sensors or any combination thereof is a unique identifier of the moduli of the layers overlaying the subgrade. Since the granular material is stress sensitive the BISTRO program was used to calculate the bulk stress ( $\theta$ ) in the middle of the granular layer. No relationships between the bulk stress and the  $M_R$  is available for granular material in Indiana and therefore a relationship was selected from the literature (76,55,26,36,43,67).

The relationship used was:

$$M_R = 5000 \theta^{0.4} \quad (9.3)$$

where

$M_R$  = resilient modulus (psi)

$\theta = \sigma_1 + \sigma_2 + \sigma_3$  = bulk stress (psi)

The bulk stress at the center of the granular layer is greatly influenced by the elastic modulus of the subgrade. It is only slightly influenced by small changes in the elastic modulus and thickness of the asphalt layers overlaying the granular layer. The bulk stress is not influenced to a great extent by the small changes in thickness of the granular layer, but by changes in the Poisson's ratio. The elastic modulus or  $M_R$  was calculated at the center of the granular layer through iterations. This left the elastic moduli of the remaining initial pavement layer, the foamed asphalt recycled layer and the asphalt surface layer undetermined. Although the  $M_R$  of the initial pavement asphalt layer was



determined it could not be used since it was not known to what extent the remaining approximately one inch was disturbed during the milling operation. The elastic modulus was arbitrarily taken to be between 10,000 psi (70 kPa) and 50,000 psi (345 kPa). The layer is thin and has only a small influence on the deflections and the bulk stress in the granular layer. The elastic moduli of the granular layer determined from the deflections taken during construction on the recycled layer on the eastbound lane were used in the BISTRO program to determine the elastic moduli of the foamed asphalt layer that gave the appropriate deflections. These moduli were used in the analysis of the deflections taken soon after construction to determine the moduli of the asphalt surface layer.

The BISTRO program calculated in the most cases deflections well above those measured in the field with the same shape of deflection basin (43). The deflections calculated by the BISTRO program can be reduced with a constant by placing a stiff layer at some depth in the hypothetical pavement (Figure 9.8). This is theoretically sound since the subgrade is stress-sensitive with the elastic modulus increasing in depth, while the BISTRO program assumes it to be constant. The elastic modulus calculated under the pavement layer combinations investigated was approximately 1,000,000 psi (6.9 MPa) at 350 inches (890 mm). Since a relationship between the deviator stress ( $\sigma_d$ ) and the  $M_R$  of the subgrade was not available for sandy silt in the study, a relationship of:

$$M_R = 27,000 \sigma_d^{-1.1} \quad (9.4)$$







FIGURE 9.8 EFFECT OF THE INCLUSION OF A STIFF  
SUBGRADE LAYER AT A DEPTH OF 350 INCHES ON  
THE DYNAFLECT DEFLECTION BASIN

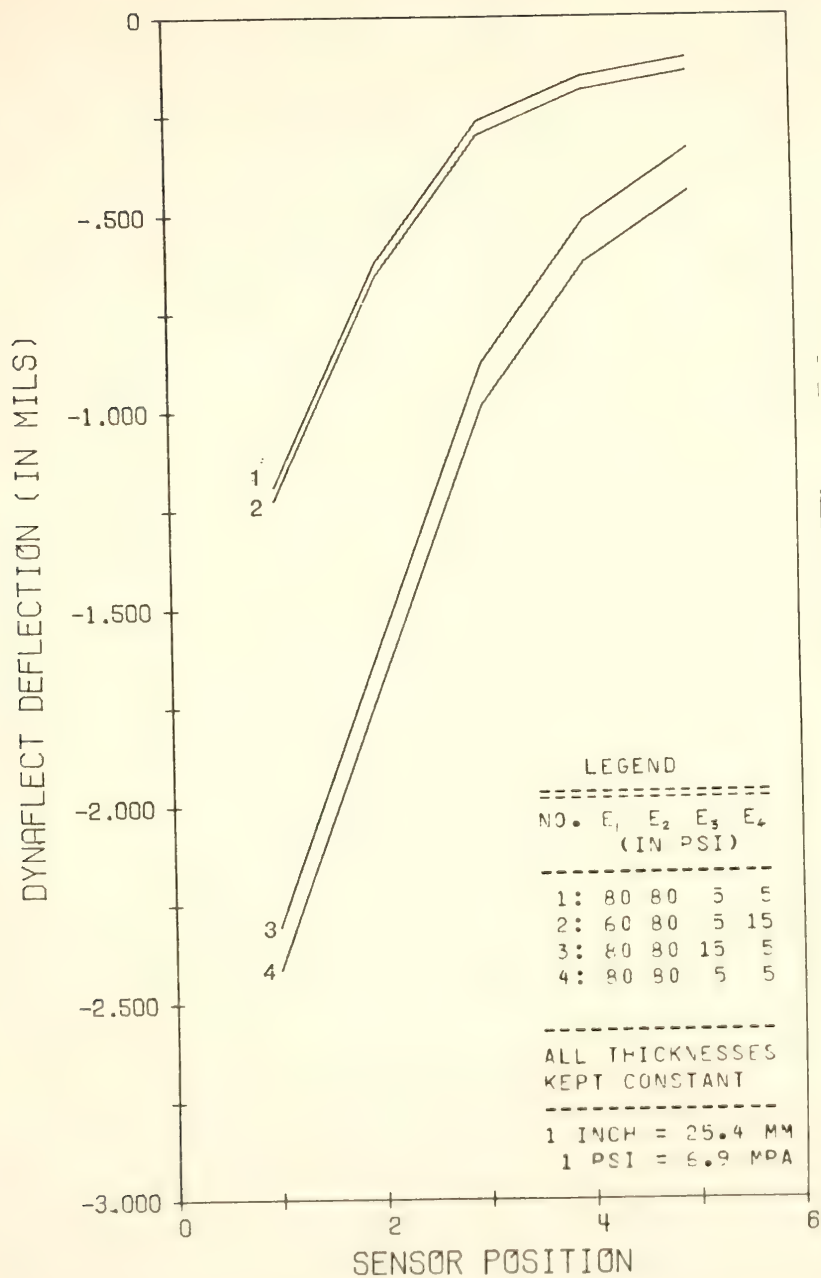


FIGURE 9.8



where

$M_R$  = resilient modulus (psi)

$\sigma_d = \sigma_3 - \sigma_1$  = deviator stress (psi)

was selected from the literature (76,55,26,67,36,43).

The magnitude of the constant by which the deflection basin is shifted with the introduction of a stiff subgrade layer at some depth depends mainly on the elastic modulus at the top of the subgrade and the depth of the stiff layer. The subgrade was therefore divided into a soft top layer and a stiff bottom layer at an arbitrarily depth of 350 inches (890 mm). In cases where it was necessary another layer was placed at some depth above the stiff layer with an appropriate elastic modulus. The elastic moduli at the depth were also determined through iterations. Although the magnitude of these layers had little effect on the deflections they can have an effect on the stresses and strains.

The pavement sections selected from the deflections taken eight months after construction (AFTER2) were simulated in a similar way except that E-values for the asphalt surface and foamed asphalt recycled material were obtained from core specimens. The cores were taken at the same time the deflections were measured.

#### 9.4. Sensitivity Analysis

The pavement cross sections selected and used in the determination of the equivalency factors and summarized in Tables 9.7 and 9.8 are by no means exactly the same as those in the actual pavement but they give deflections within 10 percent of the deflections as measured by each of the Dynaflect sensors. A sensitivity analysis was conducted on one of



Table 9.7. Selected Pavement Cross Sections (Eastbound lane)

	E <sub>1</sub> psi	E <sub>2</sub> psi	E <sub>3</sub> psi	E <sub>4</sub> psi	h <sub>4</sub> in.	E <sub>5</sub> psi	h <sub>5</sub> in.	E <sub>6</sub> psi	h <sub>6</sub> in.	E <sub>7</sub> psi
DURING										
Low 1		100,000	50,000	12,200	4	7500	200	1.3 x 10 <sup>6</sup>	140	1 x 10 <sup>6</sup>
Low 2				Same as Low 1						
Ave		40,000	40,000	11,500	4.5	5850	170	830,000	170	900,000
High 1		14,000	14,000	10,500	5	3800	80	80,000	260	4 x 10 <sup>6</sup>
High 2		15,000	15,000	11,300	4.0	4500	110	180,000	230	3.5 x 10 <sup>6</sup>
AFTER1										
Low 1	200,000	120,000	50,000	12,200	5	8800	400	9 x 10 <sup>6</sup>		
Low 2	120,000	90,000	50,000	12,100	4	8700	400	1		
Ave	180,000	40,000	50,000	10,000	4.5	5900	220	1.4	120	2.9 x 10 <sup>6</sup>
High 1	200,000	20,000	20,000	10,000	5	5000	120	240,000	220	2.4 x 10 <sup>6</sup>
High 2	200,000	30,000	20,000	7,500	3	4400	160	690,000	180	1.2 x 10 <sup>6</sup>
AFTER2										
Low 1	200,000	100,000	20,000	10,500	4	8100	400	5.6 x 10 <sup>6</sup>		
Low 2	250,000	130,000	40,000	8,000	4	5000	120	150,000	120	2.3 x 10 <sup>6</sup>
Ave	200,000	90,000	20,000	7,000	4.5	3600	120	116,000	220	1.6 x 10 <sup>6</sup>
High 1	180,000	20,000	15,000	7,800	5	4100	100	75,000	240	1.6 x 10 <sup>6</sup>
High 2	200,000	30,000	20,000	4,800	3	2450	100	100,000	240	1.9 x 10 <sup>6</sup>

1 psi = 6.9 kPa

1 in. = 25.4 mm





Table 9.8. Selected Pavement Cross Sections (Westbound lane)

	E <sub>1</sub> psi	E <sub>2</sub> psi	E <sub>3</sub> psi	E <sub>4</sub> psi	h <sub>4</sub> in.	E <sub>5</sub> psi	h <sub>5</sub> in.	E <sub>6</sub> psi	h <sub>6</sub> in.	E <sub>7</sub> psi
AFTER1										
Low 1	250,000	130,000	50,000	11,800	4	9,300	400	$10 \times 10^6$		
Low 2	120,000	90,000	50,000	11,500	5	8,300	400	$10 \times 10^6$		
Ave	180,000	40,000	50,000	8,700	4.5	4,600	150	470,000	190	$1.5 \times 10^6$
High 1	150,000	20,000	20,000	8,000	5	3,500	110	200,000	230	$2.4 \times 10^6$
High 2	120,000	40,000	20,000	6,300	3	3,150	150	600,000	190	$0.8 \times 10^6$
AFTER2										
Low 1	250,000	90,000	50,000	12,000	4	9600	450	$10^6$		
Low 2	200,000	95,000	30,000	9,300	5	5400	140	370,000	240	$2.3 \times 10^6$
Ave	200,000	60,000	30,000	6,600	4.5	3300	100	150,000	240	$3 \times 10^6$
High 1	200,000	30,000	15,000	4,700	3	2350	100	110,000	240	$2.1 \times 10^6$
High 2	180,000	33,000	15,000	5,300	4	2600	140	250,000	200	$1.6 \times 10^6$

1 psi = 6.9 kPa

1 in. = 25.4 mm.



the cross sections to investigate the effect of changes in the elastic moduli and thicknesses on strains and deformations. The selected cross section represented the average of the eastbound lane soon after construction (AFTER1). Table 9.9 exhibits the changes in the strains and deformations that were used in this study to determine structural coefficients with changes in the elastic moduli and thicknesses of the layers. The only changes that had an influence of more than 10 percent on the strain and deflection values were changes in the elastic moduli of the first five layers for the ranges analyzed. The ranges coincide with the upper and lower limits arbitrarily chosen for the first and third layer elastic moduli and 20 percent for the other layers. An accuracy of 20 percent was considered to have been easily obtained during the selection process. All the thicknesses except for  $h_4$  were further considered to have been determined through testing and were therefore fixed. The elastic modulus of the subgrade ( $E_5$ ) is the most important single parameter. For a change of plus or minus 10 percent in  $E_5$  the strains and deflections were within 10 percent of the average value. An accuracy of at least 10 percent was secured during the selection of the subgrade elastic moduli, since the deflections of sensors 3, 4 and 5 of the Dynaflect can be used and the subgrade moduli therefore uniquely be identified. The elastic moduli of the foamed asphalt recycled layer ( $E_2$ ) were within 20 percent of the correct value and had a large effect on only the radial strain below the surface layer. This is not important in this analysis since these strains were only used to determine if the fatigue life of the surface is more than that of the recycled layer. Changes in the elastic moduli of the



Table 9.9. Sensitivity Analysis

Condition			Percent Change in					
			1	2	3	4	5	6
E <sub>1</sub>	Upper limit	250000	-1	+48	-1	-2	-2	-2
	Reference	180000	0	0	0	0	0	0
	Lower limit	120000	+2	-32	0	+2	+3	+3
E <sub>2</sub>	+20%	48000	-2	-40	-2	-4	-4	-2
	Reference	40000	0	0	0	0	0	0
	-20%	32000	+4	+64	+1	+4	+6	+1
E <sub>3</sub>	Upper limit	50000	-3	- 3	-17	-8	-3	-1
	Reference	30000	0	0	0	0	0	0
	Lower limit	10000	+4	+ 3	+29	-1	+3	+2
E <sub>4</sub>	+20%	12000	-2	0	-6	-7	0	-1
	Reference	10000	0	0	0	0	0	0
	-20%	8000	+3	0	+7	+8	0	+1
E <sub>5</sub>	+20%	7080	-11	+ 7	-3	-3	-11	-13
	Reference	5900	0	0	0	0	0	0
	-20%	4720	+14	- 9	+4	+4	+13	+17
E <sub>6</sub>	Reference *2	$2.8 \times 10^{-6}$			No Change			
	Reference	$1.4 \times 10^{-6}$	0	0	0	0	0	0
	Reference/2	$0.7 \times 10^{-6}$			No Change			
E <sub>7</sub>	Reference *2	$2.0 \times 10^{-6}$			No Change			
	Reference	$1.0 \times 10^{-6}$	0	0	0	0	0	0
	Reference/2	$0.5 \times 10^{-6}$			No Change			
h <sub>5</sub>	+20%	265	+1	0	0	0	0	0
	Reference	220	0	0	0	0	0	0
	-20%	175	-2	+ 1	0	0	0	-3

1 = maximum surface deflection

2 = strain at the bottom of the surface layer

3 = strain at the bottom of the foamed asphalt recycled layer

4 = strain at the bottom of the remaining initial pavement layer

5 = maximum compressive strain on the subgrade

6 = maximum subgrade deflection

All elastic moduli(E) in psi

h in inches

1 psi = 6.9 kPa

1 inch = 25.4 mm



surface layer ( $E_1$ ) and the remaining initial pavement layer ( $E_3$ ) induced large changes in the strain at the bottom of the surface layer and the recycled layer respectively. The strain at the bottom of the surface layer was not important as explained earlier. The changes in the tensile strain at the bottom of the recycled layer due to changes in the elastic moduli of the remaining initial layer ( $E_3$ ) were important and had to be taken into consideration in comparing the structural coefficients. The value of  $E_3$  did not influence the determination of the structural equivalency factors since the corresponding pavement with the AASHTO layer had the same  $E_3$  value. The ratio of strains remained approximately the same.

#### 9.5. Determination of AASHTO Asphalt Concrete Surface Equivalent Thicknesses

Different elastic moduli ( $E$ ) for the AASHTO asphalt concrete surface were used depending upon the pavement temperature during deflection measurement. Moduli of 400,000 psi (2760 MPa), 350,000 psi (2415 MPa), 300,000 psi (2070 MPa) and 200,000 psi (1380 MPa) were selected for temperatures of 72°F, 77°F, 80°F and 85°F respectively. These elastic moduli were interpolated from values determined for the AASHTO Road Test surface material for the four seasons of the year, each at a different temperature (33) as well as a temperature-elastic modulus relationship developed from laboratory tests on a similar mixture (35).

The AASHTO layer was used in each of the 25 selected cross sections in the place of the foamed asphalt recycled layer to calculate strains and deformations for various thicknesses. With the BISTRO program increments of one inch in the AASHTO layer were used. The resilient





moduli of the granular material were also adjusted through an iteration process. Care was taken to cover a wide enough range of strains and deflections to avoid unnecessary extrapolation. Strains were calculated under one of the wheels.

#### 9.6. Determination of Equivalency Factors

The concept that the pavement fails due to functional rather than structural failure is used in the AASHTO design method. The functional failure is measured in terms of roughness, excessive deformation (rutting) and cracking. As mentioned in Chapter 2, the number of axle loads to reach a certain point of serviceability, defined as the Present Serviceability Index (PSI), was related to the, among other things, strength of the pavement, defined by the structural number (SN). For a given type of loading and serviceability at the end of a specific time the performance ( $N_f$ ) is influenced solely by the structural number.

$$N_f = f(SN) \quad (9.5)$$

where  $SN = a_1 h_1 + a_2 h_2 + a_3 h_3$

$h_1, h_2, h_3 =$  layer thickness

$a_1, a_2, a_3 =$  layer structural coefficients of the surface, base and subbase.

Pavements with the same structural number in the same region and load conditions will have the same performance. The foamed asphalt recycled pavement that has the same structural number as an AASHTO Test Road pavement will have the same performance (number of load repetitions to failure). Either the number of axle loads (repetitions) or the structural number can be used as a measure of performance.



In this study the pavement with the foamed asphalt recycled base course layer was compared to a similar pavement with an AASHTO surface layer in the place of the recycled layer. For similar SN-values or number of load repetitions:

$$SN = SN'$$

where

SN = structural number of the pavement section with the AASHTO layer.

SN' = structural number of the pavement with the foamed asphalt layer.

$$a_1 h_1 + a_2 h_2 + a_3 h_3 = a'_1 h'_1 + a'_2 h'_2 + a'_3 h'_3$$

$$\text{but } a_1 h_1 = a'_1 h'_1$$

$$\text{and } a_3 h_3 \approx a'_3 h'_3$$

Although the resilient moduli of the granular material were not the same for the sections with the AASHTO layer and those with the recycled layer, Witczak and Rada (55) concluded that the coefficient  $a_3$  is a function of the subgrade CBR, the compaction method and moisture content of the subbase. The values  $a'_3$  would therefore be equal to  $a_3$  since the subgrade moduli are the same. Even if the relationships given in NCHRP No. 128 (69), which are based on the resilient modulus of the subbase, were used the influence would be small enough to be negligible in view of all the other assumptions that were made. Therefore:

$$a'_2 h'_2 = a_2 h_2$$



$$\text{or } a_2' = a_2 h_2 / h_2'$$

with  $a_2$  fixed at 0.44 and  $D_2'$  at 5.5 inches (140mm)

$h_2$  = thickness of the AASHTO layer that would give the same strains, deflections or load repetitions as the recycled layer.

$a_2'$  = structural coefficient of the foamed asphalt recycled layer.

Equivalency factors or coefficients can be determined using various criteria. A number of different criteria were used in this study to determine the equivalencies.

#### 9.6.1. Tensile Strain at the Bottom of the Recycled Layer

This criterion of comparing the strengths of different layers has been used in the past by researchers (35,33,66). The strains are a function of only the elastic moduli of the AASHTO and foamed asphalt material. Although the stiffness, measured by the elastic modulus, is a very good indicator of the strength of the layer, it is not directly related to performance in terms of the structural number or number of load repetitions. This is therefore not a satisfactory method of determining structural equivalencies unless the materials have the same fatigue characteristics.

The thicknesses of the pavements with the AASHTO layer in them could not be compared to the corresponding foamed asphalt pavement sections without the surface layer. The strains in the recycled layer could not be uniquely assigned to a thickness of the AASHTO layer, since they fluctuated with different thicknesses with a thin AASHTO layer.



A minimum value of 0.05, corresponding to the lowest value given for any type of material in NCHRP No. 128 (69), was used in this study. Values of less than 0.05 were considered to have been too low for the recycled material and the method used to calculate them incorrect.

#### 9.6.2. Tensile Strain at the Bottom of the Remaining Initial Pavement Layer

The tensile strains in the asphalt layers are a maximum at the bottom of the remaining initial pavement layer. If all the asphalt layers had the same fatigue life, this layer would fail first. Since the remaining initial pavement layer is the same in both the pavement with the recycled layer and the pavement with the AASHTO layer, the same tensile strains will give the same fatigue life and thus SN. The strains can therefore be used to determine the equivalency factors.

#### 9.6.3. Compressive Strain on Top of the Subgrade ( $\epsilon_v$ )

Wang (72) has shown that  $\epsilon_v$  is a function of the structural number for spring conditions. The maximum compressive strain on the subgrade has also been widely used to predict the number of load repetitions until the rut depth is above the allowable. Since the subgrades in the pavements with the AASHTO sections were the same as those in the actual pavement sections, the compressive strains on top of the subgrade could have been used directly to compare the pavement layers.

#### 9.6.4. Maximum Deformation of the Subgrade

The maximum subgrade deformation has been used to predict the service life of a pavement (33). The maximum subgrade deformation can therefore also be used to calculate structural coefficients.





#### 9.6.5. Maximum Surface Deflections

The rate of rutting is a function of the maximum deflection and the number of 18,000 lb. (80 kN) axle load applications (20). For the same rate of rutting the maximum surface deflection must be the same if the number of load applications is the same. Wang (72) also correlated the maximum surface deflection with the structural number for spring conditions. The maximum surface deflection can thus be used to compare the performance of pavements.

#### 9.6.6. Fatigue Life of the Asphalt Layers

The service or fatigue life of the asphalt layers can best be predicted by using cycles-to-failure/tensile strain relationships. The relationships used in this study were described earlier. Due to the large differences among the relationships, eight different combinations were used for each pavement cross section.

They were denoted X1, X2, X3, X4, Y1, Y2, Y3, Y4 where the first symbol stands for the AASHTO material relationship (in Table 9.1) and the second symbol for the recycled material fatigue relationship (Table 9.2). Coefficients of less than 0.05 and more than 0.44 were considered to fall outside the range of structural coefficients of the foamed asphalt recycled material and a result of the wrong fatigue relationships. The fatigue relationships were arbitrarily chosen from relationships developed for different materials. The coefficients could not be determined for the case where the asphalt concrete surface had not been placed on the recycled layer (during construction) for the same reason the coefficients could not be determined from the tensile strains at the bottom of the top asphalt layer viz. fluctuation of the strains with different AASHTO layer thicknesses.



Only three of the eight combinations of fatigue characteristics of the AASHO material and foamed asphalt recycled material gave coefficients within the specified range in all the cases. If a low structural coefficient value of 0.05 is assumed for the cases where the coefficients could not be calculated another two combinations can be used.

#### 9.6.7. Results

The results are summarized in Tables 9.10 and 9.11 for the coefficients based on strains and deformations and those based on the fatigue life of the recycled layer respectively. Figures 9.9 and 9.10 display how the structural coefficients changed for the low, average and high deflection sections. The low is the average of the sections with the low deflections (stiff pavement) on both lanes at a particular time after construction. The high and average values were calculated in a similar manner.

Figures 9.11 to 9.13 depict the influence of the increase in time after construction on the structural coefficients for the low, average and high deflection cases, respectively, based on strains and deformations. Figures 9.14 to 9.16 show the influence of the increase in time after construction on the structural coefficients based on the fatigue life of the foamed asphalt recycled layer.

The tables and figures show that the structural coefficients can have virtually any value between 0.05 and 0.45, depending on which criterion is used. The average values vary between 0.10 and 0.40. There is a slight increase in general in the structural coefficients between the during construction case (DURING) and twelve days thereafter (AFTER2).



Table 9.10. Summary of Coefficients Based on Strains and Deformations

Criteria		Low	Average	High
$\epsilon_{r2}$ (A)	1	0.23	0.05	<0.05
	2	0.23	0.05	<0.05
	3	0.30	0.23	0.08
$\epsilon_{r3}$ (B)	1	0.25	0.19	0.13
	2	0.26	0.17	0.11
	3	0.33	0.26	0.12
$\epsilon_v$ (C)	1	0.27	0.22	0.18
	2	0.31	0.23	0.19
	3	0.34	0.32	0.22
$\delta_s$ (D)	1	0.30	0.24	0.19
	2	0.34	0.28	0.25
	3	0.38	0.34	0.28
$\delta_m$ (E)	1	0.30	0.25	0.18
	2	0.33	0.27	0.22
	3	0.38	0.33	0.25

1. DURING - eastbound lane
2. AFTER1 - both lanes
3. AFTER2 - both lanes

For explanation of criteria see Figure 9.1



Table 9.11. Summary of Coefficients Based on Fatigue

Fatigue Life Combination		Low	Average	High
X1	1	0.12	*	*
	2	0.19	0.12	*
X1	1	0.36	0.27	0.14
	2	0.43	0.37	0.23
Y1	1	0.39	0.33	0.26
	2	0.47	0.42	0.36
Y3	1	0.11	*	*
	2	0.36	0.27	0.10
Y4	1	0.13	0.12	0.15
	2	0.29	0.31	0.28

\*Less than 0.05

1. AFTER1 - both lanes
2. AFTER2 - both lanes

For fatigue-life combination explanation see Tables 9.1 and 9.2







**FIGURE 9.9 EFFECT OF LAYER STIFFNESS ON  
THE STRUCTURAL COEFFICIENTS  
(BASED ON STRAINS AND DEFORMATIONS)**

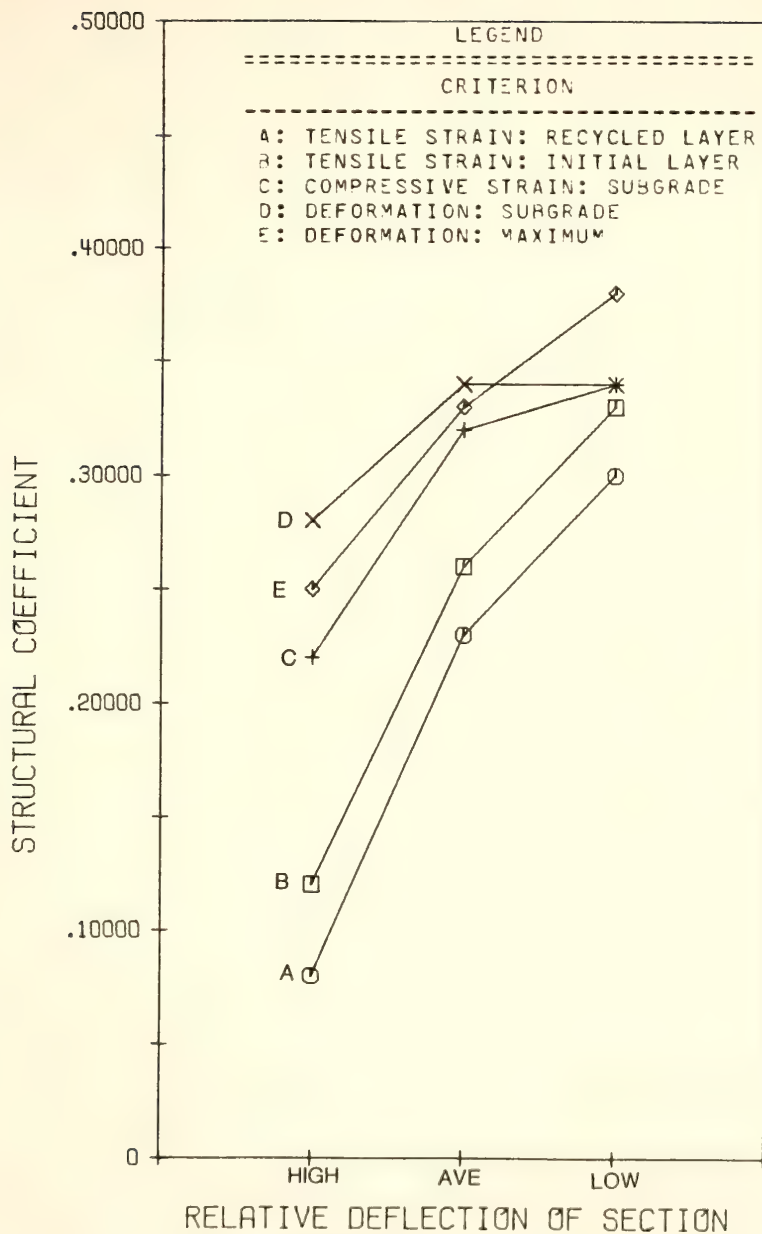


FIGURE 9.9





**FIGURE 9.10 EFFECT OF LAYER STIFFNESS  
ON THE STRUCTURAL COEFFICIENTS  
(BASED ON FATIGUE)**

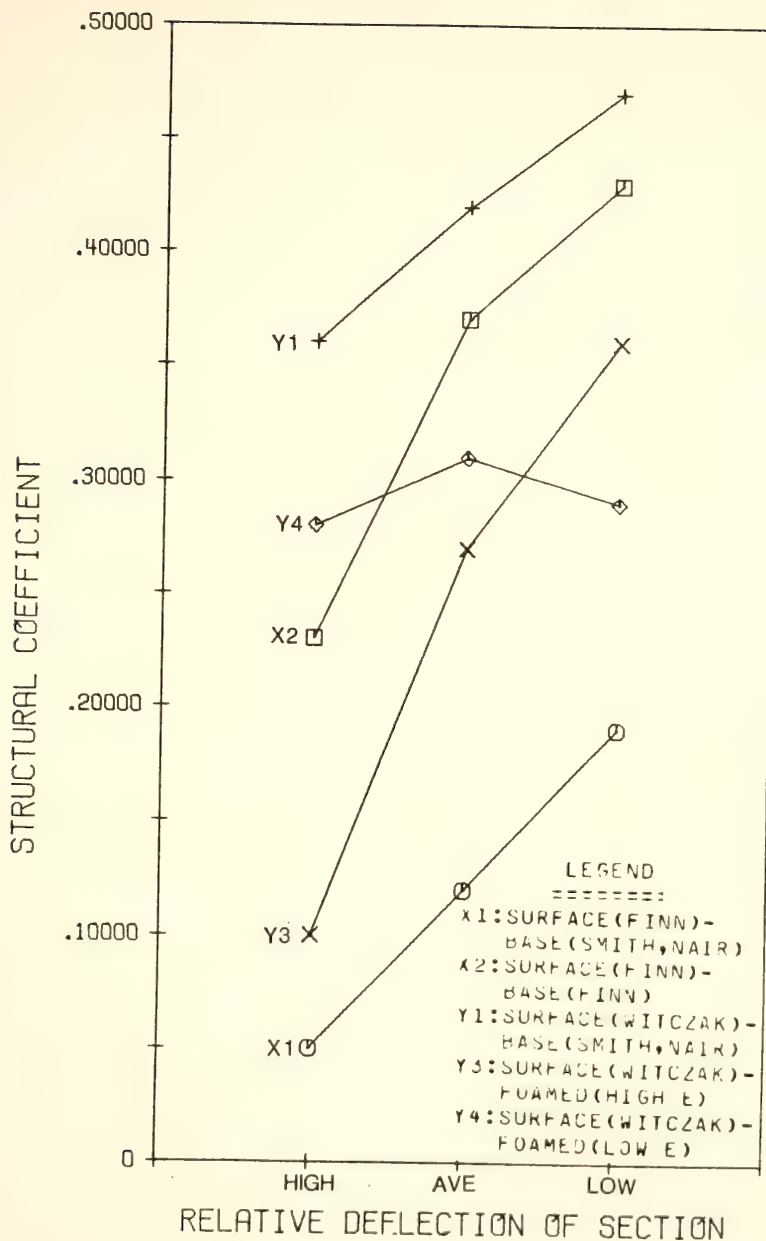


FIGURE 9.10







FIGURE 9.11 EFFECT OF TIME AFTER  
CONSTRUCTION ON THE STRUCTURAL  
COEFFICIENTS FOR LOW DEFLECTIONS  
(BASED ON DEFORMATIONS AND STRAINS)

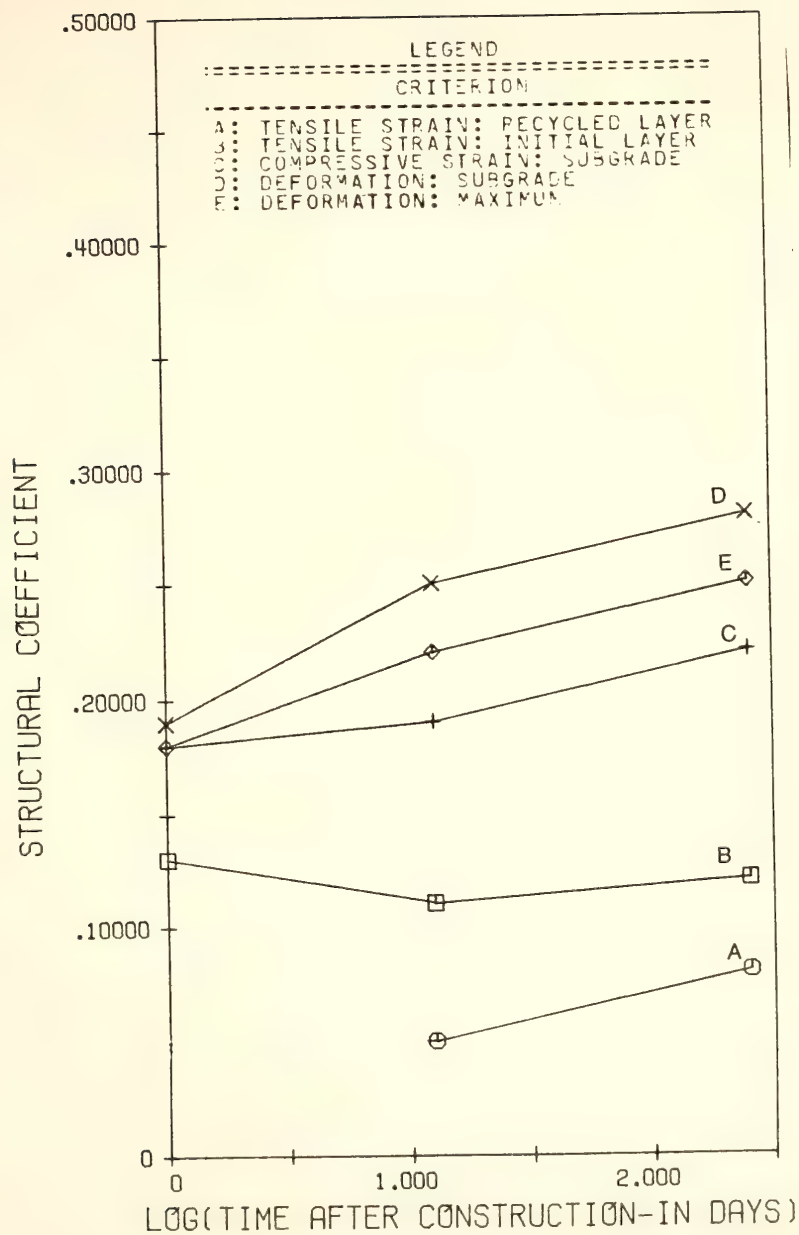


FIGURE 9.11





FIGURE 9.12 EFFECT OF TIME AFTER  
CONSTRUCTION ON THE STRUCTURAL  
COEFFICIENTS FOR AVERAGE DEFLECTIONS  
(BASED ON DEFORMATIONS AND STRAINS)

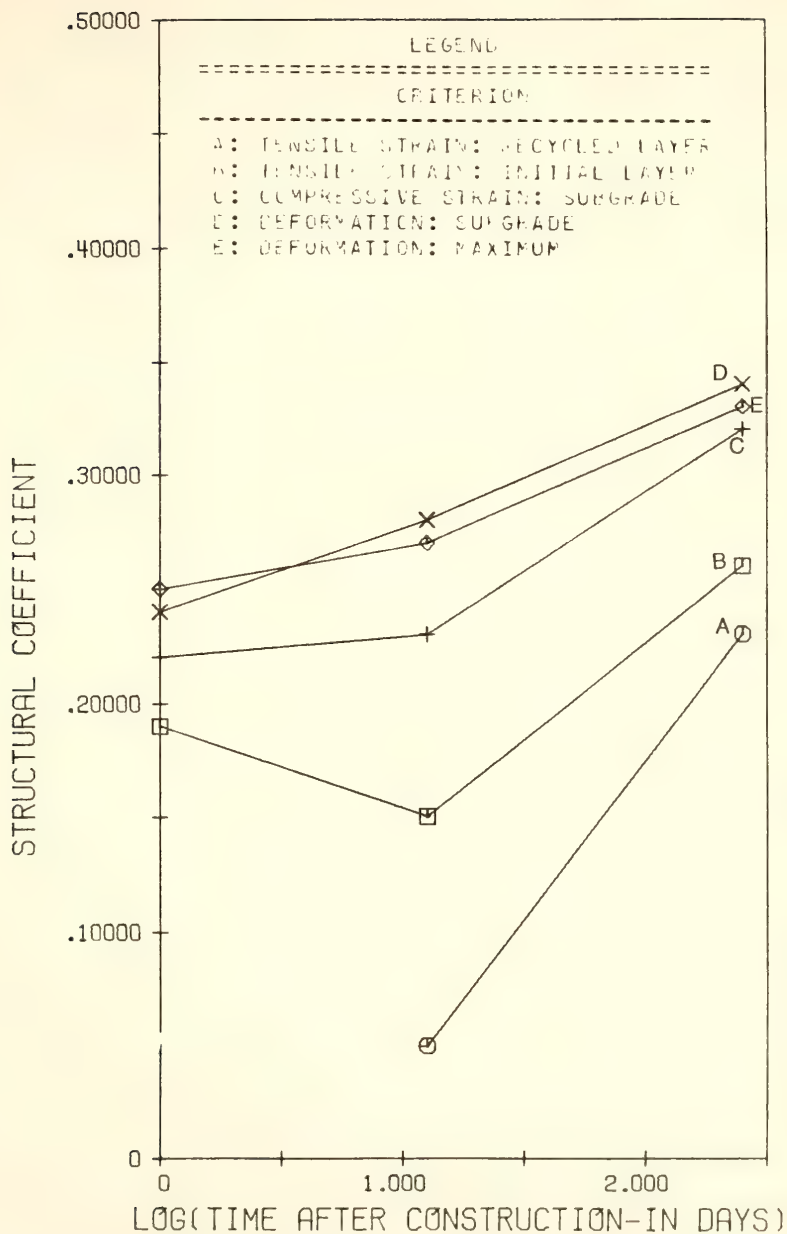


FIGURE 9.12







FIGURE 9.13 EFFECT OF TIME AFTER  
CONSTRUCTION ON THE STRUCTURAL  
COEFFICIENTS FOR HIGH DEFLECTIONS  
(BASED ON DEFORMATIONS AND STRAINS)

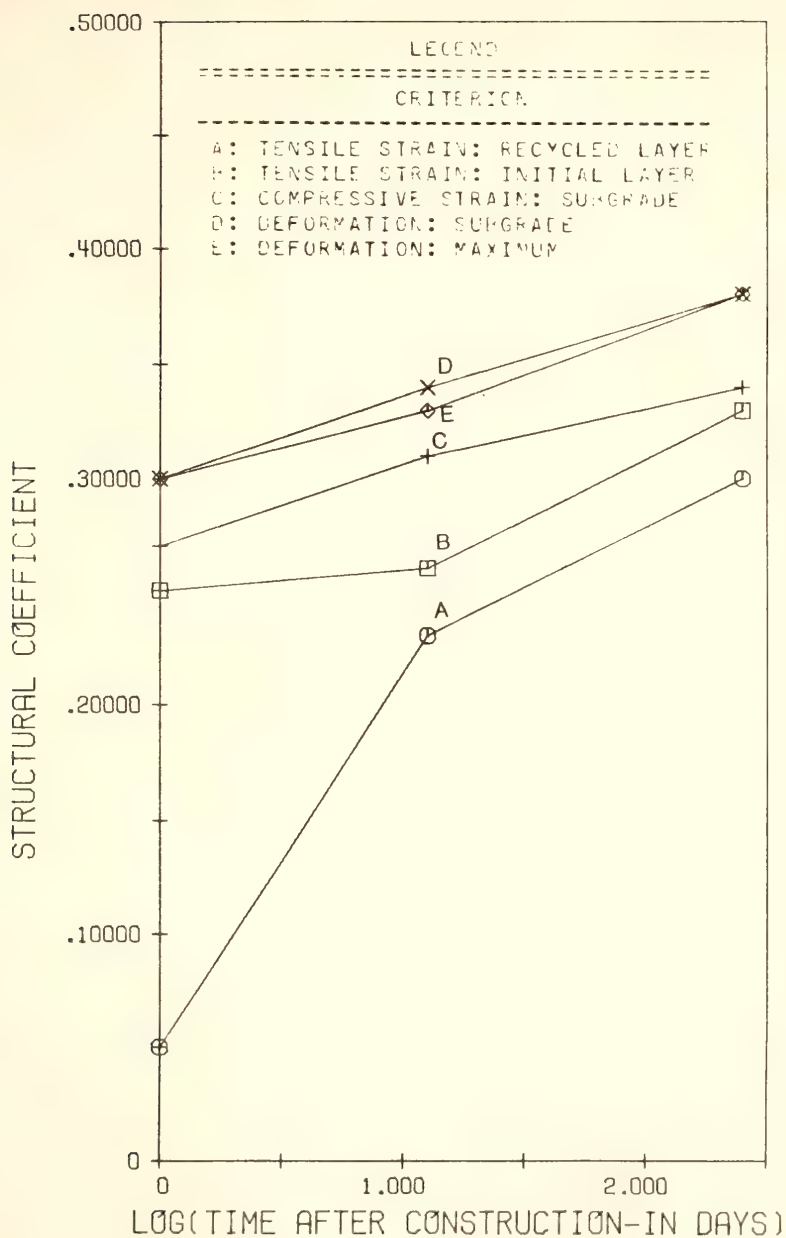


FIGURE 9.13





FIGURE 9.14 EFFECT OF TIME AFTER  
CONSTRUCTION ON THE STRUCTURAL  
COEFFICIENTS FOR LOW DEFLECTIONS  
(BASED ON FATIGUE)



FIGURE 9.15 EFFECT OF TIME AFTER  
CONSTRUCTION ON THE STRUCTURAL  
COEFFICIENTS FOR AVERAGE DEFLECTIONS  
(BASED ON FATIGUE)



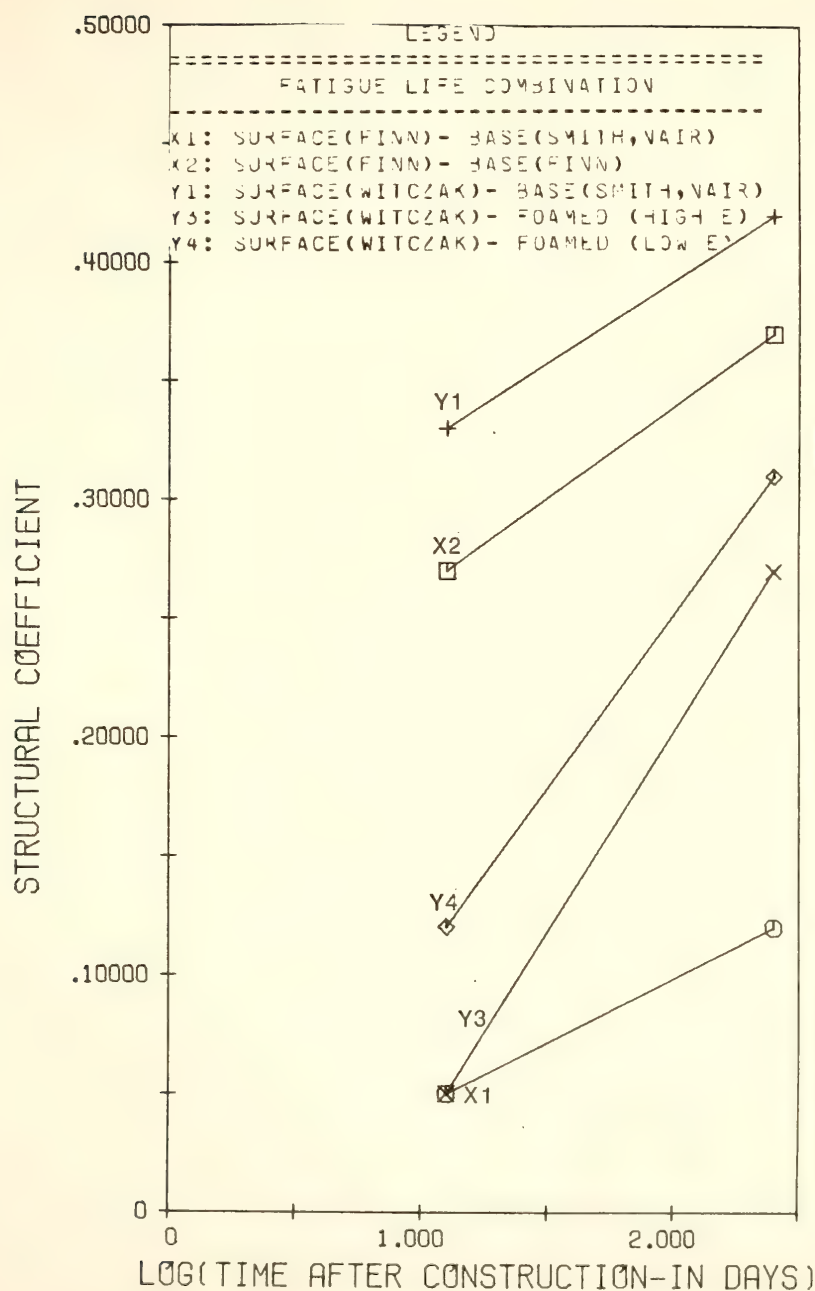


FIGURE 9.15





FIGURE 9.16 EFFECT OF TIME AFTER  
CONSTRUCTION ON THE STRUCTURAL  
COEFFICIENTS FOR HIGH DEFLECTIONS  
(BASED ON FATIGUE)

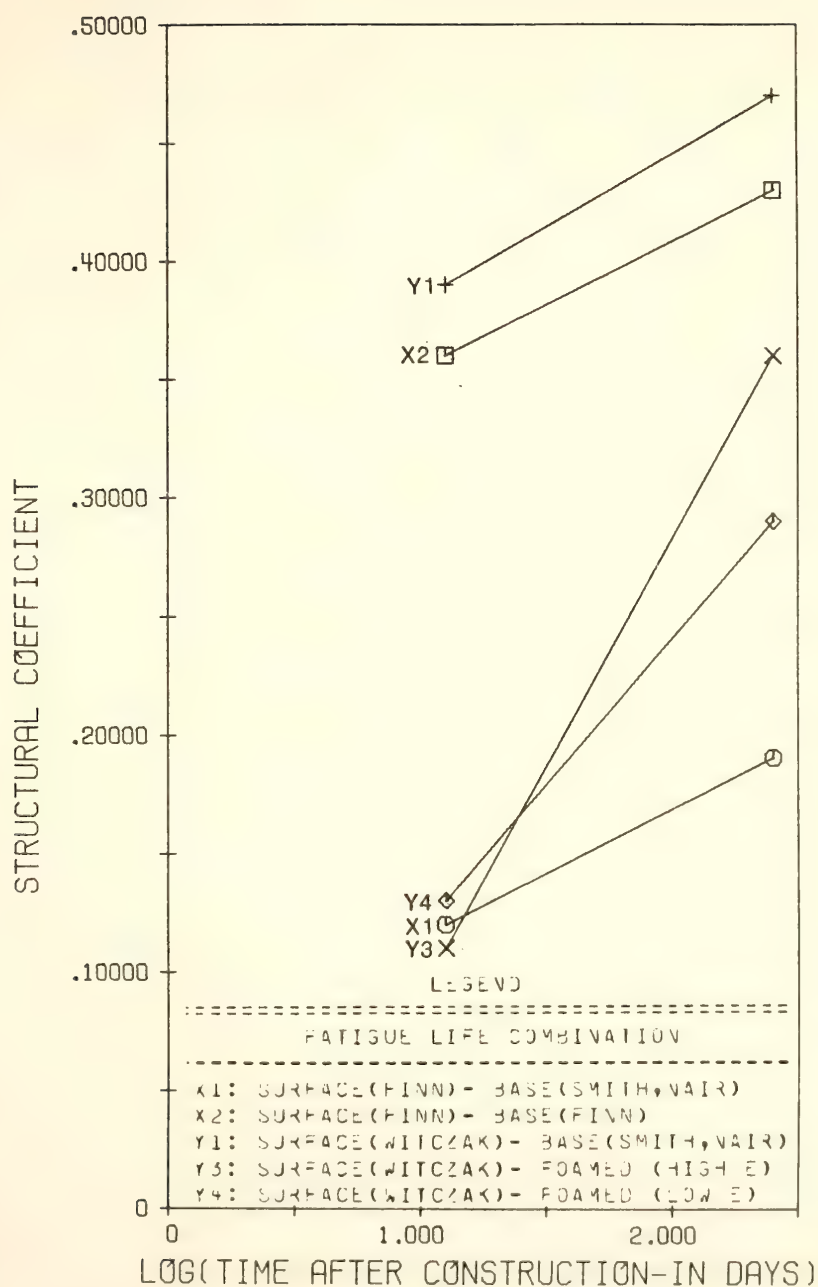


FIGURE 9.16



The structural coefficients increased further during the next eight months. It was not possible from this study to investigate the influence of seasons on the structural coefficients, since the elastic moduli of the recycled material are not the same. This was the result of not only the temperature but also the curing time. The effect of asphalt content could also not be investigated, since the total asphalt content was assumed to have been constant at approximately 7 percent by weight of the mixture. The structural coefficients increased, as expected, from the high deflection cases to the low deflection cases (Figures 9.9 and 9.10). This strengthens the idea that the structural coefficients are a function mainly of the stiffness of the layer. The only exception is the coefficient combination determined with the fatigue life combination, Y4 in which the coefficients remained constant.

#### 9.7. Controlling Criterion

All the different criteria described and used in the previous paragraphs can be used to predict the service life of the pavement, but only one will determine the service life in each case. The criterion that predicts the shortest service life will control the performance of the pavement. The controlling criterion for all the pavement sections in this study was either the subgrade deformation or the tensile strain at the bottom of the recycled layer depending on which fatigue life relationship was used. Fatigue relationship 3 (as designated in Table 9.1) predicted the shortest service lives in all cases. Structural coefficients calculated with this relationship were less than 0.05 for the AFTER1 case, but had acceptable values for the AFTER2 case. This is explainable since it is unlikely that fully cured asphalt layers will have the same fatigue





characteristics as fresh layers. The relationship for the prediction of the service life based on the subgrade deformation was also developed for conditions not necessarily similar to those in this study. The coefficients calculated from both the subgrade deformations and the fatigue life relationship 3 are nevertheless given in Table 9.12 and displayed in Figure 9.17 for the AFTER2 case.

#### 9.8. Different Recycled Layer Thicknesses

The constructed recycled layer was 5.5 inches (140 mm) and all the structural coefficients were calculated for such a thickness. Since the structural coefficients are also a function of the thickness of the layer the structural coefficients were also calculated for recycled layer thicknesses of 3 and 8 inches (75 and 200 mm). The 5.5 inch layer was replaced with the 3 and 8 inch (75 and 200mm) layers in the sections with average deflections in the AFTER2 case. The coefficients were calculated as previously described. The coefficients are summarized in Table 9.13 and displayed in Figure 9.18. Only two combinations of fatigue life relationships, viz. X2 and Y3, gave realistic coefficients. The coefficients seem to increase in general from layers of 5.5 inches (140 mm) to layers of 8 inches (200 mm), independent of which criterion is used. The increases were small. The differences between the coefficients of the layers of 3 and 5.5 inches (75 and 140 mm) were large in general, but they decreased or increased depending on which criterion was used. The coefficients calculated from the tensile strains in the recycled and remaining initial pavement layer were substantially lower than the coefficients calculated from other criteria for a thickness of 3 inches (75 mm). The tensile strains at the bottom of the asphalt



Table 9.12. Structural Coefficients Based on the Controlling Criteria

Criteria		Low	Average	High
AFTER1	$\delta_v(D)$	0.34	0.28	0.25
	$\epsilon_{r2}(A)$	0.11	*	*
AFTER2	$\delta_v(D)$	0.38	0.34	0.28
	$\epsilon_{r2}(A)$	0.36	0.27	0.10

\*: less than 0.05.

For an explanation of the criteria see Figure 9.1.





FIGURE 9.17 STRUCTURAL COEFFICIENTS BASED  
ON THE CONTROLLING CRITERIA  
(AFTER 1 AND AFTER 2 CASES)

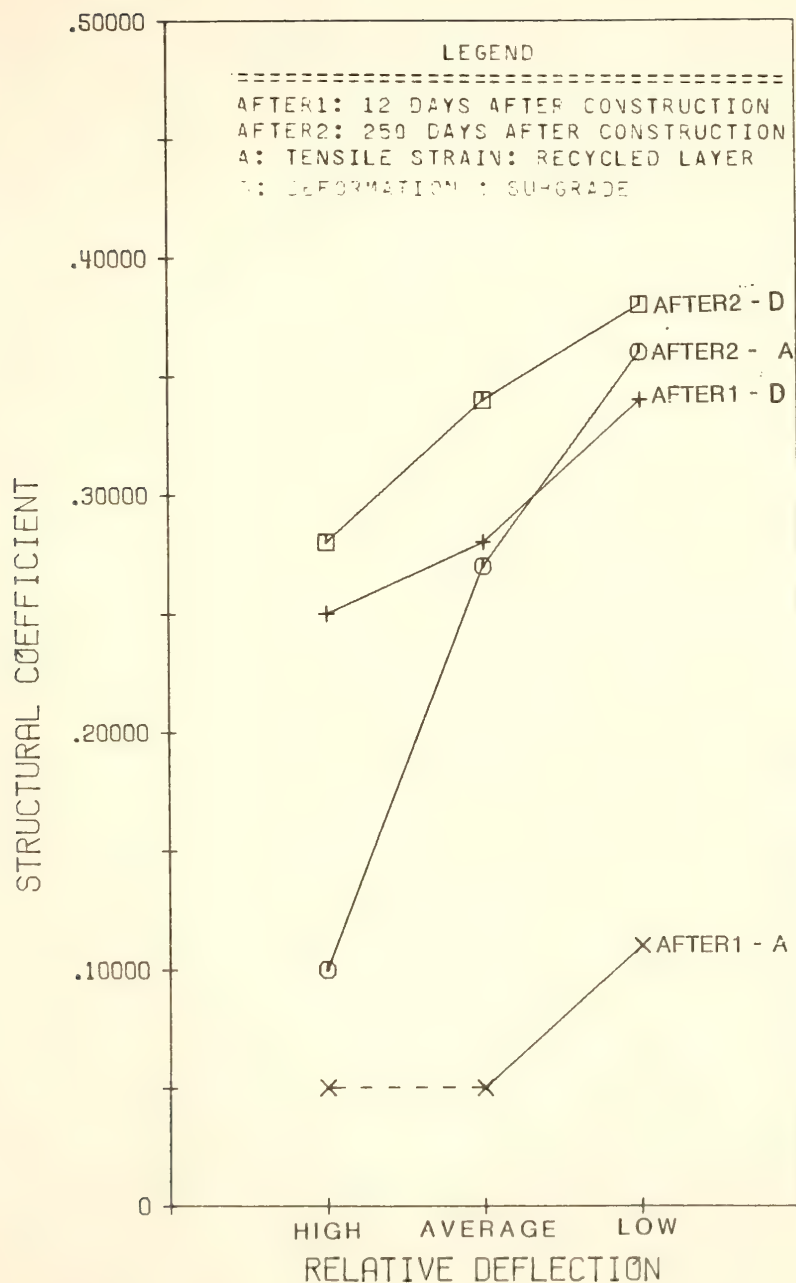


FIGURE 9.17





Table 9.13. Effect of Recycled Layer Thickness on the Structural Coefficient (AFTER2 - case)

Criteria	Thickness (inches)		
	3	5.5	8
A ( $\epsilon_{r2}$ )	0.03	0.23	0.27
B ( $\epsilon_{r2}$ )	0.16	0.26	0.28
C ( $\epsilon_v$ )	0.32	0.32	0.32
D ( $\delta_s$ )	0.36	0.34	0.35
E ( $\delta_m$ )	0.33	0.33	0.32
X2	0.42	0.37	0.38
Y3	0.09	0.27	0.30

For explanation of criteria see Tables 9.1, 9.2 and 9.3.

1 inch = 25.4 mm





FIGURE 9.18 EFFECT OF THE RECYCLED LAYER  
THICKNESS ON THE STRUCTURAL COEFFICIENT  
(AFTER 2 CASE)

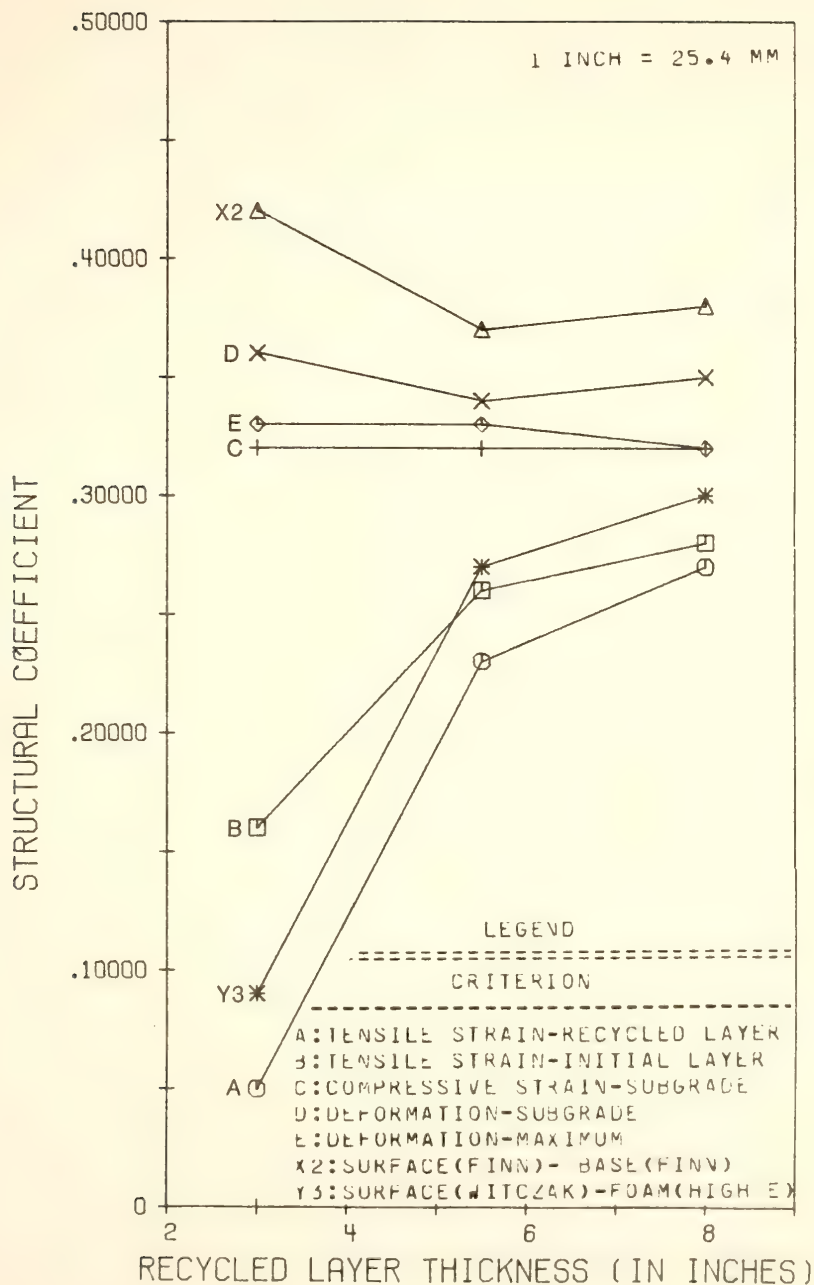


FIGURE 9.18



layers were sensitive to changes in thickness of these layers especially thin layers. The elastic modulus of the recycled layer used in this analysis was 75000 psi (517.5 MPa).

#### 9.9. Effect of the Elastic Modulus on the Recycled Layer

The structural coefficients increased with the increase in the stiffness of the layer. This was evident from the increase in coefficient values from low deflection to high deflection pavement sections and from the AFTER1 to the AFTER2 case. This was further verified by regression analysis on the coefficients developed from the subgrain strain and deflection and the tensile strain at the bottom remaining layer, as well as the fatigue life combination X2. The regression coefficients are summarized in Table 9.14. Figure 9.19 illustrates the influence of the resilient modulus on the structural coefficient with  $E_2$  (elastic modulus of the recycled layer) as the only independent variable.

#### 9.10. Summary of Results

##### 9.10.1. Criteria Used in the Final Analysis

The following criteria were selected for future use in order to establish some reliable ranges within which the structural coefficients of the foamed asphalt recycled layer will fall and which can be used in design:

1. The subgrade deformation since it predicted the shortest service life (designated as D).
2. The maximum compressive strength on top of the subgrade, since it has been widely used to determine structural coefficients (designated as C).





Table 9.14. Regression Coefficients of the Structural Coefficient vs. Elastic Modulus of the Recycled Layer

$$a_2 = m(E_2) + c$$

Criteria	m	c	n	R <sup>2</sup>
X2	$0.2497 \times 10^{-5}$	0.1304	24	0.78
C ( $\epsilon_v$ )	$0.1428 \times 10^{-5}$	0.1665	24	0.84
D ( $\delta_s$ )	$0.1296 \times 10^{-5}$	0.2170	24	0.79
B ( $\epsilon_{r3}$ )	$0.2071 \times 10^{-5}$	0.0697	24	0.84

$E_2$  in psi.

1 psi = 6.9 kPa.



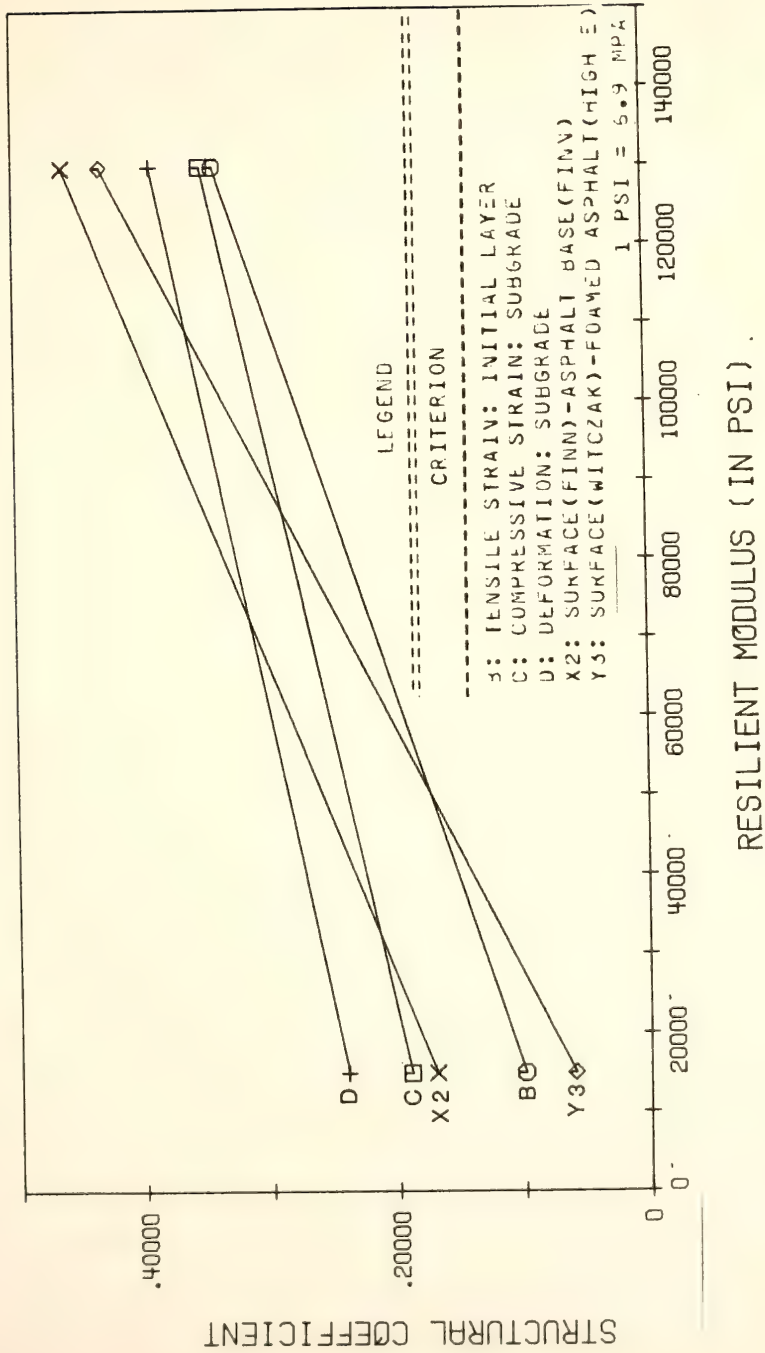


FIGURE 9.19 EFFECT OF THE LAYER ELASTIC MODULUS ON THE STRUCTURAL COEFFICIENTS



3. Tensile strain at the bottom of the remaining initial pavement layer, since the maximum tensile strain in the asphalt layers occurred in this position. This layer was the same in both the pavement systems with the recycled and the AASHTO layer. Equal tensile strain would therefore predict equal performances (designated as B).
4. Fatigue life of the recycled and AASHTO layers, based on the maximum tensile strain at the bottom of these layers. One relationship combination (X2) for both the AFTER1 and AFTER2 cases and another combination for each of the cases were selected. The section was based on the coefficients that were calculated using all eight different combinations. The foamed asphalt recycled layer is expected to have different fatigue characteristics for the three time periods, since it had different curing times. Combinations that gave coefficients of less than 0.05 or more than 0.44 were considered to be not applicable to the foamed asphalt recycled material studied here. The two combinations used were Y1 for the AFTER1 case and Y3 for the AFTER2 case.

#### 9.10.2. Assumptions Made

It is important to reconsider the assumptions made in the evaluation of the results. Table 9.15 summarizes the most important assumptions made in the determination of the structural coefficients. Although these assumptions are valid they could have influenced the results.

The final conclusions were made from the coefficients calculated from the criteria selected in section 9.10.1.



Table 9.15 Assumptions

Procedure	Assumption
A. Selection of cross sections	<ol style="list-style-type: none"> <li>1. Mr-<math>\theta</math> relationships for the granular material were valid for fall and spring conditions</li> <li>2. <math>\theta</math> calculated at the center of the granular layer represented the <math>\theta</math> of the layer.</li> <li>3. Mr-<math>\sigma_d</math> relationships for the subgrade were valid for the fall and spring conditions</li> <li>4. The conversion factor to convert Dynaflect deflections to Benkelman-beam deflections was valid for deflections at all 5 sensors.</li> <li>5. The range of <math>E_1</math> was 120000 to 250000 psi.</li> <li>6. The range of <math>E_3</math> was 10000 to 50000 psi.</li> </ol>
B. AASHTO layer	<ol style="list-style-type: none"> <li>1. The pavement temperatures were accurately measured during deflection measurements.</li> <li>2. AASHTO layer E-temperature relationships used to adjust the <math>E_1</math>-values are applicable.</li> </ol>
C. Coefficient determination	<ol style="list-style-type: none"> <li>1. The fatigue life relationships used were applicable to materials in this study. (for the asphalt materials as well as the subgrade).</li> </ol>
D. General	<ol style="list-style-type: none"> <li>1. The BISTRO elastic layer program is a good representation of the actual conditions in all cases investigated.</li> </ol>

$E_1$  = elastic modulus of the surface layer.

$E_3$  = elastic modulus of the remaining initial pavement layer.

Mr = resilient modulus.

$\theta$  = bulk stress

$\sigma_d$  = deviator stress

1 psi = 6.9 kPa.





### 9.10.3. Conclusions

1. The structural coefficients of the recycled layer increased with time after construction.
2. The structural coefficients were largely dependent upon the elastic modulus of the recycled layer. The influence of the characteristics of the surrounding layers were very small for the pavement studied.
3. The thickness of the recycled layer influenced the coefficient values. The values seem to have increased with thickness, but were largely dependent on the criterion used in their calculation.
4. The structural coefficients of the recycled material one day after construction (DURING case) varied from 0.13 to 0.30 calculated from the tensile strain at the bottom of the remaining initial pavement layer, subgrade compressive strain and deformation. The section with the average deflections had coefficients between 0.19 and 0.24. (Table 9.16)
5. The structural coefficients of the recycled layer 12 days after construction (AFTER1) varied from 0.11 to 0.39 when calculated from the finally selected criteria. The average value ranged between 0.17 and 0.33. Removal of the 0.17 value led to ranges from 0.23 to 0.33. (Table 9.16)
6. The coefficient 250 days after construction varied from 0.10 to 0.43. The values of the selections with the average deflections ranged from 0.26 to 0.37. (Table 9.16)



Table 9.16. Summary of Structural Coefficients

Time After Construction (in days)	Structural Coefficients	
	All 5 Cross Sections Per Lane	Only Average Sections
1 (DURING)	0.13 to 0.30	0.19 to 0.24
12 (AFTER1)	0.11 to 0.39	0.17 to 0.33 0.23 to 0.33*
250 (AFTER2)	0.10 to 0.43	0.26 to 0.37

\*without the 0.17.



7. The structural coefficients varied with thickness of the foamed asphalt recycled layer. The structural coefficient increased slightly from a range of 0.26 to 0.37 to a range of 0.28 to 0.39 with an increase in thickness from 5.5 inches (140 mm) to 8 inches (200 mm). The range of structural coefficients for a thickness of 3 inches (75 mm) was 0.16-0.42.
8. The structural coefficients were influenced mainly by the elastic modulus ( $E_2$ ) of the recycled layer. The coefficients of determination ( $R^2$ ) ranged from 0.78 to 0.84 for the four criteria with only  $E_2$  as independent variable.
9. It is not possible to determine a single structural coefficient value for a pavement material even if it is placed in a constant thickness, without knowing the exact fatigue characteristics of the material. The structural coefficient is extremely dependent on the distress criteria used in the determination process.

The condition of the pavement 250 days after construction is a good representation of the fully cured and compacted in-situ condition of the pavement. Structural coefficients are developed from and for the fully cured and compacted pavement layers. The coefficients determined for the AFTER2 case represent the structural coefficients of such a condition. The coefficients were further developed for spring conditions, which represents the poorest condition of the subgrade. Structural coefficient values of 0.26 to 0.37 can therefore be used for foamed asphalt recycled layers of approximately 5 to 8 inches (125-200 mm) with a resilient modulus at 70°F (21°C) of approximately 140,000 to 150,000 psi (966 to 1035 MPa). (Figure 9.20)



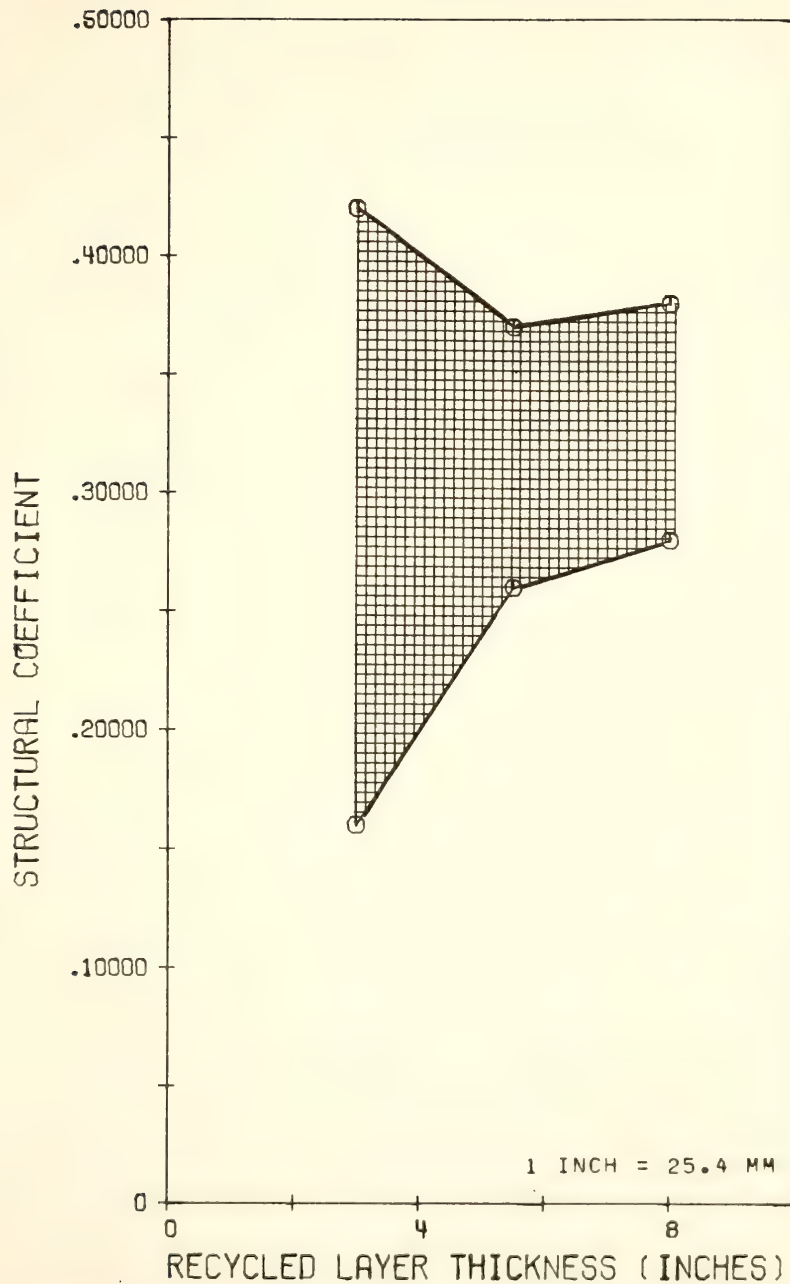


FIGURE 9.20 RECOMMENDED RANGES OF STRUCTURAL COEFFICIENTS





## CHAPTER 10: CONCLUSIONS AND RECOMMENDATIONS

### 10.1. Conclusions

1. The main purpose of this study was to determine structural coefficients for a specific foamed asphalt recycled layer. Different criteria were used to determine these structural coefficients. All the criteria gave different coefficients. The coefficients further changed with changes in thickness and elastic modulus of the recycled layer. The structural coefficients tended to increase slightly for layer thicknesses of eight inches (200 mm) instead of 5.5 inches (140 mm). Although the thicknesses and properties of the surrounding layers influenced the structural coefficient, the elastic modulus of the foamed asphalt layer had the largest influence on the coefficients independent of which criteria were used. The structural coefficients also increased with time after construction.

Assumptions had to be made in this study regarding the resilient modulus properties of the asphalt concrete surface, the remaining initial pavement layer, the subbase and the subgrade material, as well as the fatigue life properties of the asphalt layers and the subgrade. Without this information it was not possible to determine a single structural coefficient even for a specific thickness, elastic modulus and



time after construction of the foamed asphalt recycled layer. Four criteria, used to determine the structural coefficients, were selected to be applicable to the material and conditions in the study. Three were based on subgrade deformation, maximum compressive strain in the subgrade and the maximum tensile strain at the bottom of the remaining initial pavement layer. The fourth criterion was based on a chosen fatigue-life relationship of the recycled material and a hot asphalt surface material. Coefficients determined from all four criteria were used to predict a range of structural coefficients for each case investigated. The values were given in Table 9.16.

2. The behavior of the foamed asphalt mixture was investigated as part of a secondary study. Results of tests showed that the strength of the foamed asphalt recycled mixture, whether it is measured as resilient modulus, Marshall variables, Hveem-R-value or tensile strength decreased with stockpiling of the material in the open, as well as with the submission to water. Results of water sensitivity tests indicated that the introduction of water had a deleterious effect on the strength of the foamed asphalt mixtures. The recycled foamed asphalt mixture also behaved as conventional asphalt mixtures in that the resilient modulus and tensile strength values increased with a decrease in testing temperature and increase in curing time. The foamed asphalt mixture was strong enough hours after construction to carry traffic.



3. Dynaflect deflection characteristics revealed that the maximum deflections and surface curvature index were higher a few days after construction on the pavement with the recycled layer than on the initial pavement. This situation changed over time and 250 days after construction the deflection characteristics were very similar, indicating that the recycled pavement is probably equal to, and surpassing, the initial pavement in strength. Care must be taken in using the Dynaflect deflection characteristics as indicators of specific properties of the pavement.

#### 10.2. Recommendations

1. The structural coefficients were developed for a specific foamed asphalt recycled layer. The structural coefficients determined for the layer 250 days after construction, under spring conditions can be used in the design of a similar layer. The structural coefficient range suggested for use in design is valid for a foamed asphalt recycled mixture of approximately five to eight inches (125 to 200 mm) thick, with a resilient modulus value of approximately 140,000 to 150,000 psi (966 to 1035 MPa) at 70°F (21°C) and a total asphalt content of about 7 percent by weight of the mixture. The structural coefficient range is 0.26 to 0.37 (Figure 9.20).
2. Foamed asphalt recycled mixtures are also susceptible to water. The layer should therefore be protected from water by sufficient side drainage where needed and the penetration of water from the surface. A loss in strength of the foamed asphalt recycled



mixture should also be minimized by avoiding stockpiling for long periods of time.

### 10.3. Recommendations for Future Research

The structural coefficients developed in this study are only applicable for a foamed asphalt mixture with a rather narrow range of properties. Future research should be conducted to determine the structural coefficients of other widely used recycled mixtures in a similar manner. The structural coefficients should also be based on the in-situ properties of the recycled layers where possible. In the analysis it is important to know the resilient modulus properties of the granular layers and the subgrade. These properties should be determined for commonly available materials in Indiana, not only for the determination of structural coefficients, but also for use in the mechanistic design procedure.

The fatigue characteristics of the subgrade and especially the fatigue characteristics of recycled layers are of the utmost importance in the determination of structural coefficients. The range of structural coefficients given in this study and in future studies, where the fatigue characteristics of the recycled layer are not known, can only be narrowed down if the fatigue characteristics are known. Very little research has been done to establish fatigue life relationships for cold recycled mixtures. Research in this area should be conducted, ideally, prior to the developing of further structural coefficients.





## REFERENCES



## REFERENCES

1. Abel, F. and Hines, C. R., "Base Stabilization with Foamed Asphalt." Colorado Highway Dept. Interim Report, June 1979.
2. Abel, F. "Base Stabilization with Foamed Asphalt." Paper presented at the 60th Annual TRB Meeting 1981.
3. Acott, S. M. "Sand Stabilization Using Foamed Asphalt." Proceedings Third CAPSA Conference 1979. Durban, South Africa.
4. Acott, S. M. "Stabilization of Sand Using Foamed Asphalt." Ph.D. Thesis, Natal University, Pietermaritzburg, South Africa.
5. Bandyopadhyay, S. S. "Structural Performance Evaluation of Recycled Pavements Using Dynamic Deflection Measurements." Paper presented at the 61st Annual TRB Meeting 1982.
6. Barksdale, R. D. and Hicks, R. B. "Material Characterization and Layered Theory for use in Fatigue Analysis." Transportation Research Board, Special Report 140, 1973. pp. 20-48.
7. Bowering, R. H. and Martin, C. L. "Foamed Bitumen: Production and Application of Mixtures: Evaluation and Performance of Pavements," Proceedings of the Association of Asphalt Paving Technologists, 1976.
8. Brennen, M., Tia, M., Altschaeffl, A. and Wood, L. "A Laboratory Investigation on the Use of Foamed Asphalt for Recycled Bituminous Pavements." Paper presented at the 60th Annual TRB Meeting 1981.
9. Brown, S. F., Pell, P. S. and Stock, A. F. "The Application of Simplified, Fundamental Design Procedures for Flexible Pavements." Fourth International Conference on Structural Design of Asphalt Pavements, 1977. pp. 327-341.
10. Brown, S. F., Stock, A. F. and Pell, P. S. "Structural Design of Asphalt Pavements by Computer." The Journal of the Institute of Highway Engineering. March 1980. pp. 3-10.
11. Carneiro, F. B. L. "Benkelman Beam-Auxiliary Instrument of the Maintenance Engineer." Transportation Research Board, Report 129, 1966. pp. 42-46, 54.



12. Castedo, H. L. and Shofstall, R. L. "Stabilization of Three Typical Indiana Aggregates Using Foamed Asphalt." Research Report Joint Highway Research Project, Purdue University, West Lafayette, Indiana, 1981.
13. Coffman, B. S., Ilves, G. and Edwards W. "Theoretical Asphalt Concrete Equivalencies." Transportation Research Board Report 239, 1968. pp. 95-119.
14. Cooper, T. W. "State Highway Finance Trends." Transportation Research News, No. 98, Jan.-Feb. 1982. pp. 1-5.
15. Csanyi, L. H., "Foamed Asphalt in Bituminous Paving Mixtures." Transportation Research Board Report 160, 1957. pp. 108-122.
16. Deacon, J. A. "Fatigue Life Prediction." Transportation Research Board Special Report 140, 1973. pp. 73-92.
17. Epps, J. A., Little, D. N., Holmgreen, R. Journal, et.al. "Recycling Materials for Highways." National Cooperation of Highway Research Projects Synthesis 54, 1978.
18. Epps, J. A., Little, D. N., Holmgreen, R. Journal, Terrell, R. L. and Ledbetter, W. B. "Guidelines for Recycled Pavement Materials." National Cooperation of Highway Research Projects 224, 1980.
19. Faiz, A. "Evaluation of Continuously Reinforced Concrete Pavements in Indiana." Research Report JHRP-75-17, Joint Highway Research Project, Purdue University, West Lafayette, Indiana, 1975.
20. Finn, F., Saraf, C., Kulkarni, R., Nair, K., Smith, W. and Abdullah, A. "The Use of Distress Prediction Subsystems for the Design of Pavement Structures." Fourth International Conference on the Structural Design of Asphalt Pavements, 1977, pp. 10-20.
21. Francken, L. "Fatigue Performance of a Bituminous Road Mix Under Realistic Test Conditions." Transportation Research Board Report 712, 197 . pp. 30-36.
22. Gadallah, A. A., Wood, L. E. and Yoder, E. J. "Marshall Stiffness Characteristics of Asphalt Emulsion Treated Mixtures." Paper presented at the Annual Meeting of the Canadian Technical Asphalt Association, 1977.
23. Hadley, W. O., Hudson, W. R. and Kennedy, T. W. "A Method of Estimating Tensile Properties of Materials Tested in Indirect Tension." Texas Research Report 98-7, Center for Highway Research, The University of Texas at Austin, 1970.
24. Hicks, R. G., Hatch, D. R., Williamson, R. and Steward, J. "Open Graded Emulsion Mixes for Use as Road Surfaces." Transportation Research Board Report 702, 1979. pp. 64-72.



25. Hixon, C. D. and Kidd, E. B. "Foamed Asphalt in Oklahoma: A Beginning." Paper presented at the 60th Annual TRB Meeting 1981.
26. Hoffman, M. S. and Thompson, M. R. "Backcalculating Nonlinear Resilient Moduli from Deflection Data." Paper presented at the 61st Annual TRB Meeting 1982.
27. Huang, Y. H. "Strain and Curvature as Factors for Predicting Pavement Fatigue." Third International Conference on the Structural Design of Asphalt Pavements, 1972. pp. 622-628.
28. Iida, A. "Effects of Added Softening Agents Upon the Behavior of Cold Recycled Asphalt Mixtures." Research Report JHRP-80-13, Joint Highway Research Project, Purdue University, West Lafayette, Indiana, 1980.
29. Kennedy, T. W. "Characterization of Asphalt Pavement Materials Using Indirect Tensile Tests." Proceedings of the Association of Asphalt Paving Technologists, 1977. pp. 132-149.
30. Kercher, K. J. "Cold Recycling on SR-16: Project B, Emulsified Asphalt." Interim Report, Indiana Dept. of Highways. May 1982.
31. Kumar, A. and Goetz, W. "The Gyrotory Testing Machine as a Design Tool and as an Instrument for Bituminous Mixture Evaluation." Research Report JHRP-74-1, Joint Highway Research Project.
32. Lee, D. Y. "Treating Marginal Aggregates and Soils with Foamed Asphalt." Proceedings of the Association of Asphalt Paving Technologists, 1981. pp. 211-212.
33. Little, D. N. and Epps, J. A. "Effects of Recycling Agents on Structural Performance of Recycled Asphalt Concrete Materials." Proceedings of the Association of Asphalt Paving Technologists, 1982.
34. Little, D. N. and Epps, J. A. "Evaluation of Certain Structural Characteristics of Recycled Pavement Materials." Proceedings of the Association of Asphalt Paving Technologists, 1981. pp. 219-249.
35. Little, D. N., Button, J. W. and Epps, J. A. "Structural Properties of Laboratory Mixtures of Foamed Asphalt and Marginal Aggregates." Paper presented at the 60th Annual TRB Meeting 1981.
36. Luhr, D. R. and McCullough, B. F. "Development of a Rationally Based AASHO Road Test Algorithm." Transportation Research Board, Report 766, 1980. pp. 10-17.
37. Luhr, D. R. and McCullough, B. F. "Structural Analysis of AASHO Road Test Flexible Pavements for Performance Evaluation." Paper presented at the 61st Annual TRB Meeting 1982.





38. Majidzadeh, K. "An Evaluation of Reological Properties and Thickness Layer Equivalencies for Four Asphaltic Paving Mixtures." Report submitted to Mobil Research and Development Corporation, 1976.
39. Mamlouk, M. S. "Characterization of Cold Mixed Asphalt Emulsion Treated Bases." Research Report JHRP-79-19, Joint Highway Research Project, Purdue University, West Lafayette, Indiana, 1979.
40. Marshall, P. B. and Kennedy, T. W. "Tensile and Elastic Characteristics of Pavement Materials." Texas Research Report 183-1, Center for Highway Research, The University of Texas at Austin, 1974.
41. Maupin, G. W. "Implementation of Stripping Test for Asphaltic Concrete." Transportation Research Board, Report 712, 1979. pp. 8-12.
42. Maupin, G. W. and Freeman, J. R. "Simple Procedure for Fatigue Characterization of Bituminous Concrete." Research Report FHWA-RD-76-102, Federal Highway Administration, Washington, D. C., 1976.
43. McCullough, B. F. and Taute, A. "Use of Deflection Measurements for Determining Pavement Material Properties." Paper presented at the 61st Annual TRB Meeting 1982.
44. McComb, R. W. "Pueblo West, Colorado: Foamix Experience." Paper presented at the 61st Annual TRB Meeting, 1982.
45. McDonald, C. H. "Foamed Asphalt: An Eighteen Year Performance Record on Four Major Projects." Paper presented at the 60th Annual TRB Meeting, 1981.
46. McKinney, J. L. "An Investigation of Recycling Bituminous Pavements." Research Report JHRP-80-15, Joint Highway Research Project, Purdue University, West Lafayette, Indiana, 1980.
47. McKinney, J. L. "Recycling of Bituminous Pavements." Proceedings of the 65th Annual Road School, 1979.
48. Metwali, E. S. W. "Framework for a Pavement Evaluation System." Research Report JHRP-81-7, Joint Highway Research Project, Purdue University, West Lafayette, Indiana, 1981.
49. Meyer, F. P. R., Cheetham, H. and Haas, R. C. G. "A Coordinated Method for Structural Distress Prediction in Asphalt Pavements." Proceedings of the Association of Asphalt Paving Technologists, 1978. pp. 160-189.
50. Monismith, C. L. and Deacon, J. A. "Fatigue of Asphalt Paving Mixtures." Transportation Engineering Journal of ASCE, Vol. 95, May 1969. pp. 317-345.



51. Monismith, C. L. and Finn, F. N. "Recent Developments in Pavement Design and Structural Rehabilitation," Proceedings of the 9th Australian Road Research Board Conference, 1978. Vol. 9 Part 1, pp. 113-142.
52. Mosey, J. and Welke, R. A. "Use of In-Situ Foamed Asphalt in Michigan." Paper presented at the 61st Annual TRB Meeting, 1982.
53. Oglesby, C. H. and Hicks, R. G. Highway Engineering, Fourth Edition, John Wiley and Sons, 1982. pp. 666-667.
54. Phillips, B. A. and Beaman, R. T. "Dollar Needs to Preserve and Restore U.S. Roads." Transportation Research Board Research News, No. 93, March-April 1981. pp. 1-5.
55. Rada, G. and Witczak, M. W. "Material Layer Coefficients of Unbound Granular Materials from Resilient Modulus." Paper presented at the 61st Annual TRB Meeting 1982.
56. Rauhut, J. B. and Kennedy, T. W. "Characterizing Fatigue Life for Asphalt Concrete Pavements." Paper presented at the 61st Annual TRB Meeting, 1982.
57. Schmidt, R. J. "A Practical Method for Measuring the Resilient Modulus of Asphalt Treated Mixes." Transportation Research Board, Report 404, 1973. pp. 22.
58. Sriver, F. H., Peohl, R., Moore, W. M. and Phillips, M. B. "Detecting Seasonal Changes in Load-Carrying Capacities of Flexible Pavements." National Cooperation of Highway Research Projects 76, 1969. pp. 3-8, 19-27.
59. Sharpe, G. W., Southgate, H. F. and Deen, R. C. "Pavement Evaluation by Using Dynamic Deflections." Transportation Research Board, Report 700, 197 . pp. 34-36.
60. Shurig, D. G., Hittle, J. E. "Field Identification of Soils and Aggregates for County Roads." HERPIC County Highway Series No. 13, Purdue University, West Lafayette, Indiana, 1971.
61. Shurig, D. G., Hittle, J. E., Yoder, E. J. and Goetz, W. H. "Field Investigation of County Road Bases and Subgrades." HERPIC County Highway Series No. 14, Purdue University, West Lafayette, Indiana, 1977.
62. Skok, E. L., Doty, R. N., Finn, F. N. and Lyon, J. W. "Traffic Factors Used in Flexible Pavement Design." Transportation Research Circular, April 1982.
63. Southgate, H. F. and Deen, R. C. "Temperature Distribution Within Asphalt Pavements and its Relationship to Pavement Deflection." Transportation Research Board, Report 291, 1970. pp. 116-127.



64. Kingham, R. I. and Kallas, B. F. "Laboratory Fatigue and its Relationship to Pavement Performance." Proceedings 3rd International Conference on the Structural Design of Asphalt Pavements. pp. 849-865.
65. Tia, M. "A Laboratory Investigation of Cold Mix Recycled Bituminous Pavements." Research Report JHRP-78-23, Joint Highway Research Project, Purdue University, West Lafayette, Indiana, 1978.
66. Tia, M. "Characterization of Cold-Recycled Asphalt Mixtures." Research Report JHRP-82-5, Joint Highway Research Project, Purdue University, West Lafayette, Indiana, 1982.
67. Treybig, H. J., McCullough, B. F., Smith, P. and Von Quintus, H. "Overlay Design and Reflection Cracking Analysis for Rigid Pavements." Vol. 1, Development of New Design Criteria." Research Report FHWA-RD-77-66, Federal Highway Administration, Washington, D. C., 1977.
68. Van Dijk, W., Moreaud, H., Quadiville, A. and Uge, P. "The Fatigue of Bitumen and Bituminous Mixes." Third International Conference on the Structural Design of Asphalt Pavements, 1972. pp. 354-366.
69. Van Til, C. J., McCullough, B. F., Vallergera, B. A. and Hicks, G. "Evaluation of AASHO Interim Guides for Design of Pavement Structures." National Cooperation of Highway Research Projects 128, 1972.
70. Vaswani, N. K. "Design of Pavements Using Deflection Equations from AASHO Road Test Results." Transportation Research Board, Report 239, 1968. pp. 76-94.
71. Vaswani, N. K. "Method for Separately Evaluating Structural Performance of Subgrade and Overlying Flexible Pavements." Transportation Research Board, Report 365, 1971. pp. 40-61.
72. Wang, M. C. "Performance Analysis for Flexible Pavements with Stabilized Bases." Paper presented at the 61st Annual TRB Meeting, 1982.
73. Wang, M. C. and Kilareski, W. P. "Field Performance of Aggregate-Lime-Pozzolon Base Material." Transportation Research Board, Report 725, 1980. pp. 74-80.
74. Wang, M. C. and Larson, T. D. "Evaluation of Structural Coefficients of Stabilized Base-Coarse Materials." Transportation Research Board, Report 725, 1980. pp. 58-67.
75. Woods, K. B. Highway Engineering Handbook. First Edition, McGraw-Hill Book Company.



76. Yoder, E. J. and Witczak, M. W. Principles of Pavement Design. Second Edition, John Wiley and Sons, Inc., 1975.
77. A Basic Asphalt Emulsion Manual. Asphalt Institute MS-19, March 1979.
78. AASHTO Materials. Part II: Tests. Second Ed. 1978. Pp. 247-272.
79. ASTM Test Procedures. Part 15: Road, Paving, Bituminous Materials: Travelled Surface Characteristics. Annual Book of ASTM Stand., 1981.
80. "Asphalt Concrete Overlays of Rigid and Flexible Pavements." Louisiana Highway Research, Final Report.
81. Computer Program for Layered Systems Under Normal Surface Loads. "BISTRO". CDC-6500 Version. Koninklijke/Shell-Laboratorium, Amsterdam, Netherlands.
82. "Clegg Impact Soil Tester". Information published by the manufacturers of the Clegg Impact Soil Tester, Australia.
83. Conoco Technical Bulletin, April 1981.
84. Construction Proposal. Contract No. RS-13064. Indiana State Highway.
85. Federal Aviation Administration, Circular AC 150/5320-6c.
86. "Foamed Asphalt Resilient Modulus Tests." Foamed Asphalt Technology Joint Project, CR-42 Project MOBIL OIL, 1975.
87. "Foamed Asphalt/Crushed Rock Pavements." Foamed Asphalt Technology Joint Project, CR-42 Project MOBIL OIL, 1976.
88. "Foamed Asphalt: Water Resistance." Foamed Asphalt Technology Joint Project, CR-42 Project MOBIL OIL, 1977.
89. "Indirect Tensile Test." Transportation Research Board Special Report 162. Pp. 32-34.
90. "International Aspects of Recycling." Rural and Urban Roads. July 1981. Pp. 22.
91. "Is This the Road Ahead?" Asphalt Institute Publication.
92. Mix Design Methods for Asphalt Concrete and Other Hot-Mix Types. Asphalt Institute MS-2, March 1979.
93. "Plant Set-Up for Foamed Asphalt." Construction Canada. July 1964. pp. 20-23.





94. Soils Manual for the Design of Asphalt Pavement Structures.  
Asphalt Institute MS-10, February 1969.
95. Thickness Design - Asphalt Pavements for Highways and Streets.  
Asphalt Institute MS-1, September 1981.
96. Thickness Design - Full Depth Asphalt Pavement Structures for Highways and Streets. Asphalt Institute MS-1, August 1970. P. 42.
97. "What's Wrong with U.S. Transportation Infrastructure." Civil Engineering ASCE, Nov. 1981. pp. 58-61.



## APPENDIX



## APPENDIX : DYNAFLECT DEFLECTION DATA

TABLE A.1 : DYNAFLECT DEFLECTIONS TAKEN IN NOVEMBER 1980  
(BEFORE1) ON THE EASTBOUND LANE

STATION (0.1 MI)	1	2	3	4	5
1	1.630	1.230	.780	.430	.170
2	1.960	1.200	.760	.380	.260
3	1.620	1.450	.800	.420	.220
4	2.370	2.190	1.030	.690	.350
5	3.410	2.680	1.390	.730	.380
6	1.530	1.320	1.040	.380	.200
7	1.690	1.190	.510	.280	.160
8	1.260	.850	.520	.230	.140
9	1.230	.950	.570	.330	.240
10	1.230	.950	.560	.330	.240
11	1.710	1.120	.480	.250	.220
12	1.130	.930	.460	.320	.240
13	.710	.550	.290	.260	.190
14	1.840	1.350	.690	.670	.480
15	2.010	1.340	.910	.650	.540
16	1.430	1.200	.790	.350	.260
17	1.110	.680	.440	.250	.160
18	.960	.780	.460	.290	.170
19	.840	.620	.390	.340	.180
20	.650	.540	.400	.220	.190
21	1.040	.800	.430	.260	.170
22	.840	.510	.290	.250	.180
23	1.350	1.130	.780	.490	.330
24	1.290	1.000	.700	.420	.260
25	.960	.760	.410	.230	.130
26	1.380	.980	.530	.290	.180
27	1.520	1.190	.790	.350	.210
28	1.260	1.020	.430	.360	.150
29	1.530	1.160	.620	.340	.160
30	1.040	.740	.340	.300	.100
31	1.120	.900	.640	.260	.150
32	1.060	.870	.440	.290	.180
33	1.590	1.080	.720	.600	.350
34	2.240	1.420	1.310	.360	.220
35	1.510	.900	.560	.280	.170
36	2.610	1.550	1.210	.490	.390
37	1.980	1.350	.780	.300	.130
38	1.490	.980	.700	.290	.150
39	2.040	1.400	.780	.490	.230
40	2.290	1.430	.780	.420	.240
41	2.050	1.330	.540	.410	.230
42	1.140	1.020	.510	.380	.310
43	2.080	1.580	.900	.460	.340



TABLE A.2 : DYNAFLECT DEFLECTIONS TAKEN IN NOVEMBER 1980  
(BEFORE1) ON THE WESTBOUND LANE

STATION (0.1 MI)	DYNAFLECT SENSOR NUMBER				
	1	2	3	4	5
1	2.735	1.694	.774	.345	.153
2	1.874	1.287	.551	.290	.147
3	1.704	1.132	.807	.306	.231
4	1.886	1.358	.787	.328	.183
5	2.244	1.785	1.047	.557	.305
6	2.060	1.642	.915	.653	.315
7	1.420	1.141	.544	.294	.196
8	1.232	1.117	.540	.420	.307
9	1.674	1.055	.780	.533	.175
10	1.205	1.078	.601	.339	.198
11	1.344	1.054	.505	.290	.182
12	1.117	.777	.412	.293	.164
13	1.030	.766	.374	.280	.178
14	.686	.437	.332	.269	.208
15	2.253	1.548	1.017	.735	.433
16	1.918	1.511	.792	.555	.321
17	1.768	1.244	.738	.410	.252
18	1.140	.810	.478	.328	.204
19	.840	.584	.421	.319	.199
20	.930	.687	.374	.275	.172
21	.627	.539	.328	.209	.165
22	.902	.631	.420	.273	.185
23	1.123	.894	.616	.440	.308
24	1.561	1.204	.771	.486	.326
25	1.458	1.158	.609	.391	.245
26	1.033	.744	.438	.300	.190
27	1.541	.926	.490	.395	.253
28	1.622	1.172	.601	.376	.238
29	1.339	.916	.445	.259	.186
30	1.193	.983	.372	.274	.149
31	1.133	.742	.402	.222	.092
32	1.088	.773	.464	.290	.175
33	.718	.464	.342	.233	.155
34	1.193	1.114	.762	.721	.577
35	1.203	.837	.445	.303	.184
36	1.595	1.055	.677	.364	.170
37	2.090	1.384	.870	.580	.268
38	1.642	.952	.818	.294	.208
39	1.164	.952	.818	.294	.208
40	1.079	.956	.557	.317	.164
41	1.980	1.466	.879	.517	.221
42	1.358	1.172	.661	.404	.241
43	1.768	1.365	1.151	1.096	1.047

ALL DEFLECTIONS IN MILS  
1 INCH = 25.4 MM





TABLE A.3 : DYNAFLECT DEFLECTIONS TAKEN IN MAY 1981  
(BEFORE2) ON THE EASTBOUND LANE

STATIONS (0.1 MI)	1	2	3	4	5
1	2.650	1.556	1.111	.375	.181
2	1.537	1.121	1.102	.328	.199
3	2.441	1.698	1.499	.589	.302
4	3.413	2.330	1.080	.632	.373
5	3.525	3.010	1.478	.736	.292
6	3.219	1.654	1.308	.537	.250
7	3.875	2.238	1.127	.423	.210
8	3.871	1.408	.717	.392	.266
9	3.780	2.265	1.696	.596	.257
10	3.578	1.840	.798	.358	.193
11	3.705	1.800	1.614	.372	.174
12	3.524	1.110	.531	.290	.238
13	3.240	1.045	.748	.397	.206
14	3.850	.649	.496	.396	.214
15	3.317	2.441	1.353	.785	.417
16	3.471	2.500	1.501	.583	.322
17	3.208	1.529	1.126	.547	.271
18	3.230	1.371	.677	.389	.187
19	3.544	1.102	.616	.383	.230
20	3.172	.780	.452	.296	.177
21	3.247	.867	.559	.338	.213
22	3.664	.512	.296	.286	.157
23	3.536	1.310	.966	.635	.536
24	3.562	1.979	1.062	.598	.379
25	3.524	.966	.805	.376	.230
26	3.004	.876	.525	.491	.391
27	3.800	1.866	.973	.588	.235
28	3.427	1.636	1.483	.531	.216
29	3.078	2.075	1.728	.477	.268
30	3.911	1.391	1.317	.382	.211
31	3.435	1.121	1.115	.386	.232
32	3.898	.572	.443	.214	.177
33	3.160	.841	.755	.399	.230
34	3.066	2.155	1.148	.692	.295
35	3.613	1.571	.943	.294	.176
36	3.443	3.035	1.426	.899	.306
37	3.002	2.015	.795	.392	.176
38	3.861	2.930	1.703	.486	.250
39	3.995	1.619	1.585	.434	.416
40	3.207	1.975	1.640	.474	.276
41	3.616	2.080	1.310	.594	.358
42	3.356	1.005	.540	.412	.285
43	3.149	2.171	1.341	.347	.235

ALL DEFLECTIONS IN MILS  
1 INCH = 25.4 MM



TABLE A.4 : DYNAFLECT DEFLECTIONS TAKEN IN MAY 1981  
(BEFORE2) ON THE WESTBOUND LANE

STATIONS (0.1 MI)	1	2	3	4	5
1	1.364	.845	.720	.524	.147
2	2.957	1.936	.997	.625	.226
3	2.483	1.866	1.630	.479	.271
4	3.073	2.371	1.156	1.070	.248
5	2.329	1.617	.862	.422	.189
6	1.845	1.069	.519	.324	.144
7	1.725	1.072	.586	.435	.199
8	2.555	1.516	.681	.465	.245
9	2.790	1.740	1.327	.628	.170
10	2.025	1.243	.555	.325	.150
11	1.140	.780	.566	.368	.197
12	1.007	.708	.505	.403	.207
13	1.705	.502	.290	.209	.174
14	2.377	1.477	.674	.407	.324
15	2.266	1.650	.892	.424	.284
16	2.752	1.708	.953	.431	.224
17	1.460	1.013	.497	.323	.148
18	1.368	.926	.459	.305	.179
19	1.191	.869	.481	.302	.187
20	1.068	.793	.413	.226	.184
21	1.734	.434	.291	.204	.167
22	1.623	1.380	.928	.509	.485
23	2.624	1.844	.767	.411	.379
24	1.504	1.057	.628	.355	.260
25	1.634	1.160	.668	.305	.197
26	2.114	1.340	.723	.387	.191
27	1.808	1.209	.502	.308	.120
28	2.103	1.256	.662	.307	.169
29	1.364	.775	.402	.204	.138
30	1.094	.875	.751	.281	.158
31	1.979	1.602	.961	.238	.175
32	1.214	.967	.587	.403	.218
33	2.169	1.512	1.420	.388	.171
34	1.995	1.568	1.281	.489	.173
35	2.277	1.747	1.058	.467	.351
36	2.500	1.656	.951	.282	.174
37	2.246	1.694	.660	.469	.183
38	1.597	.918	.560	.253	.151
39	2.206	1.438	.663	.409	.255
40	2.255	1.628	.851	.518	.350
41	1.973	.725	.528	.333	.258
42	1.845	1.242	1.223	.350	.175
43	2.149	1.353	.882	.440	.276

ALL DEFLECTIONS IN MILS  
1 INCH = 25.4 MM



TABLE A.5 : DYNAFLECT DEFLECTIONS TAKEN IN SEPTEMBER 1981  
(DURING) ON THE EASTBOUND LANE

STATION (0.1 MI)	1	2	3	4	5
0	2.100	1.630	.870	.490	.250
1	2.170	1.340	.460	.220	.120
2	1.440	.950	.420	.240	.150
3	1.560	1.210	.610	.410	.220
4	2.360	1.640	1.190	.530	.210
5	3.630	2.630	1.260	.600	.260
6	2.980	2.040	.810	.380	.180
7	2.360	1.410	.480	.230	.130
8	1.890	1.290	.550	.300	.170
9	3.100	1.780	.470	.220	.120
10	2.940	1.840	.640	.300	.140
11	2.220	1.540	.580	.270	.140
12	1.450	1.040	.470	.270	.160
13	1.480	1.010	.500	.330	.200
14	1.480	1.210	.700	.510	.320
15	2.210	1.750	.970	.620	.350
16	2.250	1.750	.930	.560	.270
17	1.450	1.100	.580	.360	.200
18	1.590	1.010	.450	.260	.140
19	1.290	.880	.430	.260	.160
20	1.560	1.060	.460	.250	.140
21	1.680	1.280	.610	.360	.200
22	.870	.670	.380	.270	.180
23	2.090	1.730	1.020	.730	.470
24	2.330	1.770	.850	.470	.260
25	1.470	1.070	.470	.260	.150
26	2.440	1.560	.670	.350	.190
27	2.500	1.670	.700	.350	.190
28	1.980	1.300	.520	.240	.100
29	1.760	1.220	.530	.280	.140
30	1.650	1.010	.380	.200	.100
31	1.610	1.170	.490	.250	.140
32	1.110	.770	.380	.240	.150
33	2.600	2.020	1.160	.820	.500
34	2.300	1.640	.710	.310	.150
35	1.590	1.170	.540	.290	.150
36	2.920	2.060	.790	.350	.150
37	2.850	1.900	.700	.290	.130
38	3.030	2.170	.880	.410	.190
39	2.900	1.800	.560	.200	.070
40	2.910	1.910	.800	.410	.200
41	2.320	1.560	.670	.410	.220
42	1.910	1.360	.810	.510	.340

ALL DEFLECTIONS IN MILS  
1 INCH = 25.4 MM



TABLE A.6 : DYNAFLECT DEFLECTIONS TAKEN IN SEPTEMBER 1981  
(AFTER) ON THE EASTBOUND LANE

STATION (0.1 MI)	1	2	3	4	5
1	1.800	1.140	.670	.420	.230
2	2.090	1.220	.580	.330	.170
3	2.070	1.280	.670	.370	.190
4	1.850	1.260	.770	.510	.290
5	3.080	1.930	.790	.630	.300
6	2.280	1.510	.880	.540	.290
7	2.230	1.470	.840	.500	.260
8	2.050	1.150	.550	.320	.130
9	1.710	1.010	.520	.300	.180
10	2.230	1.260	.590	.320	.180
11	2.080	1.270	.660	.400	.230
12	1.670	1.020	.530	.300	.160
13	1.160	.730	.420	.290	.180
14	1.220	.860	.610	.420	.260
15	.760	.500	.330	.260	.180
16	2.750	1.990	1.390	1.050	1.030
17	1.900	1.360	.900	.650	.380
18	1.500	.980	.580	.400	.230
19	1.260	.840	.490	.340	.200
20	1.280	.840	.490	.340	.200
21	1.340	.850	.490	.330	.200
22	1.280	.840	.490	.350	.220
23	.760	.510	.340	.280	.190
24	1.510	1.120	.830	.710	.510
25	2.140	1.490	.920	.630	.350
26	1.900	1.220	.700	.470	.380
27	1.520	.980	.570	.400	.230
28	1.690	1.050	.560	.350	.190
29	2.200	1.350	.700	.420	.200
30	1.720	1.080	.600	.380	.180
31	1.120	.690	.370	.230	.120
32	1.130	.720	.390	.260	.150
33	.830	.540	.320	.240	.160
34	2.180	1.450	.950	.740	.490
35	2.100	1.380	.810	.520	.270
36	1.530	.980	.560	.370	.200
37	2.680	1.750	1.010	.650	.330
38	2.180	1.430	.780	.460	.200
39	2.290	1.390	.690	.370	.150
40	2.080	1.350	.760	.460	.210
41	2.970	1.820	1.000	.620	.310
42	2.280	1.470	.850	.550	.300
43	.640	.570	.510	.490	.400

ALL DEFLECTIONS IN MILS  
1 INCH = 25.4 MM





TABLE A.7 : DYNAFLECT DEFLECTIONS TAKEN IN SEPTEMBER 1981  
(AFTER1) ON THE WESTBOUND LANE

STATION (0.1 MI)	1	2	3	4	5
1	1.920	1.350	.840	.570	.310
2	3.000	1.790	.850	.410	.170
3	2.050	1.250	.640	.380	.190
4	1.780	.910	.420	.250	.150
5	2.800	1.670	.800	.410	.170
6	4.600	2.800	1.390	.640	.200
7	3.880	2.480	1.290	.680	.270
8	1.050	.600	.320	.220	.150
9	1.420	.980	.620	.430	.260
10	1.320	.840	.470	.300	.160
11	1.890	1.250	.720	.450	.230
12	2.210	1.420	.770	.420	.200
13	2.080	1.190	.530	.280	.150
14	1.360	.860	.490	.320	.180
15	.910	.610	.390	.290	.200
16	2.330	1.660	1.120	.830	.470
17	2.840	1.960	1.160	.750	.380
18	3.800	2.350	1.160	.610	.260
19	1.850	1.160	.610	.370	.200
20	1.370	.910	.560	.380	.230
21	1.100	.710	.410	.280	.170
22	1.180	.830	.510	.360	.220
23	1.060	.700	.430	.310	.200
24	1.550	1.130	.760	.580	.360
25	2.330	1.580	.950	.620	.330
26	2.970	1.820	.970	.600	.330
27	1.550	.970	.510	.320	.170
28	2.150	1.360	.740	.470	.260
29	1.850	1.240	.720	.460	.250
30	1.280	.800	.460	.310	.170
31	1.230	.730	.360	.220	.120
32	1.380	.860	.440	.270	.150
33	1.310	.880	.530	.360	.220
34	.810	.530	.350	.270	.190
35	2.270	1.390	.720	.420	.220
36	2.410	1.460	.690	.360	.170
37	3.220	2.060	1.120	.680	.330
38	2.980	1.830	.910	.480	.190
39	2.550	1.520	.800	.460	.220
40	1.430	.830	.440	.260	.130
41	2.750	1.640	.840	.500	.270
42	2.470	1.520	.810	.510	.280
43	2.660	2.130	1.950	2.030	1.780

ALL DEFLECTIONS IN MILS  
1 INCH = 25.4 MM



TABLE A.8 : DYNAFLECT DEFLECTIONS TAKEN IN MAY 1982 :  
(AFTER2) ON THE EASTBOUND LANE

STATION (0.1 MI)	DYNAFLECT SENSOR NUMBER				
	1	2	3	4	5
0	2.330	1.810	1.120	.640	.360
1	2.930	1.920	.900	.390	.180
2	2.190	1.460	.730	.340	.180
3	2.560	1.930	1.190	.680	.400
4	2.440	1.800	.980	.470	.230
5	3.200	2.410	1.400	.710	.340
6	2.920	2.250	1.280	.610	.280
7	2.400	1.420	.690	.370	.230
8	2.050	1.480	.820	.430	.230
9	2.310	1.310	.560	.260	.150
10	2.830	1.840	.890	.410	.200
11	1.720	1.200	.640	.330	.190
12	1.770	1.170	.610	.320	.200
13	1.240	.990	.680	.450	.310
14	.810	.560	.370	.260	.190
15	3.620	2.990	2.060	1.290	.800
16	2.310	1.730	.990	.560	.320
17	1.670	1.200	.700	.380	.220
18	1.460	1.020	.570	.320	.190
19	1.630	1.170	.660	.370	.230
20	1.140	.790	.500	.310	.210
21	1.470	1.100	.690	.430	.280
22	1.100	.770	.480	.300	.210
23	1.670	1.390	1.070	.810	.630
24	2.070	1.480	.870	.490	.300
25	1.790	1.160	.640	.400	.280
26	2.010	1.350	.760	.440	.280
27	1.740	1.120	.540	.260	.150
28	2.560	1.690	.890	.440	.220
29	2.270	1.570	.880	.450	.230
30	1.670	1.100	.550	.270	.140
31	1.480	1.010	.570	.330	.200
32	.780	.560	.380	.270	.200
33	1.560	1.210	.830	.570	.420
34	2.400	1.840	1.100	.590	.320
35	2.080	1.330	.720	.380	.220
36	3.830	2.720	1.520	.790	.430
37	3.200	2.160	1.150	.520	.210
38	3.270	2.240	1.160	.530	.240
39	1.580	1.130	.610	.300	.140
40	2.950	2.070	1.150	.610	.350
41	2.570	1.780	1.000	.570	.360

ALL DEFLECTIONS IN MILS  
1 INCH = 25.4 MM



TABLE A.9 : DYNAFLECT DEFLECTIONS TAKEN IN MAY 1982  
(AFTER2) ON THE WESTBOUND LANE

STATION (0.1 MI)	1	2	3	4	5
0	2.960	1.900	.900	.420	.200
1	2.960	1.900	.900	.420	.200
2	2.960	1.900	.900	.420	.200
3	5.670	4.110	2.320	1.220	.580
4	4.650	2.710	1.090	.410	.150
5	3.530	2.380	1.240	.610	.290
6	3.050	2.010	.970	.430	.210
7	2.170	1.370	.690	.370	.220
8	1.580	1.150	.680	.400	.230
9	1.640	1.130	.640	.360	.210
10	2.540	1.850	1.060	.570	.300
11	2.060	1.220	.590	.310	.170
12	1.860	1.180	.590	.320	.190
13	1.280	.910	.600	.390	.260
14	1.060	.820	.580	.430	.330
15	4.790	3.660	2.360	1.470	.900
16	2.460	1.810	1.090	.640	.380
17	2.830	1.670	.750	.340	.180
18	1.730	1.150	.620	.350	.210
19	1.650	1.170	.680	.400	.250
20	1.140	.790	.470	.310	.230
21	1.200	.840	.490	.310	.230
22	.740	.530	.380	.280	.220
23	1.300	1.020	.700	.500	.360
24	2.300	1.790	1.090	.650	.390
25	1.990	1.390	.810	.480	.300
26	1.960	1.390	.780	.450	.270
27	1.930	1.170	.560	.280	.170
28	2.080	1.480	.820	.450	.250
29	2.010	1.400	.790	.440	.240
30	1.540	.950	.470	.250	.150
31	1.700	1.110	.580	.320	.200
32	1.180	.880	.560	.370	.260
33	1.910	1.370	.900	.620	.470
34	2.560	1.710	.900	.490	.280
35	3.200	2.160	1.140	.550	.270
36	4.670	3.370	1.870	.960	.490
37	3.150	2.090	1.030	.470	.200
38	3.090	2.150	1.150	.580	.300
39	1.710	1.210	.690	.400	.230
40	3.440	2.530	1.380	.740	.390
41	2.420	1.850	1.080	.650	.420
42	2.470	1.800	1.050	.610	.380

ALL DEFLECTIONS IN MILS  
1 INCH = 25.4 MM







COVER DESIGN BY ALDO GIORGINI